AD NUMBER

AD903501

NEW LIMITATION CHANGE

TO

Approved for public release, distribution unlimited

FROM

Distribution authorized to U.S. Gov't. agencies only; Test and Evaluation; 09 JUN 1972. Other requests shall be referred to Air Force Materials Command, Attn: AFML/LAE, Wright-Patterson AFB, OH 45433.

AUTHORITY

AFML ltr, 18 Jan 1974

NOTICE

When Government drawings, specifications, or other data are used for any purpose other than in connection with a definitely related Government procurement operation, the United States Government thereby incurs no responsibility nor any obligation whatsoever; and the fact that the government may have formulated, furnished, or in any way supplied the said drawings, specifications, or other data, is not to be regarded by implication or otherwise as in any manner licensing the holder or any other person or corporation, or conveying any rights or permission to manufacture, use, or sell any patented invention that may in any way be related thereto.

Copies of this report should not be returned unless return is required by security considerations, contractual obligations, or notice on a specific document.

NOTICE

When Government drawings, specifications, or other data are used for any purpose other than in connection with a definitely related Government procurement operation, the United States Government thereby incurs no responsibility nor any obligation whatsoever; and the fact that the government may have formulated, furnished, or in any way supplied the said drawings, specifications, or other data, is not to be regarded by implication or otherwise as in any manner licensing the holder or any other person or corporation, or conveying any rights or permission to manufacture, use, or sell any patented invention that may in any way be related thereto.

Copies of this report should not be returned unless return is required by security considerations, contractual obligations, or notice on a specific document.

AFML-TR-72-95

EVALUATION OF MATERIALS APPLICABLE TO AEROSPACE SYSTEMS

D. A. Gerdeman

W. E. Berner

G. J. Petrak

University of Dayton Research Institute
Dayton, Ohio

FOREWORD

This report covers work performed during the period from 1 September 1970 to 29 February 1972 under Air Force Contract F33615-71-C-1054. This contract was initiated under Project Number 7381, "Materials Application". The work was administered under the direction of the Materials Support Division of the Air Force Materials Laboratory, Wright-Patterson Air Force Base, Ohio. Mr. A. Olevitch (LAE) acted as Project Engineer.

University of Dayton personnel who made major contributions to the program include: D. A. Gerdeman, Project Leader; W. E. Berner, R. E. Jones, G. J. Petrak, R. R. Cervay, Research Engineers; and J. A. Ziegenhagen, Research Chemist. Research technicians participating in this program were P. J. Allen, S. W. Brzezicki, W. D. Cambron, J. H. Eblin, P. J. Larger, S. C. Macy, R. J. Marton, D. C. Maxwell, J. C. McKiernan, D. S. Opela, L. D. Pike, G. E. Price, P. L. Proshek, C. W. Schroll, L. W. Sears, E. Soltis, and D. W. Woleslagle. This report was released by the authors in June 1972. The contractor's report number is UDRI-TR-72-39.

This technical report has been reviewed and is approved.

Albert Olevitch

ALBERT OLEVITCH, Chief
Materials Engineering Branch
Materials Support Division
Air Force Materials Laboratory

ABSTRACT

This report describes the materials evaluations and related efforts completed under contract to the Air Force Materials Laboratory. It is divided into three sections: properties of metals, nonmetallic materials evaluation, and other efforts related to materials evaluation.

The first section describes programs which involved the evaluation of the mechanical properties of metal alloys. The crack growth properties of D6ac steel were determined and actual components constructed of D6ac and 4340 were fatigue tested. The tensile, crack growth, and fracture toughness properties of roll-extruded HP 9-4-25 were determined as a function of degree of roll-reduction. Fracture and fatigue crack growth studies were conducted on 7175-T736 aluminum forgings. Design data were generated on the newly developed 7049 aluminum alloy extrusion in the T73 and T76 conditions. The effect of annealing on the tensile and fatigue properties of centrifugally cast Ti-6Al-4V were investigated as were the tensile, fracture, fatigue crack growth and stress corrosion properties of beta annealed Ti-6Al-4V plate. Tensile, fracture, fatigue, and static crack growth, and notched and unnotched fatigue test data were generated for Ti-6Al-6V-2Sn. A parametric analysis of creep stress rupture data as it pertains to the refractory metal alloys is presented. Two laminated composites were also evaluated. One was a simple adhesively bonded 2024 aluminum composite and the other was composed of alternating layers of Ti-6Al-4V and boron/epoxy. The results of the preliminary evaluation of these composites are presented.

The second section describes the evaluation of nonmetallic materials. One program discussed involves the storage life of elastomeric fuel tank sealants. Thirty-three materials manufactured by five different companies are involved in this 24 month program. The hydrolytic stability of several potting compounds was also determined. Included were flexible epoxies, polyester and polyether polyurethanes, and polysulfides. The compatibility of elastomeric sealing compounds and seals with different fluids was determined and is discussed. Compatibility studies involved a silicone compound helicopter engine seal in eleven approved engine lubricants, two O-ring packings in Type I, Type III, JP-4, and JP-7 fuels, as well as Buna-n, ethylene propylene, and neoprene pump seals in a 55% mono-ethanol-amine/45% amon-isopropyl-amine decontaminant. A discussion of dynamic O-ring endurance testing is also included.

Three additional areas of support are described in the third section. Included as a discussion of a program to increase the density of 3-D carbon/carbon composites by hot pressing. The hot pressing conditions which were used are described. Additional development of a foam-in-place liner for helmets and the development of suitable photochromic compounds for camera filters are also discussed.

TABLE OF CONTENTS

SECTION			PAGE
I	MECHANICAL PROPERTIES OF METAL ALLOYS		1
	1.1	INTRODUCTION	1
	1.2	EVALUATION OF MATERIALS FOR SPECIFIC SYSTEMS	2
		1.2.1 Crack Growth Properties of D6ac Steel	2
		1.2.1.1 Tensile Test Results	3
		1.2.1.2 Fracture Toughness Results	3
		1.2.1.3 Fatigue Crack Growth Test Results	12
		1.2.1.4 Stress Corrosion Crack Test Results	24
		1.2.2 Fatigue of Steel Bomb Hooks	24
		1.2.2.1 Results and Discussion	29
	1.3	DATA ON EMERGING MATERIALS AND PROCESSES	34
		1.3.1 Roll-Extruded HP 9Ni-4Co-25C Steel	34
		1.3.1.1 Test Materials	34
		1.3.1.2 Results and Discussion	36
		1.3.1.3 Summary	47
		1.3.2 Fracture and Fatigue Crack Growth of 7175-T736 Forgings	47
		1.3.2.1 Results and Discussion	49
		1.3.3 Design Properties of 7049 Extrusions	58
		1.3.3.1 Results and Discussion	58
		1.3.4 Evaluation of Ti-6Al-4V Castings	76
		1.3.4.1 Results and Discussion	78
		1.3.5 Beta Annealed T-6Al-4V Plate	78
		1.3.5.1 Results and Discussion	83
		1.3.6 Evaluation of Ti-6Al-6V-2Sn Alloy	83
		1.3.6.1 Results and Discussion	88
		1.3.7 Parametric Analysis of Creep and Stress Rupture Data	88
		1.3.7.1 Procedure	101
		1.3.8 Laminated Metal Composites	119
		1.3.8.1 Laminated Aluminum	119
		1.3.8.2 Titanium-Boron Composite	122
II	EVALUATION OF NONMETALLIC MATERIALS		129
	2.1	INTRODUCTION	129
	2.2	STORAGE LIFE TESTING OF FUEL TANK SEALANTS	130
		2.2.1 Procedure	130
		2.2.2 Results	131
		2.2.2.1 Application Life Tests	131
		2.2.2.2 Standard Curing Rate Tests	146

TABLE OF CONTENTS (cont)

SECTION			PAGE
		2.2.2.3 Tack-Free Time	146
	2.2.3	Discussion	147
2.3	HYDROLYTIC STABILITY TESTING OF ELASTOMERS		148
	2.3.1	PC-1 Potting Compound	148
		2.3.1.1 Part One Testing	148
		2.3.1.2 Part Two Testing	150
	2.3.2	Compounds PC-2, PC-3, and PC-4	153
		2.3.2.1 Test Procedure	153
		2.3.2.2 Results	156
	2.3.3	Evaluation of PC-5	156
		2.3.3.1 Procedures	156
		2.3.3.2 Results	159
	2.3.4	FTS-B Sealant	159
		2.3.4.1 Procedure	160
		2.3.4.2 Results	160
	2.3.5	FTS-C Sealant	160
		2.3.5.1 Procedures	160
		2.3.5.2 Results	164
	2.3.6	Evaluation of MC-A and MC-B Materials	164
		2.3.6.1 Procedure	164
		2.3.6.2 Results	164
	2.3.7	Cover Material CM-A	167
		2.3.7.1 Procedure	167
		2.3.7.2 Results	167
2.4	COMPATIBILITY OF ELASTOMERS		170
	2.4.1	Elastomers in Lubricants	170
		2.4.1.1 Procedure	170
		2.4.1.2 Results	170
		2.4.1.3 Summary	177
	2.4.2	Elastomers in Fuels	177
		2.4.2.1 Procedure	177
		2.4.2.2 Results	177
	2.4.3	Elastomers in a Decontaminant	179
		2.4.3.1 Procedure	179
		2.4.3.2 Test Results	179
2.5	DYNAMIC O-RING EVALUATIONS		182
	2.5.1	Modifications to Test Equipment	182
	2.5.2	Tests Conducted	184
	2.5.3	Results of Baseline Testing	184
	2.5.4	Conclusions and Recommendations	188
III	ADDITIONAL AREAS OF ACTIVITY		189

TABLE OF CONTENTS (cont)

SECTION		PAGE
3.1	INTRODUCTION	189
3.2	HOT PRESSING 3-D CARBON COMPOSITES	189
	3.2.1 Procedure	189
	3.2.2 Results	190
3.3	DEVELOPMENT OF FOAM-IN-PLACE HELMET LINERS	195
	3.3.1 Improvement in Molds	195
	3.3.2 Foam Formulation Improvements	197
3.4	PHOTOCHROMIC FILTERS FOR CAMERAS	198
	3.4.1 Preliminary Studies	198
	3.4.2 Development of Suitable Compounds	198
	3.4.3 Evaluation of Filters	199
REFERENCES		200

LIST OF ILLUSTRATIONS

Figure		Page
1	Medium Toughness D6ac Plate Steel Mechanical Properties vs. Temperature	7
2	Effect of Temperature on Fracture Toughness of D6ac Steel	11
3	Fracture Toughness of D6ac Plate at Room Temperature in Three Heat Treatment Conditions	13
4	Comparison of Fracture Toughness Values Obtained From SF Specimens and CT Specimens Machined From SF Specimens	14
5	Effect of Toughness on Crack Growth Rate, CT Specimen	15
6	Effect of Toughness on Crack Growth Rate, DCB Specimen	16
7	Effect of Loading Ratio and Frequency on Crack Growth Rate	18
8	Effect on Loading Ratio and Frequency on Crack Growth Rate	19
9	Effect of Specimen Configuration on Crack Growth Rate D6ac Medium Toughness Plate	20
10	Effect of Loading Ratio and Frequency on Surface Flaw Crack Growth Rate	21
11	Effect of Distilled Water Environment on Crack Growth Rate	22
12	Effect of Grain Direction on Crack Growth Rate, D6ac Medium Toughness Plate	23
13	D6ac Static Crack Growth Rate vs. Stress Intensity In a Distilled Water Environment	26
14	Bomb Lug	28

Figure		Page
15	S/N Fatigue Curve for D6ac and 4340 Steel in Two Heat Treatments (Notched Specimens, R = 1.0)	30
16	Fatigue Data for D6ac and 4340 Bomb Hooks	32
17	Typical Types of Bomb Hook Failures	33
18	Fractured HP-9-4-25 Tensile Specimens	38
19	Fractured HP-9-4-25 Tensile Specimens	39
20	Fractured HP-9-4-25 Tensile Specimens	39
21	Photomicrograph of Laminations in Axial Tensile Specimen (600X)	40
22	Stress Intensity Factor Range Versus Fatigue Crack Growth Rate for Roll Extruded HP 9-4-25 Steel, Rectangular DCB Specimen and Other Data	43
23	Stress Intensity Factor Range Versus Fatigue Crack Growth Rate for HP 9-4-25 Steel, Mostovy DCB Specimen, and Other Data	44
24	SCC Crack Growth Rate Versus Stress Intensity for HP 9-4-25 Steel	45
25	SCC Crack Growth Rate Versus Stress Intensity for D6ac and HP 9-4-25 (Reference 10)	46
26	Flaw Sensitivity Index Versus Yield Strength Normalized by Young's Modulus for Several Steel Alloys	48
27	Stress Intensity Factor Range Versus Crack Growth Rate for 7175-T736 Forging at Room Temperature	53
28	Stress Intensity Factor Range Versus Crack Growth Rate for 7175-T736 Forging at Elevated Temperatures, Compared with Room Temperature	54
29	Stress Intensity Factor Range Versus Crack Growth Rate for 7175-T736 Forging At Low Temperatures, Compared with Room Temperature	56

Figure		Page
30	Fatigue Crack Growth Rate Versus the Reciprocal of Test Temperature for 7175-T736 Forging	57
31	Tensile Property Data for the Longitudinal Direction of Three 7049 Extrusions	59
32	Tensile Property Data for the Transverse Direction of Three 7049 Extrusion	60
33	Tensile Property Data for the Short Transverse Direction of Three 7049 Extrusions	61
34	Elongation and Reduction of Area for the Longitudinal Direction of Three 7049 Extrusions	62
35	Elongation and Reduction of Area for the Transverse Direction of Three 7049 Extrusions	62
36	Elongation and Reduction of Area for the Short Transverse Direction of Three 7049 Extrusions	62
37	Fracture Toughness, K_{IC}, for the Longitudinal (LW) Orientation in Three 7049 Extrusions	64
38	Fracture Toughness, K_{IC}, for the Transverse (WL) Orientation in Three 7049 Extrusions	64
39	Fracture Toughness, K_{IC}, for the Short Transverse (TW) Orientation in Three 7049 Extrusions	64
40	S/N Fatigue Curve at Room Temperature for 7049-T73 Aluminum Bar Extrusion	65
41	S/N Fatigue Curve at 250°F for 7049-T73 Aluminum Bar Extrusion	66
42	S/N Fatigue Curve at 350°F for 7049-T73 Aluminum Bar Extrusion	67
43	S/N Fatigue Curve at Room Temperature for 7049-T73 Integrally Stiffened Aluminum Extrusion	68
44	S/N Fatigue Curve at 250°F for 7049-T73 Integrally Stiffened Aluminum Extrusion	69

Figure		Page
45	S/N Fatigue Curve at 350°F for 7049-T73 Integrally Stiffened Aluminum Extrusion	70
46	S/N Fatigue Curves for 7049-T73 Aluminum Bar Extrusion	71
47	S/N Fatigue Curves for 7049-T73 Integrally Stiffened Aluminum Extrusion	72
48	S/N Fatigue Curves for Several Tempers of 7049 and 7075 Aluminum Alloys in the Smooth Condition	74
49	Stress Intensity Factor Range Versus Crack Growth Rate for 7049-T73 Bar Extrusion	77
50	S/N Fatigue Curve for Ti-6Al-4V Casting Smooth Specimens Tested at Room Temperature	80
51	Ti-6Al-4V Casting (as cast)	81
52	Ti-6Al-4V Casting (Annealed); Smooth Specimen Tested at Room Temperature	82
53	Air Environment Crack Growth Data for Beta Annealed Mill Annealed Ti-6Al-4V (R = 0.1; Lab Air, Relative Humidity >30%)	86
54	Crack Growth Rate for Ti-6Al-6V-2Sn (MCAIR)	95
55	Crack Growth Rate Data for Ti-6Al-6V-2Sn (MCAIR)	96
56	Crack Growth Rate Data for Ti-6Al-6V-2Sn (MCAIR)	97
57	Titanium 6Al-6V-2Sn Room Temperature Fatigue Data (NAR Annealed Plate, R = 0.1)	99
58	Larson-Miller Parameter Plot (C = 13.5) for T-222 and T-111 at 0.5% Creep	107
59	Manson-Haferd Parameter Plot (T = 1000 t_a = 7.0 for T-222 and T-111 at 0.5% Creep)	108
60	Dorn Parameter Plot (H = 70,000) for T-222 and T-111 at 0.5% Creep	109

Figure		Page
61	Larson-Miller Parameter Plot (C = 13.5) for T-222, T-111, and Cb-752 at 1.0% Creep	110
62	Manson-Haferd Parameter Plot (T_a = 1000, t_a = 7.0) for T-222, T-111, and Cb-752	111
63	Dorn Parameter Plot (H = 70,000) for T-222, T-111, and Cb-752 at 1.0% Creep	112
64	Larson-Miller Parameter Plot (C = 13.5) for D-43 and Cb-752 at 5.0% Creep	113
65	Manson-Haferd Parameter Plot (T_a = 1000, t_a = 7.0) for D-43 and Cb-752 at 5.0% Creep	114
66	Dorn Parameter Plot (H = 70,000) for D-43 and Cb-752 at 5.0% Creep	115
67	Larson-Miller Parameter Plot (C = 13.5) for T-222, D-43, and Cb-752 at Rupture	116
68	Manson-Haferd Parameter Plot (T_a = 1000, t_a = 7.0) for T-222, and D-43, and Cb-752 at Rupture	117
69	Dorn Parameter Plot (H = 70,000) for T-222, D-43 and Cb-752 at Rupture	118
70	Laminated Aluminum Composite Compact Tension Fracture Toughness Specimen	123
71	Fractured Surface of Aluminum Composite CT Specimen	124
72	Stress-Strain Curves for Titanium/Boron/Epoxy	128
73	Results of Application Life Tests for Class A-2 Materials in Semkit Form	140
74	Results of Application Life Tests for Class B-2 Materials in Semkit Form	141
75	Results of Application Life Tests for Class B-1/2 Materials in Semkit Form	142

Figure		Page
76	Results of Application Life Tests for Class A-2 Materials in Semkit Form	143
77	Results of Application Life Tests for Class B-2 Materials in Can Form	144
78	Results of Application Life Tests for Class B-1/2 Materials in Can Form	145
79	PC-2 Insulation Resistance Sample Before and After Exposure	158
80	FTS-C Test Specimens Indicating Reversion and Collapsing Voids	166
81	L/C-1 Chevron Helicopter Seal and Cut Test Sections	172
82	Endurance -Cycling Test Circuit Schematic (Reference 54)	183
83	Resistance-Heated Hot Press Graphite Die	191
84	Change in Dimensions Resulting from Hot Pressing of 3-D Carbon/Carbon Composite	194
85	Newly Developed Mold for Foam-In-Place Helmet Liners	196

LIST OF TABLES

Table		Page
I	Tensile Properties of D6ac Steel Plates	4
II	Plane Strain Fracture Toughness, K_{IC}, Of D6ac Compact Tension Specimens	8
III	Plane Strain Fracture Toughness, K_{IC}, of D6ac Surface Flaw Specimens	10
IV	CT Specimen Stress Corrosion Cracking Test Results; Medium Toughness D6ac Plate	25
V	Double Cantilever Beam Stress Corrosion Cracking Test Results; Medium Toughness D6ac Plate	27
VI	Bomb Hook Fatigue Data R = 0.1, Room Temperature	31
VII	Chemical Analysis of HP 9-4-25 Steel Alloy (Ref. 9)	35
VIII	Heat Treatment of HP 9-4-25 Motor Case (Ref. 10)	35
IX	Tensile Properties of HP 9-4-25 Steel Alloy Solid Rocket Motor Case	37
X	Fracture Toughness Properties of HP 9-4-25 Steel Alloy Solid Rocket Motor Case	41
XI	Tensile Properties of 7175-T736 Aluminum Alloy Forging	50
XII	Fracture Toughness Properties of 7175-T736 Aluminum Alloy Forging	51
XIII	Typical Room Temperature Fracture Toughness Properties for Several High Strength Aluminum Alloys	52
XIV	Fatigue Limits for 7049-T73 Aluminum Extrusions at 10^7 Cycles	73
XV	Time-To-Failure Stress Corrosion Properties of 7049 Aluminum Extrusions in 3.5% Sodium Chloride Solution	73

Table		Page
XVI	Alternate Immersion Stress Corrosion Results of 7049-T73 Integrally Stiffened Extrusion in a 3.5% Sodium Chloride Solution	75
XVII	Tensile Properties of Cast Ti-6Al-4V	79
XVIII	Fatigue Properties of Cast Ti-6Al-4V at Room Temperature, R = 0.1, K_t = 1.0	79
XIX	Tensile Properties of Ti-6Al-4V Beta Annealed-Mill Annealed Plate	84
XX	Plane Strain Fracture Toughness of Ti-6Al-4V Beta Annealed-Mill Annealed Plate (All Specimens 0.5 Inch Thick)	85
XXI	SCC Properties of Ti-6Al-4V Beta-Annealed-Mill Annealed Plate (3.5% NaCl Solution)	87
XXII	Tensile Properties of NAR Ti-6Al-6V-2Sn	89
XXIII	Tensile Properties of MCAIR Ti-6Al-6V-2Sn	90
XXIV	Fracture Toughness Properties of NAR Ti-6Al-6V-2Sn (Specimen Thickness = 0.5 Inch)	91
XXV	Fracture Toughness Properties of MCAIR Ti-6Al-6V-2Sn	93
XXVI	Crack Growth Rate of MCAIR Ti-6Al-6V-2Sn In Air and Various Environments (R = 0.1)	94
XXVII	K_{ISCC} Test Results for Ti-6Al-6V-2Sn In Distilled H_2O (MCAIR)	98
XXVIII	Room Temperature Fatigue Results From NAR Ti-6Al-6V-2Sn (R = 0.1)	100
XXIX	Creep Data Plotted By Parametric Methods	102
XXX	Tensile Properties of Laminated Aluminum Composite	120
XXXI	Compressive Properties of Laminated Aluminum Composites	121

Table		Page
XXXII	Tensile Properties of Titanium/Boron/ Epoxy Composite	125
XXXIII	Compressive Properties of Titanium/Boron/ Epoxy Composite	127
XXXIV	Results of Storage Life Tests	132
XXXV	Application Time or Work Life for Materials Stored for 9 Months	149
XXXVI	Tack-Free Time and Curing Rate for Materials Stored for 9 Months	149
XXXVII	Hydrolytic Stability Test Results of Six Color Colorations PC-1 Potting Compound	151
XXXVIII	Hardness of PC-1 Potting Compound for Different Mix Ratios	154
XXXIX	Hardness and Insulation Resistance Test Results	157
XL	Hydrolytic Stability of PC-5 Potting Compound	161
XLI	Test Result of Sealant FTS-B	162
XLII	Test Results of FTS-C Fuel Tank Sealant	165
XLIII	Mechanical Property Test Results on MC-A and MC-B	168
XLIV	Hydrolytic Stability Test Results on CM-A Cover Material	171
XLV	Results of L/C-1 Chevron Test Seal Tests	173
XLVI	Results of Lubricant/Seal Compatibility Tests	175
XLVII	Fuel Compatibility Test Results	178
XLVIII	Results of Elastomer/Decontaminant Compatibility Tests	180
XLIX	Results of Baseline O-Ring Cycling Tests	185
L	Results of Hot-Pressing 3-D Carbon/Carbon Composites	192

SECTION I

MECHANICAL PROPERTIES OF METAL ALLOYS

1.1 INTRODUCTION

Over the past year and a half the University of Dayton Research Institute (UDRI) has participated in a large number of engineering mechanical property development programs in conjunction with the Air Force Materials Laboratory (AFML). Generally these programs are required to provide an assessment of the suitability of materials proposed for use in an Air Force system or to provide a basis for recommending a material for use in an Air Force system.

The studies have included the determination of tensile, fatigue, fracture, and creep properties and have ranged from simple data generation programs to the development of testing systems, techniques and criteria. Although the materials involved are generally of interest to the aerospace community, particular emphasis was placed on materials specifically for use in present or future Air Force systems.

1.2 EVALUATION OF MATERIALS FOR SPECIFIC SYSTEMS

Air Force systems do experience occasional failures due to poorly manufactured or inadequately designed components. Although these deficiencies often entail only minor parts, they are in other instances associated with the critical or major components of the system and may result in catastrophic failures.

To evaluate or define the problem associated with any failed component, it is usually a requirement that mechanical property data be developed under conditions which are similar to those encountered by the component in the actual system. These data may be used to define a shortcoming in the material itself or they may be used to infer the life expectancy of systems which remain operational.

The following is a synopsis of the results of two of the more critical data programs performed to assess the suitability of the materials used in operational systems.

1.2.1 Crack Growth Properties of D6ac Steel

A program was performed to evaluate the crack growth properties of D6ac steel. The results of the program were used as input to a large effort involving a number of different laboratories. All of the material involved was obtained from General Dynamics, Fort Worth (GD).

The majority of the D6ac was received and tested with a shot peened and cadmium plated and painted surface. The material involved was designated as being high, medium, or low toughness. These toughness levels were controlled by adjusting the cooling rate during heat treatment. This cooling rate was controlled largely by the initial plate thickness, the thicker plate giving the slower cooling rate and hence lower toughness. Ultimate and yield strength values were not affected by the above variations in processing. The categories of toughness were defined by GD as follows.

Low toughness, $K_{IC} = 35\text{-}50\ KSI\sqrt{IN}$

Medium toughness, $K_{IC} = 51\text{-}70\ KSI\sqrt{IN}$

High toughness, $K_{IC} = 80\text{-}100\ KSI\sqrt{IN}$

Tensile specimens were taken from each plate and tested to guarantee that the proper strength levels were obtained. Unless

otherwise identified, the specimens in the basic program were taken from the plate material with their load axes in the longitudinal direction; cracks were oriented in the transverse direction.

The compact tension (CT) specimens utilized in the K_{IC} tests were machined according to ASTM Standard E339-70T, except that the thickness was left as received (0.690-inch) and the plan for of a 3/4-inch CT specimen was used. The CT specimens used in the stress corrosion cracking (SCC) tests and the cyclic crack growth tests were identical with the exception that a hole was drilled and tapped into the forward face of the crack growth specimens. A shelf, which activated a linear variable differential transformer (LVDT), was also attached to the specimen. This apparatus was used during the SCC tests to monitor crack growth by a compliance technique.

The same technique used on the CT specimens to monitor crack opening displacement (COD) was used for the double cantilever beam (DCB) SCC testing. A surface flaw specimen was also used for cyclic crack growth studies and for K_{IC} testing. This specimen was an adapation of a Boeing design. Lips were Eloxed into the flaw to monitor the COD during K_{IC} tests. All sawed surfaces were ground to dimensions. The pin holes and the starter notches were all eloxed into the specimens.

1.2.1.1 Tensile Test Results

The tensile data are given in Table I. There was no noticeable variation in the tensile strength of this material as a function of toughness. There was likewise no observable trend in hardness with changing toughness. All the material tested had a Rockwell hardness on the "C" scale from 42-50 (data not reported). There were some plates that did not fall exactly within the 220-240 KSI ultimate strength range. They were, however, sufficiently close so as not to be rejected from the test program. In only one case was it felt the variation in tensile strength could affect the results. In addition, there was no difference in the tensile strength between plate and forged material of the same toughness tested at the same temperature. The tensile strength increased slightly as a result of reducing the test temperature from room temperature to -40°F (see Figure 1).

1.2.1.2 Fracture Toughness Results

The fracture toughness (K_{IC}) test results for CT and surface flaw (SF) specimens are presented in Tables II and III, respectively. In the medium and low toughness range, the forging material has slightly higher toughness than the plate material (Figure 2). Some of the data presented in this plot have been reported in Reference 1.

Text continued on page 12

TABLE I

TENSILE PROPERTIES OF D6ac STEEL PLATES

Spec. No.	Heat Treat Toughness	Form	Temp. (°F)	UTS (ksi)	0.2%, Y.S. (ksi)	Elong. (%)	R.A. (%)
PHT-1	High	Plate	RT	231.8	210.0	13.0	51.4
PHT-2				231.7	211.3	12.1	51.3
FHT-5		Forging	RT	230.1	206.2	13.7	49.0
FHT-1				229.8	202.9	14.9	49.1
FHT-2				230.5	206.3	14.7	50.5
FHT-3				230.0	203.2	13.8	49.5
FHT-4				227.7	206.0	14.7	51.0
PMT-1	Med	Plate	RT	240.0	218.9	9.9	42.1
PMT-2				237.5	219.9	12.0	46.9
PMT-3				237.5	218.9	11.8	46.9
PMT-4				237.9	223.3	11.9	49.1
PLT-1				242.1	221.7		
PLT-2				234.2	213.9		
PMT-9				244.2	223.2	9.0	36.0
PMT-11				232.3	222.2	10.3	38.9
PMT-13				242.3	221.7	10.3	38.4
PMT-19				240.2	226.7		48.0
PMT-20				240.2	232.0	14.5	49.0
PMT-21				242.4	229.1	14.5	48.0
PMT-22				242.4	228.3	14.2	48.0
PMT-23				240.2	227.4		
PMT-24				240.3	226.0		
PMT-25				239.4	218.2		
PMT-26				234.3	208.1		

TABLE I (continued)

TENSILE PROPERTIES OF D6ac STEEL PLATES

Spec. No.	Heat Treat Toughness	Form	Temp. (°F)	UTS (ksi)	0.2%, Y.S. (ksi)	Elong. (%)	R.A. (%)
PMT-27	Med	Plate	RT	231.0	203.8		49.5
PMT-28				238.3	213.3		48.7
PMT-29				242.2	227.7		49.1
PMT-7	Med	Plate	-40	244.4	227.1		
PMT-8				252.7	236.1		
PLT-3				244.4	230.8		
PLT-4				243.3	225.9		
PMT-10				248.5	228.9	10.0	37.0
PMT-12				249.5	230.1	9.7	35.6
PMT-14				250.5	229.1	9.4	36.0
FMT-1		Forging	RT	238.0	221.3	11.0	42.6
FMT-2				237.0	219.2	11.1	41.2
FMT-6				238.1	221.5		
FMT-9				238.3	220.8		
FMT-10				238.3	223.6		
FMT-5		Forging	-40	246.3	225.9		
FMT-7				254.7	237.9		
FMT-8				244.4	226.1		
FMT-3				247.4	228.6	11.0	37.0
FMT-4				244.3	227.6	11.0	44.0

TABLE I (concluded)

TENSILE PROPERTIES OF D6ac STEEL PLATES

Spec. No.	Heat Treat Toughness	Form	Temp. (°F)	UTS (ksi)	0.2%, Y.S. (ksi)	Elong. (%)	R.A. (%)
PLT-8	Low	Plate	RT	236.3	215.4	11.9	39.0
PLT-9				219.5	192.5	15.3	50.0
PLT-10				217.7	188.4	16.2	52.0
PLT-11				217.7	187.9	15.5	51.0
FLT-2	Low	Forging	RT	226.0	207.2	14.0	53.0
FLT-6				231.0	214.6	12.8	42.0

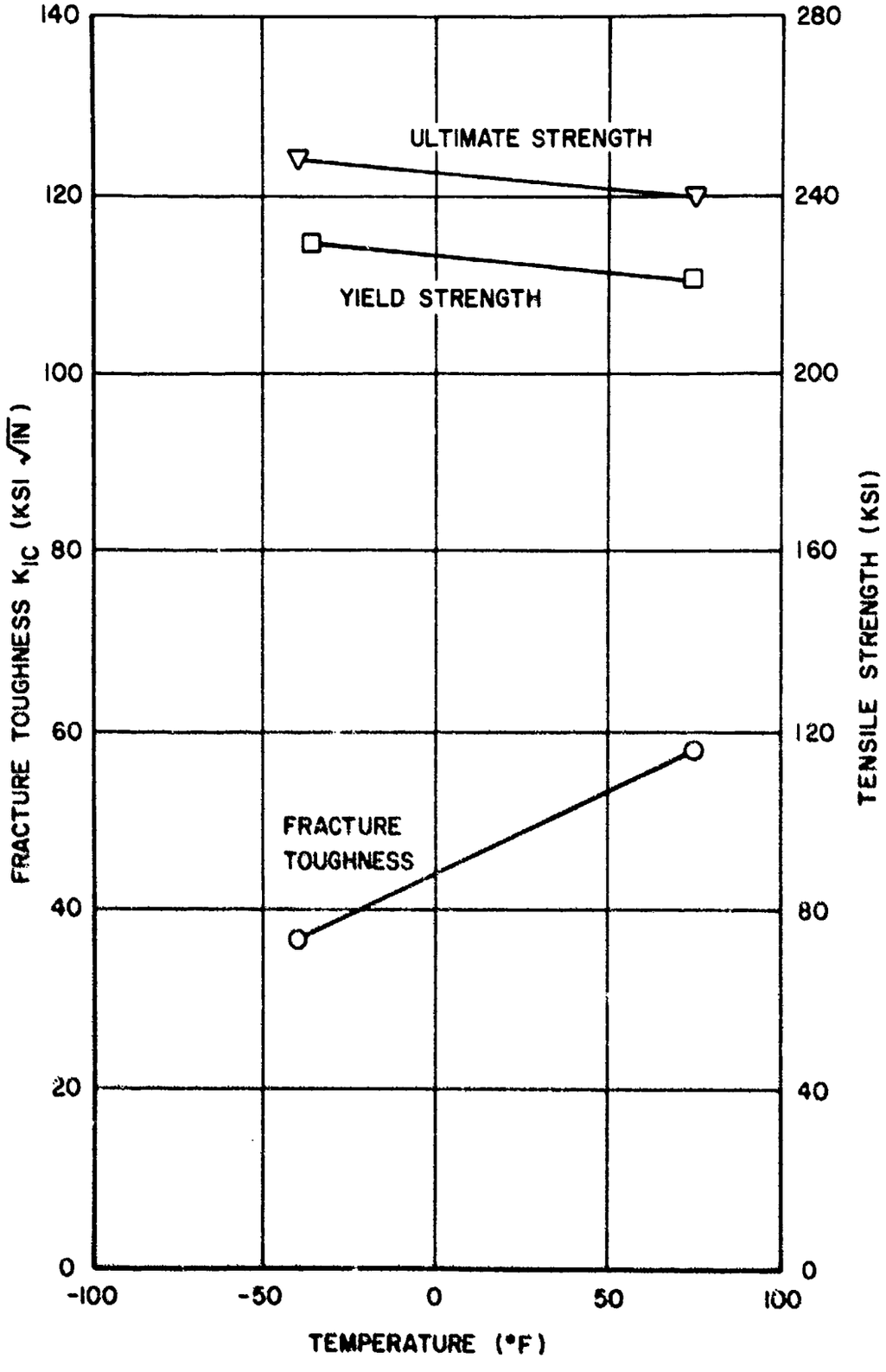

Figure 1. Medium Toughness D6ac Plate Steel Mechanical Properties vs. Temperature.

TABLE II

PLANE STRAIN FRACTURE TOUGHNESS, K_{IC}, OF D6ac COMPACT TENSION SPECIMENS

Spec. No.	Heat Treat Toughness	Form	Test Temp. (°F)	K_{IC} (KSI$\sqrt{IN}$)
PHC-1	High	Plate	RT	96.2
PHC-2				94.0
FHC-1		Forging	RT	93.7
FHC-2				96.3
PMC-12	Med	Plate	RT	55.8
PMC-13				53.4
PMC-14				57.3
PMC-15				53.6
PMC-16				54.5
MA-1				81.7
MA-2				82.9
PMC-18				61.8
PMC-19				55.2
PMC-20				53.9
PMC-21				57.1
PMC-22				56.0
PMC-24				55.3
PMC-25				59.1
PMC-26				59.9
PMC-27				60.2
PMC-28				57.7
PMC-29				60.9
PMC-30				59.4
PMC-31				63.0
PMC-32				61.7
PMC-10			-40	37.4
PMC-11				37.0
MA-3				36.4
MA-4				31.5
FMC-1	Med	Forging	RT	60.0
FMC-4				57.5
BO-1				58.5
BO-2				66.7
FMC-2			-40	39.7

TABLE II (Included)

PLANE STRAIN FRACTURE TOUGHNESS, K_{IC}, OF D6ac COMPACT TENSION SPECIMENS

Spec. No.	Heat Treat Toughness	Form	Test Temp. (°F)	K_{IC} (KSI$\sqrt{IN}$)
FMC-3	Med	Forging	-40	41.6
PLC-1	Low	Plate	RT	44.5
PLC-2				43.9
FLC-1		Forging	RT	54.1
FLC-2				47.4

TABLE III

PLANE STRAIN FRACTURE TOUGHNESS, K_{IC},
OF D6ac SURFACE FLAW SPECIMENS

Spec. No.	Heat Treat Toughness	Form	Test Temp. (°F)	K_{IC} (KSI$\sqrt{IN}$)	a (in.)	2c (in.)
PHS-1	High	Plate	RT	108.9	0.1684	0.415
FHS-2		Forging	RT	106.8	0.1178	0.3577
PMS-1*	Med	Plate	RT	120.0	0.300	0.820
PMS-2				110.0	0.1158	0.3726
PLS-1				92.3	0.1328	0.3702
PLS-2			-40	55.1	0.0995	0.3555
PMS-4				42.9	0.1904	0.4534
FMS-1		Forging	RT	83.0	0.1495	0.3795
FMS-3				115.0	0.1126	0.3787
FMS-2			-40	44.9	0.1744	0.4027
PLS-4	Low	Plate	RT	76.3	0.1362	0.375
FLS-1	Low	Forging	RT	94.4	0.1189	0.3574

*Specimen Through Cracked

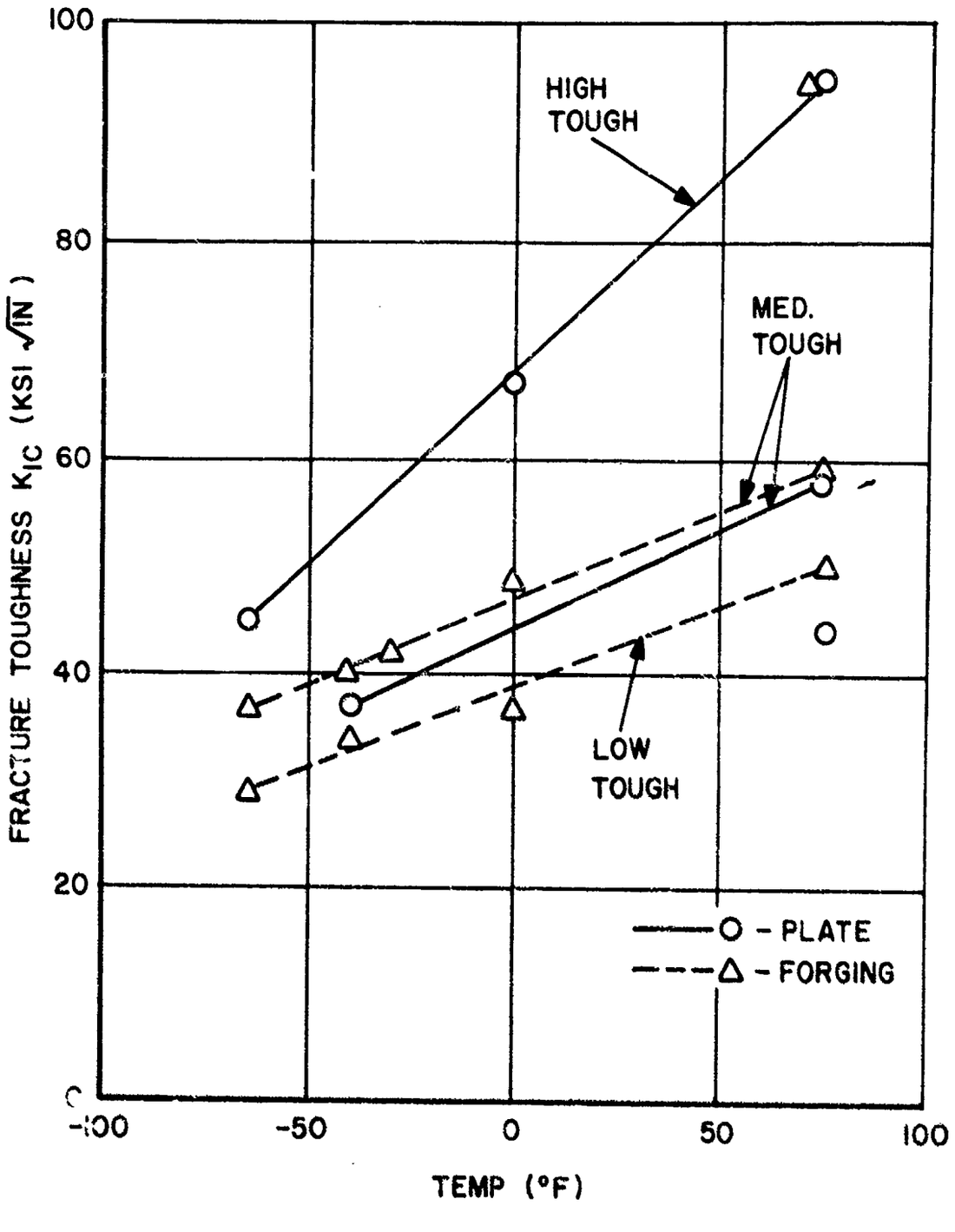

Figure 2. Effect of Temperature on Fracture Toughness of D6ac Steel.

No distinction can be made between plate and forging at the high toughness level.

The toughness of D6ac decreases with decreasing temperature (Figure 2). The high toughness material was more temperature-sensitive than the medium or low toughness material, and the toughness of all the materials appears to converge at some temperature far below those involved in these tests.

The level of toughness is controlled by the material's cooling rate during heat treatment. The areas which receive the more rapid quench attain the greater toughness. Therefore, the toughness of any one area in a piece is dependent on location in the piece and the section size. Because of this variation within the plate, a statistical value for the fracture toughness of the plate could not legitimately be established within the scope of this test program.

For the toughness levels and temperature range investigated, there appeared to be a definite difference in the test results obtained by the use of the CT and SF specimens. The SF specimen consistently yielded a higher value of fracture toughness (Figure 3). However, as was previously discussed, the fracture toughness can vary (by as much as a factor of two) in plates undergoing apparently identical heat treatments. To substantiate the observed discrepancy, CT specimens were machined from two SF specimens tested at room temperature (RT). In this way the fracture faces of the two specimen configurations were approximately three-quarters of an inch apart. It can be assumed that over this brief span the toughness could not vary radically, provided no great section size variation existed. This procedure was repeated on a SF specimen tested at -40°F. At -40°F one would expect the best correlation between the CT and SF specimen because of the low toughness.

The results of these supplementary tests (Figure 4) substantiate the initially observed effect. The SF specimen produced a higher K_{IC} value at RT and -40°F. Note that the difference between the CT and SF specimen configuration is far less at -40° F than at RT. It appears that if the temperature were decreased even further, the fracture toughness of the two specimens would coincide. It was concluded that the SF specimen is not producing a true K_{IC} value as currently defined by ASTM, even though the SF test produces more reliable information for certain specific applications. Obviously additional studies are required in this area.

1.2.1.3 Fatigue Crack Growth Test Results

Figures 5 and 6 show crack growth data from plate material of the three toughness levels tested in the program. All

Text continued on page 17

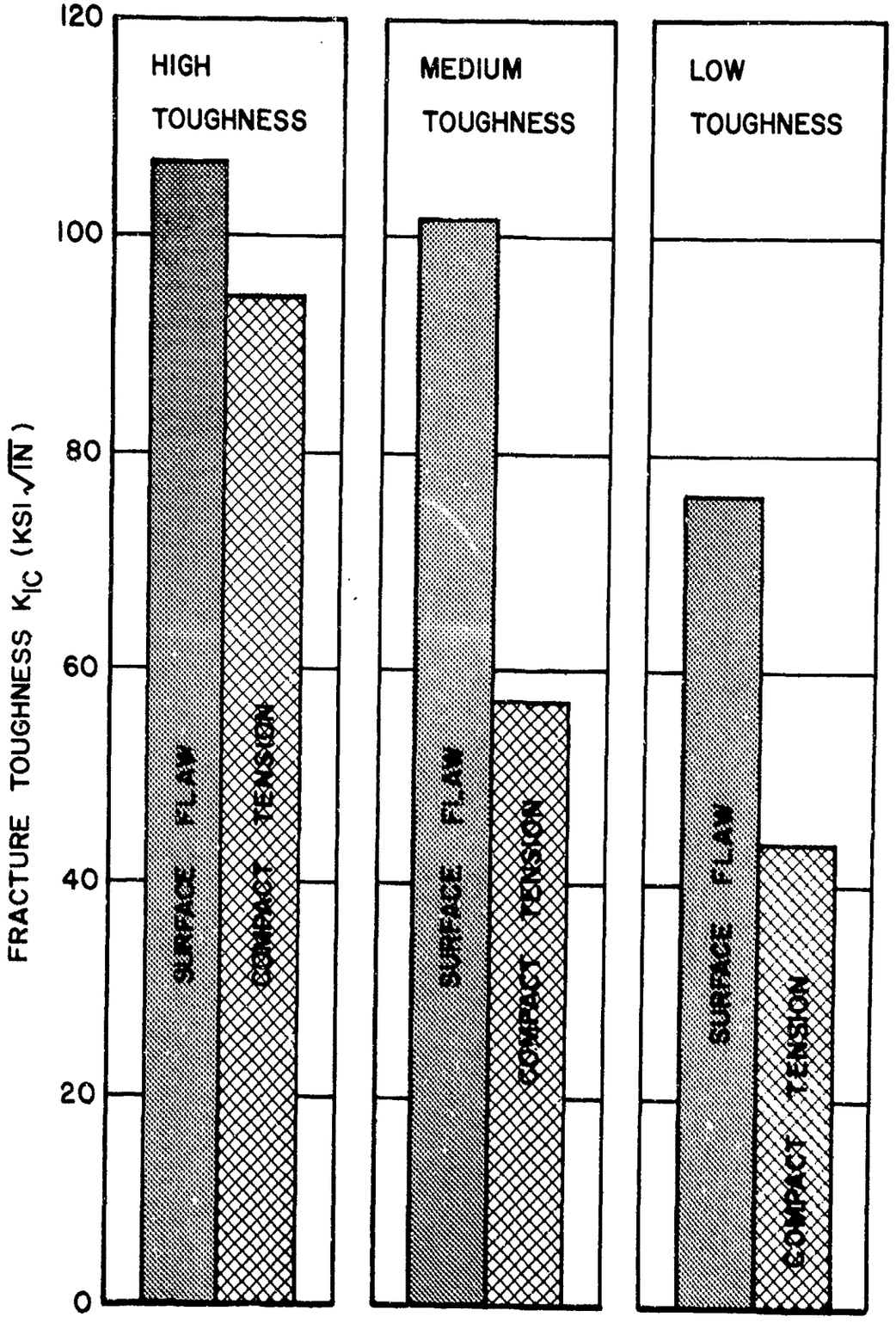

Figure 3. Fracture Toughness of D6ac Plate at Room Temperature in Three Heat Treatment Conditions.

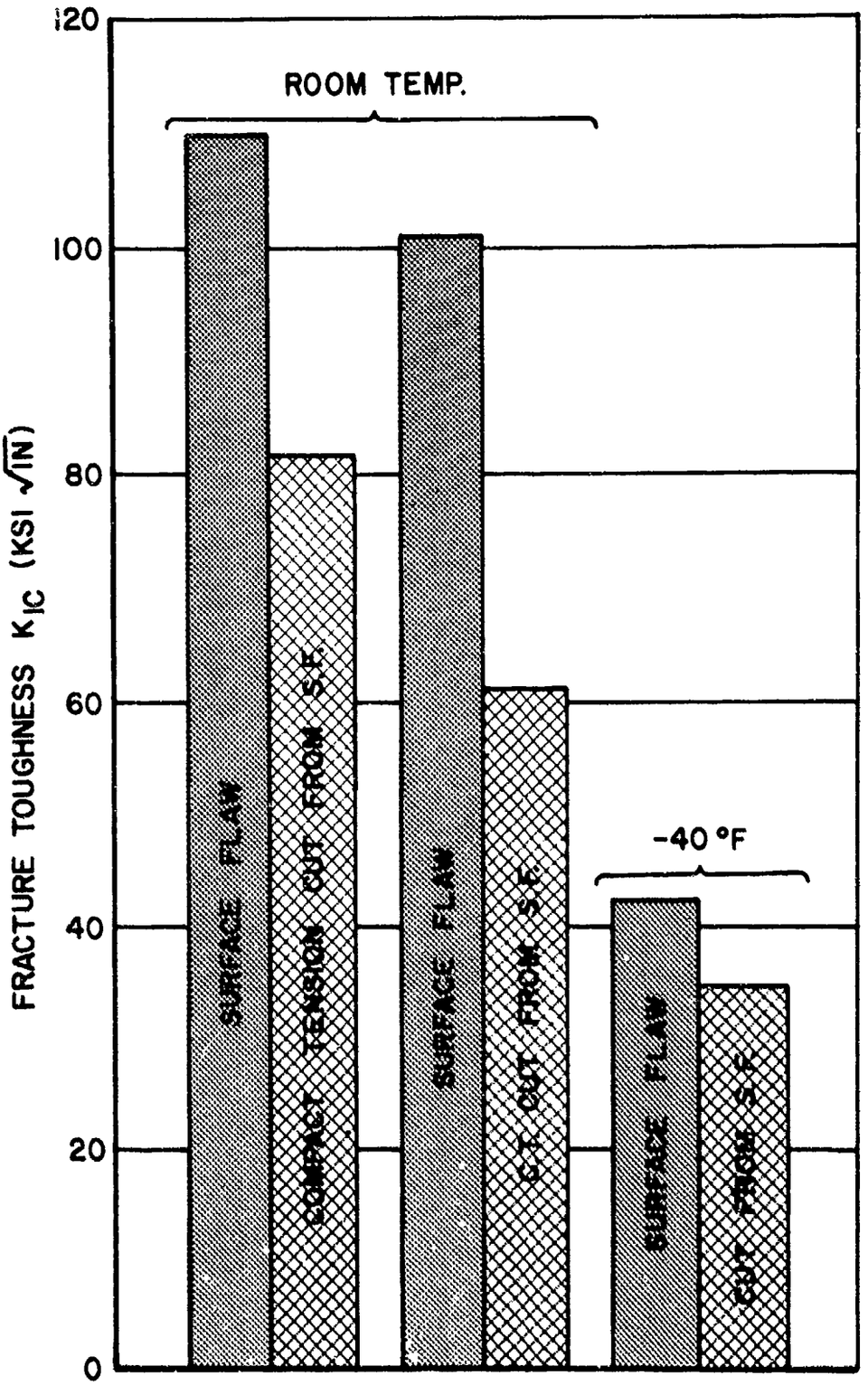

Figure 4. Comparison of Fracture Toughness Values Ootained from SF Specimens and CT Specimens Machined from SF Specimens.

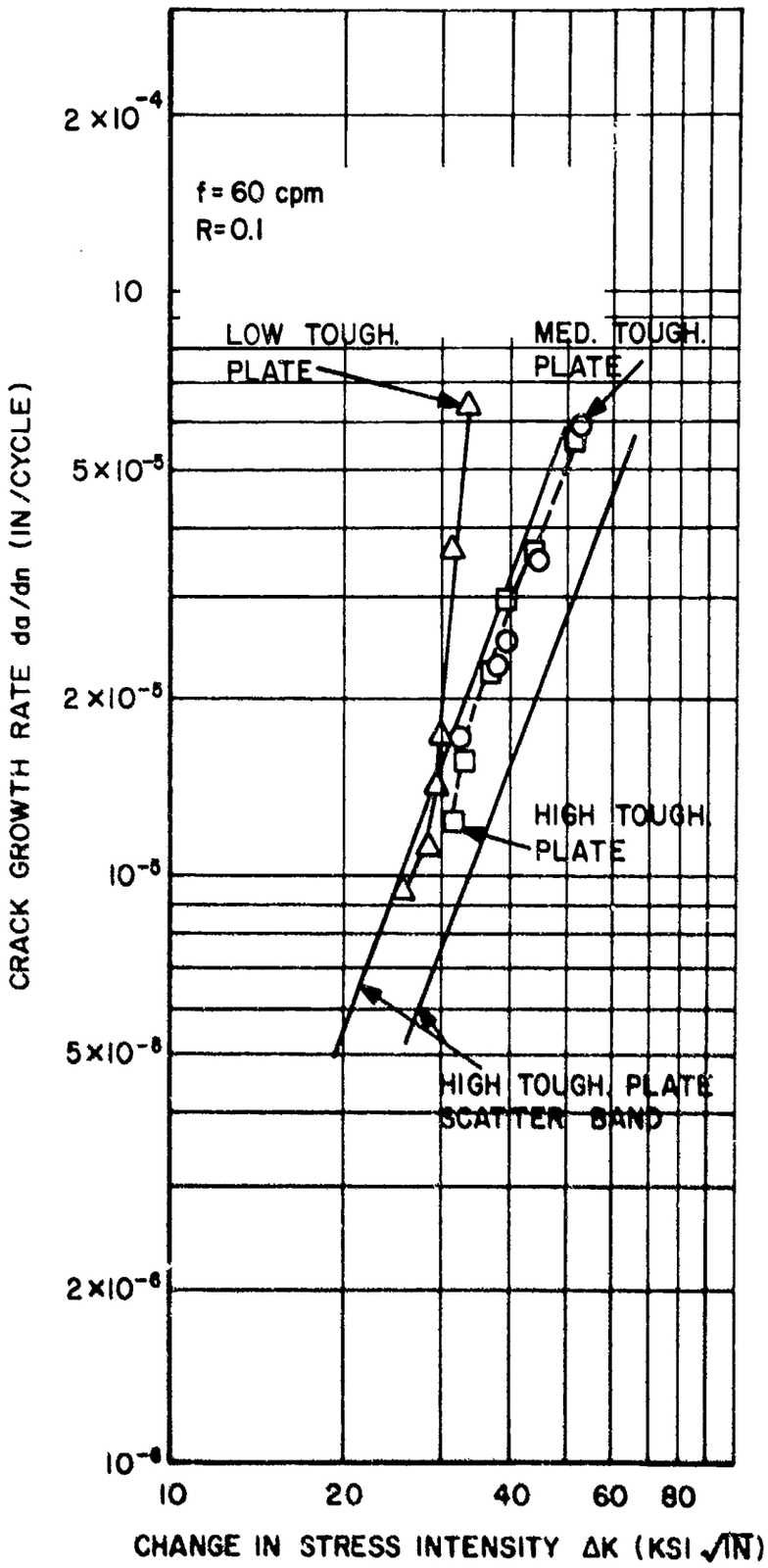

Figure 5. Effect of Toughness on Crack Growth Rate. CT Specimen.

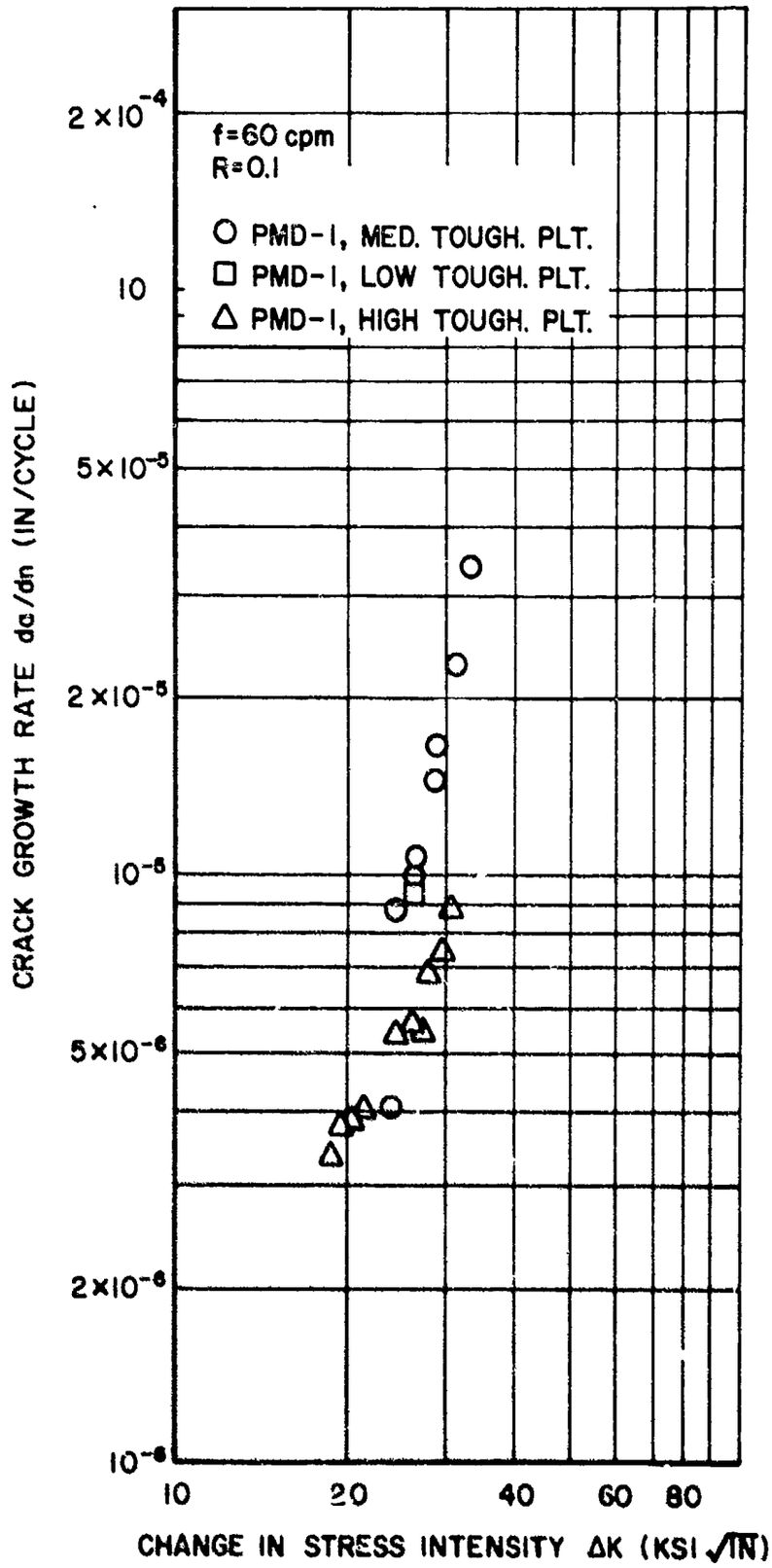

Figure 6. Effect of Toughness on Crack Growth Rate, DCB Specimen.

three CT and DCB crack growth specimens were subjected to the same test conditions of 60 cpm, load ratio of 0. 1, and laboratory air (relative humidity 55%) environment. There was very little difference in the crack growth rate between the medium and high toughness specimens. However, Figure 5 indicates that the low toughness material may have a higher crack growth rate at the higher stress intensities. This apparent variation in crack growth rate with toughness may or may not be consistent due to the possible variation in toughness in a single plate as previously discussed. Alternately the noticable difference in the response of the low toughness plate to an increase in ΔK could be due to the somewhat lower tensile strength of the low toughness plate used in the program (Table I, Specimens PLT-9, PLT-10, PLT-11).

The crack growth rate vs. change in stress intensity and the effect of frequency, load ratio, and specimen type on crack growth rate are shown in Figures 7 through 10. In Figure 9 the test results of a CT and DCB specimen tested at 60 cpm and a load ratio of 0. 1 are plotted together. Any difference between the two is small and within the narrow scatter band that could exist in a single plate. Again, such observations are based on very few specimens.

The SF specimen data were not compared directly to the other specimen results because of the difference in the shape of the crack front and the orientation of the crack front to material grain direction. However, the relative effects of stress ratio and frequency appear to be confirmed by the SF data. The SF specimen dynamic crack growth test results are reported in Figure 10.

The graphs of the data for all specimens indicate that the higher load ratio resulted in a faster crack growth rate at a given stress intensity range. This was expected. No consistent frequency effect was observed in the tests conducted in lab air even though the frequencies differed by a factor of ten. A frequency effect could possible be more apparent at lower ΔK levels than those incorporated into this test program. Figures 10 and 11 show that the water environment has a small effect (increase) on the crack growth rate at the test conditions indicated.

It was of interest to see what influence the crack directionality would have on the crack growth rate. Two specimens with the crack progressing parallel to the grain, WR orientation, were, therefore, tested. No definite effect on the crack growth rate could be ascertained (Figure 12).

Text continues on page 24

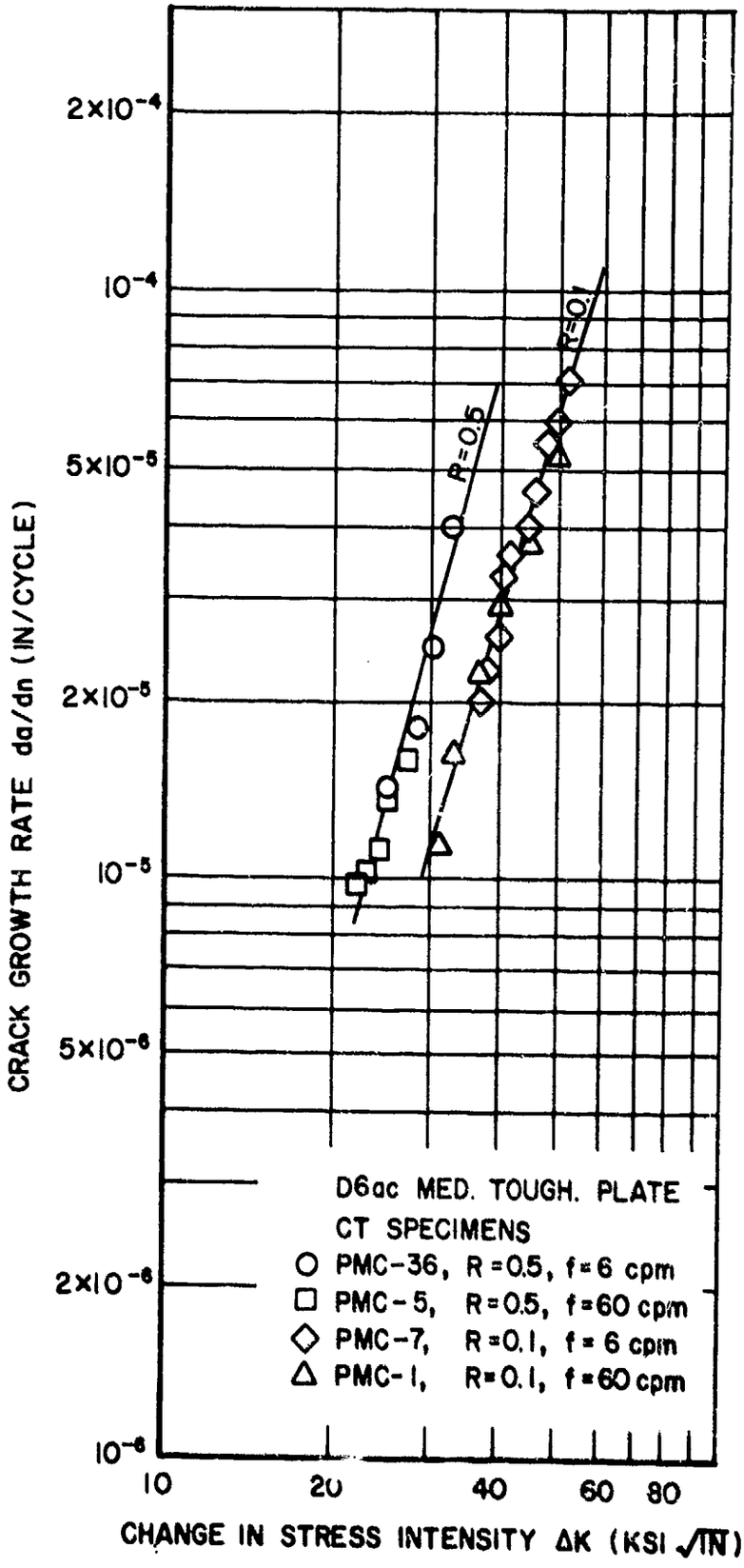

Figure 7. Effect of Loading Ratio and Frequency on Crack Growth Rate.

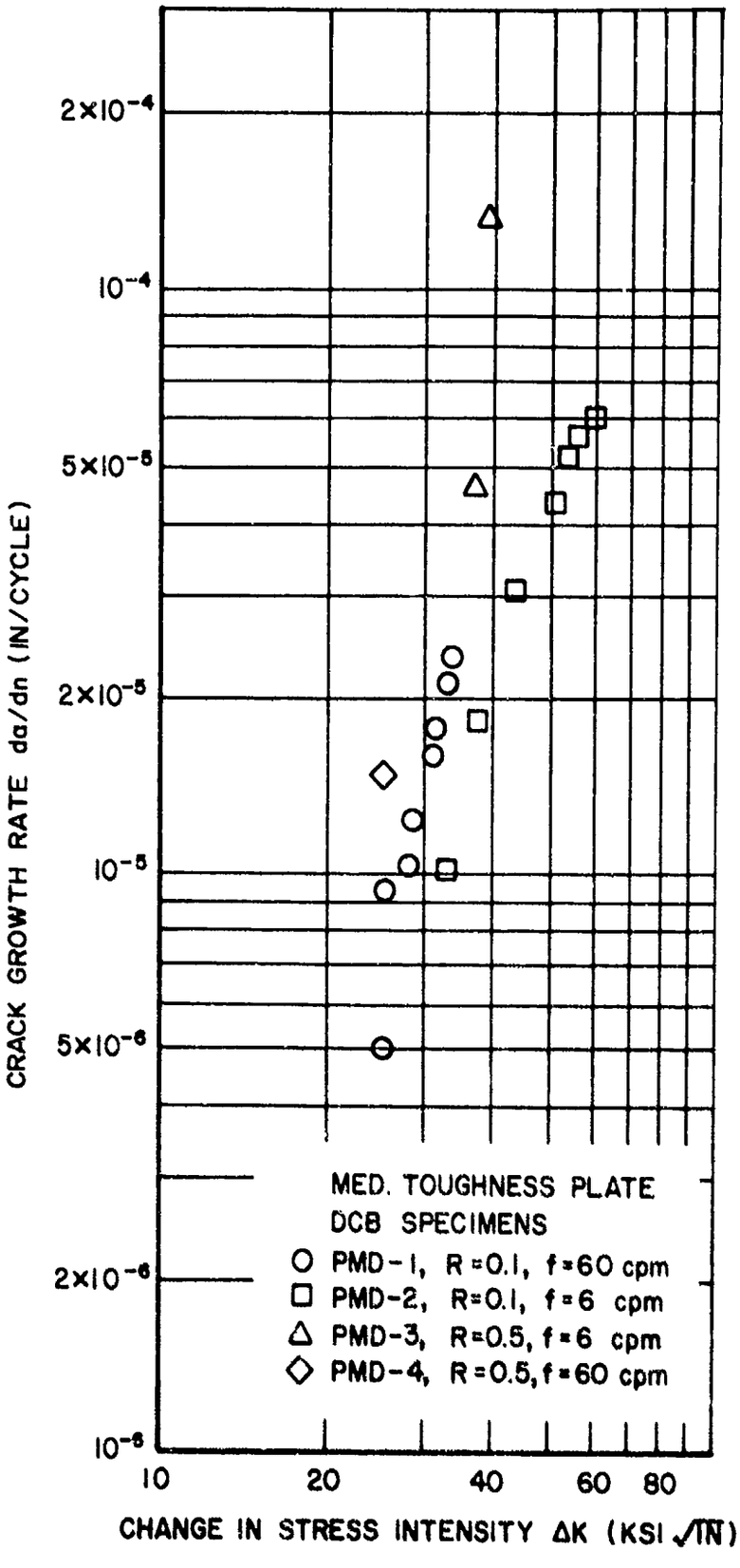

Figure 8. Effect on Loading Ratio and Frequency on Crack Growth Rate.

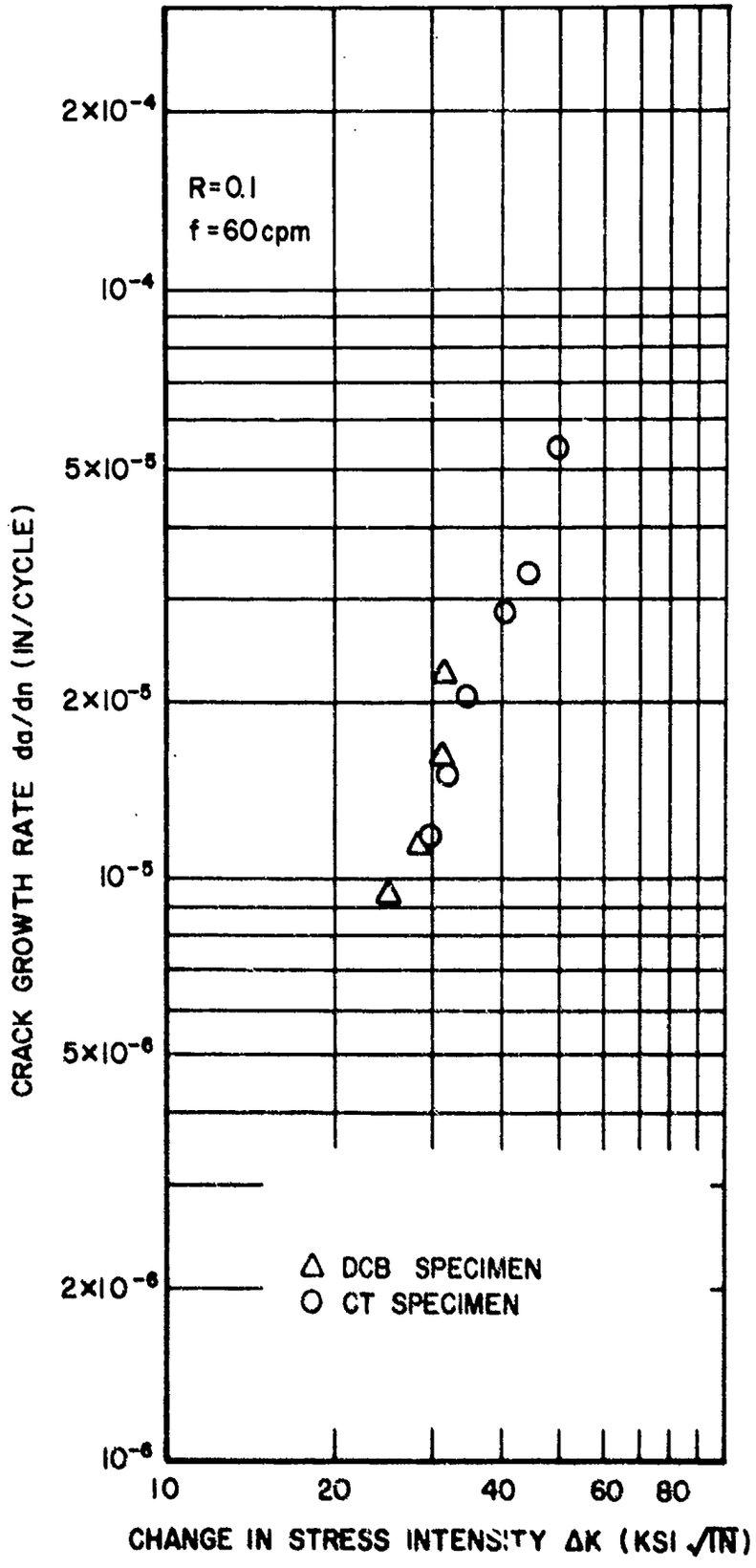

Figure 9. Effect of Specimen Configuration on Crack Growth Rate D6ac Medium Toughness Plate.

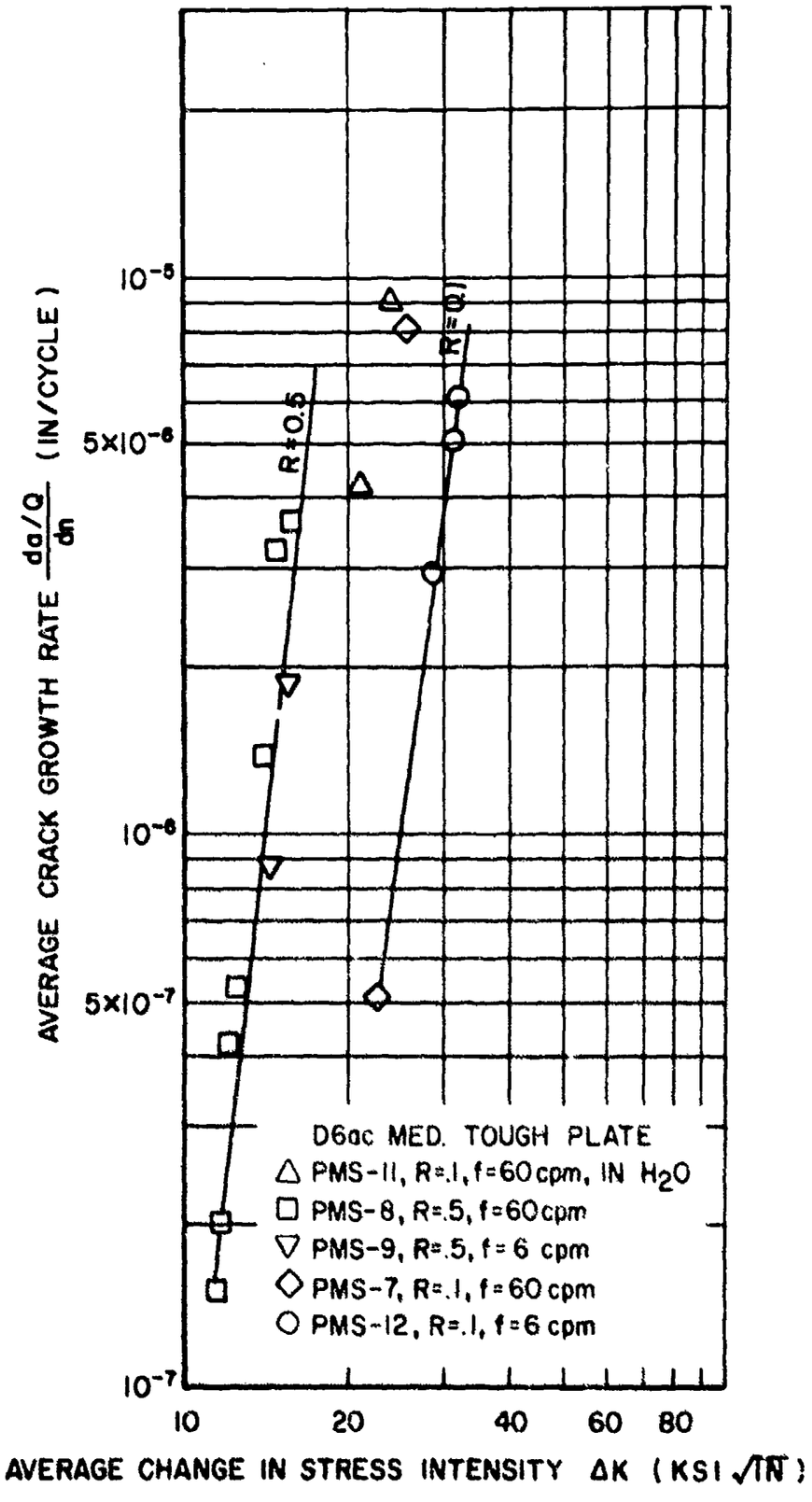

Figure 10. Effect of Loading Ratio and Frequency on Surface Flaw Crack Growth Rate.

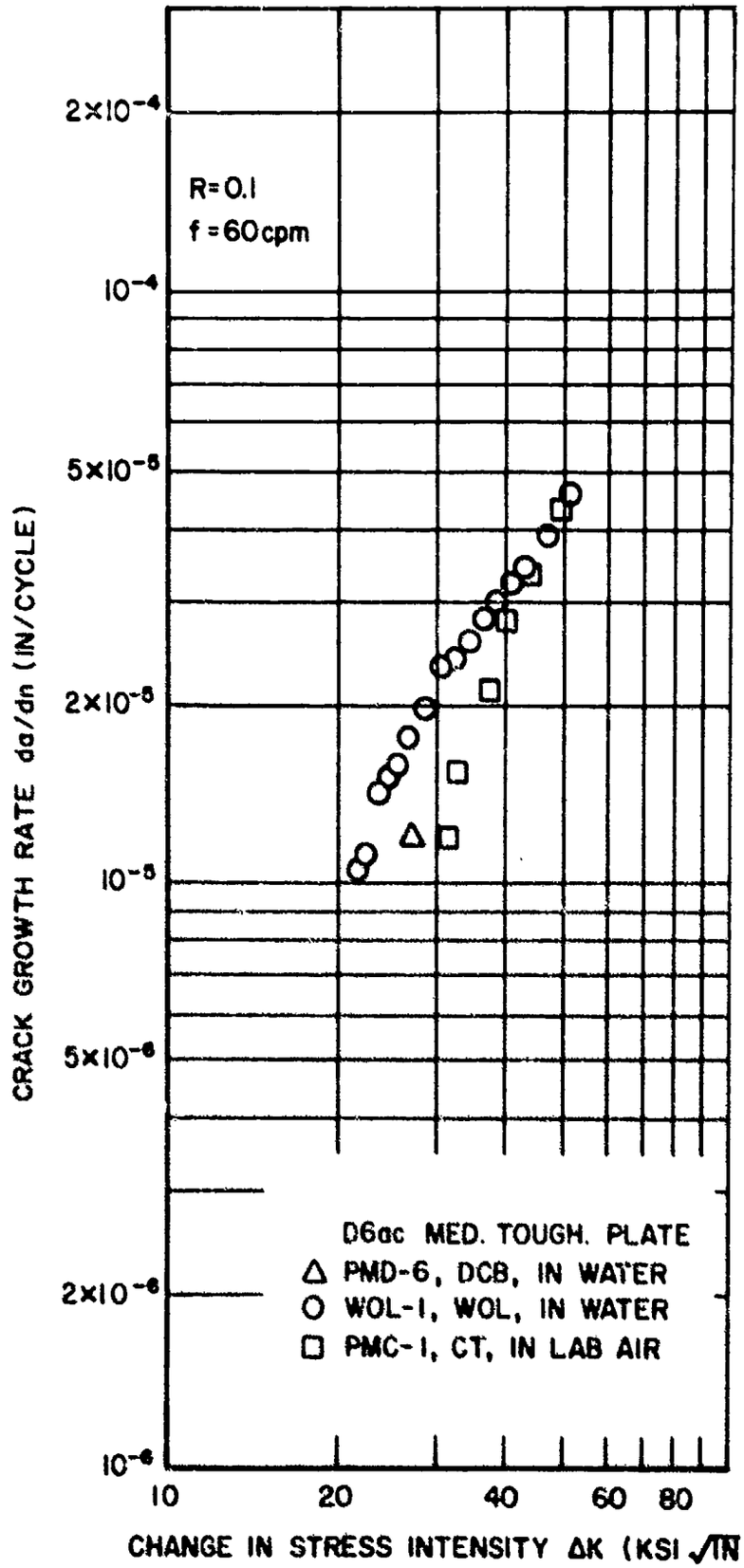

Figure 11. Effect of Distilled Water Environment on Crack Growth Rate.

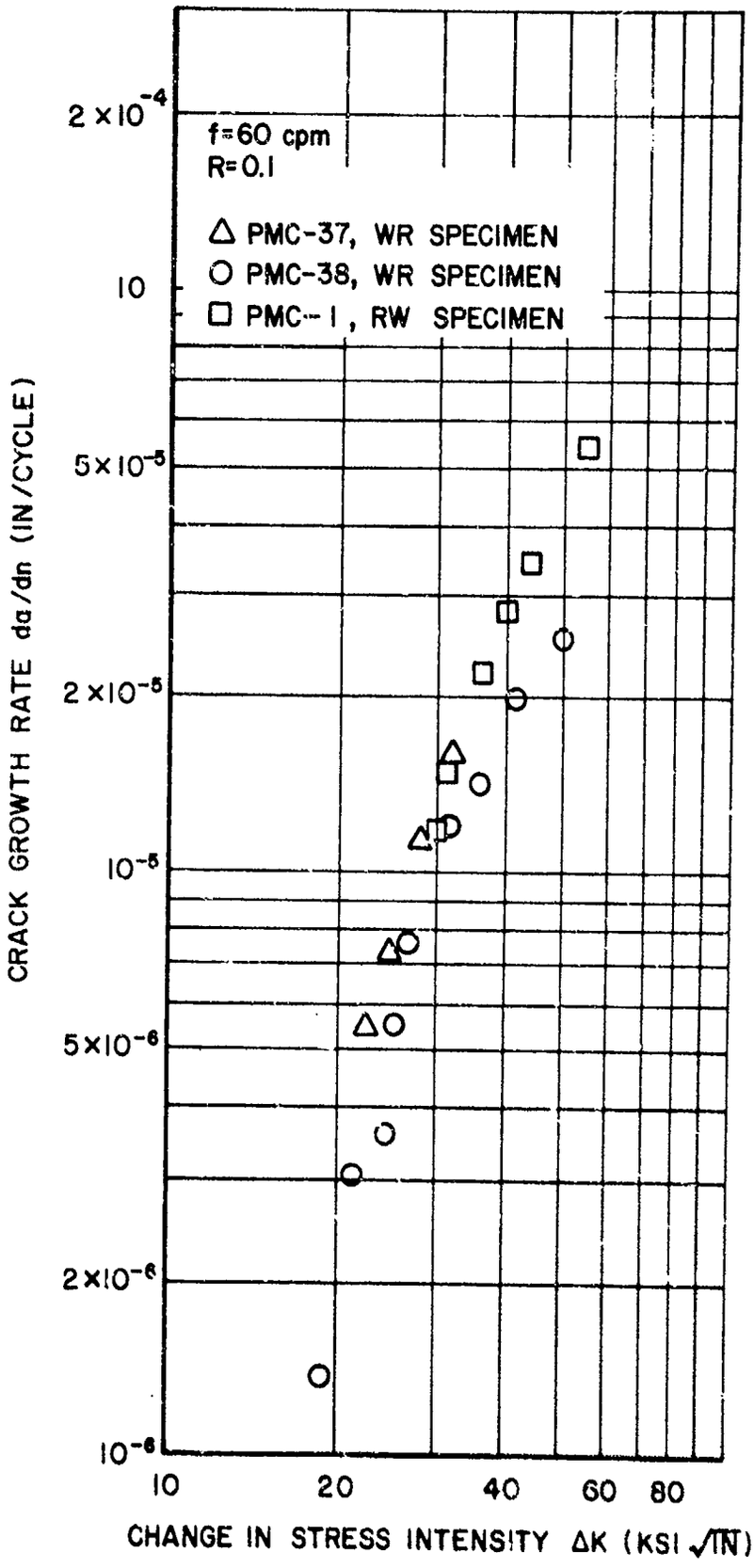

Figure 12. Effect of Grain Direction on Crack Growth Rate, D6ac Medium Toughness Plate.

1.2.1.4 Stress Corrosion Crack Test Results

All of the static crack growth tests were performed in distilled water. The test results for the CT specimens are given in Table IV. These specimens were loaded with a fairly high initial stress intensity ($K_{initial}$) of 30-40 KSI$\sqrt{IN}$ so that the tests would not be of especially long duration.

The CT specimens exhibited a three-part failure pattern. That is, there was an incubation period, a steady crack growth period, and a rapid crack growth period that led to failure over a short period of time. All of the CT specimens had a constant crack growth rate of approximately 2×10^{-3} (in/hr) over the slow crack growth period (Figure 13).

The DCB specimen SCC test results are given in Table V. Similar to the CT specimens, the DCB specimen exhibited an incubation period before a period of steady crack growth.

In Reference 1 it was reported that the crack front led at the free surface and trailed at the center of the specimen. This did not occur in the CT specimens tested in this program. It was assumed that the tests were not of sufficient duration to allow the inversion in the crack front shape to occur. The DCB specimens SCC tests were of considerably longer duration and confirmed the observations of Reference 1. Upon inspection of the fracture faces, it was readily observable that the shape of the crack front went through an inversion and actually led at the free surface when it arrested.

1.2.2 Fatigue of Steel Bomb Hooks

The UDRI evaluated the fatigue properties of a series of new bomb hooks that had evolved from an older configuration. The program was a two-stage progression and involved several physical changes in the hooks. The first change to the hook was a change in the hardness of the 4340 steel from which the original hooks were constructed. A change in the heat treatment increased the R_c hardness from 38 to 49. The second change was the substitution of D6ac steel for the 4340 steel, along with an increase in the dimensions of the hook. The hardness of the D6ac material was R_c 46 to 49.

Both new hook configurations were fatigue tested along with the original hooks. The tests involving all three bomb hook designs (the original, the higher heat treatment 4340, and the D6ac) were performed using actual bomb lugs (Figure 14) as a method of applying the load and also by loading with a special grip designed to simulate the lugs.

Text continued on page 29

TABLE IV

CT SPECIMEN STRESS CORROSION CRACKING TEST RESULTS; MEDIUM TOUGHNESS D6ac PLATE

Specimen	$K_{initial}$ ($KSI\sqrt{IN}$)	Time to Failure (hr.)
PMC-2	39.1	68
PMC-4	36.0	75
PMC-6	27.5	107
PMC-9	34.2	80
PMC-34	41.6	42
PMC-35	40.0	43

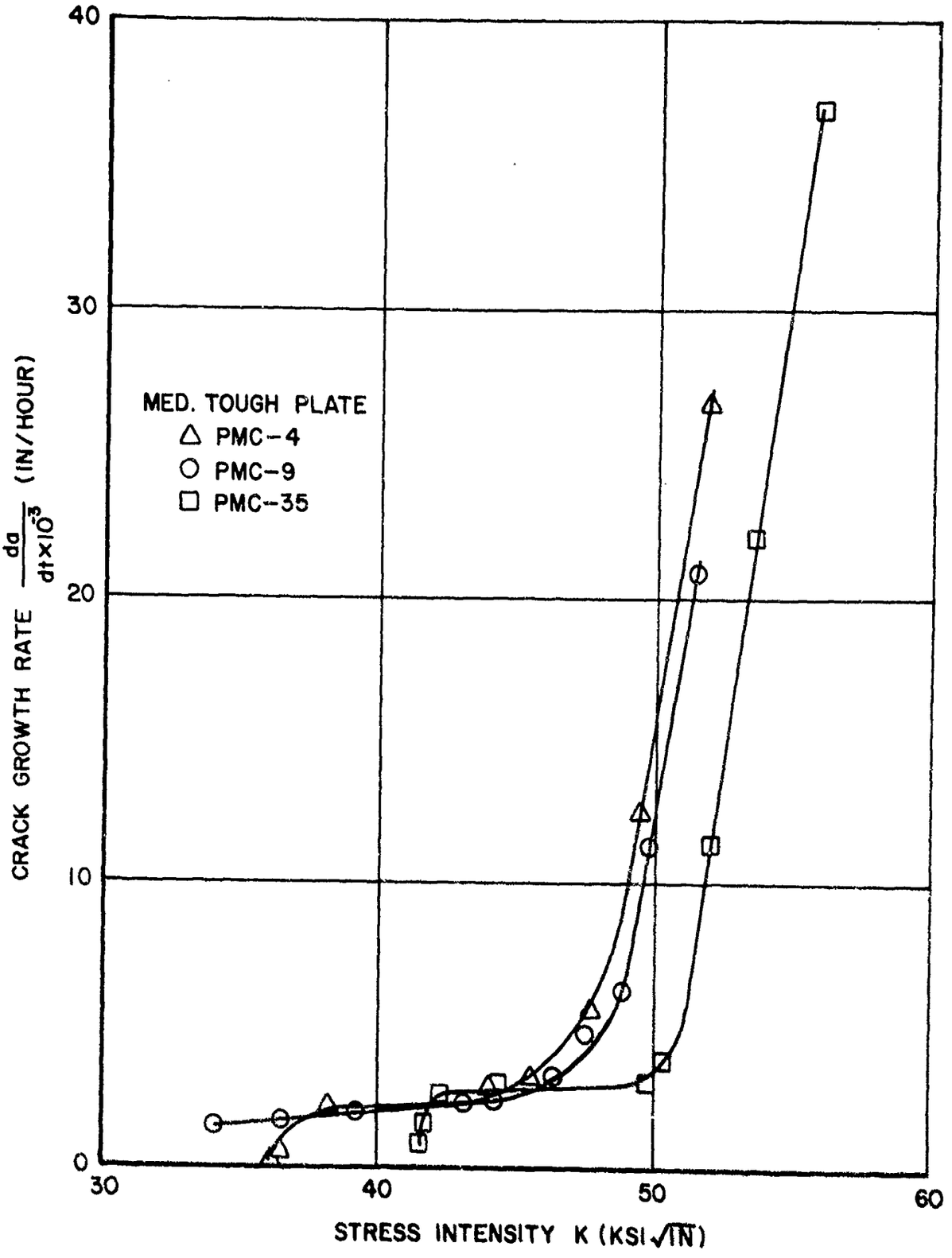

Figure 13. D6ac Static Crack Growth Rate vs. Stress Intensity In a Distilled Water Environment.

TABLE V

DOUBLE CANTILEVER BEAM STRESS CORROSION CRACKING TEST RESULTS; MEDIUM TOUGHNESS D6ac PLATE

Specimen	$K_{initial}$ (KSI$\sqrt{IN}$)	da/dt (in/hr)
PMD-5	31.40	4.1×10^{-5}
PMD-5	31.40	1.25×10^{-5}
PMD-5	34.0	4.57×10^{-5}
PMD-7	40.2	2.15×10^{-5}
PMD-8	36.33	2.27×10^{-5}
PMD-8	39.9	5.1×10^{-5}

Figure 14. Bomb Lug

1.2.2.1 Results and Discussion

Figure 15 presents S/N curves for the same types of materials used to fabricate the bomb hooks. These data are from References 7 and 8. D6ac has a slightly higher endurance limit than either of the two heat treatments of 4340 steels. Both heat treatments of the 4340 steel have about the same fatigue life in high cycle fatigue. However, it is possible that the soft 4340 may be inferior to the hard 4340 since the soft material was tested at a lower K_t.

A summary of the bomb hook test results is presented in Table VI. The data of Table VI are plotted in Figure 16. Both the D6ac and 4340 steel had increased fatigue life when loaded with the test fixture. This was expected because the test fixture was pin loaded, thus, evenly distributing the load across the loading fixture-bomb hook interface.

The D6ac hooks were superior to the 4340 steel in fatigue. This was also expected, based on the reference test data and on the increased size of the D6ac hooks. The softer 4340 steel hooks had better fatigue properties than the harder 4340 steel hooks.

The other area of interest in this program was in the mode of failure in the bomb lugs (Figure 17 and Table VI). Test points were duplicated for the two hook configurations at a maximum load of 14,000 pounds. At first glance it appears as though the D6ac hooks have a detrimental effect on the lugs compared to the 4340 hooks. However, the fatigue life of the D6ac hooks was approximately seven times that of the high strength 4340 steel. The average life of the bomb lugs was about the same (70,000 cycles/lug failure) whether loading the D6ac or 4340 steel hook configuration.

Text continued on page 34

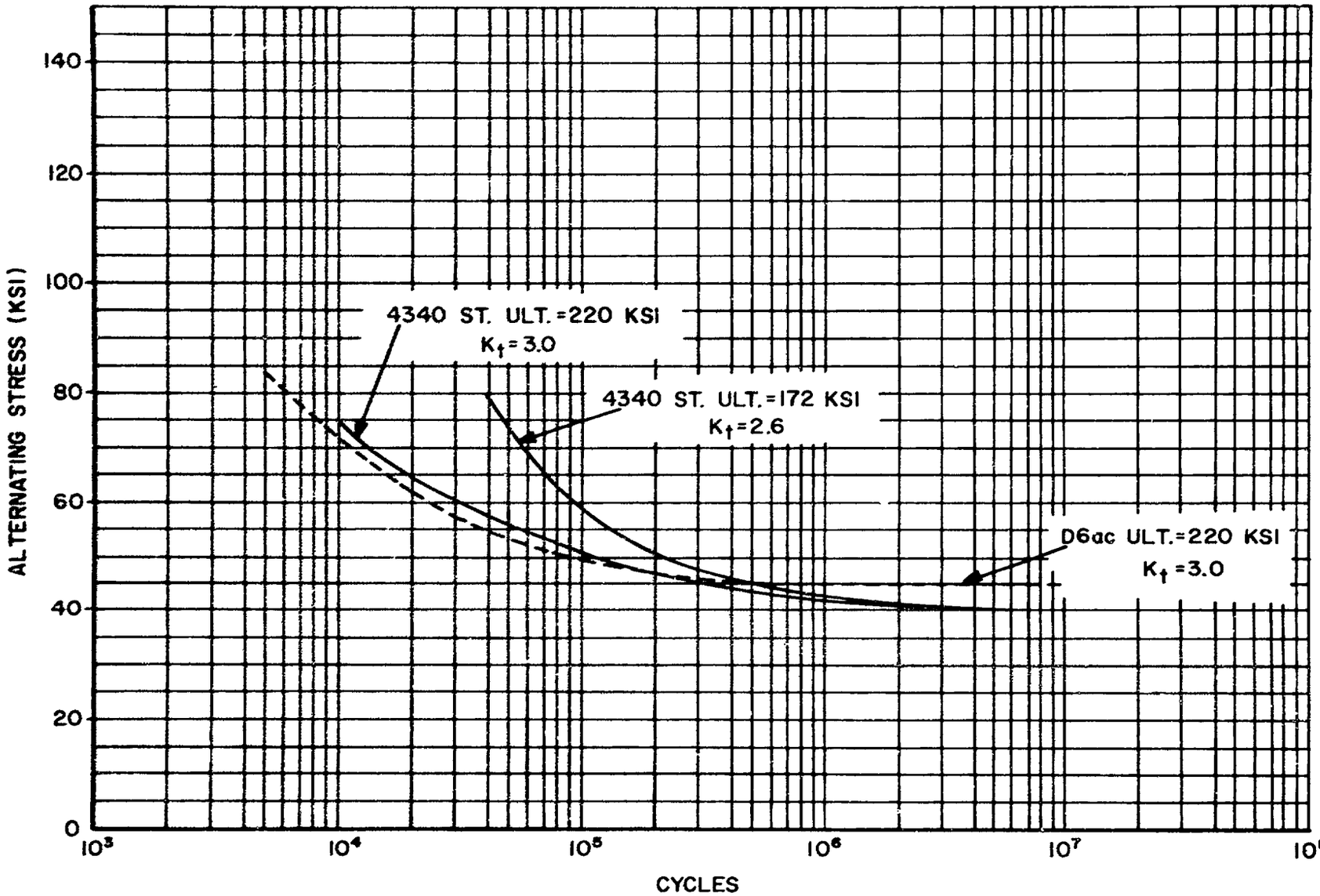

Figure 15. S/N Fatigue Curve for D6ac and 4340 Steel In Two Heat Treatments (Notched Specimens, R = 1.0).

TABLE VI

BOMB HOOK FATIGUE DATA
R = 0.1, Room Temperature

Specimen Number	Matl.	Hardness (R_C)	Max. Load (lbs) / Min. Load (lbs)	Cycles to Failure	Loading Apparatus	Freq. (cpm)	Comment
D6-1	D6ac	47	34000/3400	6,000	Test Fixture	40	Failed across body of hook*
D6-2	D6ac	47	28000/2800	24,215	Test Fixture	60	Failed across body of hook
43-1	4340	38	23000/2300	35,000	Test Fixture	2000	Hook broke off
43-2	4340	38	17000/1700	138,000	Test Fixture	2000	Hook broke off
43-4	4340	46	17000/1700	98,000	Test Fixture	2000	Hook broke off
D6-4	4340	48	17000/1700	38,000	Test Fixture	2000	Hook broke off
D6-5	4340	48	14000/1400	174,000	Test Fixture	2000	Hook broke off
43-6	4340	46	14000/1400	215,000	Test Fixture	2000	Pivots broke off
D6-6	4340	49	12000/1200	144,000	Test Fixture	2000	Failed across body of hook
43-5	4340	46	12000/1200	400,000	Test Fixture	2000	Pivot broke off
D6-7	D6ac	46	17000/1700	63,000	Test Fixture	2000	Pivot broke off
D6-8	D6ac	46	17000/1700	867,000	Test Fixture	2000	Pivot broke off
D6-9	D6ac	46	17000/1700	1,258,000	Test Fixture	2000	Pivot broke off
D6-10	D6ac	46	17000/1700	117,000	Bomb lug	2000	Pivots broke, failed 1 lug
D6-11	D6ac	46	14000/1400	504,000	Bomb lug	2000	Pivots broke, failed 4 lug's
D6-12	D6ac	46	14000/1400	495,000	Bomb lug	2000	Hook broke off, failed 6 lugs
43-7	4340	46	14000/1400	85,000	Bomb lug	2000	Failed across body of hook
43-8	4340	46	14000/1400	69,000	Bomb lug	2000	Failed across body of hook, failed 1 lug
43-9	4340	46	14000/1400	63,000	Bomb lug	2000	Failed across body of hook, failed 1 lug

*See Figure 17

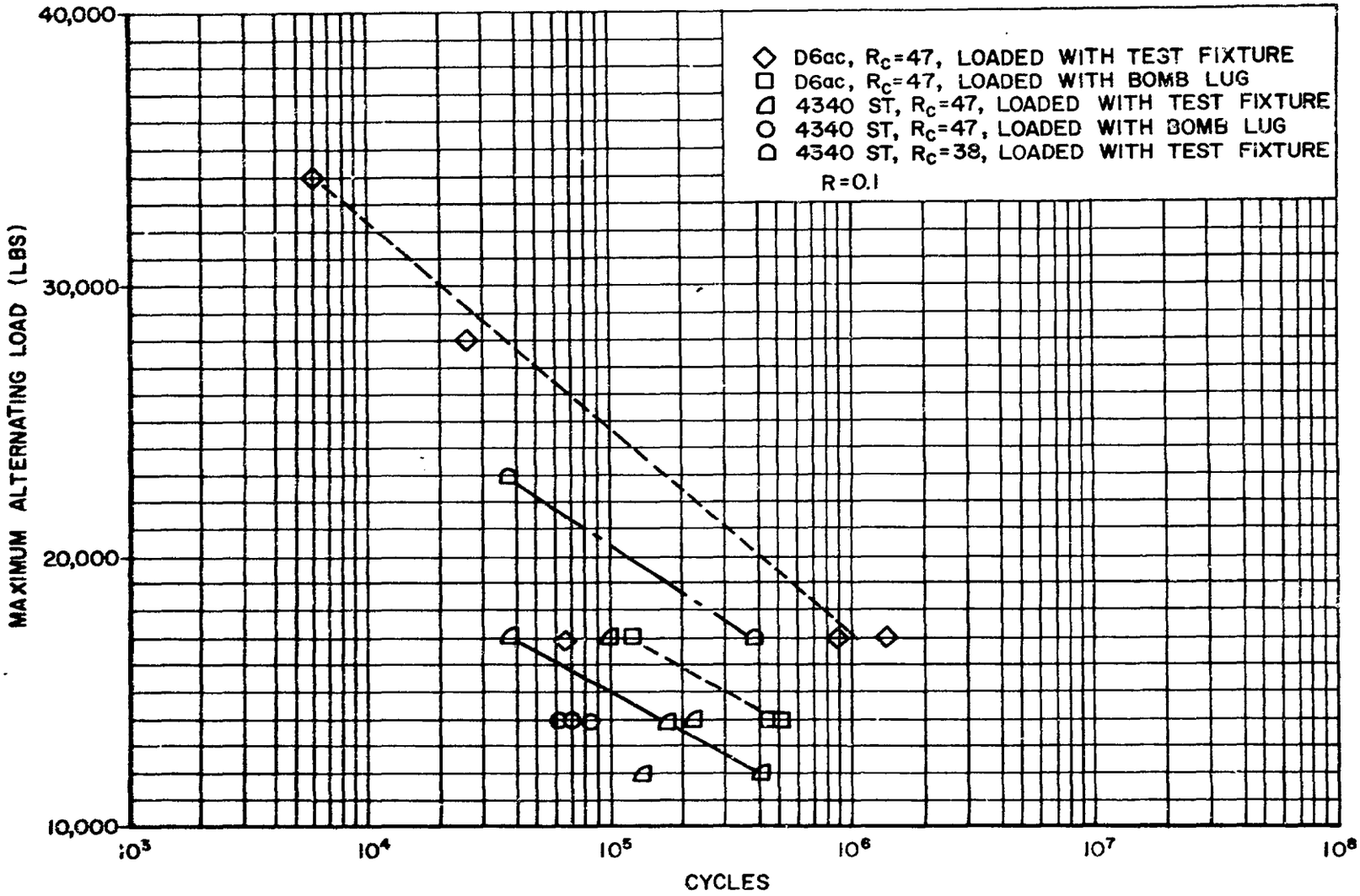

Figure 16. Fatigue Data for D6ac and 4340 Bomb Hooks.

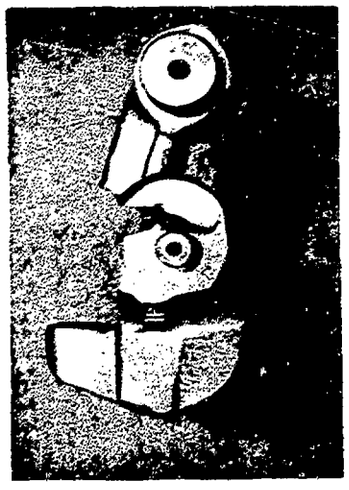

Failed across body of hook

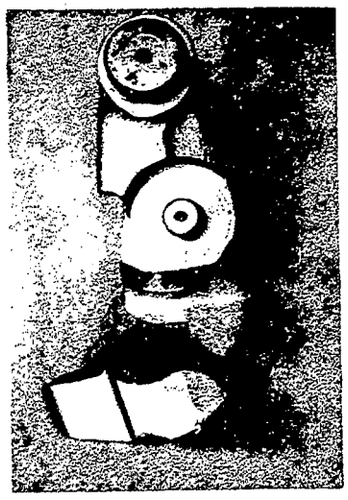

Hook Failed

Pivot Failed

Figure 17. Typical Types of Bomb Hook Failures.

1.3 DATA ON EMERGING MATERIALS AND PROCESSES

The UDRI has over the period of this effort performed a number of investigations of emerging materials and material fabrication techniques. These investigations were intended to qualify the material or process for incorporation in future Air Force procurements whether they be initial system procurements or an Engineering Change Proposal (ECP) to be executed on presently operational systems. A review of some of the more significant programs is presented in the following sections.

1.3.1 Roll-Extruded HP 9Ni-4Co-25C Steel

A cold forming internal roll-extrusion process has been developed to improve the fabrication of large diameter solid rocket motor (SRM) case segments for the Titan III Missile. Many alloys had been fabricated into SRM cases with varying degrees of success. Two of the materials suitable for this fabricating processes, HP 9-4-25 and D6ac steel alloys, were selected for further processing examination. The results of a processing investigation indicated that the HP 9-4-25 alloy had higher potential because of its improved mechanical properties and ease of fabrication.

A section of the as-worked HP 9-4-25 steel was procured for additional mechanical property evaluation by UDRI. It was the intent of this program to evaluate the effect of varying degrees of rolling reduction on the tensile and fracture toughness properties of HP 9-4-25 steel. Crack growth properties were also studied in some detail.

1.3.1.1 Test Materials

A 25 x 31-inch section was removed from a 120-inch diameter HP 9-4-25 test ring (S/N 004). The thinnest section of the ring had been reduced a total of 74% (to a 0.423-inch thick section) in five passes. One part of the ring was of varying thickness, tapering from a 1.637-inch thick section to the highly worked 0.423-inch thick section.

The basic material was produced by Republic Steel with a vacuum arc remelt carbon-deoxidized process to meet the requirements of AM 6541 material specification. The material was obtained from heat No. 391419, and had the chemical composition shown in Table VII. The heat treatment of the forged preformed ring before and during internal roll-extrusion processing is presented in Table VIII. The data in Tables VII and VIII are from Reference 9.

All specimens were removed from the as-received material. In the terminology of this report, the "axial direction" is the

TABLE VII

CHEMICAL ANALYSIS OF HP 9-4-25 STEEL ALLOY (*REF. 9*)

Chemical Composition (weight %)									
C	Mn	P	S	Si	Ni	Cr	Mo	Na	Co
0.28	0.29	0.008	0.009	0.02	8.40	0.44	0.50	0.09	3.95

TABLE VIII

HEAT TREATMENT OF HP 9-4-25 MOTOR CASE (REF. 9)

The heat treatment of rough forged ring (S/N 004) before internal roll-extrusion processing was as follows:

A. Austenitized for 1 hour at 1650°F.

B. Temperature dropped to 1,550 ±25°F for 2 hours.

C. Oil quenched in room temperature oil.

D. Furnace tempered at 1,000 ±25°F for 4 hours.

E. Air-cooled.

After pass No. 3, an intermediate stress-relief cycle was utilized to reduce the internal hardness of the roll-extruded cylinder from R_c of 49 to an R_c of 44. The final configuration of the SRM segment was not heat treated.

long direction of the SRM case with longitudinal grain orientation and the "hoop direction" is the circumferential direction of the SRM case with transverse grain orientation (verified by metallography).

1. 3. 1. 2 Results and Discussion

The tensile properties developed for the HP 9-4-25 steel alloy are presented in Table IX. In both the hoop and axial directions, the decrease in ductility and increase in strength at both room temperature and -65°F can be attributed to the cold working reduction process. At room temperature the ultimate strength was increased 22% in the hoop direction and 30% in the axial direction by the increased cold working required to reduce the section thickness from 1. 5-inches to 0. 4-inch. As can be observed, no highly directional tensile properties were detected.

Representative tensile specimens are shown in Figures 18, 19, and 20. These figures illustrate the laminations observed after testing the axial and hoop specimens removed from the 0. 4-inch-thick heavily worked section. A photomicrograph of these laminations is shown in Figure 21. The distance between laminations in this figure was approximately 0. 0004-inch.

The discontinuous laminar structure observed in fractured specimens is of considerable importance. It may be speculated that fracture toughness and crack growth properties through the radial wall thickness of the SRM cases are improved due to the possibility of crack branching at the laminations. Further intermediate heat treatment during forming would be required to achieve a homogeneous material if desired.

The results of the fracture toughness tests are presented in Table X. It can be seen in this table that only K_Q values were obtained from specimens removed from the 0. 4-inch-thick section of the roll extrusion. This was because of insufficient material thickness. It can also be observed, however, that the toughness values calculated for the 0. 4-inch-thick section (even though invalid) are sufficiently lower than those for the thicker section, indicating that the toughness is lower in the highly-worked thin section than in the thick section.

Both tensile and fracture toughness data were developed by Gott, et. al. (Reference 9) for a plate which was removed from the material used to produce the forged performed test ring. This plate had the same heat treatment as that given the rough forged preformed test ring prior to roll-extrusion processing. The fracture toughness values obtained in Reference 9 from 1. 88-inch-thick unrolled plate compared favorably with data obtained from the 1. 4-inch-thick section

Text continued on page 42

TABLE IX

TENSILE PROPERTIES OF HP 9-4-25 STEEL ALLOY
SOLID ROCKET MOTOR CASE

Temperature (°F)	Direction	Section Thickness (inches)	Ultimate Strength (KSI)	Yield Str. 0.2% Offset (KSI)	Elongation in 1 inch G. L. (%)	Reduction Of Area (%)
Room	Hoop	1.5	170.1	156.8	15.7	50.2
		*	167.7	159.4	17.4	57.8
		*	172.1	168.0	16.7	57.2
		*	173.8	172.8	16.8	56.9
		0.8	186.6	173.4	11.9	50.7
		0.4	208.0	180.3	9.3	40.6
		0.4	210.6	188.1	9.2	42.5
		0.4	207.4	181.7	9.0	38.6
-65	Hoop	1.5	183.3	-----	16.2	48.8
		*	179.0	165.6	17.3	51.0
		*	174.9	164.1	18.2	53.9
		1.2	173.2	165.5	17.6	54.0
		0.4	210.5	178.6	9.1	35.5
		0.4	207.6	184.0	9.1	35.2
		0.4	208.3	178.9	9.8	36.2
Room	Axial	1.4 **	166.7	158.4	16.4	54.9
		1.4 **	166.7	159.6	16.4	53.3
		1.4 **	167.4	158.1	16.6	55.0
		1.4 **	167.7	159.4	17.1	54.7
		1.4 **	167.4	159.1	16.4	55.0
		1.0 **	177.0	177.0	20.0	59.7
		0.4	217.7	211.0	10.1	52.4
		0.4	217.4	209.6	9.7	49.7
		0.4	217.0	207.9	10.3	51.1
-65	Axial	1.4 **	171.5	162.2	16.5	50.2
		1.0 **	187.2	183.2	19.6	57.7
		1.0 **	187.1	181.5	19.8	57.9
		0.4	214.7	210.6	11.0	49.7
		0.4	228.0	219.8	10.4	45.0
		0.4	227.9	223.8	10.4	43.5

* Decreasing section thickness

** Section thickness measured at center of tensile specimen gage length

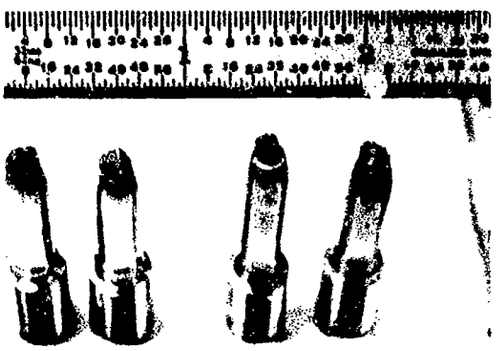

Figure 18. Fractured HP-9-4-25 Tensile Specimens: Axial direction, room temperature test, removed from 1.4-inch thick section Left: Axial direction, room temperature Test, removed from 0.4-inch thick section.

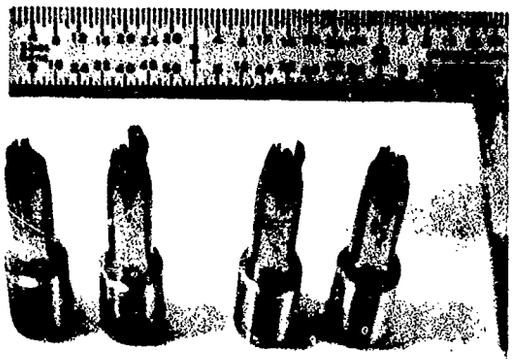

Figure 19. Fractured HP-9-4-25 Tensile Specimens. Right: Hoop direction, room temperature test, removed from 1.4-inch thick section. Left: Hoop direction, room temperature test, removed from 0.4-inch thick section.

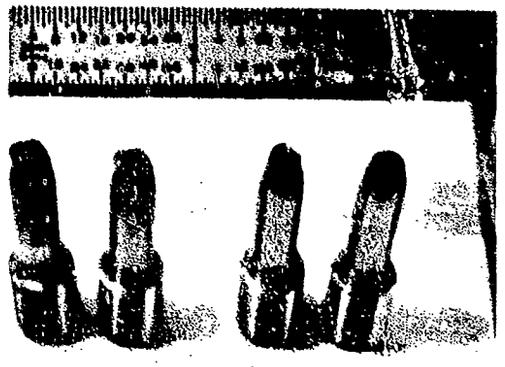

Figure 20. Fractured HP-9-4-25 Tensile Specimens. Right: Axial direction, -65°F test temperature, removed from 0.4-inch thick section. Left: Axial direction, -65°F test temperature removed from 0.4-inch thick section.

Figure 21. Photomicrograph of Laminations in Axial Tensile Specimen (600X).

TABLE X

FRACTURE TOUGHNESS PROPERTIES OF HP 9-4-25 STEEL ALLOY SOLID ROCKET MOTOR CASE

Temperature (°F)	Section Thickness (inches)	Direction	K_{IC} (KSI $\sqrt{IN}$)
Room	1.4 1.0 1.0 * 0.4 0.4	Axial (WR)	113.5 118.5 126.0 (72.8) *** (73.9) ***
-65	1.4 1.4 * 0.4	Axial (WR)	125.6 111.5 (61.2) ***
Room	1.4 1.4 1.4 1.0 ** 0.4 0.4	Hoop (RW)	117.3 113.9 108.7 121.2 (57.0) *** (53.1) ***
-65	1.4 1.0 0.4 ** 0.4	Hoop (RW)	111.7 99.0 (74.4) *** (71.6) ***
Room	1.5 1.5	Short Hoop (RT)	(88.9) *** (85.8) ***
-65	1.5 1.5	Short Hoop (RT)	(87.7) *** (91.3) ***
Room	1.5 1.5 **	Short Axial (RT)	93.9 94.4
-65	1.5 **	Short Axial (WT)	(83.4) ***

* Section thickness measured at plane through which specimen fractured

** Section thickness measured at specimen notch tip

*** K_Q values which did not meet ASTM K_{IC} thickness criteria are given in parentheses ( )

reported here, although the 0.2% offset yield strength in the 1.4-inch-thick section was as much as 11% lower than the plate material before preforming.

The fatigue crack growth rate versus the stress intensity factor range for the rectangular Double Cantilever Beam and the Mostovy DCB are presented in Figure 22 and Figure 23, respectively. Fatigue crack growth rate data were essentially the same for both types of specimen and were also compatible with other high strength steel data presented in the literature from a ΔK value of 29.0 to a ΔK value of 50.0.

Neither a distilled water environment nor variations in the relative humidity of the laboratory air appreciably influenced the fatigue crack growth behavior (Figure 23). Accelerated environmental crack growth which occurs in some high strength steels was not observed in HP 9-4-25 steel.

Statically loaded SCC properties are presented in Figure 24. A comparison of these data with data generated by Harmsworth and Cer ay (Reference 10) using medium toughness D6ac steel shows the HP 9-4-25 steel to be significantly less sensitive to an aqueous environment under static load conditions (Figure 25).

A very discernable difference was observed in the behavior of the K_I dependent of crack length (rectangular) specimens and the K_I independent of crack length (Mostovy) specimens under SCC conditions. Both types of specimen experienced an incubation period and slow subcritical crack growth. However, while the Mostovy specimen exhibited an unexpected crack arrest, the crack growth in the rectangular specimen continued on normally until fracture. The slow subcritical crack growth rate data obtained from the Mostovy specimen prior to arrest were very erratic (Figure 24). A corroded precrack was shown to affect only the incubation period and not the crack growth rates (Figure 24).

The HP 9-4-25 steel alloy is attractive for use in structural members for several reasons. First, the plane strain flaw sensitivity index (FSI),

$$\left(\frac{K_{IC}}{\sigma_{ys}}\right)^2$$

of this alloy is 0.510-inches in the axial direction (crack parallel to longitudinal grain direction). This FSI is for the low tensile strength-high toughness unworked material. This compares favorable with other

Text continued on page 47

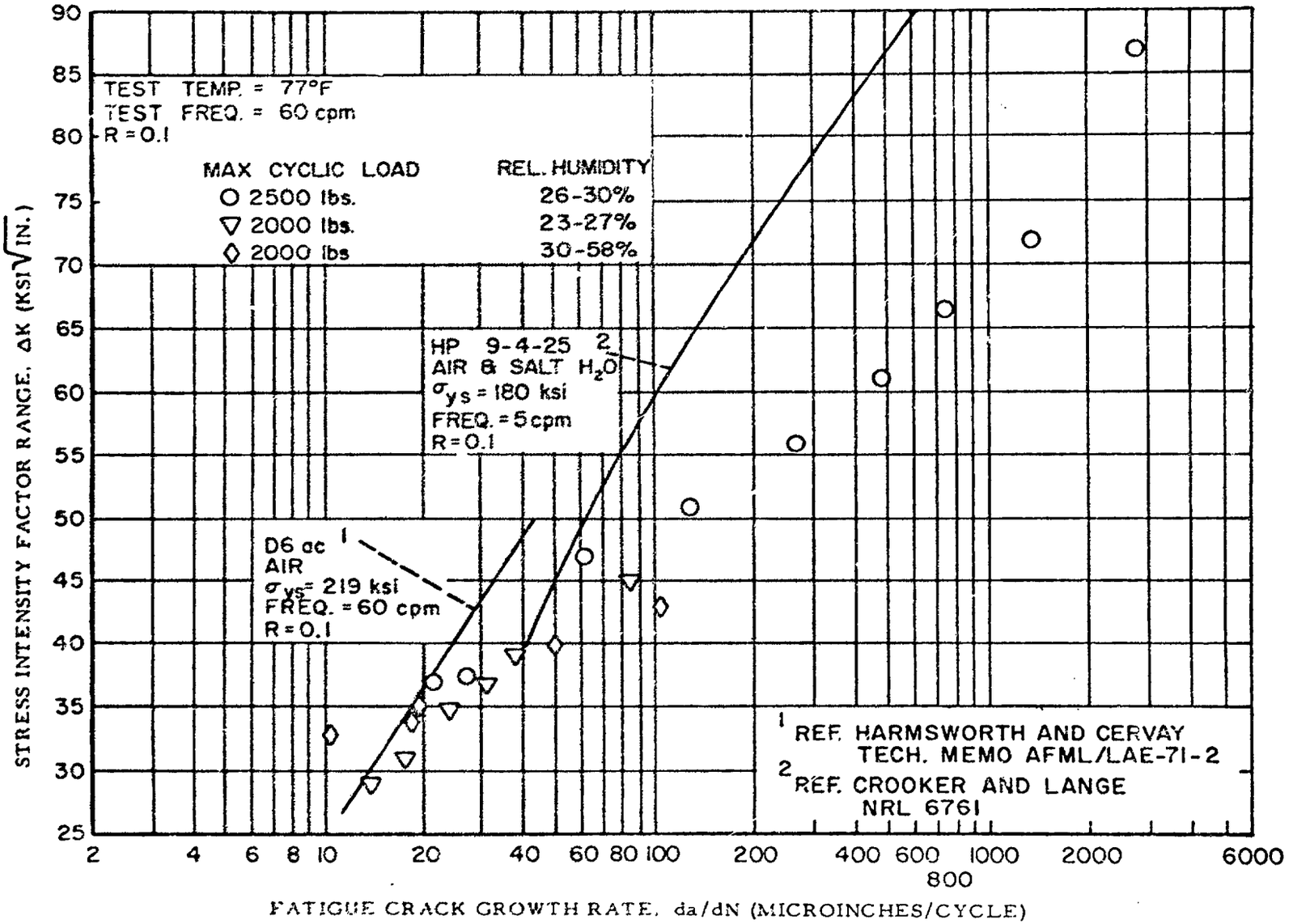

Figure 22. Stress Intensity Factor Range Versus Fatigue Crack Growth Rate for Roll Extruded HP 9-4-25 Steel, Rectangular DCB Specimen and Other Data.

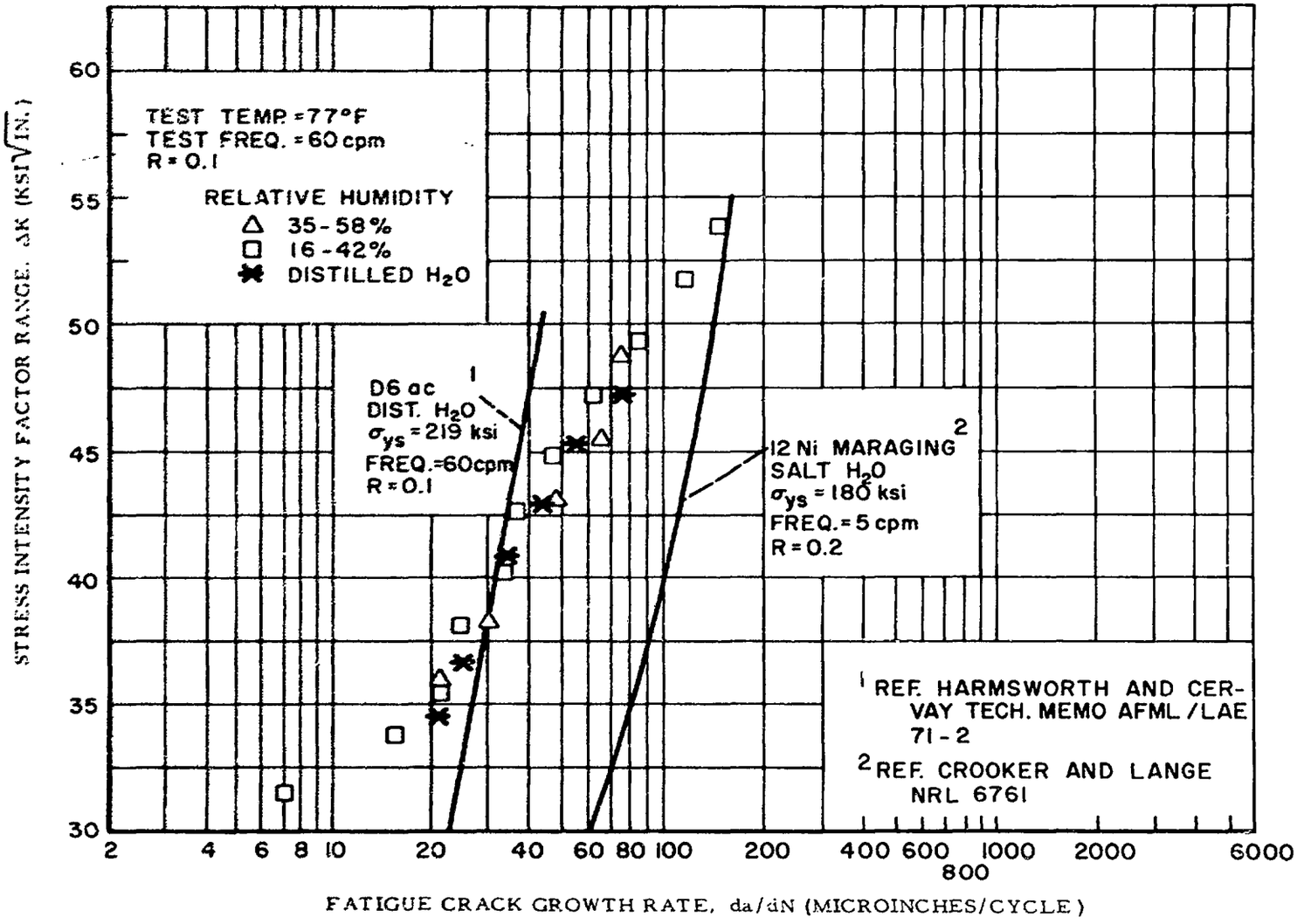

Figure 23. Stress Intensity Factor Range Versus Fatigue Crack Growth Rate for HP 9-4-25 Steel, Mostovy DCB Specimen, and Other Data.

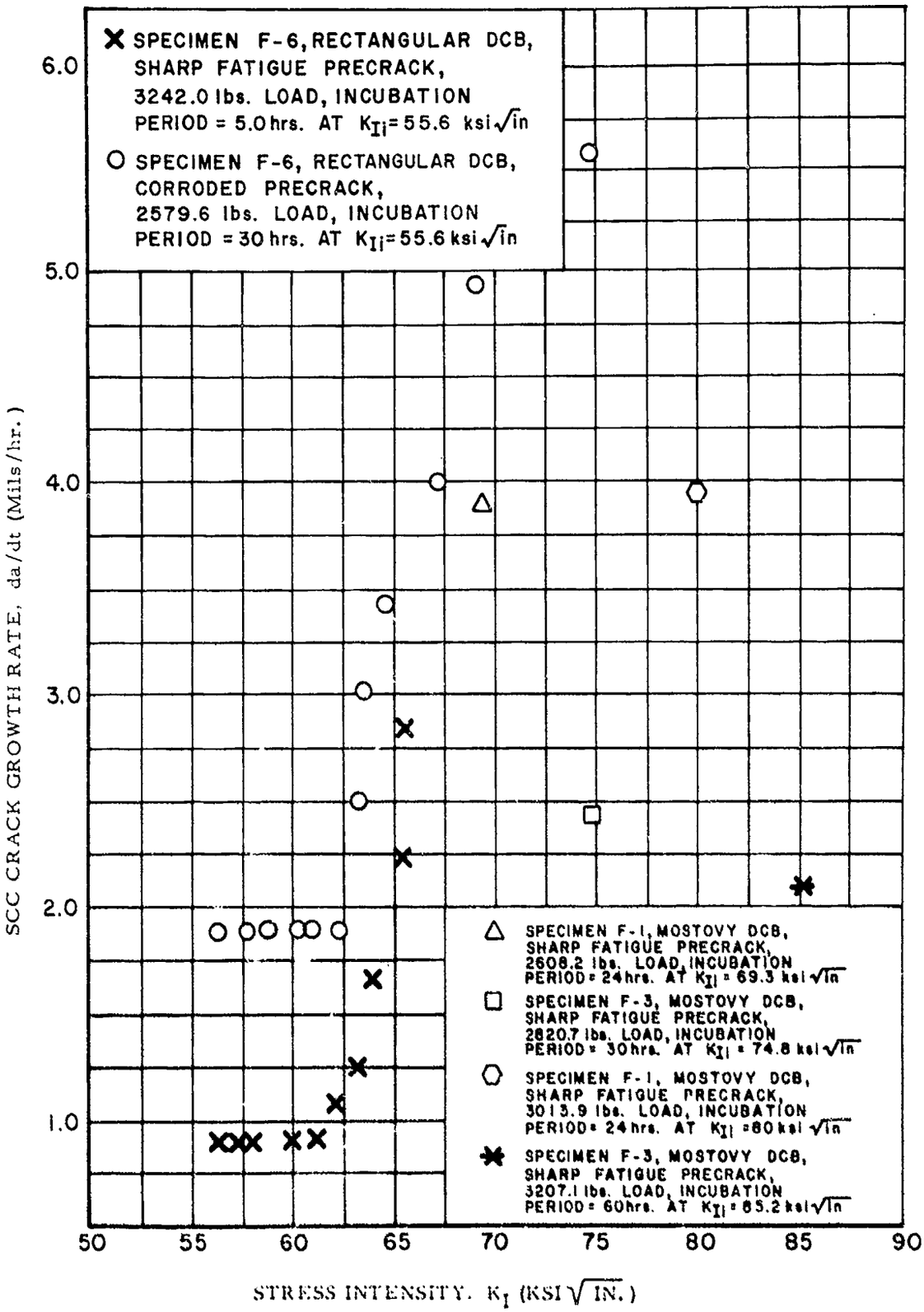

Figure 24. SCC Crack Growth Rate Versus Stress Intensity for HP 9-4-25 Steel.

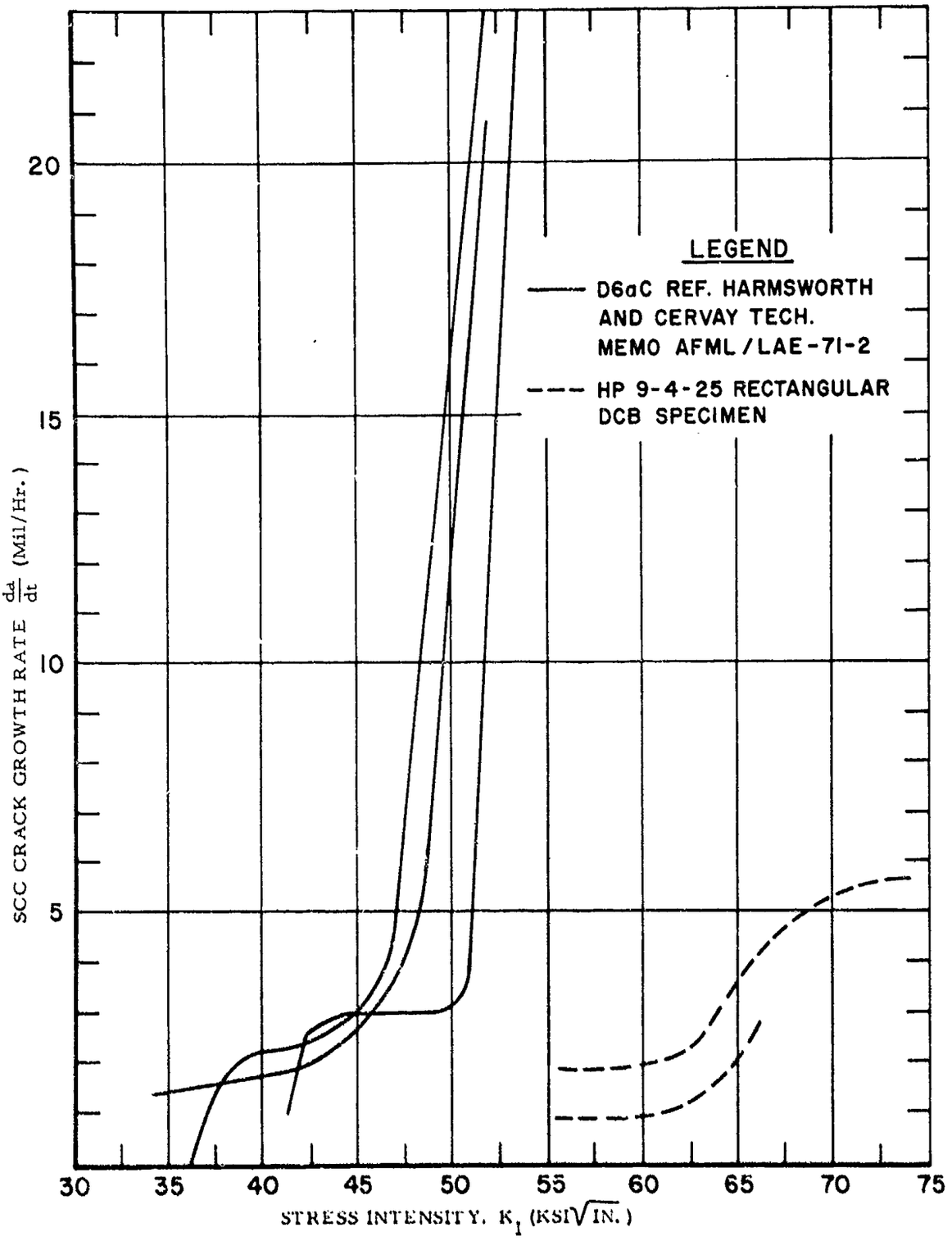

Figure 25. SCC Crack Growth Rate Versus Stress Intensity for D6ac and HP 9-4-25 (Reference 10).

high strength steel alloys having the same yield strength (Figure 26). Since the critical flaw size is proportional to the FSI, it is of prime concern from a structural integrity viewpoint to keep the index as high as possible. As expected, the highly worked roll-extruded material appears to have a lower FSI value than the unworked material. However, due to material thickness limitations, the plane strain FSI was not evaluated for both states of the material.

The second advantage of the HP 9-4-25 is that the fatigue crack growth behavior of this alloy is relatively stable and generally superior to other steels of comparable strength in an aqueous environment. In air the fatigue crack growth properties are comparable to other steels up to a ΔK value of 50.0. Static load SCC crack growth in an aqueous environment is also equal or superior to comparable steels.

1.3.1.3 Summary

The thin section highly worked HP 9-4-25 steel alloy displayed an increase in tensile strength and an apparent decrease in fracture toughness when compared with the thick section unprocessed material of the experimental SRM case. The exact reduction in toughness due to processing could not be definitely substantiated because of thickness limitations in the processed section. That is, the thickness of the material was not sufficient by ASTM standards for a valid K_{IC} test. However, the toughness values calculated are sufficiently lower in the thin section than in the thick section to indicate that the thin section has lower fracture toughness. It is not conclusive that the degradation of toughness negates the other desirable attributes of the process.

Fatigue crack growth properties of the processed HP 9-4-25 at the lower ΔK levels in both air and distilled water environment were comparable to other high strength steels. Acceleration of growth rate was not discernible in an aqueous solution under fatigue loading. Statically loaded SCC properties were excellent when compared to medium toughness D6ac steel alloy.

Because of its relative insensitivity to crack acceleration in an aqueous environment and its excellent flaw sensitivity index, the HP 9-4-25 steel alloy is attractive for use in structural members.

1.3.2 Fracture and Fatigue Crack Growth of 7175-T736 Forgings

A preliminary investigation of Petrak (Reference 11) has shown aluminum alloy 7175-T736 to have superior fracture toughness and stress corrosion properties relative to 7075-T6. In the initial investigation both constantly-immersed precracked compact tension specimens and

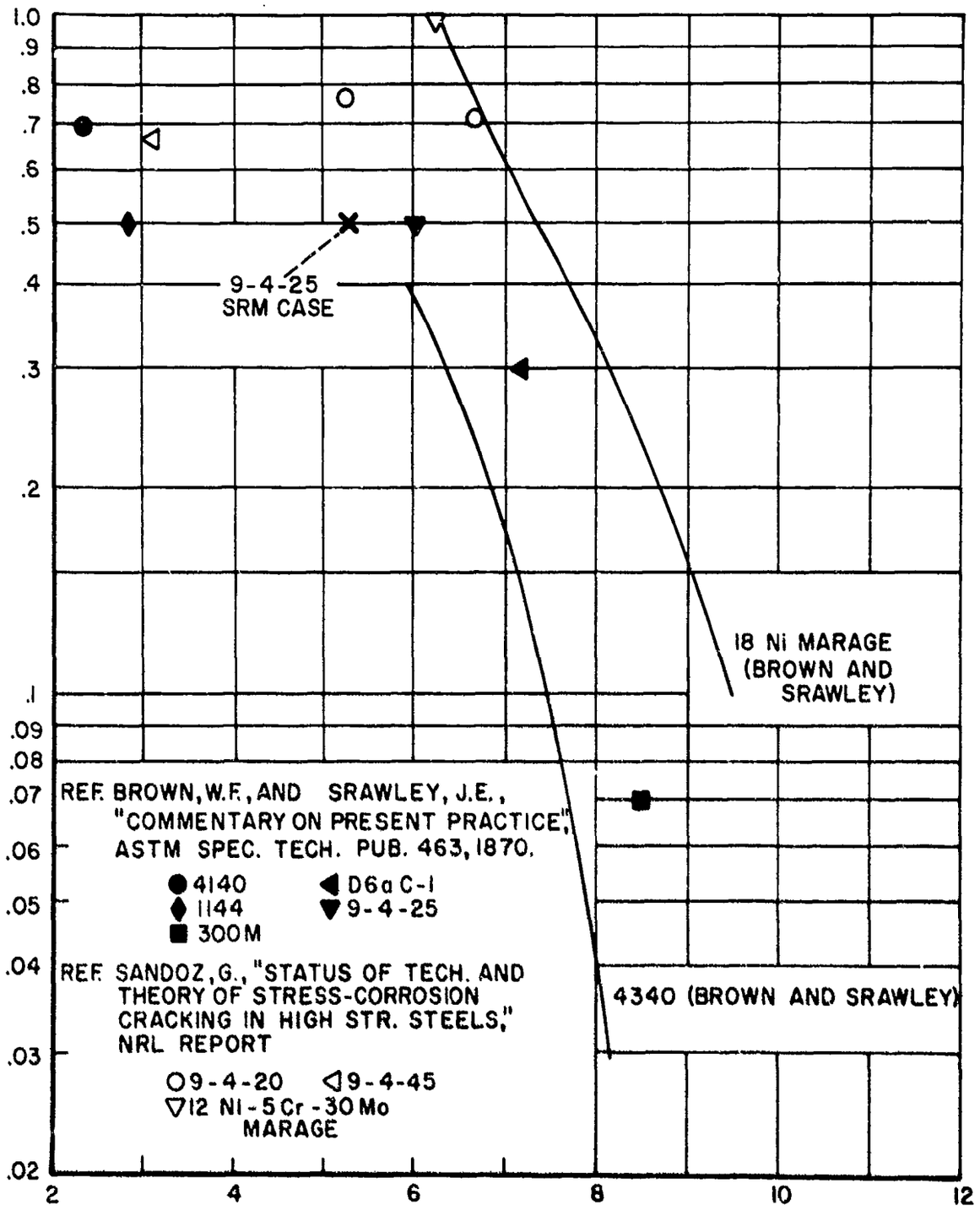

Figure 26. Flaw Sensitivity Index Versus Yield Strength Normalized by Young's Modulus for Several Steel Alloys.

alternately-immersed smooth specimens were tested to study stress corrosion behavior. In order to further evaluate this promising alloy, fatigue crack growth properties at expected operating temperatures were determined in a more comprehensive test program. Consequently, a section of a forging was procured from the Aluminum Company of American (ALCOA) in order to study tensile, fracture toughness, and fatigue crack growth properties at several temperatures. A linear elastic fracture mechanics approach was used to analyze and present the fatigue crack growth data.

1.3.2.1 Results and Discussion

The tensile properties developed for the 7175-T736 forging are presented in Table XI. The room temperature tensile values are slightly less than those of 7075-T651 for the 11/16 by 16-inch ribbed extrusion presented in Reference 12.

Fracture toughness properties of the 7175-T736 forging are shown in Table XII. Although fracture toughness specimens were tested in the longitudinal (WL) direction, all WL data were invalid by ASTM E-399 criteria due to the irregular crack front curvatures. obtained when precracking the specimens. These irregular crack fronts were probably due to anisotropic material properties in the forging, as a specimen rejection rate of this size because of crooked crack fronts is extremely rare. Exceptionally high toughness (K_{IC}) values were obtained in the short transverse direction while low toughness was detected in the transverse direction of the forging. This odd occurrence may be a result of the forging process. Comparable toughness data were generated in other investigations (References 13, 14, and 15) for several high strength aluminum alloys as shown in Table XIII. The fracture toughness of 7175-T736 in the short transverse (TW) direction appears to be superior to the other alloys listed.

The transverse fatigue crack growth properties of the 7175 forging at room temperature are presented in Figure 27. The crack growth data generated in this program at room temperature compare favorably with 7075-T6 and 7075-T736 crack growth data published in References 13 and 16, respectively.

A frequency change from 60 to 120 cpm had very little effect on the crack growth behavior. However, an R (ratio of minimum fatigue load to maximum fatigue load) change from 0.1 to 0.5 produced an increase in crack growth rate. This is to be expected since the maximum stress intensity is higher for the larger R.

Fatigue crack growth data at 350°F, 400°F, and room temperature are shown in Figure 28. The elevated test temperature

TABLE XI

TENSILE PROPERTIES OF 7175-T736 ALUMINUM ALLOY FORGING

Number of Tests	Temperature (°F)	Direction	Ultimate Strength (KSI)	Yield Strength (KSI)	Elong. in 1" G. L. (%)	Reduction of Area (%)
3	-65	Longitudinal	85.1	78.1	11.7	28.8
3	0	"	83.2	76.0	12.4	34.0
3	R. T.	"	81.2	74.6	12.2	37.5
3	200	"	70.2	65.5	14.6	44.9
2	-65	Transverse	78.6	68.6	7.2	9.6
3	0	"	75.1	65.2	8.0	17.0
3	R. T.	"	74.5	66.3	9.3	22.3
3	200	"	64.0	61.7	10.2	32.7
3	-65	Short Transverse	76.8	66.6	6.6	9.9
3	0		75.6	65.9	7.4	13.0
3	R. T.	"	73.6	64.9	7.8	15.6
3	200	"	64.0	60.5	9.6	26.2

TABLE XII

FRACTURE TOUGHNESS PROPERTIES OF
7175-T736 ALUMINUM ALLOY FORGING

Temperature	Direction	K_{IC} (KSI$\sqrt{IN}$)
Room	Transverse (WL)	22.7 (23.4)* (23.8)*
Room	Short Transverse (TW)	33.1 29.1 33.5 31.9 Avg.
200°F	"	33.0 35.0 34.4 34.1 Avg.
0°F	"	26.4 27.1 26.3 26.6 Avg.
-65°F	"	26.0 26.7 26.1 26.3 Avg.

* Invalid test results; crack length did not meet ASTM standards.

TABLE XIII

TYPICAL ROOM TEMPERATURE FRACTURE TOUGHNESS PROPERTIES FOR SEVERAL HIGH STRENGTH ALUMINUM ALLOYS

Alloy and Temper	Configuration	Cross Sectional Configuration (in x in)	K_{IC} (KSI$\sqrt{IN}$)		
			Long. LW	Trans. WL	Short Trans. TW
7075-T7352(Ref. 13)	Hand Forging	2 x 8	31.4	24.0	-
7075-T7352(Ref. 13)	Hand Forging	6 x 24	39.5	27.7	25.6
7075-T651 (Ref. 14)	Plate	1 x 20	30.6	27.8	-
7075-T7351(Ref. 14)	Plate	1 x 20	35.3	31.1	-
7075-T6511(Ref. 15)	Extrusion	3 1/2 x 7 1/2	30.9	20.8	19.0
7175-T736	Die Forging	2 1/2 x 2 1/2	-	22.7	31.9

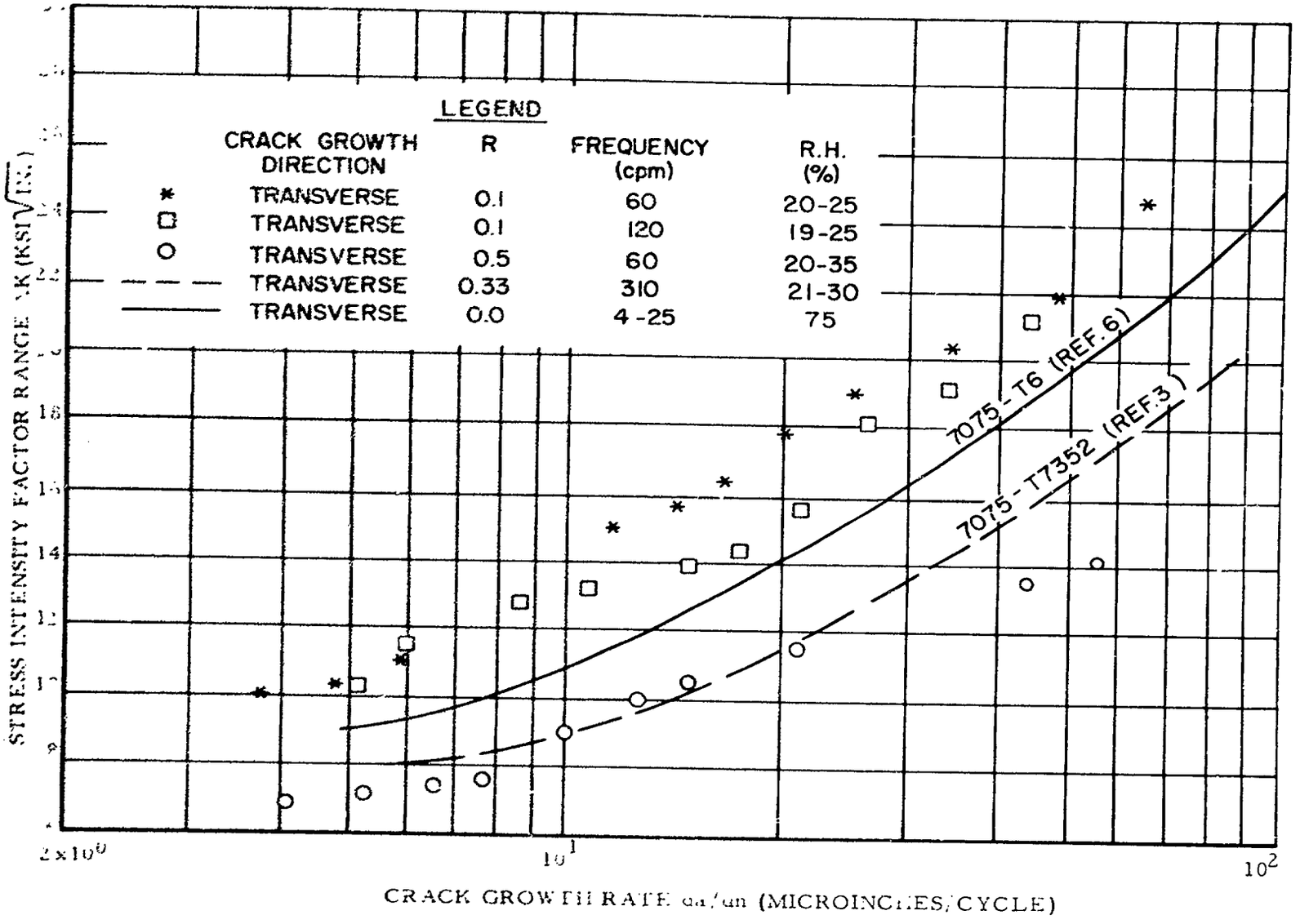

Figure 27. Stress Intensity Factor Range Versus Crack Growth Rate for 7175-T736 Forging at Room Temperature.

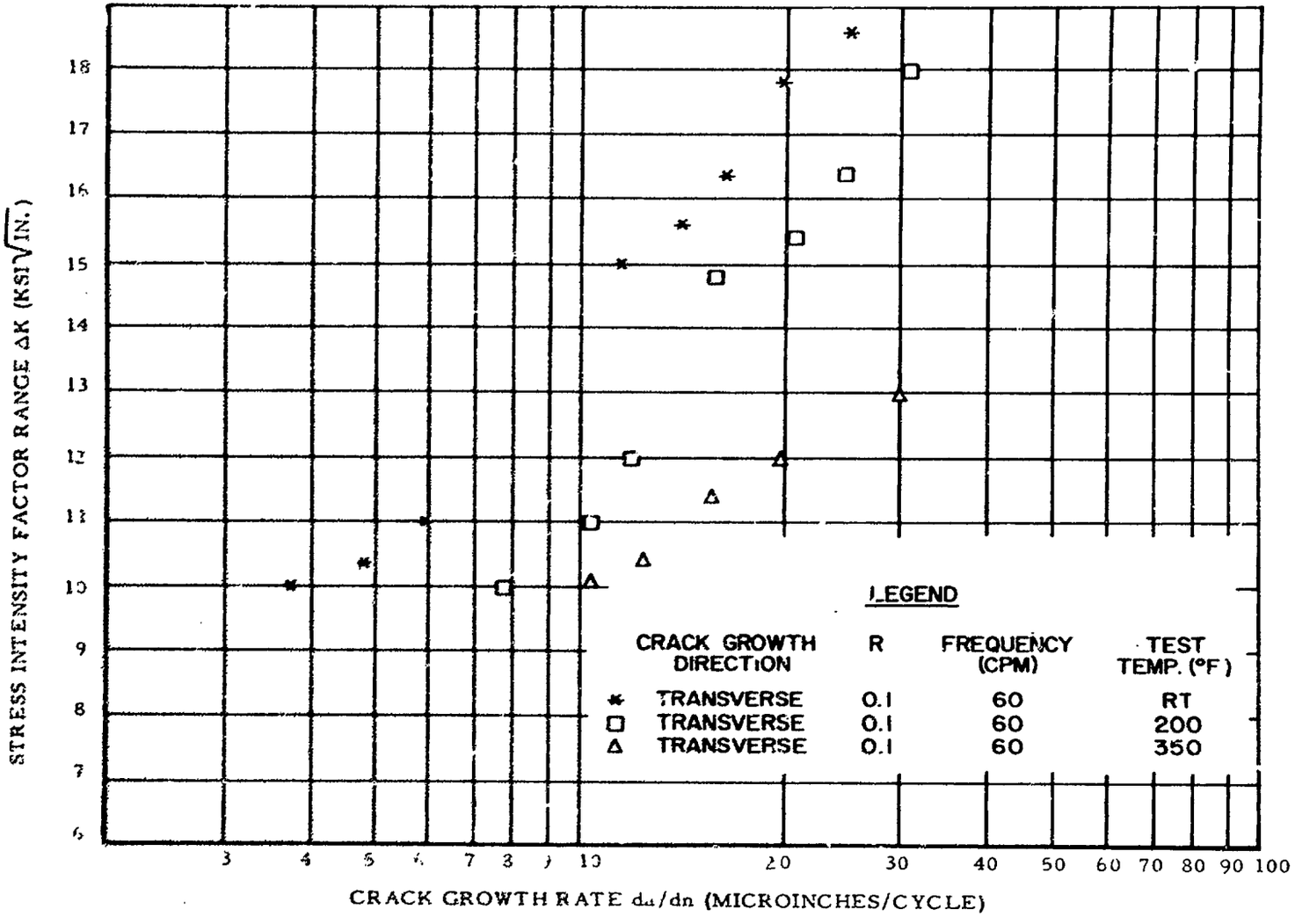

Figure 28. Stress Intensity Factor Range Versus Crack Growth Rate for 7175-T736 Forging at Elevated Temperatures, Compared with Room Temperature

had a detrimental effect on the crack growth properties of 7175-T736. Fatigue crack growth data at -65°F, 0°F, and room temperature are shown in Figure 29. Observation of the results shown in Figure 29 would tend to indicate that (relative to R.T.) the growth rate increased at 0°F and decreased at -65°F. However, the apparent trends are probably caused by normal scatter in these test data and are not considered real, particularly since only one specimen was run at R.T. and -65°F and only two at 0°F.

This scatter could be attributed to humidity variations, since humidity was neither controlled nor monitored, leading to varying amounts of frost and ice condensing at the crack tip at low temperatures. The above speculation connotes that although 7175-T736 is not sensitive to cracking in a corrosive environment when statically loaded, it may be environment-sensitive while fatigue cracking at low temperatures. Further testing is necessary to establish this fact.

Wei (Reference 17) has suggested that fatigue crack growth under the influence of low or elevated temperatures may behave according to an Arrhenius-type rate process as presented in the following equation:

$$da/dN = A\, f(\Delta K)\, \exp\left[\frac{-u(\Delta K)}{kT}\right]$$

where:

A	=	a constant
$f(\Delta K)$	=	a stress intensity function
$u(\Delta K)$	=	apparent activation energy as a function of stress intensity
k	=	Boltzmann's constant
T	=	absolute temperature

Wei also presented data to verify this equation for 7075-T651 in a distilled water environment from temperature of 180°F to 32°F. Johnson and Wilner (Reference 18) have presented H-11 steel alloy data in distilled water environment from temperatures of 180°F to 32°F which agree with this equation. The Arrhenius-type of correlation would fit the elevated and room temperature data presented in this report (Figure 30), but when considering the 0°F and -65°F crack growth data the Wei relationship is no longer valid for predicting the results. It is essential that environmental influences as well as loading parameter not vary during crack growth testing at elevated and low temperatures for the application of the Wei rate process equation.

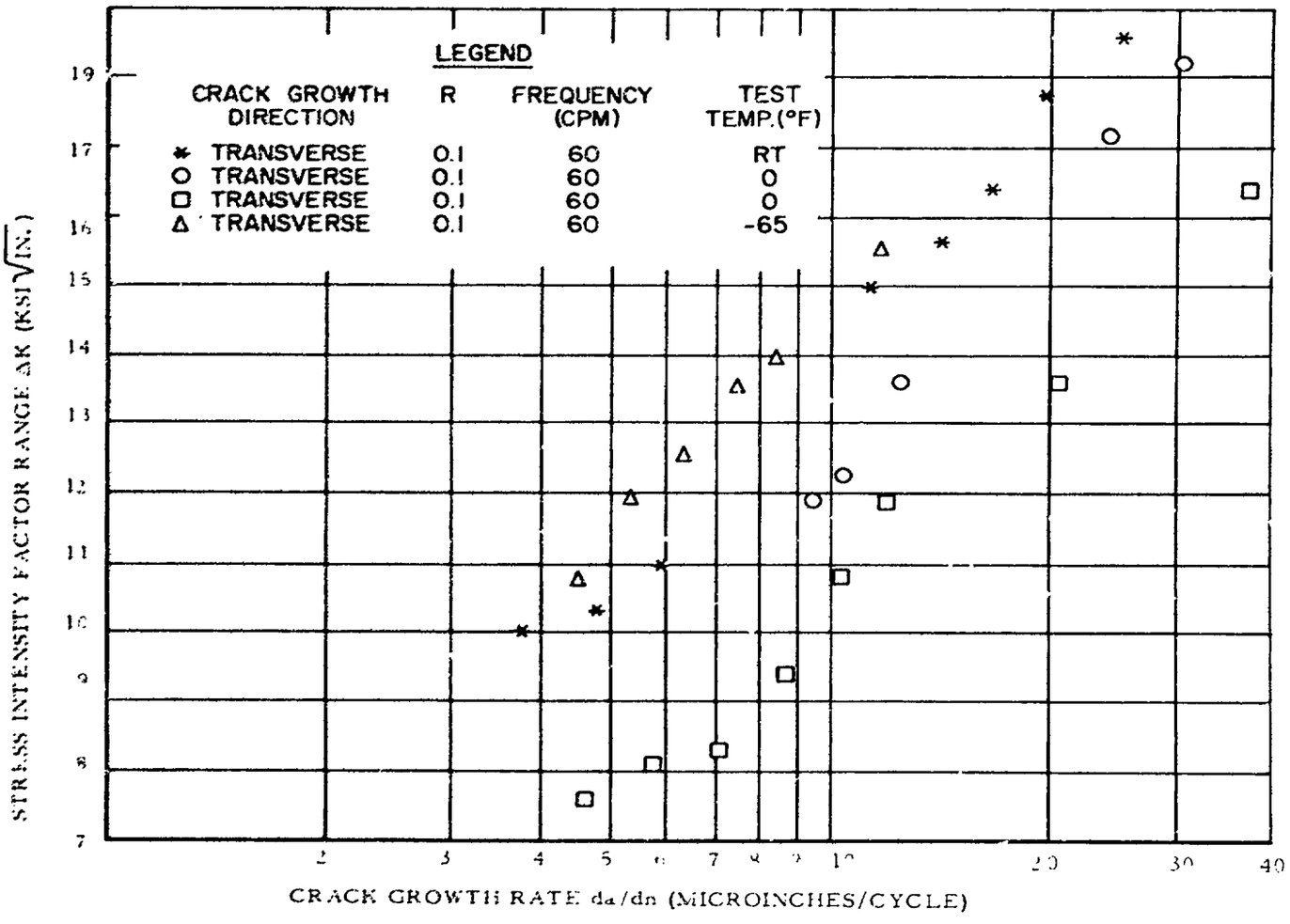

Figure 29. Stress Intensity Factor Range Versus Crack Growth Rate for 7175-T736 Forging At Low Temperatures, Compared with Room Temperature.

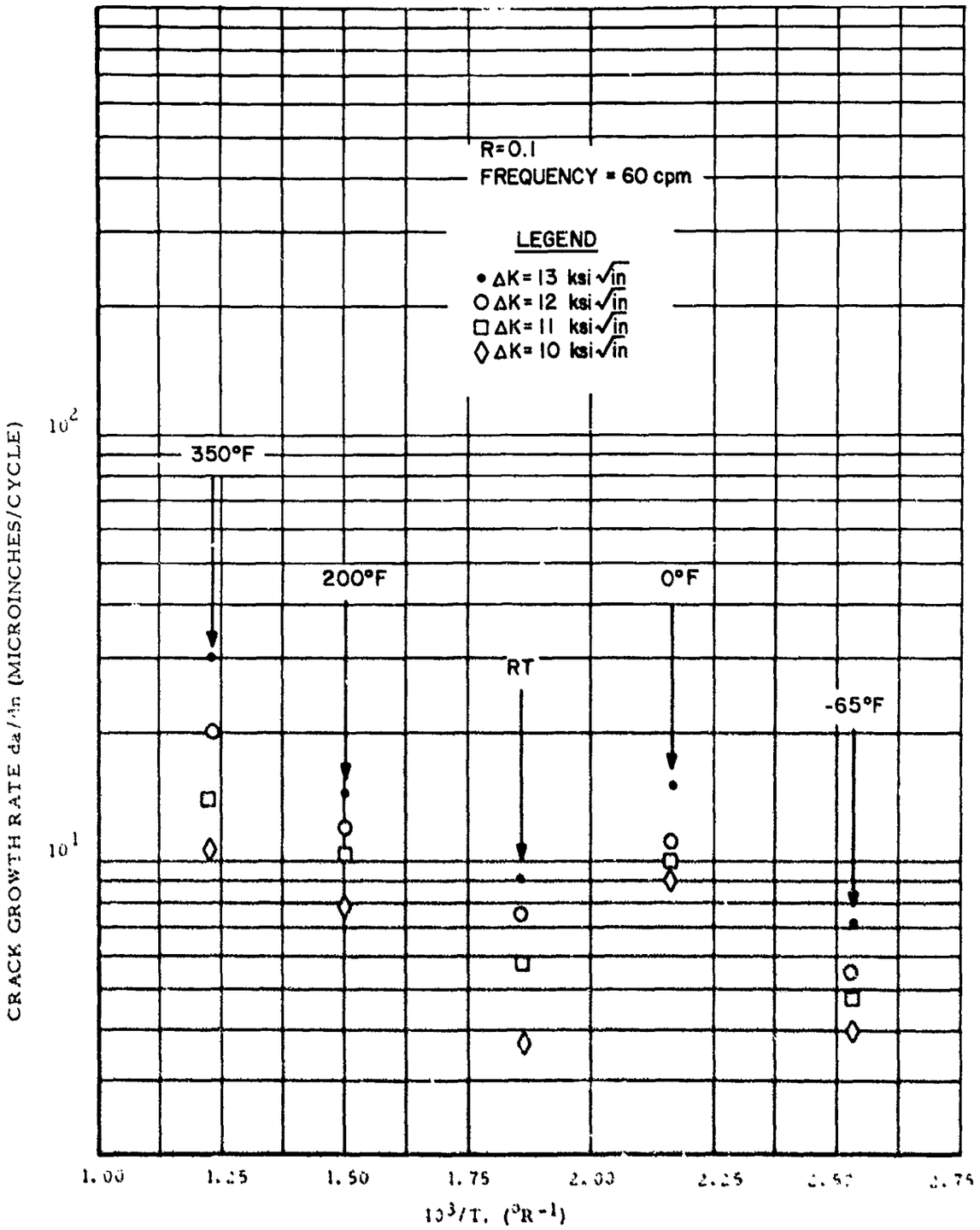

Figure 30. Fatigue Crack Growth Rate Versus the Reciprocal of Test Temperature for 7175-T736 Forging.

1.3.3 Design Properties of 7049 Extrusions

Extruded aluminum alloys have come into use extensively as structural members in Air Force systems. Due to the reduction in machining time and cost to produce complicated structural configurations, extrusions are considered advantageous where they can be used. A newly developed aluminum alloy extrusion in two heat treatment conditions, 7049-T73 and 7049-T76, is being manufactured by the Kaiser Aluminum and Chemical Corporation. Because it is expected to have strength levels comparable to that of 7075, combined with excellent fracture toughness and stress corrosion cracking resistance, the 7049 extrusion is considered a prime candidate for future aircraft structural applications.

Two 7049-T73 extrusions and one 7049 extrusion were procured for mechanical property evaluation. Tensile and fracture toughness properties at several temperature were determined for all three extrusions. In addition, for the two T73 extrusions, fatigue, corrosion, and crack growth properties were determined as limitations in available material permitted.

1.3.3.1 Results and Discussion

The potential usefulness of a material can be ascertained by comparing its properties with those of a material it could possibly replace. Since the T651 heat treatment of the 7075 gives it a strength equal to the 7049 strength levels, the data developed in this program will be compared to 7075-T651 extrusion data in the literature, whenever possible. In general, a comparison between 7049-T76 or T73 and the lower strength 7075-T73 would be inappropriate.

The average tensile properties of the three 7049 extrusions are presented in Figures 31 through 36. The 7049-T76 bar is the strongest of the three extrusion in the longitudinal direction at all test temperatures except 500°F (Figure 31). The 7049-T73 integrally stiffened extrusion is the strongest in the transverse and short transverse directions (Figures 32 and 33). The best overall average strength was exhibited by the 7049-T73 integrally stiffened extrusion. As can be observed, an acute loss of strength occurred at the 500°F temperature for all materials. The elongation and reduction of area was comparable for all three extrusion (Figure 34 through 36). The tensile properties of the three extrusions are comparable to 7075-T651 extrusion properties reported by Kaufman, et. al. (Reference 19). The values obtained were 85.4 KSI and 90.4 KSI for the longitudinal ultimate strength of 3-1/2-inch and 11/16-inch extruded shapes, respectively. Similar properties for the transverse direction were 77.3 and 87 KSI. These properties are somewhat higher than the same properties for 7075 extrusions in the T7351 condition also reported in Reference 19.

Text continued on page 63

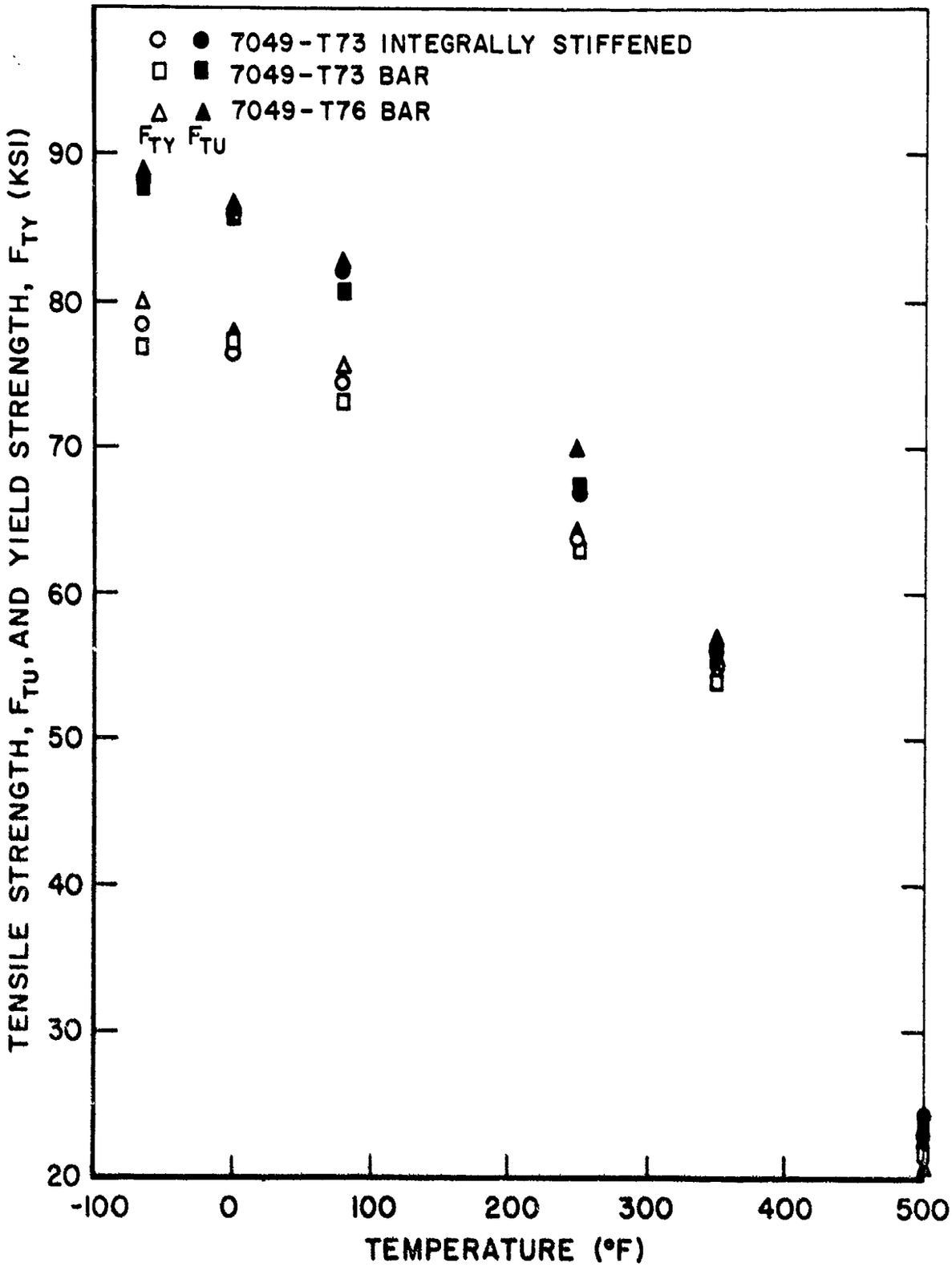

Figure 31. Tensile Property Data for the Longitudinal Direction of Three 7049 Extrusions.

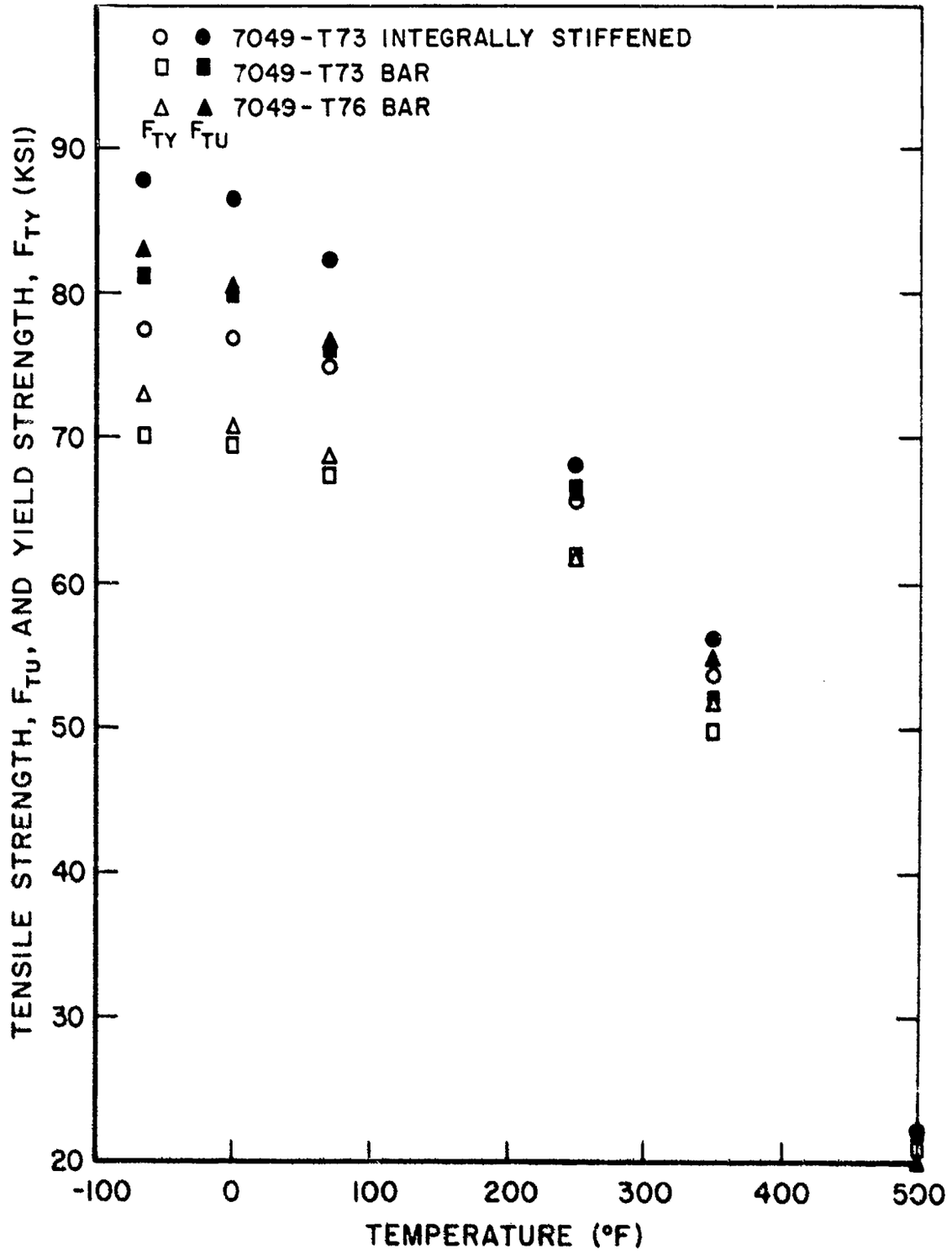

Figure 32. Tensile Property Data for the Transverse Direction of Three 7049 Extrusions.

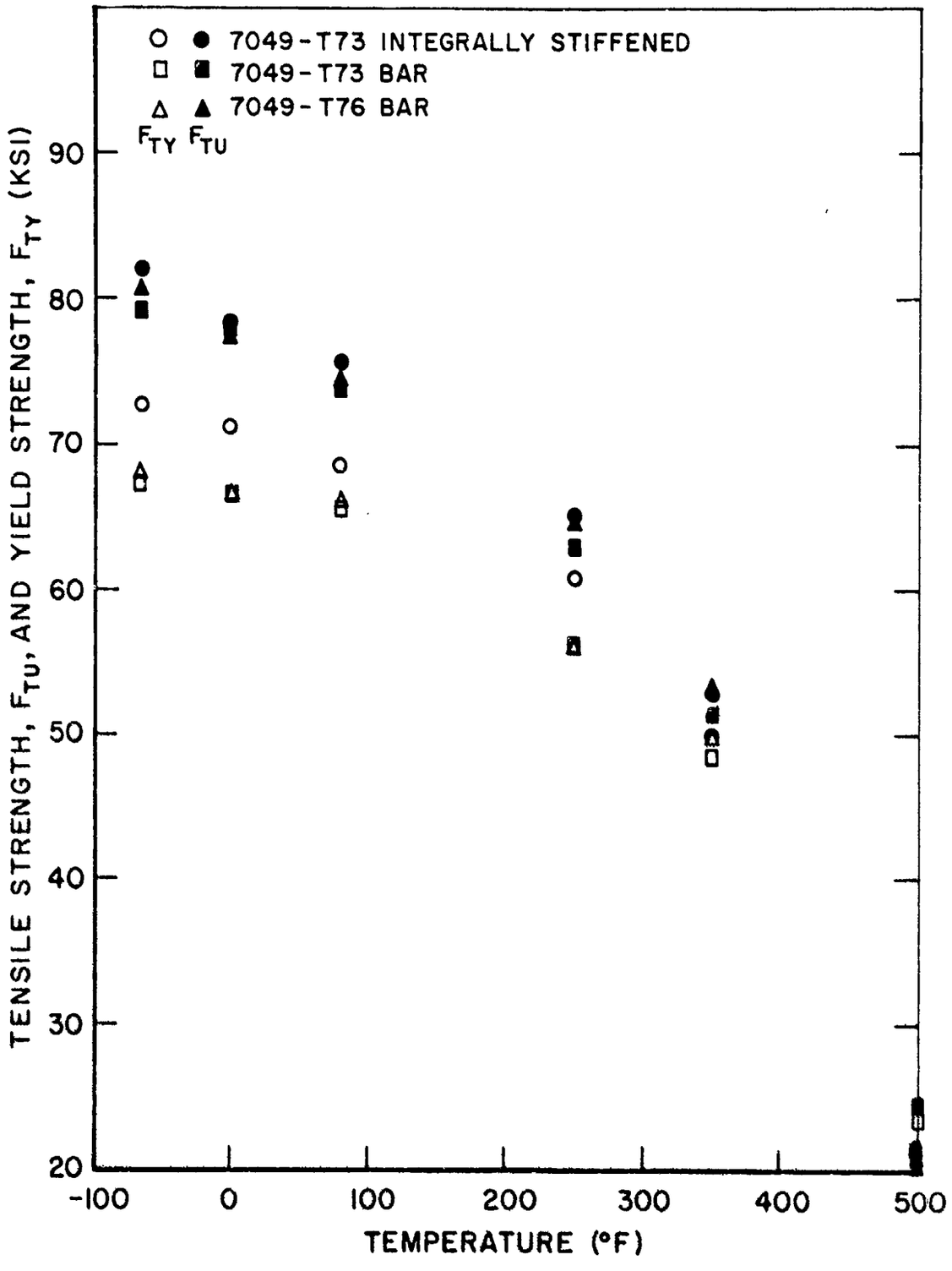

Figure 33. Tensile Property Data for the Short Transverse Direction of Three 7049 Extrusions.

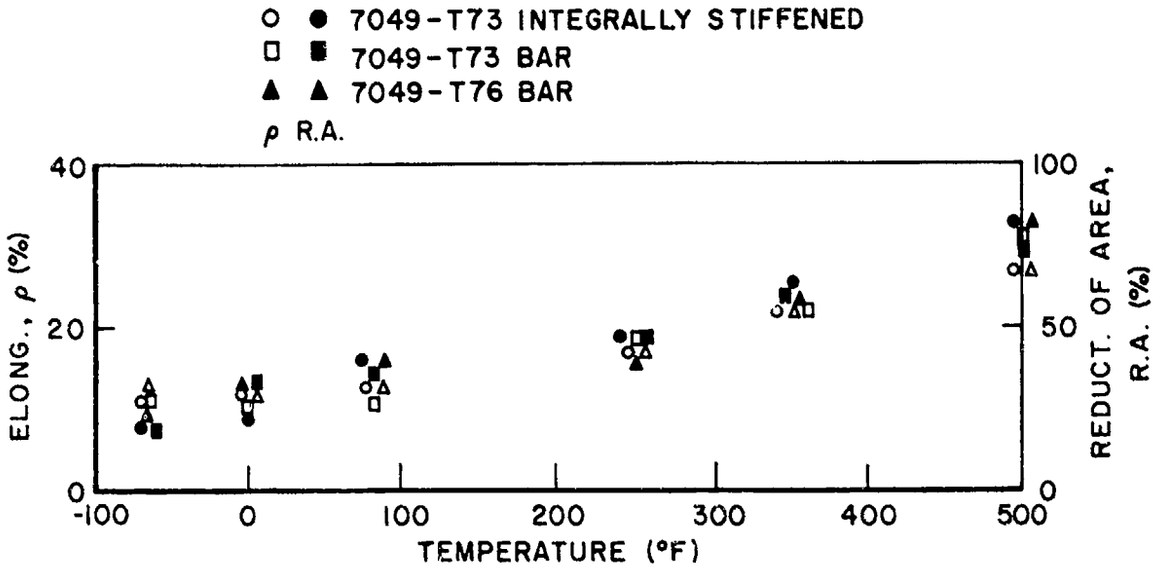

Figure 34. Elongation and Reduction of Area for the Longitudinal Direction of Three 7049 Extrusions.

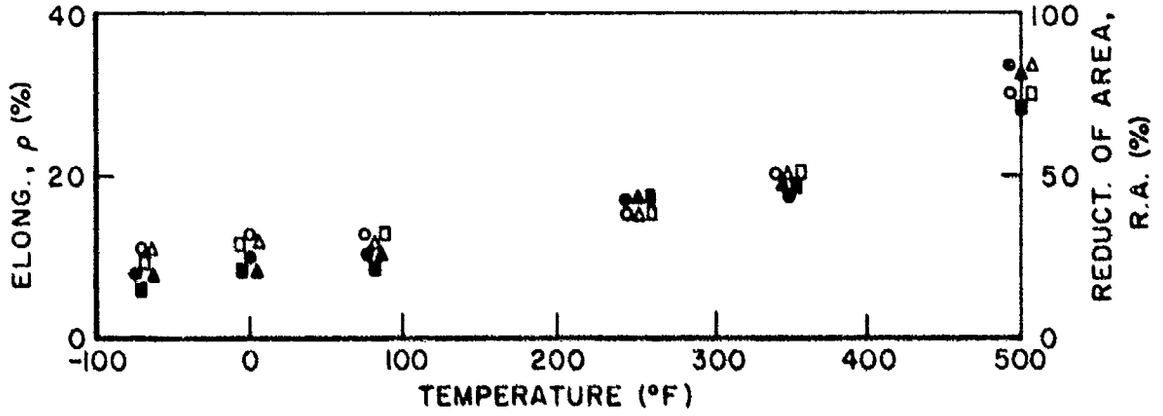

Figure 35. Elongation and Reduction of Area for the Transverse Direction of Three 7049 Extrusions.

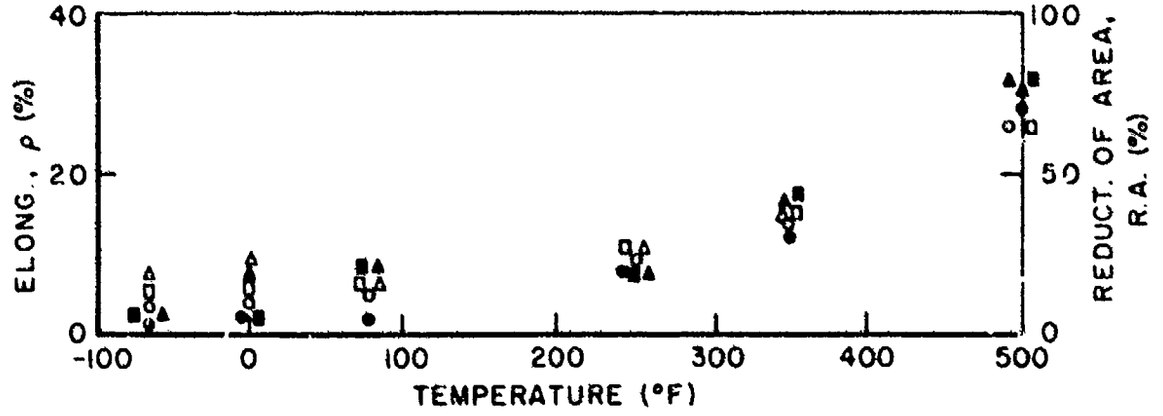

Figure 36. Elongation and Reduction of Area for the Short Transverse Direction of Three 7049 Extrusions.

Fracture toughness properties are presented in Figures 37 through 39. The T73 and T76 bar extrusions had longitudinal toughness values significantly better than those for 7075-T6510 extrusion reported in Reference 19, while the toughness for the integrally stiffened extrusion was equal to the 7075-T651 longitudinal toughness. It is apparent from Figures 37 and 38 that the more homogeneous toughness properties are possessed by the integrally stiffened extrusion. There was a 6 percent loss in longitudinal toughness of the T73 bar due to a change in temperature from room to -65°F. The T73 bar also displayed the highest toughness of the three extrusions at room temperature in the short transverse direction.

Axial fatigue properties of the 7049-T73 bar and integrally stiffened extrusions are shown in Figures 40 through 45. Composite fatigue curves are presented in Figures 46 and 47. In a smooth condition and at room temperature, the T73 integrally stiffened extrusion had the better fatigue properties of the two extrusions at the higher stress levels. At the lower stress levels the extrusion with the better fatigue properties was a function of the test temperature. In the notched condition both extrusions had similar fatigue properties. Both extrusions were superior in room temperature smooth axial fatigue to 7075-T6510 extruded panel and 7075-T7351 extruded panel. They were also superior to 7049-T73 forging (Figure 48). Fatigue limits are presented in Table XIV. The fatigue limits of both extrusions were similar.

Time-to-failure stress corrosion cracking properties of the T73 materials are presented in Table XV. Precracked compact tension specimens were utilized in this phase of the testing. Neither extrusion was susceptible to cracking in a corrosive environment for the indicated elapsed test periods. However, extensive pitting was observed in the precracked region of the specimens during post-test examinations.

Alternate immersion stress corrosion results of the 7049-T73 integrally stiffened extrusion in the short transverse direction are presented in Table XVI. Failure did not occur at a stress level of 61.7 KSI in the 1000-hour elapsed test periods using smooth tensile specimens. Since failure did not occur in either type of stress corrosion test it appears that the materials tested are not susceptible to cracking in a 3.5 percent salt solution within the reported time periods. On first observation these results are somewhat surprising. Initial data from the literature show that while the material has good corrosion resistance it is nevertheless sensitive to corrosive attack above approximately 35 KSI. Because of this discrepancy between the two sets of corrosion tests an examination of the microstructure of the specimens tested in this program was initiated. It was felt that the reason for the apparent insensitivity to corrosion might have been that

Text continued on page 76

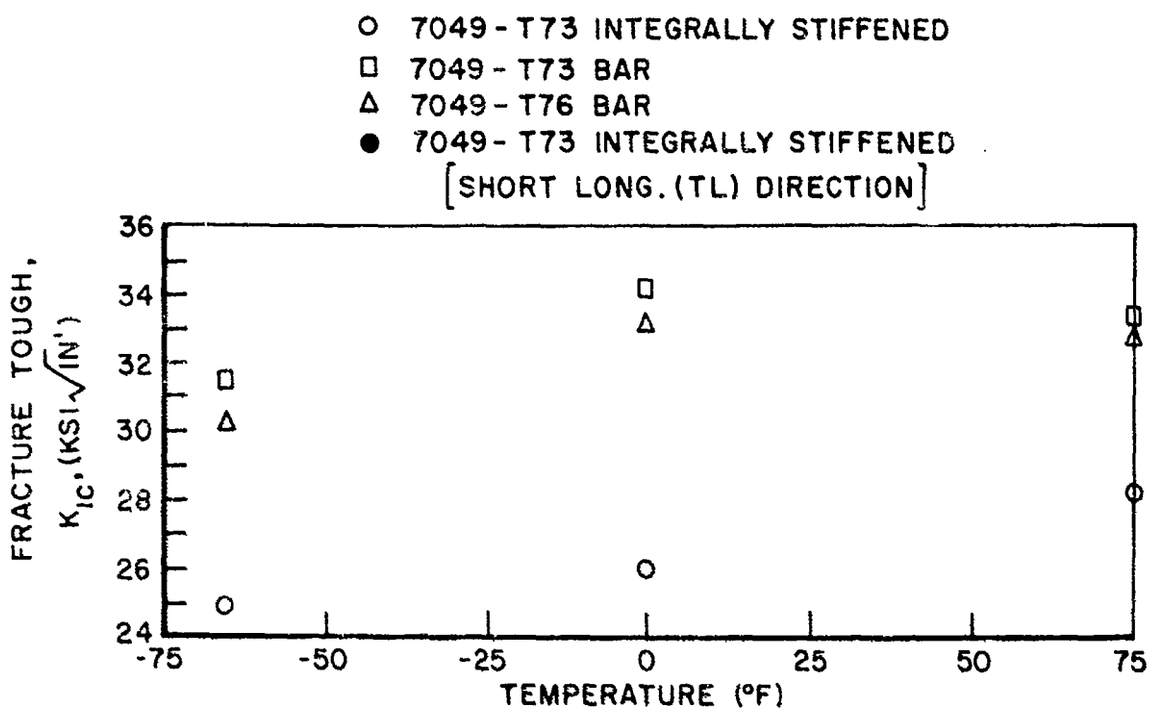

Figure 37. Fracture Toughness, K_{IC}, for the Longitudinal (LW) Orientation in Three 7049 Extrusions.

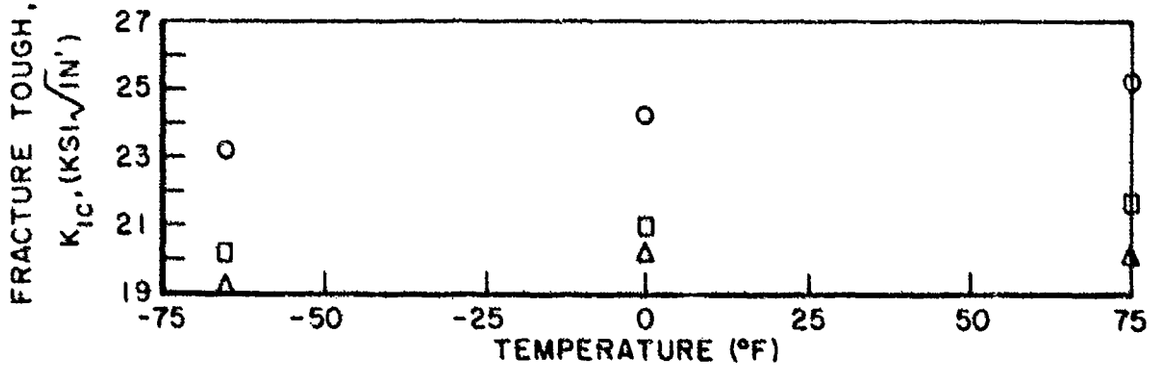

Figure 38. Fracture Toughness, K_{IC}, for the Transverse (WL) Orientation in Three 7049 Extrusions.

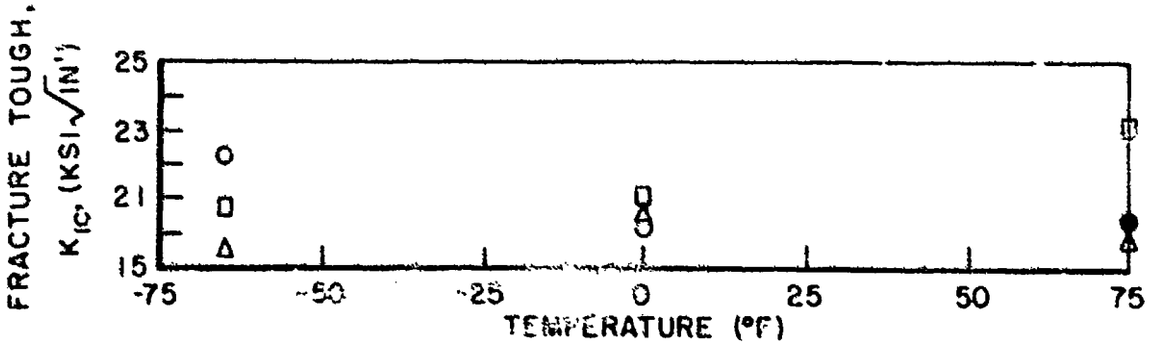

Figure 39. Fracture Toughness, K_{IC}, for the Short Transverse (TW) Orientation in Three 7049 Extrusions.

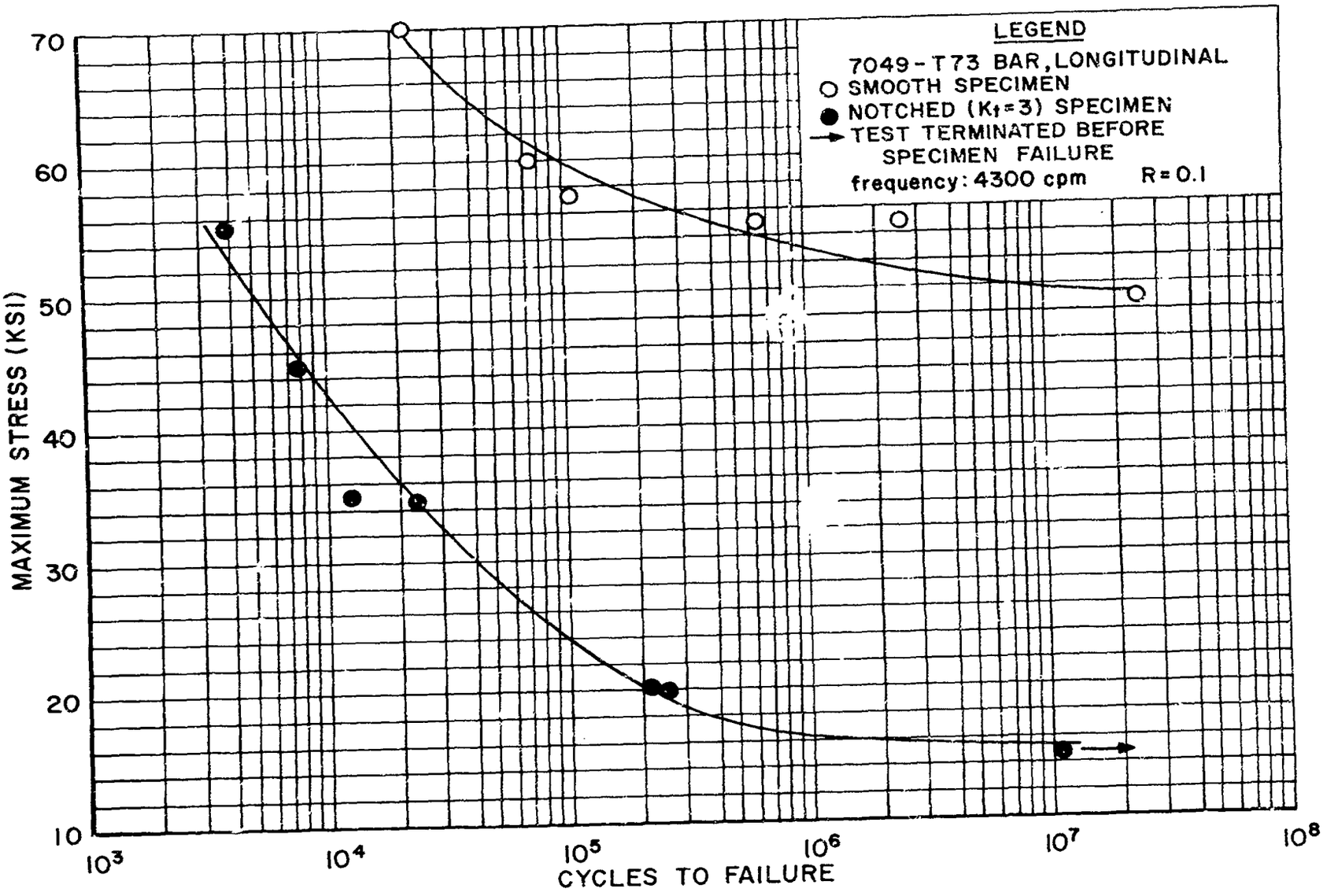

Figure 40. S/N Fatigue Curve at Room Temperature for 7049-T73 Aluminum Bar Extrusion.

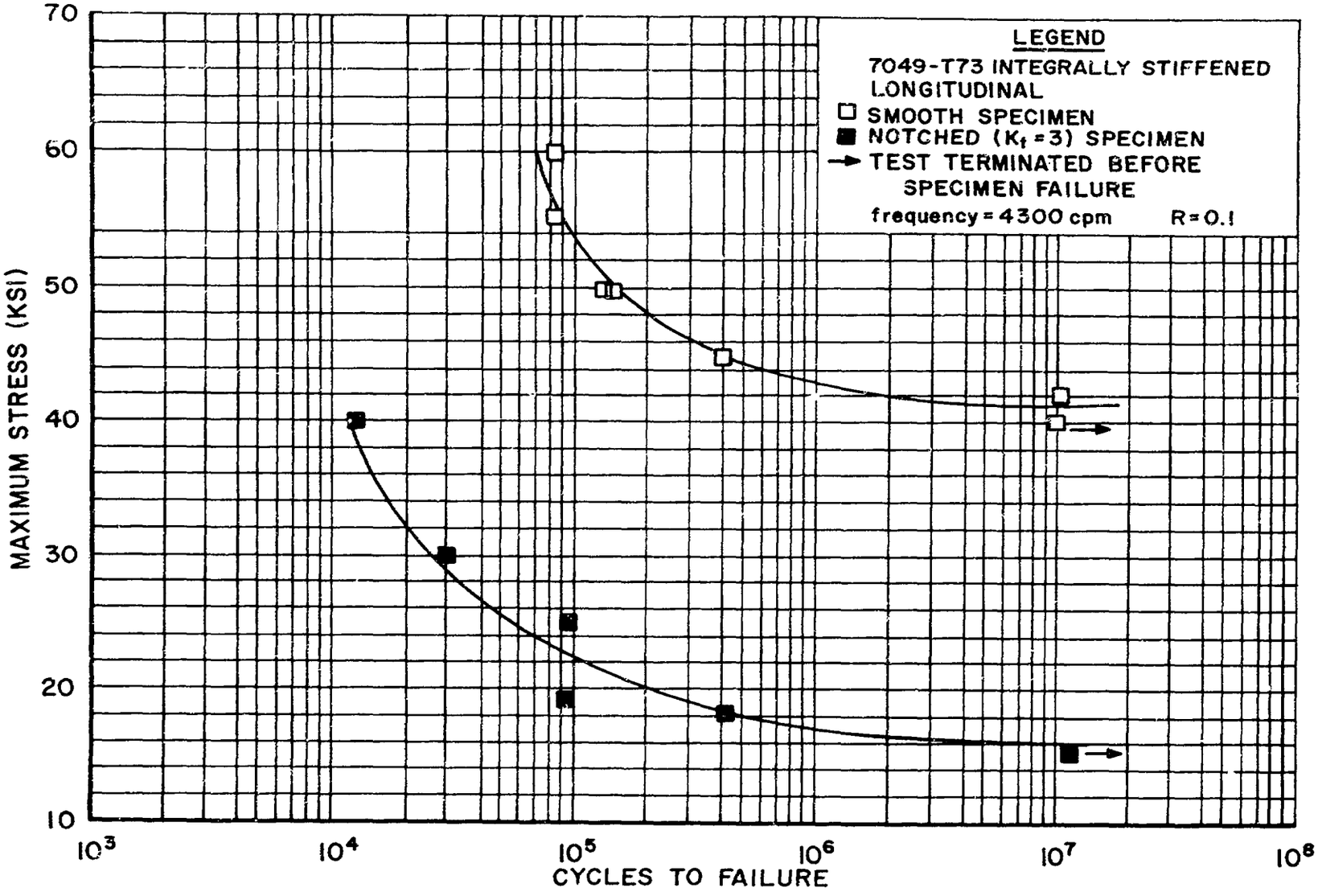

Figure 41. S/N Fatigue Curve at 250°F for 7049-T73 Aluminum Bar Extrusion.

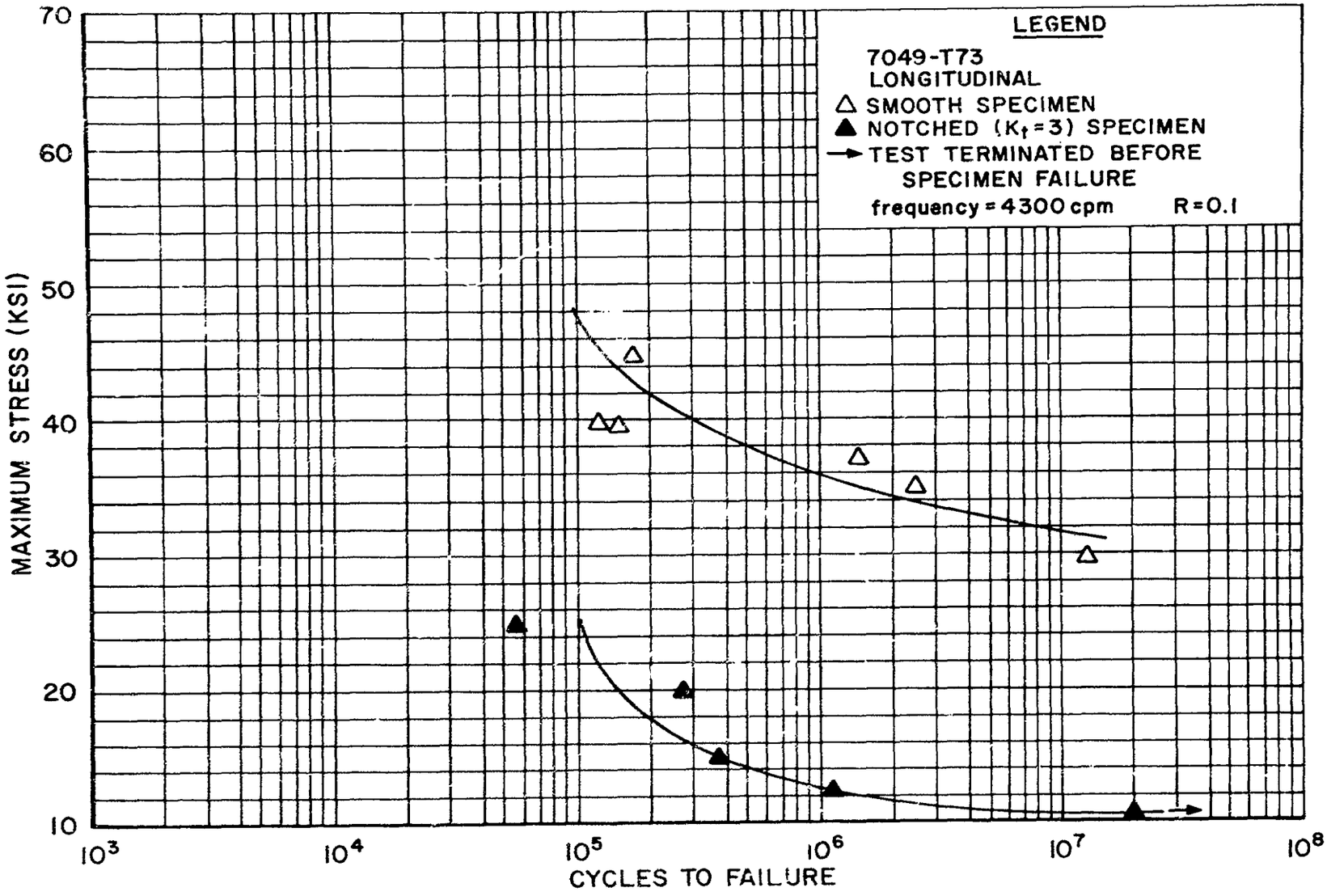

Figure 42. S/N Fatigue Curve at 350°F for 7049-T73 Aluminum Bar Extrusion.

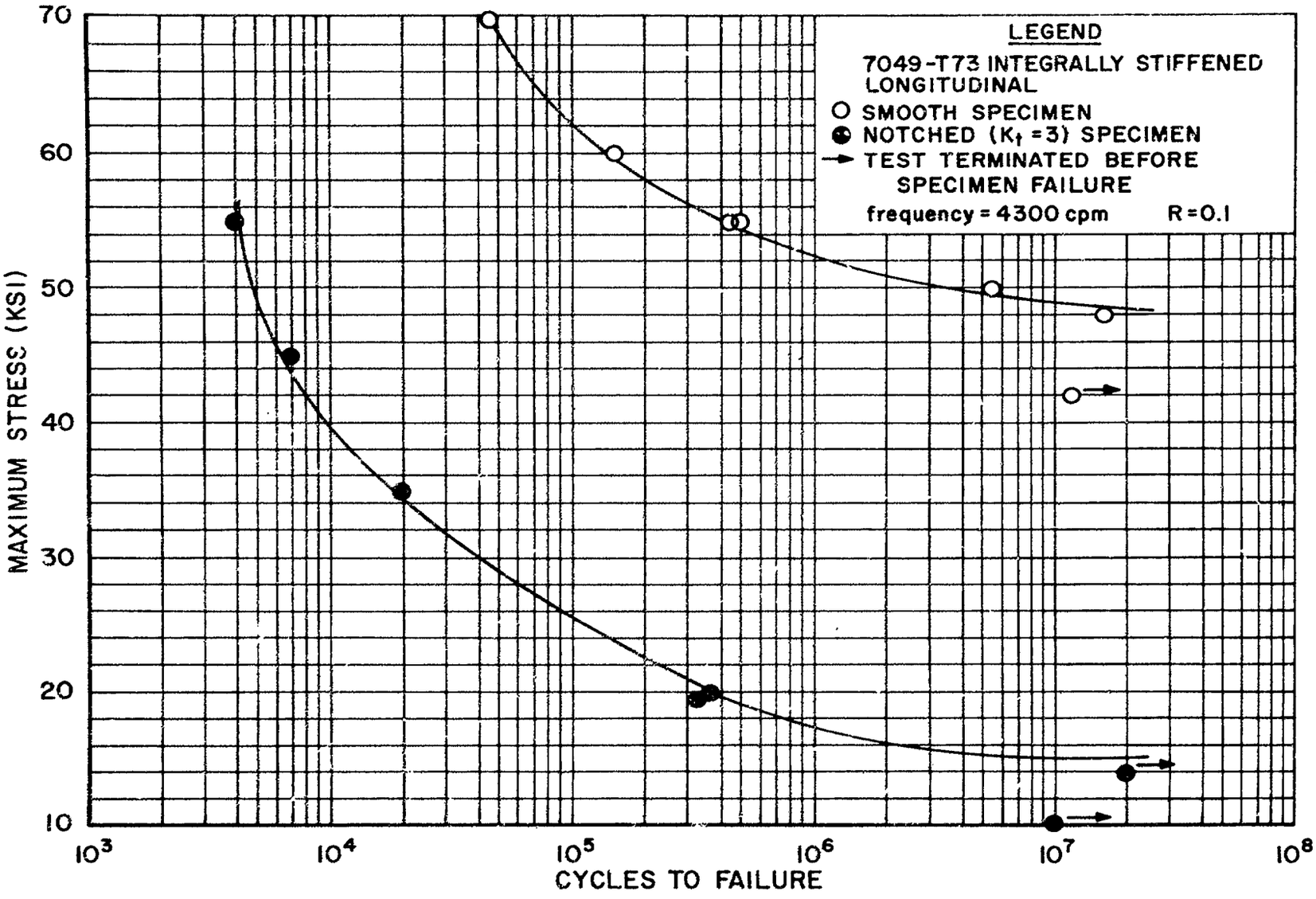

Figure 43. S/N Fatigue Curve at Room Temperature for 7049-T73 Integrally Stiffened Aluminum Extrusion.

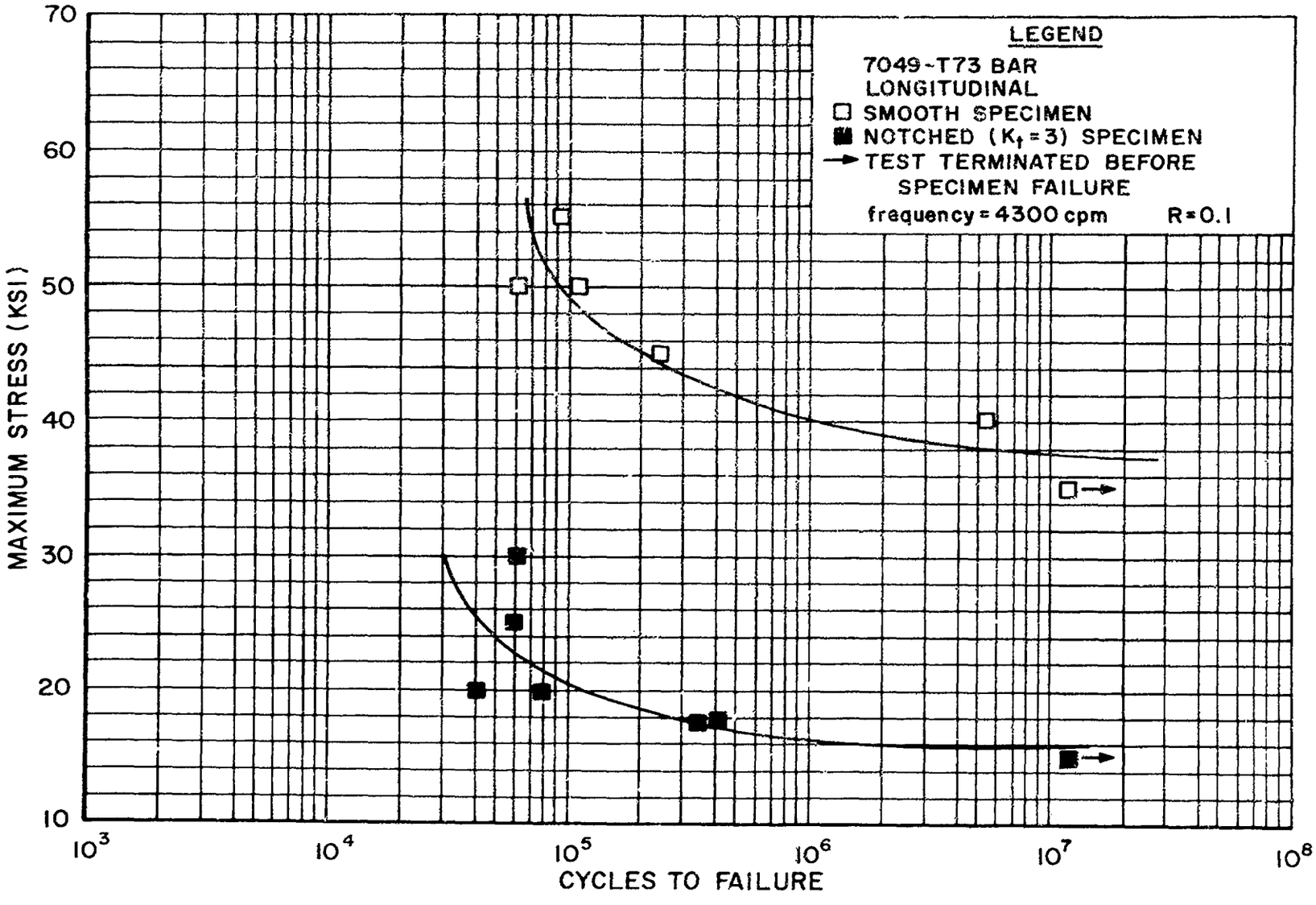

Figure 44. S/N Fatigue Curve at 250°F for 7049-T73 Integrally Stiffened Aluminum Extrusion.

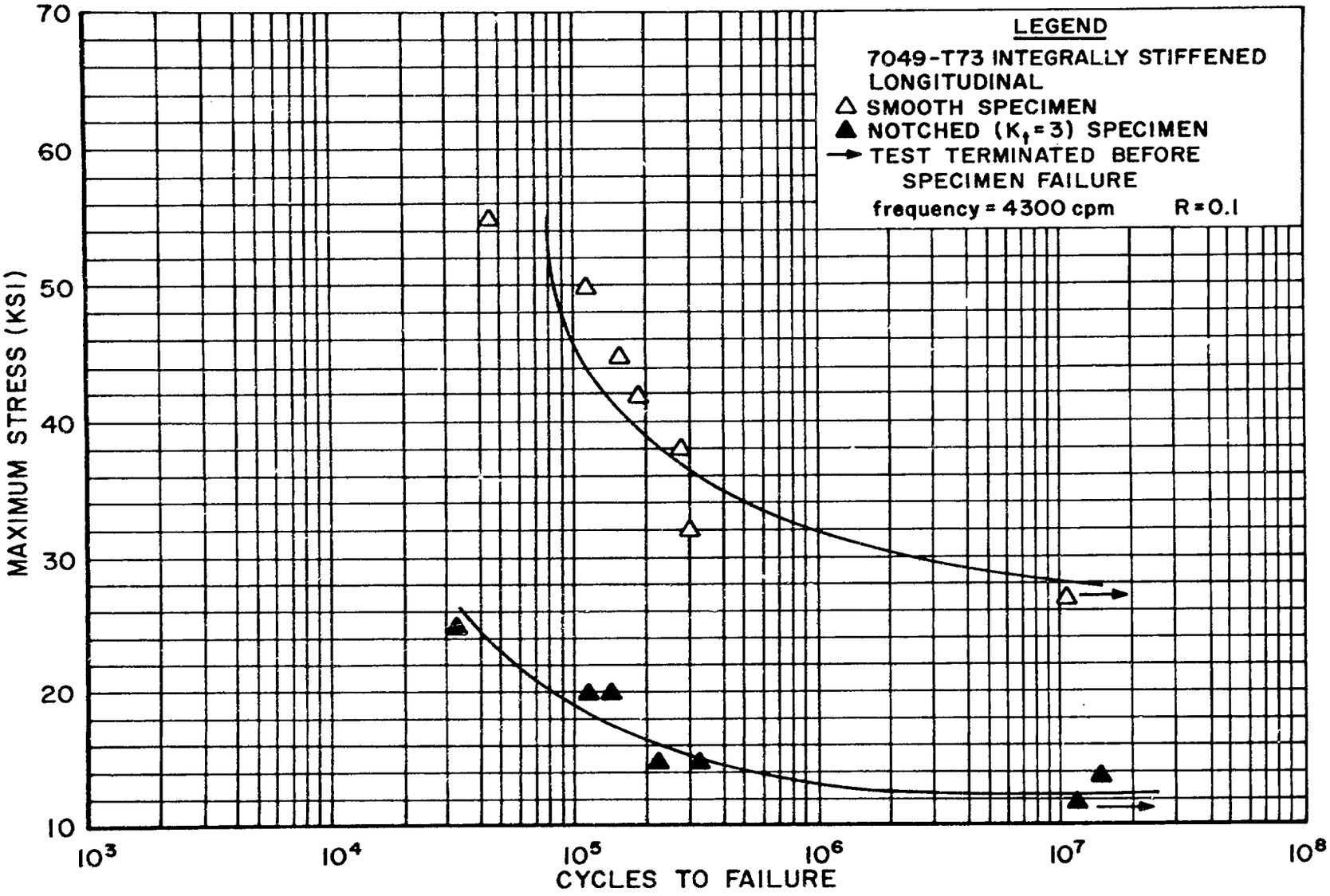

Figure 45. S/N Fatigue Curve at 350°F for 7049-T73 Integrally Stiffened Aluminum Extrusion.

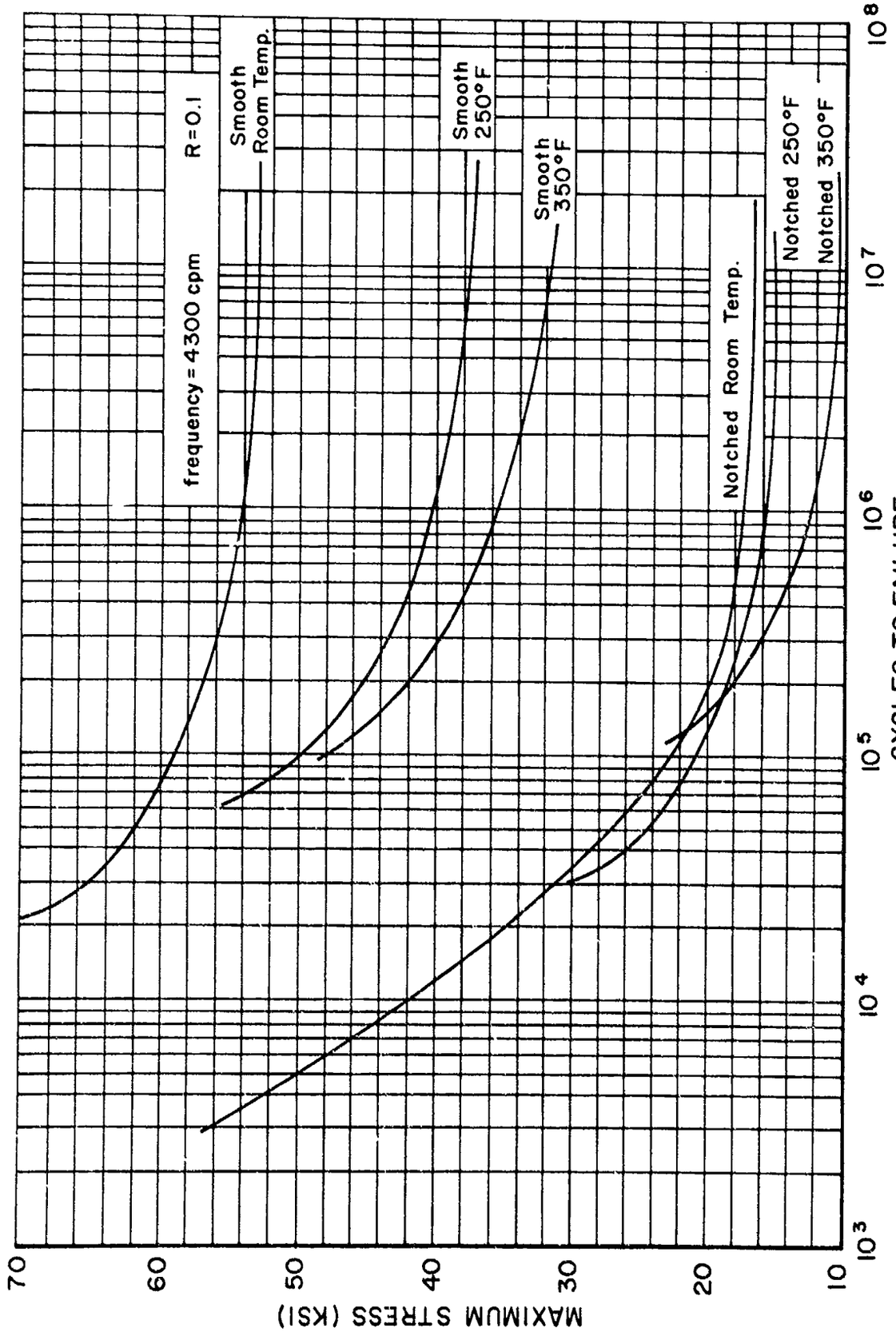

Figure 46. S/N Fatigue Curves for 7049-T73 Aluminum Bar Extrusion.

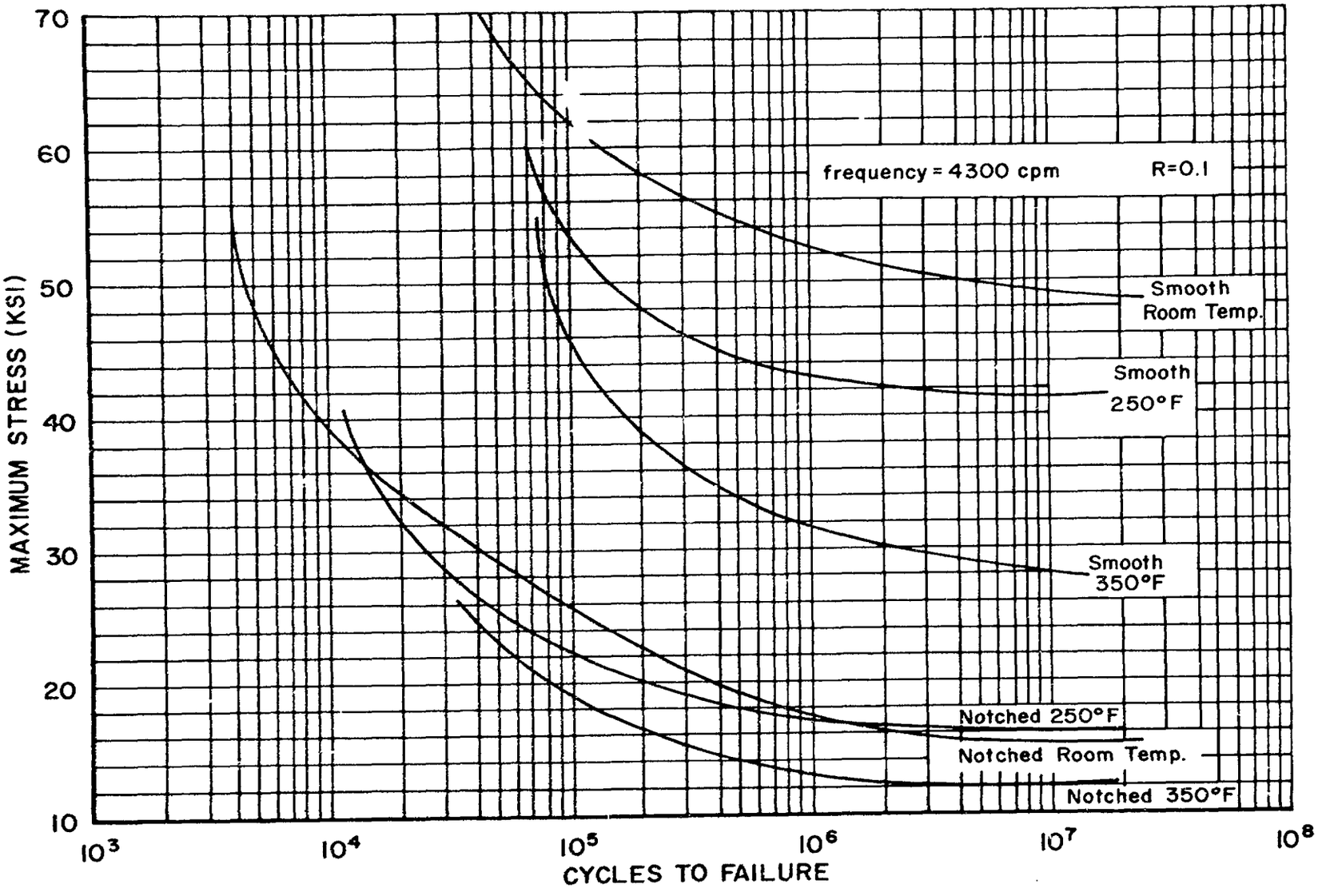

Figure 47. S/N Fatigue Curves for 7049-T73 Integrally Stiffened Aluminum Extrusion.

TABLE XIV

FATIGUE LIMITS FOR 7049-T73 ALUMINUM EXTRUSIONS AT 10^7 CYCLES

Test Condition / Extrusion Configuration	SMOOTH			NOTCHED		
	RT	250°F	350°F	RT	250°F	350°F
Bar	53.0 KSI	37.5 KSI	31.5 KSI	16.6 KSI	15.0 KSI	10.5 KSI
Integrally Stiffened	49.0 KSI	41.0 KSI	28.0 KSI	15.0 KSI	16.0 KSI	12.0 KSI

TABLE XV

TIME-TO-FAILURE STRESS CORROSION PROPERTIES OF 7049 ALUMINUM EXTRUSIONS IN 3.5% SODIUM CHLORIDE SOLUTION

Material	Loading Direction	K_I Initial ($KSI\sqrt{IN}$)	Elapsed Test Time (hrs)	Results
7049-T73 Integrally Stiffened	Longitudinal	24.7	265.9	No failure
		26.7	285.5	No failure
	Short Transverse	19.4	0.0	Failed on loading
		19.4	670.6	No failure
7049-T73 Bar	Longitudinal	22.9	0.0	Failed on loading
		19.2	285.5	No failure
		23.9	0.0	Failed on loading
		20.4	353.8	No failure
		21.2	287.3	No failure
	Short Transverse	16.0	330.0	No failure
		20.3	330.0	No failure

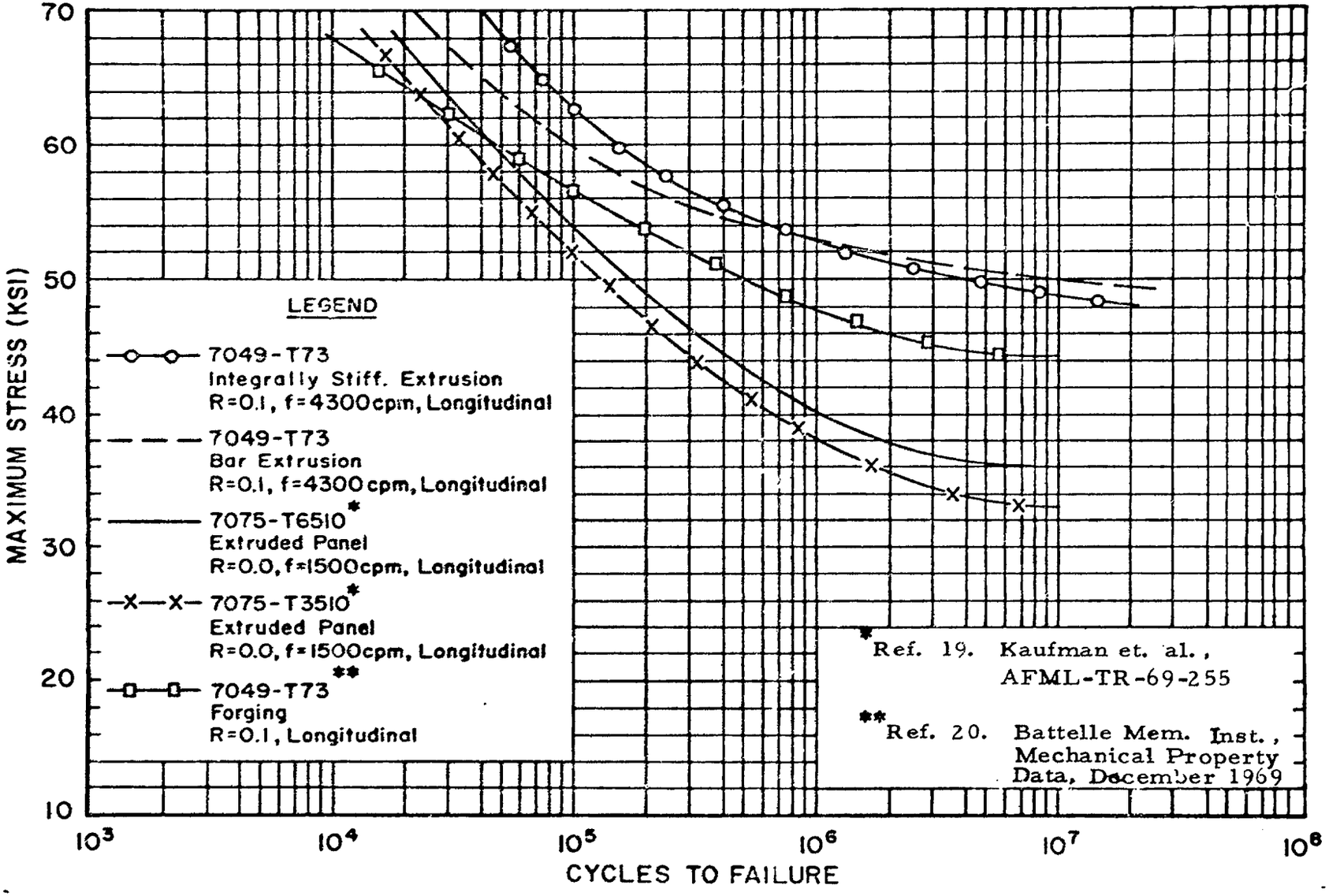

Figure 48. S/N Faituge Curves for Several Tempers of 7049 and 7075 Aluminum Alloys in the Smooth Condition.

TABLE XVI

ALTERNATE IMMERSION STRESS CORROSION RESULTS OF 7049-T73 INTEGRALLY STIFFENED EXTRUSION IN A 3.5% SODIUM CHLORIDE SOLUTION *

Stress Level (KSI)	Test Period ** (hrs)
30.0	2016
40.0	2016
45.0	2016
54.9 (80% of yield stress)	1000
61.7 (90% of yield stress)	1000

* Specimen Removed from Short Transverse Direction of Extrusion

** No Failure

the specimens were taken from a somewhat complicated shape and the possibility did exist of having specimens with their grain structure oriented other than in the short transverse direction. Since in aluminum alloys the short transverse grain direction is sensitive to corrosion attack, any misorientation of the grain structure would cause the test results to be misleading.

Each of the alternate immersion specimens were mounted, polished, etched, and photomicrographed. From these photomicrographs it appears the specimens were located with their pull direction parallel to the short transverse direction. Other possibilities for the difference in results are associated with metallurgical differences, such as grain size, and with specimen size effects. The specimens used in this investigation were 1/4-inch in diameter while those in the literature were 1/8-inch in diameter. Since it was not possible to check the grain structure of the specimens tested in the reference programs, no further comparison was made.

Fatigue crack growth rate data are presented in Figure 49. Although crack growth tests were planned for both of the T73 extrusions, crack growth testing was possible only in the bar extrusion because of the arm break-off problems in the integrally stiffened extrusion. This arm break-off problem could be caused by anisotropic material properties in the test sample. Fatigue crack growth rate data similar to the 7049-T73 bar growth data were obtained by Brownhill, et al. (Reference 20) for a 7075-T7352 hand forging and by Dubensky for 7075-T6 sheet (see Figure 49 and Reference 21).

From the limited number of tests, of which none were duplicates, it appears that the 7049 has the same general crack growth rates as the 7075 materials reported in the literature. Crack growth tests were performed with cracks oriented in the short transverse and the longitudinal directions of the bar extrusion. Little difference was observed in crack growth rates below 10 micro-inch/cycle. It appears that above this value the curve for the specimen with its crack oriented in the short transverse direction may behave differently from the other specimens. This adds proof to the indication that the crack growth rates are dependent on grain orientation. Crack growth in the T73 bar extrusion shows loading rate sensitivity in the frequency range of 200 to 600 cpm. It must be cautioned that these conclusions are drawn from a very limited number of tests.

1.3.4 Evaluation of Ti-6Al-4V Castings

A centrifugally cast peice of Ti-6Al-4V alloy was procured in the as-cast condition from Titanium Technology Corporation. After cut the casting in half, one portion was sent to General Electric Company to be annealed. The annealing heat treatment was carried out at 1350°F

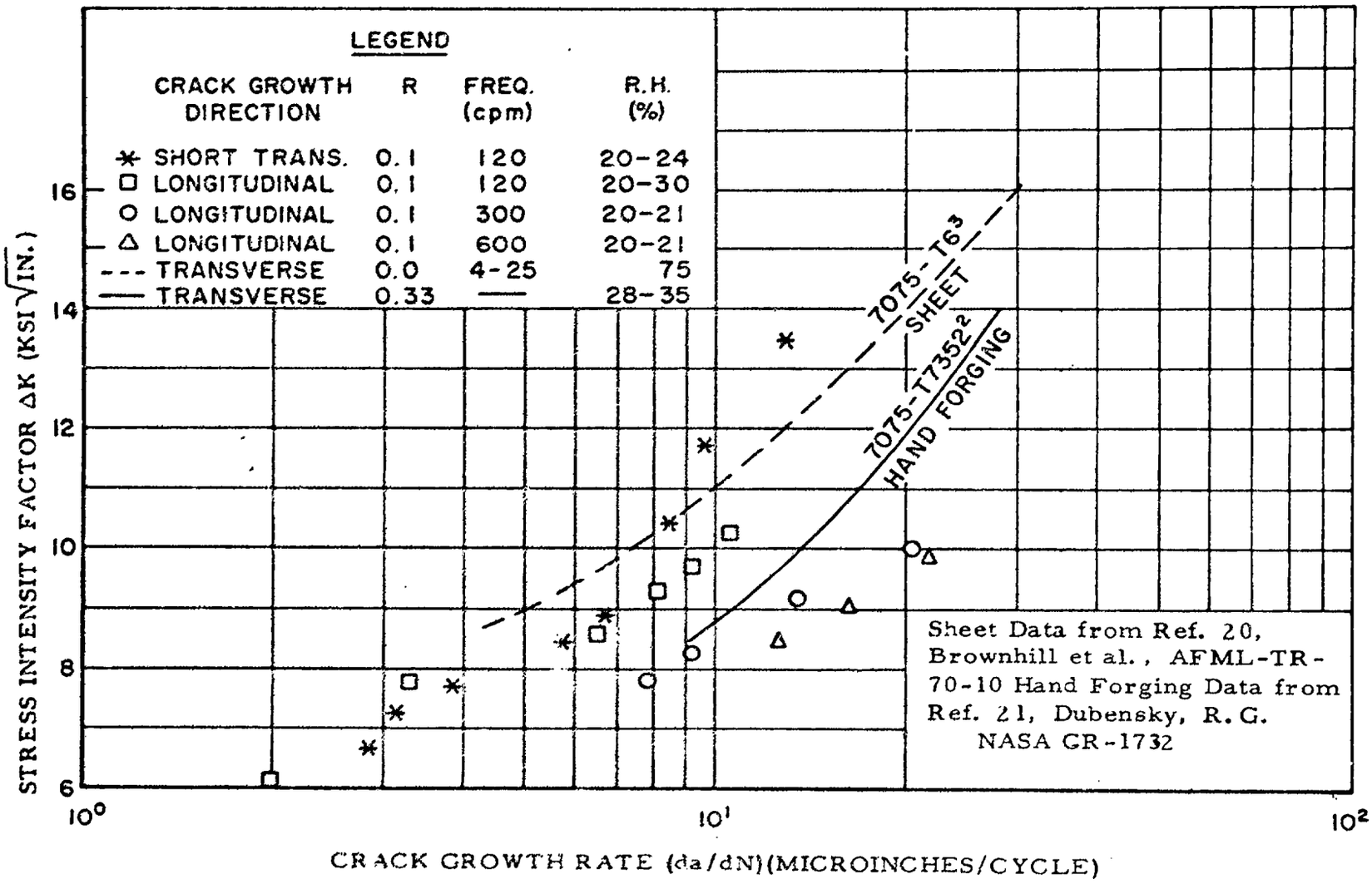

Figure 49. Stress Intensity Factor Range Versus Crack Growth Rate for 7049-T73 Bar Extrusion.

+ 25°F for four hours, followed by a furnace cool to between 800°F and 1000°F, and then air cooled. The remaining portion of the casting was tested in the as-cast condition, the objective being to investigate possible changes as a result of the annealing.

1.3.4.1 Results and Discussion

Three tensile specimens and five fatigue specimens were machined from each portion of the casting and evaluated. The results of the tensile tests are presented in Table XVII. As can be observed, the ultimate strength was not affected by the annealing heat treatment; however, the annealing did increase the yield strength slightly. The ductility of the material was reduced slightly by the annealing operation. These data agree with the tensile data found in References 22 through 24.

The fatigue test data are reported in Table XVIII. The S/N curves of this data are represented in Figure 50. The annealing cycle has a significant effect on the fatigue properties in the range of 5×10^4 to 10^6 cycles. In this range the annealed material has considerably reduced load-carrying capability. It appears that at other stress levels there is little difference between the fatigue properties of the two materials.

The fatigue data below 10^6 cycles for the as-cast material falls within the scatter band for data found in References 22 and 24 (Figure 51). However, the endurance limit (10^7 cycles) of the Titanium Technology casting is 15 KSI below the data found in Reference 22. Figure 51 presents the upper and lower limits of the data found in References 22 and 24, along with the as-cast material test results from this program.

The fatigue data generated from the annealed material are plotted in Figure 52 along with the scatter band for annealed material found in Reference 23. The fatigue properties of the annealed material used in this program were inferior to those reported in Reference 23.

1.3.5 Beta Annealed T-6Al-4V Plate

One of the older titanium alloys, Ti-6Al-4V, is being heat treated by a number of new cycles with the intent of developing superior fracture, crack growth, and stress corrosion properties. One of the new heat treat cycles was developed by Boeing and was applied to plate specimens. The heat treatment is referred to as beta annealed-mill annealed.

A half of a large center cracked fracture toughness sample that was previously tested by Boeing was obtained for use in this test program. The sample, which was 17 x 12 x 0.5-inches was cut into tensile, fracture, fatigue crack growth, and stress corrosion specimens.

Text continued on page 83

TABLE XVII

TENSILE PROPERTIES OF CAST Ti-6Al-4V

AS-CAST					ANNEALED				
Specimen No.	UTS (KSI)	Yield (KSI)	Elong. (%)	Red. Area (%)	Specimen No.	UTS (KSI)	Yield (KSI)	Elong. (%)	Red. Area (%)
T1	739.2	125.6	7.8	15.1	T4	138.7	131.4	8.7	14.7
T2	140.0	-	8.7	17.3	T5	137.9	130.7	8.3	15.9
T3	137.6	122.9	7.5	17.2	T6	138.6	131.8	7.6	12.5

TABLE XVIII

FATIGUE PROPERTIES OF CAST Ti-6Al-4V AT ROOM TEMPERATURE, R=0.1, K_t=1.0

Specimen Number		Maximum Stress (KSI)	Cycles to Failure
As Cast		87.3	170,000
	F2	100.0	30,000
	F3	70.0	1,200,000
	F4	60.0	3,400,000
	F5	55.0	11,000,000
Annealed	F6	70.0	56,000
	F7	60.0	4,100,000
	F8	80.0	41,000
	F9	65.0	67,000
	F10	62.0	420,000

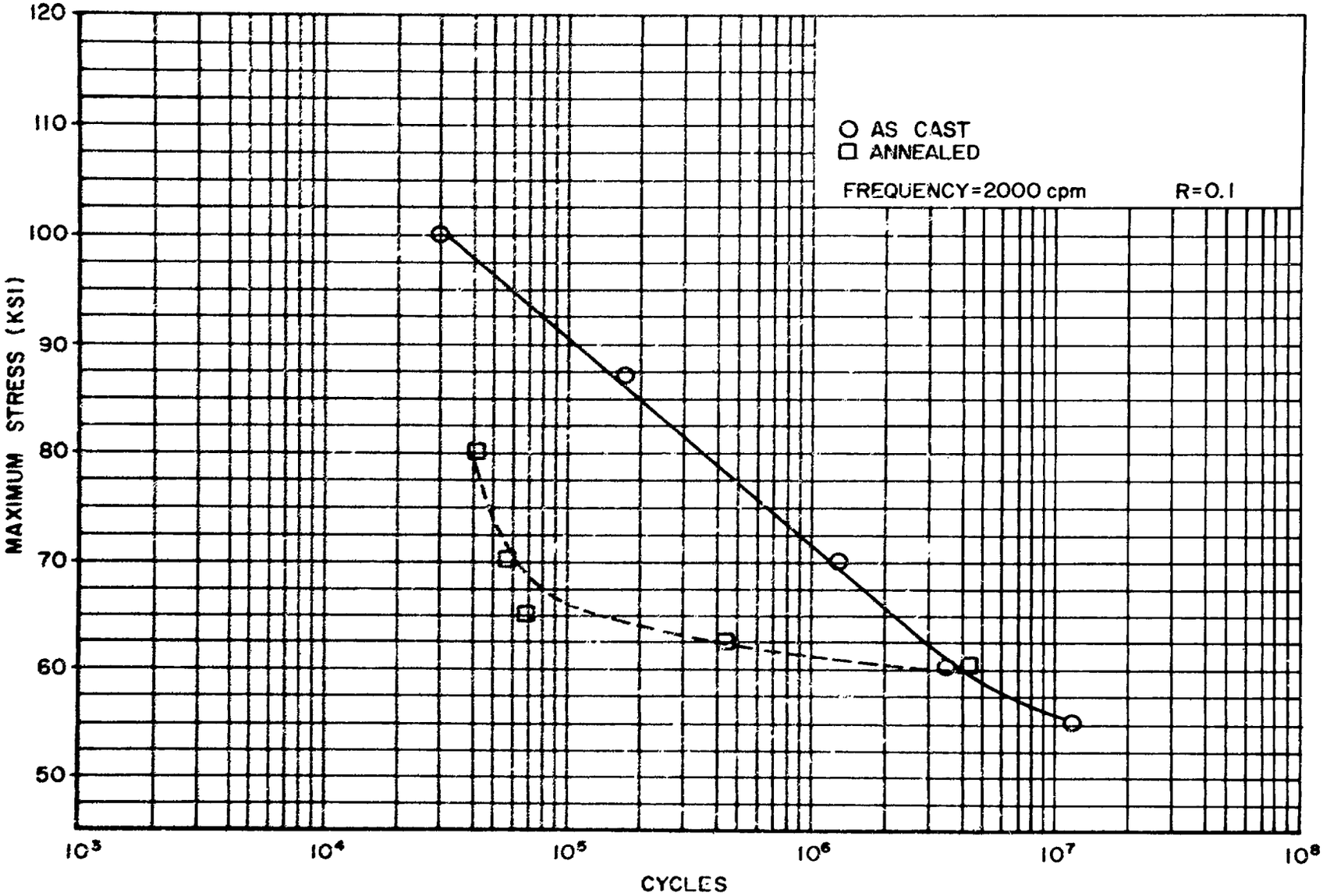

Figure 50. S/N Fatigue Curve for Ti-6 Al-4V Casting Smooth Specimens Tested at Room Temperature.

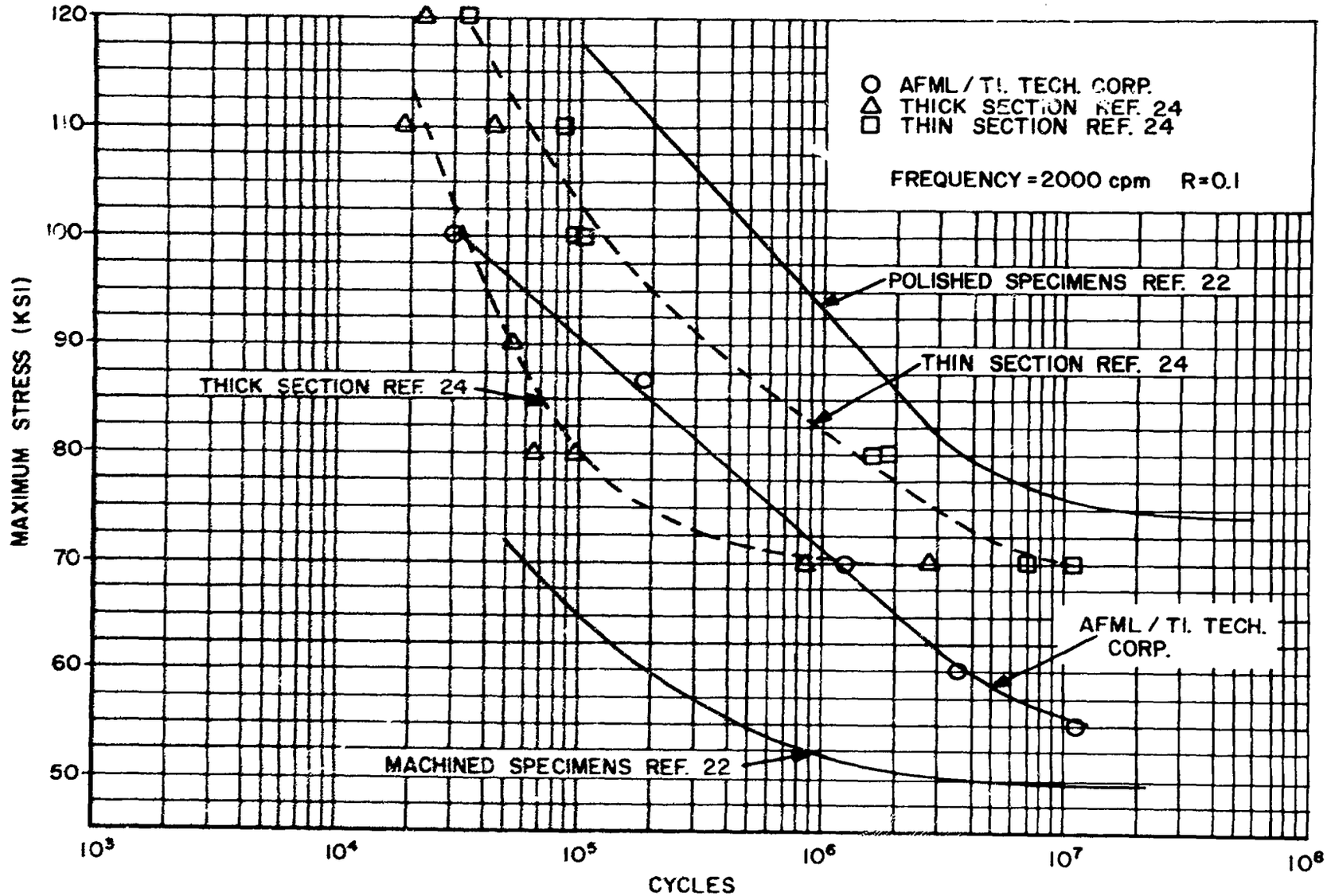

Figure 51. Ti-6Al-4V Casting (as cast).

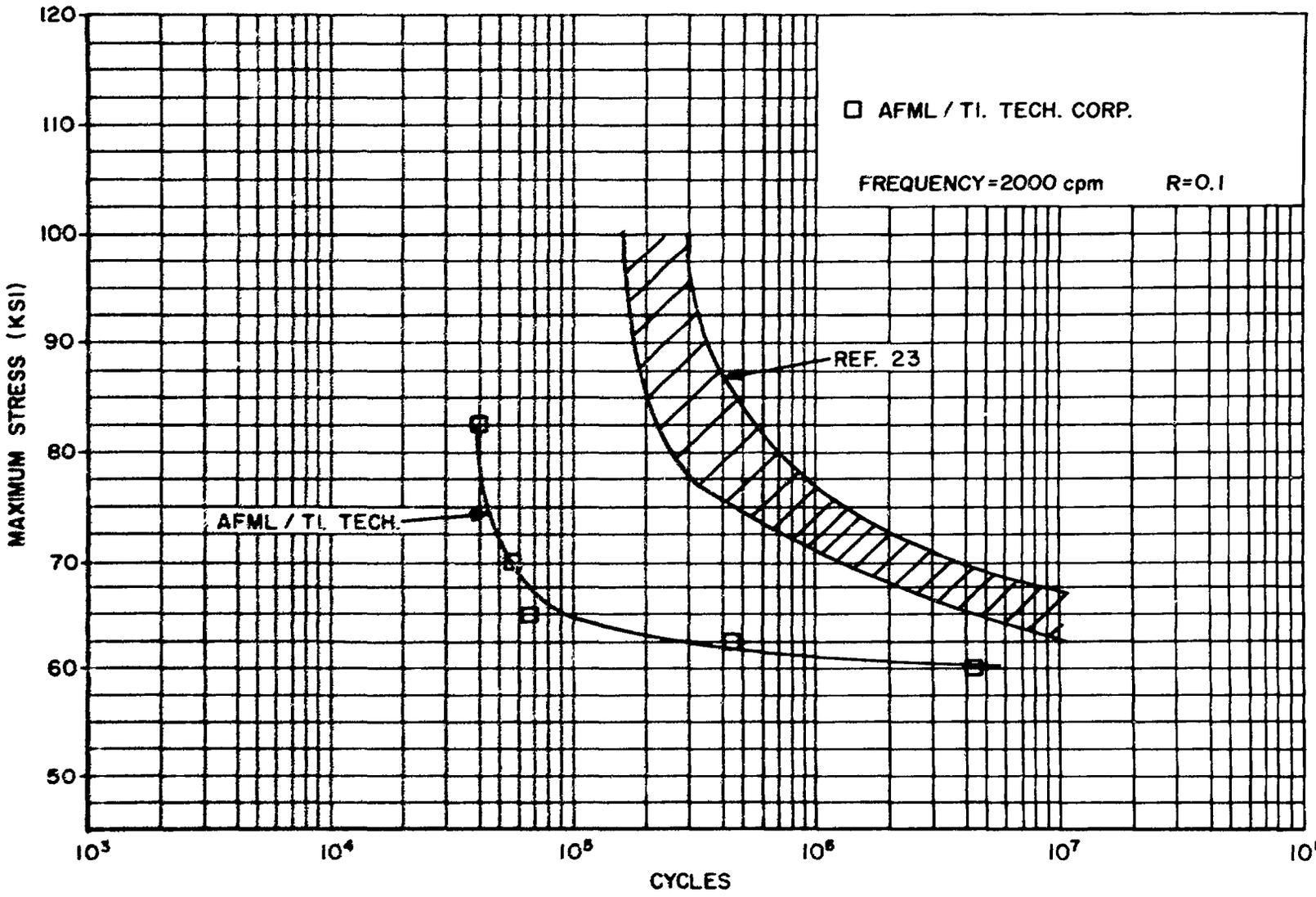

Figure 52. Ti-6Al-4V Casting (Annealed); Smooth Specimen Tested at Room Temperature.

1.3.5.1 Results and Discussion

The results of the tensile and fracture toughness tests are presented in Tables XIX and XX, respectively. Specimens designated by a "T" are transverse to the grain, while "L" indicates longitudinal. The fatigue crack growth rate test results are shown in Figure 53. The SCC results are presented in Table XXI.

The main purpose for developing the beta-annealing process was to increase the toughness and stress corrosion properties of the material to which it is applied. The success of the new heat treating technique can, therefore, be evaluated by comparing the mechanical properties developed by the new heat treatment to mechanical properties developed by a conventional heat treating procedure on the same material. A comparison of this type is somewhat difficult because the majority of the toughness tests were invalid. Most of the other mechanical properties that did compare with literature data are of little aid in the comparison because these properties are not expected to be greatly affected by heat treatment.

The fracture toughness test results were invalid by ASTM criteria for 80 percent of the samples tested. ASTM presently requires a minimum thickness of $2.5\ (K_Q/YS)^2$. It is anticipated that in the future this value will be raised which could invalidate all these fracture toughness test results presented in Table XX. Because most of the data was invalid, no conclusion can be drawn concerning the toughness ranking of this material relative to other aerospace materials or compared to other Ti-6Al-4V heat treatments.

The SCC tests did show the material to be essentially insensitive to SCC attack by a 3.5 percent NaCl solution. Again, this is not surprising when other K_{ISCC} results for Ti-6Al-4V are considered (References 25 and 29).

The fatigue crack growth rate results also agree with those in the literature (References 26, 27, and 28). As can be seen in Figure 53, there is no effect of crack orientation on the crack growth rate.

1.3.6 Evaluation of Ti-6Al-6V-2Sn Alloy

A candidate material for new Air Force systems, Ti-6Al-6V-2Sn, was procured from two different sources. North American Rockwell (NAR) provided a plate which had been obtained from Titanium Metals Corporation of America, while McDonnell-Douglas (MCAIR) supplied a forging they had procured from Reactive Metals. The NAR

Text continued on page 88

TABLE XIX

TENSILE PROPERTIES OF Ti-6Al-4V BETA ANNEALED-MILL ANNEALED PLATE

Specimen	Direction	Temp (°F)	Ultimate Strength (ksi)	Yield Strength (ksi)	R. A. (%)	Elongation (%)
T-12	Transverse	-65	162.9	154.2	10	6
T-15			152.6	152.1	17	7
T-18			162.4	154.2	16	5
T-13		0	157.1	147.0	9	6
T-16			158.0	150.2	12	7
T-19			158.2	149.4	9	4
T-14		RT	149.5	136.1	26	9
T-17			146.7	137.2	20	8
T-20			147.1	137.3	21	8
L-23	Longitudinal	-65	168.3	163.2	11	8
L-26			166.5	163.3	12	6
L-29			169.7	163.0	10	6
L-27		0	160.1	153.0	12	7
L-30			160.3	15[illegible].7	9	6
L-24			160.5	153.5	13	7
L-25		RT	150.6	142.6	19	8
L-28			151.1	142.7	20	9
L-31			148.7	140.4	16	8

TABLE XX

PLANE STRAIN FRACTURE TOUGHNESS OF
Ti-6Al-4V BETA ANNEALED-MILL ANNEALED PLATE
(ALL SPECIMENS 0.5 INCH THICK)

Specimen	Direction	Temperature (°F)	K_Q (KSI$\sqrt{IN}$)
T-1	Transverse	-65	76.2*
T-4			70.5*
T-7			70.8*
T-23			77.1*
T-2		0	72.2*
T-8			69.7*
T-21			65.1**
T-3		RT	75.0*
T-6			66.0*
T-9			65.3*
T-22			72.6*
L-1	Longitudinal	-65	71.7
L-4			68.8
L-7			74.5*
L-35			72.9
L-2		0	75.4*
L-5			67.2
L-8			66.7
L-33			69.1*
L-6		RT	73.9*
L-9			69.8*
L-32			75.5*
L-34			70.9*

* Violates ASTM K_{IC} specimen size requirements
** Excess deviation from linearity

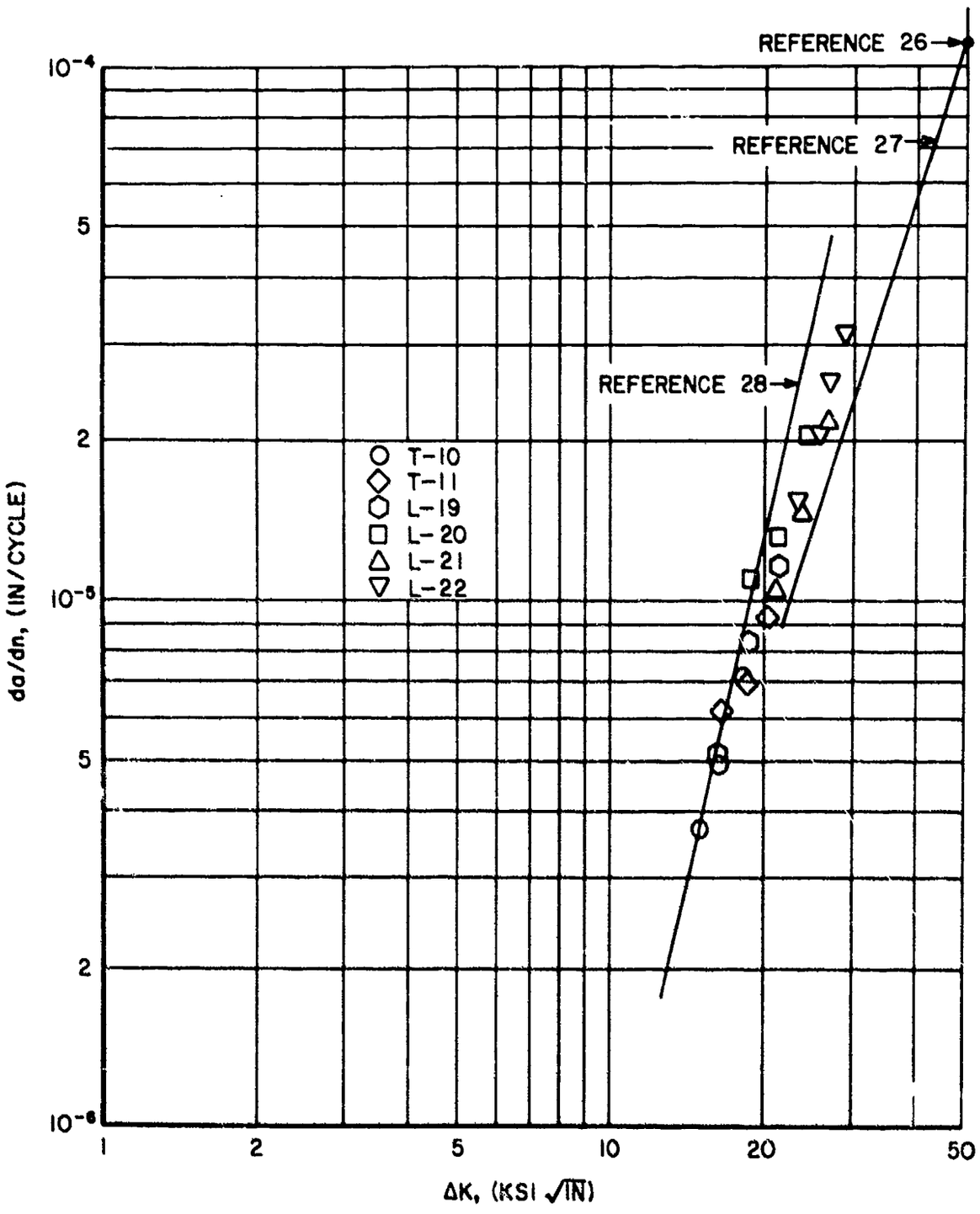

Figure 53. Air Environment Crack Growth Data for Beta Annealed-Mill Annealed Ti-6Al-4V (R = 0.1; Lab Air, Relative Humidity > 30%).

TABLE XXI

SCC PROPERTIES OF Ti-6Al-4V
BETA-ANNEALED-MILL ANNEALED PLATE
(3.5% NaCl SOLUTION)

Specimen No.	$K_{initial}$ (KSI$\sqrt{IN}$)	Time (hrs.)	
		Failure	No Failure
L-10	50	---	621
L-10	81.5	0.01	---
L-11	55	---	162
L-12	45	---	378
L-13	62	---	141
L-14	68	---	333
L-15	74.4	0.1	---
L-16	70.5	0.1	---

and MCAIR plates were annealed at 1300°F and 1350°F, respectively. The material properties investigated were tensile, fracture, fatigue crack growth, static crack growth, and fatigue (notched and unnotched).

1.3.6.1 Results and Discussion

The results of the tensile tests are presented in Tables XXII and XXIII. The fracture toughness test results are presented in Tables XXIV and XXV. Fatigue crack growth rate data are presented in Table XXVI and Figures 54, 55, and 56. Static environmental crack growth data are presented in Table XXVII. Fatigue results are presented in Table XXVIII and Figure 57.

Although the specimens (except N7) used in these tests met all the criteria imposed by ASTM Committee E-24 for K_{IC} testing, some of the values presented in Tables XXIV and XXV may be invalid. There is presently some though among ASTM members that the thickness criterion, $2.5\ (K_{IC}/Y.S.)^2$, may not be sufficiently strict for titanium alloys. This should be considered when using these data.

The laboratory air (relative humidity greater than 40%) fatigue crack growth data agree with other data from a number of sources (References 30, 31, and 32. See Figures 54). It also appears that for the range of crack growth rates investigated, there is no effect of H_2O or JP-4 on the crack growth rate. All the crack growth data fall in a scatter band slightly above the Naval Aresearch Laboratory (NRL) data and on the low side of a scatter band for MCAIR data. Other data for this alloy (not shown) indicate no change in growth rate from dry air to lab air (Reference 32).

The stress corrosion test results (Table XXVII) show the material to have a threshold stress intensity for crack growth in a distilled H_2O environment of 40 KSI$\sqrt{IN}$. These tests were originally intended to give results in terms of K versus crack growth rate (da/dt). However, the raw data were unrepeatable and could not be confidently correlated to crack growth rate.

1.3.7 Parametric Analysis of Creep and Stress Rupture Data

Future flight vehicle requirements present a need for reusable components which will sustain temperatures in the regime of 1832°F (1000°C) to 3272°F (1800°C). Coated refractory metal alloys are being considered for utilization in a number of applications where a high-temperature load carrying capability is necessary. With this in mind, an effort has been initiated to evaluate the influence of an oxidizing environment, and the coating required for use in such an environment, on

Text continued on page 101

TABLE XXII

TENSILE PROPERTIES OF NAR Ti-6Al-6V-2Sn

Specimen	Direction	Temp. (°F)	Ultimate Strength (ksi)	Yield Strength (ksi)	Elongation (%)	Reduction of Area (%)
A2	Trans.	-65	169.8	167.5	15.8	36.8
A3			170.4	169.3	15.1	31.6
A6		0	159.0	155.6	15.2	34.0
A11			156.6	150.8	14.4	35.5
A7		R.T.	154.1	148.7	16.9	33.6
A8			152.7	146.9	18.7	37.0
A9		200	137.6	129.7	16.9	35.4
A10	↓		140.9	132.4	16.4	36.7
B3	Long.	-65	170.1	167.7	15.9	35.8
B4			167.6	165.4	14.2	33.6
B1		0	164.7	160.1	15.4	30.6
B2			162.4	158.4	13.9	31.2
B5		R.T.	152.2	147.8	17.2	39.5
B6			151.8	148.2	16.7	40.2
B7		200	141.8	133.4	17.4	42.7
B8	↓		139.9	130.5	18.2	47.6

TABLE XXIII

TENSILE PROPERTIES OF MCAIR Ti-6Al-6V-2Sn

Specimen	Direction	Temp. (°F)	Ultimate Strength (ksi)	Yield Strength (ksi)	Elongation (%)	Reduction of Area (%)
F3	Trans.	R.T.	160.7	149.9	9	14
F8	↓	↓	159.4	150.8	11	32
F10	↓	↓	162.6	152.7	15	40
G3	Long.	↓	166.2	152.8	10	26
G8	↓	↓	168.2	155.9	13	23
G11	↓	↓	165.0	152.4	13	20
F2	Trans.	0	172.1	162.2	10	19
F7	↓	↓	174.3	167.4	12	25
F12	↓	↓	167.9	159.1	15	29
G2	Long.	↓	176.9	168.6	11	24
G7	↓	↓	174.0	163.4	10	15
G10	↓	↓	174.5	163.6	12	30
F1	Trans.	-65	176.7	-	9.9	17
F6	↓	↓	180.9	173.0	9.4	19
F9	↓	↓	175.1	-	10.6	26
G1	Long.	↓	180.0	172.9	9.4	15
G6	↓	↓	178.8	-	9.0	12
G9	↓	↓	176.3	-	7.6	14
F4	Trans.	+200	153.7	135.4	14	41
F5	↓	↓	154.3	138.1	15	40
F11	↓	↓	153.1	138.5	17	45
G4	Long.	↓	157.9	137.5	17	41
G5	↓	↓	153.5	134.5	12	33
G12	↓	↓	153.9	137.8	15	36

TABLE XXIV

FRACTURE TOUGHNESS PROPERTIES OF NAR Ti-6Al-6V-2Sn
(Specimen Thickness = 0.5 inch)

Specimen	Direction	Temperature (°F)	K_{IC} (KSI$\sqrt{IN}$)
K4	Trans.	-65	34.9
K8			32.7
K12			33.3
			33.6 avg.
N4	S. Trans.	-65	35.4
N10			34.6
N15			34.4
			34.8 avg.
P4	Long	-65	36.7
P8			37.0
P12			35.9
			36.5 avg.
K3	Trans.	0	34.2
K7			33.2
K11			29.8
			32.4 avg.
N3	S. Trans.	0	36.7
N9			32.8
N14			34.6
			34.7 avg.
P3	Long	0	42.4
P7			38.9
PL			37.0
			39.4 avg.
K2	Trans.	R.T.	39.4
K6			41.5
K10			38.6
			39.8 avg.
N2	S. Trans.	R.T.	44.4
N8			47.1
N12			40.7
			44.1 avg.

TABLE XXIV (concluded)

FRACTURE TOUGHNESS PROPERTIES OF NAR Ti-6Al-6V-2Sn
(Specimen Thickness = 0.5 inch)

Specimen	Direction	Temperature (°F)	K_{IC} (KSI$\sqrt{IN}$)	
P2	Long	R.T.	45.6	
P6			43.6	
P10			44.5	
				44.5 avg.
K1	Trans.	200	56.5	
K5			53.9	
K9			55.3	
				55.2 avg.
N1	S. Trans.	200	50.8	
N7			(64.2)*	
				57.5 avg.

*Violates ASTM K_{IC} thickness criterion

TABLE XXV

FRACTURE TOUGHNESS PROPERTIES OF MCAIR Ti-6Al-6V-2Sn

Specimen	Direction	Temperature (°F)	K_{IC} (KSI$\sqrt{IN}$)
E1[1]	Trans.	R. T.	56.8
E2[1]	↓	↓	58.4
E3[1]	↓	↓	60.5
			58.6 avg.
H1[2]	S. Trans.	↓	54.1
H2[2]	↓	↓	54.5
H3[2]	↓	↓	66.4
			58.3 avg.
D3[3]	Long.	↓	57.6
D13[3]	↓	↓	52.7
D23[3]	↓	↓	47.3
			52.5 avg.
D2[3]	↓	0	51.3
D12[3]	↓	↓	45.4
D22[3]	↓	↓	36.7
			44.5 avg.
D1[3]	↓	-65	51.5
D11[3]	↓	↓	42.6
D21[3]	↓	↓	38.8
			44.3 avg.
D4[3]	↓	+200	63.2
D14[3]	↓	↓	64.6
D24[3]	↓	↓	59.8
			62.5 avg.

[1] Specimen thickness = 0.75-inch

[2] Specimen thickness = 0.50-inch

[3] Specimen thickness = 0.65-inch

TABLE XXVI

CRACK GROWTH RATE OF MCAIR-Ti-6Al-6V-2Sn IN AIR AND VARIOUS ENVIRONMENTS (R = 0.1)

Specimen	Environment	ΔK (KSI$\sqrt{IN}$)	da/dn (Inch/Cycle)
D5	Air	28.5	2.5×10^{-5}
		31.6	4.3×10^{-5}
		38.8	6.9×10^{-5}
D7	Air	26.0	2.0×10^{-5}
		27.0	3.1×10^{-5}
		25.6	1.4×10^{-6}
		19.1	5.0×10^{-6}
D8	Air	29.8	1.3×10^{-5}
		32.0	3.0×10^{-5}
		33.2	3.9×10^{-5}
D25	Air	38.7	1.1×10^{-4}
		33.5	5.2×10^{-5}
		29.5	3.1×10^{-5}
		26.3	2.0×10^{-5}
D6	H_2O	27.8	3.8×10^{-5}
		24.5	2.6×10^{-5}
		21.4	2.0×10^{-5}
D29	H_2O	21.4	1.1×10^{-5}
		24.3	1.8×10^{-5}
		27.8	2.6×10^{-5}
		34.0	3.6×10^{-5}
D31	JP4	21.3	1.0×10^{-5}
		33.8	3.5×10^{-5}
		26.4	2.9×10^{-5}
D37	JP4	53.2	7.0×10^{-4}
		45.6	2.2×10^{-4}
		42.9	1.5×10^{-4}
D40	JP4	16.8	7.4×10^{-6}
		28.4	2.2×10^{-5}
		34.3	4.9×10^{-5}

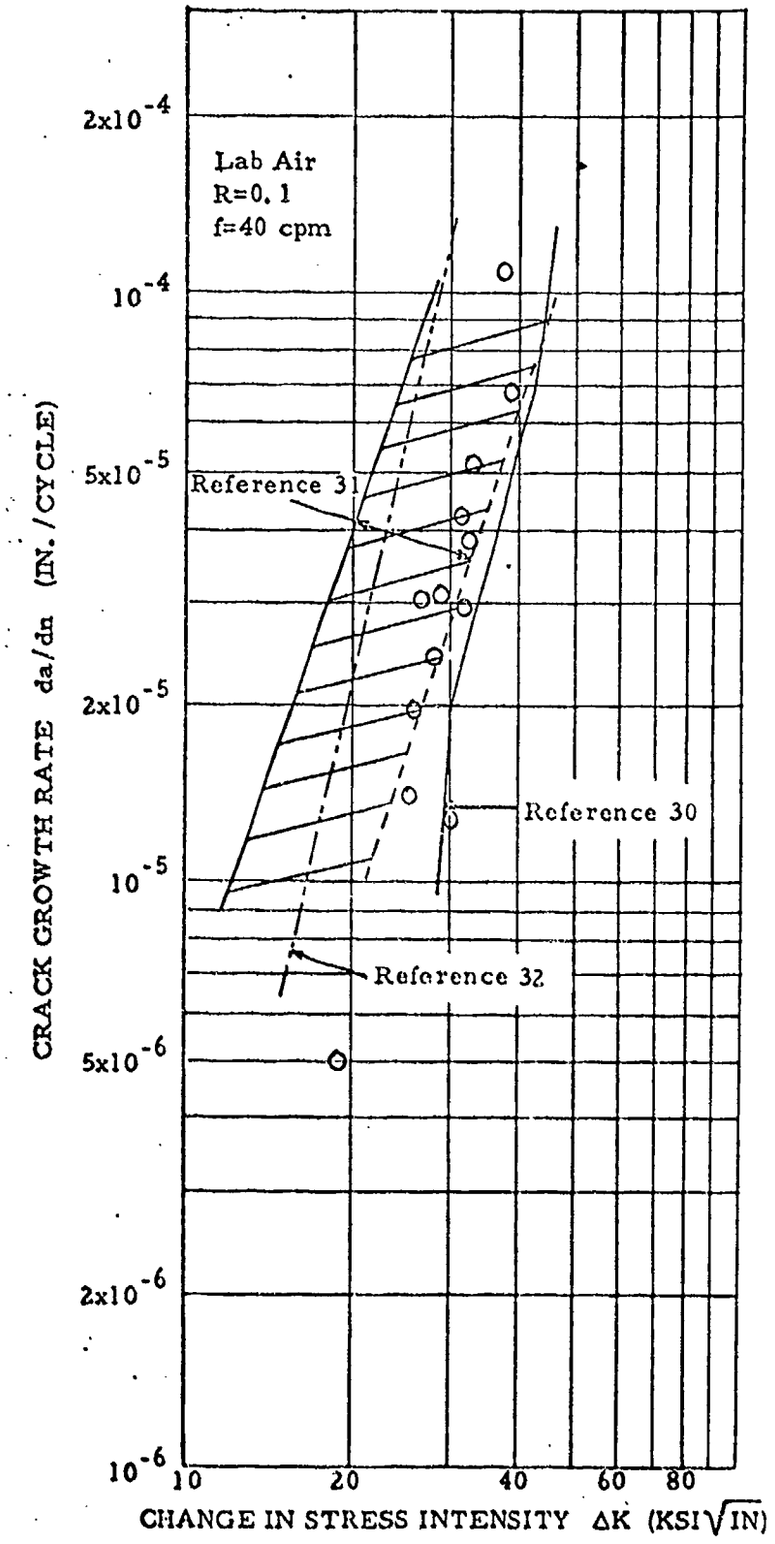

Figure 54. Crack Growth Rate for Ti-6Al-6V-2Sn (MCAIR).

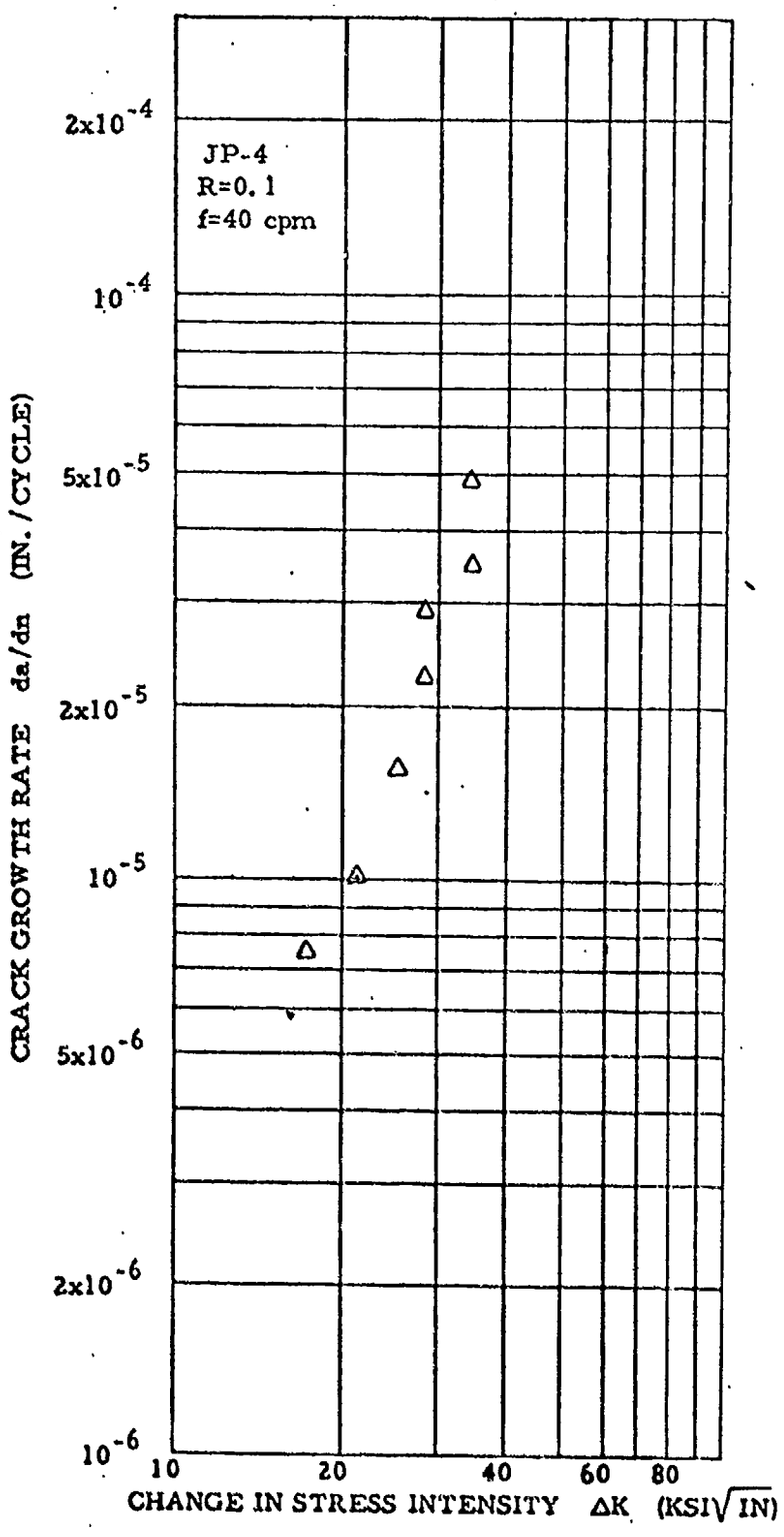

Figure 55. Crack Growth Rate Data for Ti-6Al-6V-2Sn (MCAIR).

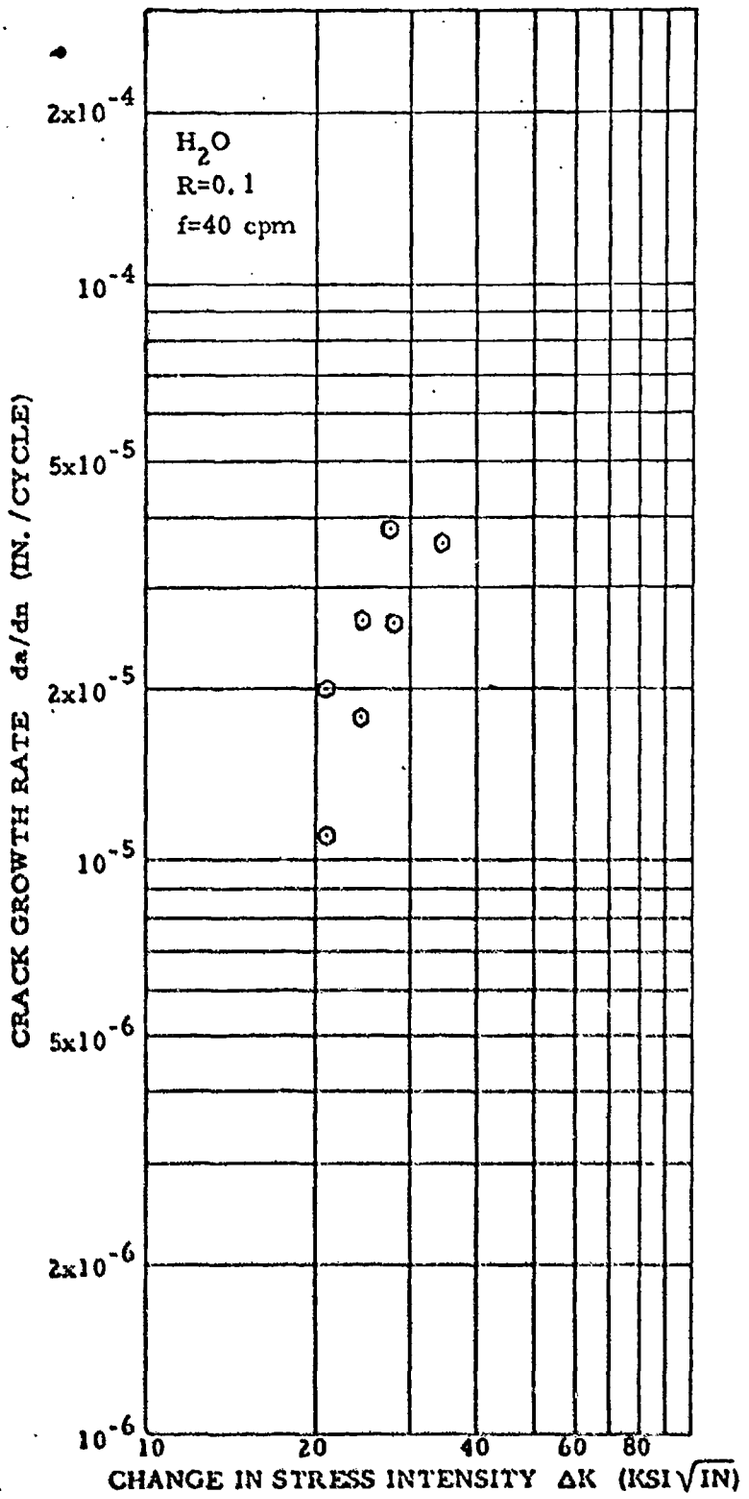

Figure 56. Crack Growth Rate Data for Ti-6Al-6V-2Sn (MCAIR).

TABLE XXVII

K_{ISCC} TEST RESULTS FOR Ti-6Al-6V-2Sn IN DISTILLED H_2O (MCAIR)

$K_{initial}$ KSI$\sqrt{IN}$)	Time (hr)	
	Failure	No Failure
36.4	-	168
44.2	1.5	-
40.0	3.0	-
39.4	-	333
39	-	119
42.6	2.4	-

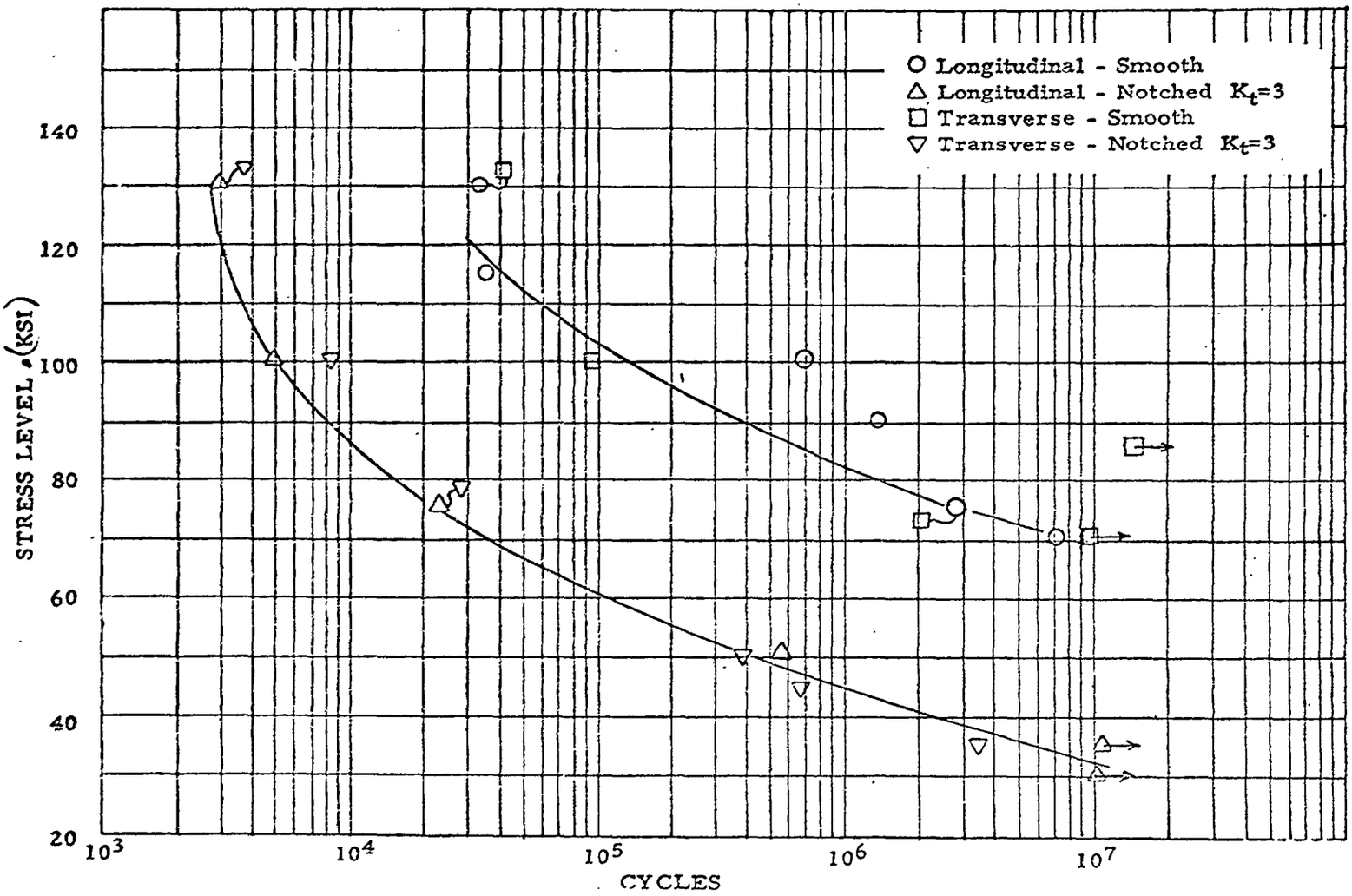

Figure 57. Titanium 6Al-6V-2Sn Room Temperature Fatigue Data (NAR Annealed Plate, R = 0.1)

TABLE XXVIII

ROOM TEMPERATURE FATIGUE RESULTS FROM
NAR Ti-6Al-6V-2Sn (R = 0.1)

LONGITUDINAL

Smooth No.	KSI	Cycles	Notched No.	KSI	Cycles
L-1	130	3.6×10^4	L-7	130	3.0×10^3
L-2	115	3.9×10^4	L-8	100	5.0×10^3
L-3	100	7.3×10^5	L-9	75	2.3×10^4
L-4	90	1.44×10^6	L-10	50	5.6×10^5
L-5	75	3.0×10^6	L-11	30	$1.04 \times 10^7 \rightarrow$
L-6	70	7.5×10^6	L-12	35	$1.1 \times 10^7 \rightarrow$

TRANSVERSE

Smooth No.	KSI	Cycles	Notched No.	KSI	Cycles
T-1	130	3.5×10^4	T-7	100	8.6×10^3
T-2	85	$1.5 \times 10^7 \rightarrow$	T-8	130	3.0×10^3
T-3	100	9.9×10^4	T-9	75	2.3×10^4
T-4	70	$1.0 \times 10^7 \rightarrow$	T-10	50	3.9×10^5
T-5	Bad Threads		T-11	45	6.8×10^5
T-6	75	2.9×10^6	T-12	35	3.5×10^6

$\rightarrow$ Indicate No Failure

the creep properties of a tantalum alloy (T-222). To date the evaluation of the T-222 is only partially complete. However, in conjunction with this effort, it was decided to investigate the tractable techniques of correlating and extrapolating creep data.

This work is oriented toward laboratory utilization for selecting a pretest estimated stress needed to obtain a percentage of creep for a specified time and temperature. Limited available data prohibit this study from producing design information since design values must be based on statistical numbers.

Much emphasis has been placed on the development of analytical methods of reducing high-temperature creep data so that it can be extrapolated over several log-cycles of stress and/or time. Several linear parametric methods using time, temperature, and stress level for the plotting and extrapolating of creep data are in existence. The three tractable parametric methods commonly in use today are the Larson-Miller, Manson-Haferd, and the Dorn parameters. This investigation was limited to these three procedures.

Although other reports have been published (References 33 and 34) in which linear parametric procedures were investigated, they have generally dealt with rupture data or with the optimization of parametric constants. This effort encompasses creep and stress rupture data along with the optimization of constants.

1.3.7.1 Procedure

Creep and stress rupture data of two tantalum alloys, T-222 and T-111 and two columbium alloys, D-43 and Cb-752 were extracted from the published literature (Reference 35 through 47). These literature data were combined with T-222 data presently being generated in the testing portion of this program. Data were selected only in the testing temperature regime of 1832°F to 3000°F. The majority of the data was chosen to have a test time duration of less than 1000 hours. The refractory alloys were generally tested in a vacuum environment of 10^{-6} TORR to 10^{-10} TORR. The data for each individual alloy were selected so as to have the same heat treatment (see Table XXIX).

The data were programmed into an IBM 7094 digital computer to produce Larson-Miller, Manson-Haferd, and Dorn parametric plots of 0.5% creep, 1% creep, 5% creep, and stress rupture data. Data for each refractory alloy were plotted for a percentage of creep only if ample data were available for that alloy. A best-fit curve was fitted to the parametric data by the least-squares method.

The empirical parametric equations used in this study are as follows:

Text continued on page 106

TABLE XXIX

CREEP DATA PLOTTED BY PARAMETRIC METHODS

(0.5% Creep)

Alloy	Temp. (°F)	Time (hrs.)	Stress Level (KSI)	Reference
T-222*	2552	0.03	40.0	Current Program
	2450	120.0	8.0	Current Program
	2400	175.0	8.0	35
	2400	500.0	6.0	35
	2200	4200.0	8.0	35
	2200	1400.0	12.0	35
	2200	550.0	16.0	35
	2056	600.0	19.2	36
	1832	90.0	54.0	Current Program
	1832	45.0	58.0	Current Program
T-111*	2500	72.0	8.3	37
	2500	67.0	9.2	37
	2400	76.0	12.7	37
	2400	27.0	14.7	37
	2200	120.0	8.0	38
	2200	24.0	21.3	37
	2000	5400.0	11.0	38
	2000	1000.0	20.0	39
	1625	12300.0	30.0	38
	1600	7000.0	35.0	38

*Final Heat Treatment: 3000°F for One Hour.

TABLE XXIX (continued)

CREEP DATA PLOTTED BY PARAMETRIC METHODS

(5% Creep)

Alloy	Temp. (°F)	Time (hrs.)	Stress Level (KSI)	Reference
D-43*	2200	180.0	9.0	42
	2200	32.0	12.0	42
	2200	12.0	18.0	42
	2000	925.0	10.0	43
	2000	250.0	15.0	42
	2000	60.0	17.0	42
	2000	5.0	25.0	42
	1808	225.0	23.0	42
	1808	42.0	28.0	42
	1808	5.0	35.0	42
Cb-752**	2500	1.0	8.5	40
	2500	0.13	15.0	40
	2200	40.0	8.9	41
	2200	24.0	11.0	41
	2200	5.0	15.0	41
	2000	220.0	10.0	43
	2000	19.0	18.0	41
	2000	5.0	22.0	41
	1800	55.0	25.0	41
	1800	3.0	35.0	41
(1.0% Creep)				
Cb-752**	2500	0.5	8.5	40
	2500	1.0	7.0	40
	2200	6.0	8.9	41
	2200	2.1	11.0	41
	2200	0.9	15.0	41
	2000	55.0	9.0	41
	2000	25.0	13.0	41
	2000	5.5	18.0	41
	1800	70.0	19.0	41
	1800	15.0	25.0	41

* Duplex Anneal

** Final Heat Treatment 2800°F Solution Anneal

TABLE XXIX (continued)

CREEP DATA PLOTTED BY PARAMETRIC METHODS

(Stress Rupture)

Alloy	Temp. (°F)	Time (hrs.)	Stress Level (KSI)	Rererence
T-222*	3000	10.0	12.0	44
	3000	1.0	18.0	44
	2552	0.1	40.0	Current Program
	2400	59.7	25.0	45
	2400	57.6	25.0	45
	2400	12.8	33.0	45
	2400	8.4	33.0	45
	2400	1.0	47.0	44
	2200	1.0	65.0	44
	1832	150.0	58.0	Current Program
D-43**	2400	10.0	10.5	46
	2400	1.0	15.0	46
	2200	95.0	12.0	42
	2200	12.0	18.0	42
	2200	6.5	20.0	42
	2000	500.0	15.0	42
	2000	10.0	28.5	46
	1800	65.0	28.0	42
	1800	7.5	30.0	42
	1800	1.8	40.0	42
(1.0% Creep)				
T-222*	2552	0.03	40.0	Current Program
	2450	220.0	8.0	Current Program
	2400	900.0	6.0	35
	2400	300.0	8.0	35
	2400	600.0	12.0	36
	2200	7500.0	8.0	35
	2200	2500.0	12.0	35
	2056	900.0	19.2	36
	1832	200.0	54.0	Current Program
	1832	140.0	58.0	Current Program

*Final Heat Treatment of 3000°F for One Hour

**Duplex Anneal

TABLE XXIX (concluded)

CREEP DATA PLOTTED BY PARAMETRIC METHODS

(1.0% Creep)

Alloy	Temp. (°F)	Time (hrs.)	Stress Level (KSI)	Reference
T-111*	2500	117.0	8.3	37
	2500	93.0	9.2	37
	2500	26.0	12.7	37
	2400	300.0	10.0	37
	2400	119.0	12.7	37
	2400	42.0	14.7	37
	2200	2900.0	8.0	38
	2200	45.0	21.3	37
	2000	670.0	20.0	37
	2000	13250.0	13.0	38
(Stress Rupture)				
Cb-752**	2400	1.7	15.0	47
	2400	80.0	9.0	47
	2200	19.8	15.0	47
	2200	200.0	8.9	41
	2000	1.9	28.0	47
	2000	18.0	22.0	41
	2000	18.0	23.0	47
	2000	70.0	18.0	41
	1800	7.5	35.0	41
	1800	140.0	25.0	41

* Final Heat Treatment: 3000°F for One Hour.

** Final Heat Treatment 2800°F Solution Anneal

Larson-Miller	$P = (T + 460)(\log + C)$
Dorn	$D = te^{-H/T}$
Manson-Haferd	$M = \frac{T - T_a}{\log t - \log t_a}$

where:

P, D, M	=	parameters
T	=	temperature
t	=	time
C, H, T_a, t_a	=	constants

The values of constants H, C, T_a and t_a were determined by graphical methods (Reference 48) for all data and then corrected to values which gave a better correlation using the computer program.

1.3.7.2 Results and Discussion

The parametric plots of 0.5% creep, 1% creep, 5% creep, and stress rupture for the aforementioned refractory alloys are presented in Figures 58 to 69.

Although parametric constants are generally considered to be material constants, it was determined that for the purpose of this investigation a single value of each constant was necessary. The constants for each individual alloy vary only slightly from those constants obtained using the entire refractory alloy data. The values of C, H, T_a, and t_a considering all refractory alloy data are as follows: C = 13.5, H = 70,000, T_a = 1000, and t_a = 7.

As can be observed by the parametric plots (Figures 58 to 69), each method correlated the data reasonably well. Since limited data were available it was impossible to statistically determine whether one method gave a better correlation than another. Extrapolation would likewise not be warranted based on the limited available data.

The most creep-resistant of the four refractory alloys parametrically compared at 0.5% creep, 1.0% creep and rupture was tantalum alloy T-222. Sparse data for T-222 at 5% creep would not allow its comparison. The ranking of the other refractory alloys from the highest to the lowest creep resistance are T-111, D-43, and Cb-752.

Text continued on page 119

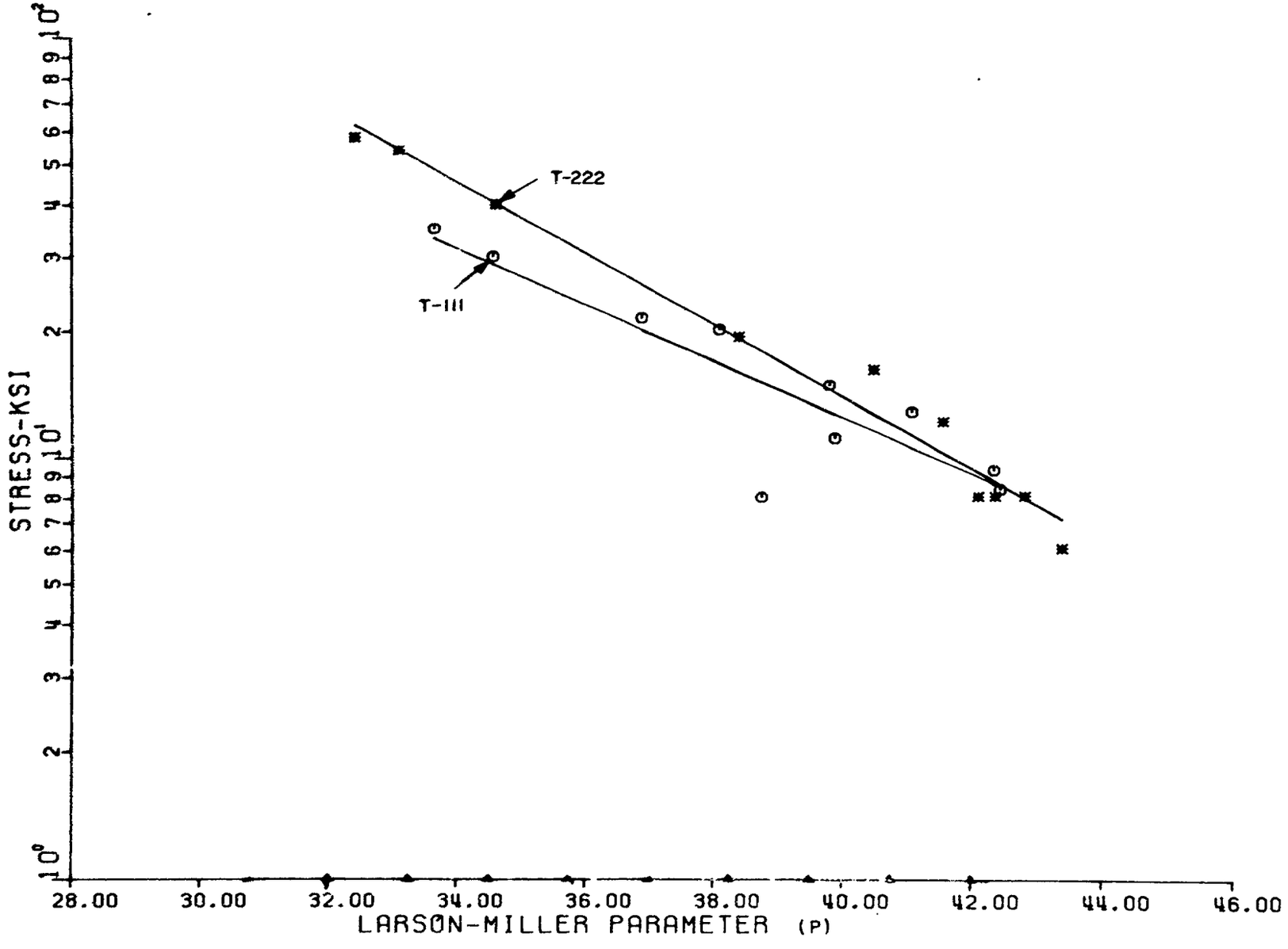

Figure 58. Larson-Miller Parameter Plot (C = 13.5) for T-222 and T-111 at 0.5% Creep.

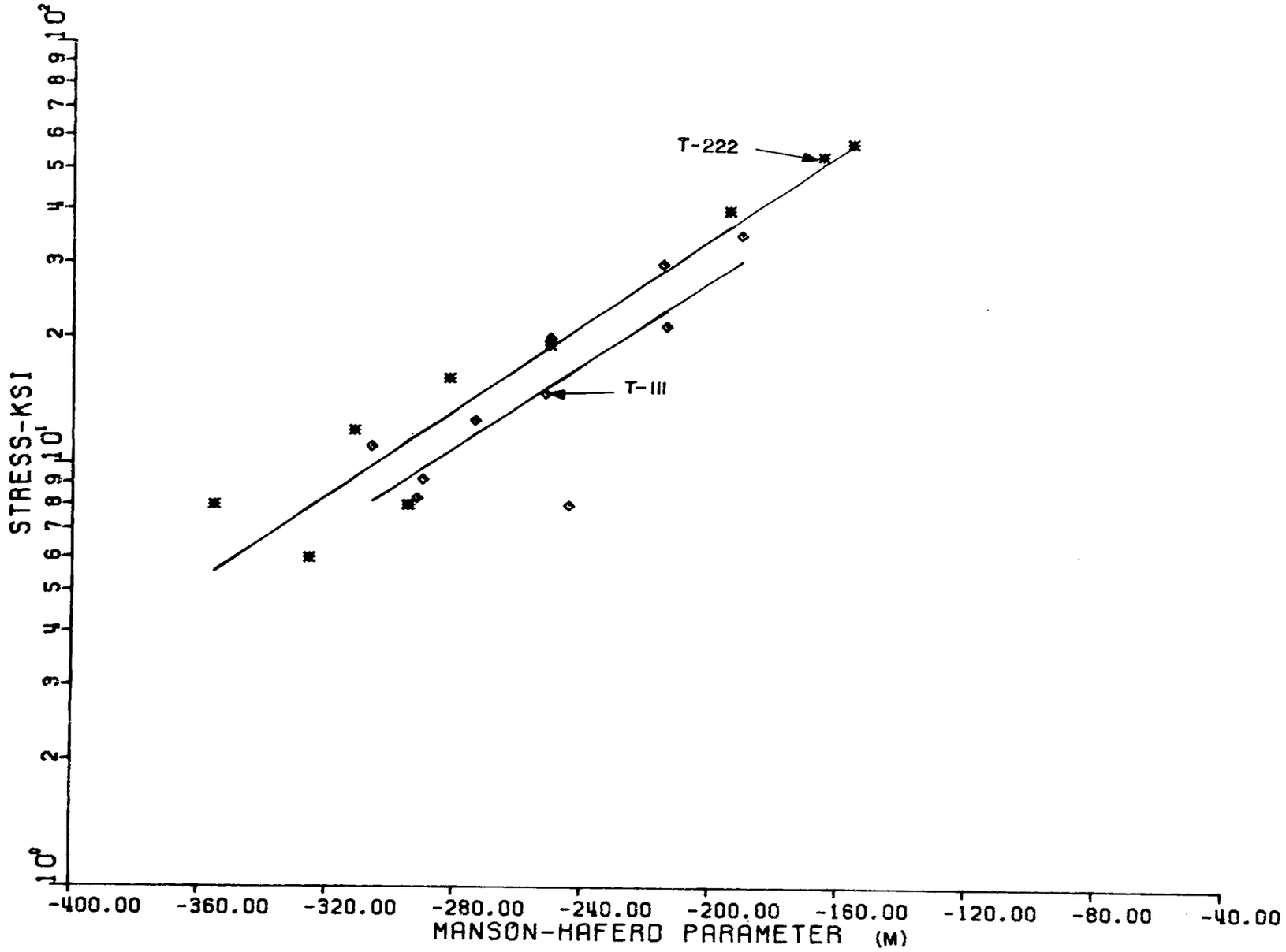

Figure 59. Manson-Haferd Parameter Plot (T = 1000, t_a = 7.0 for T-222 and T-111 at 0.5% Creep.

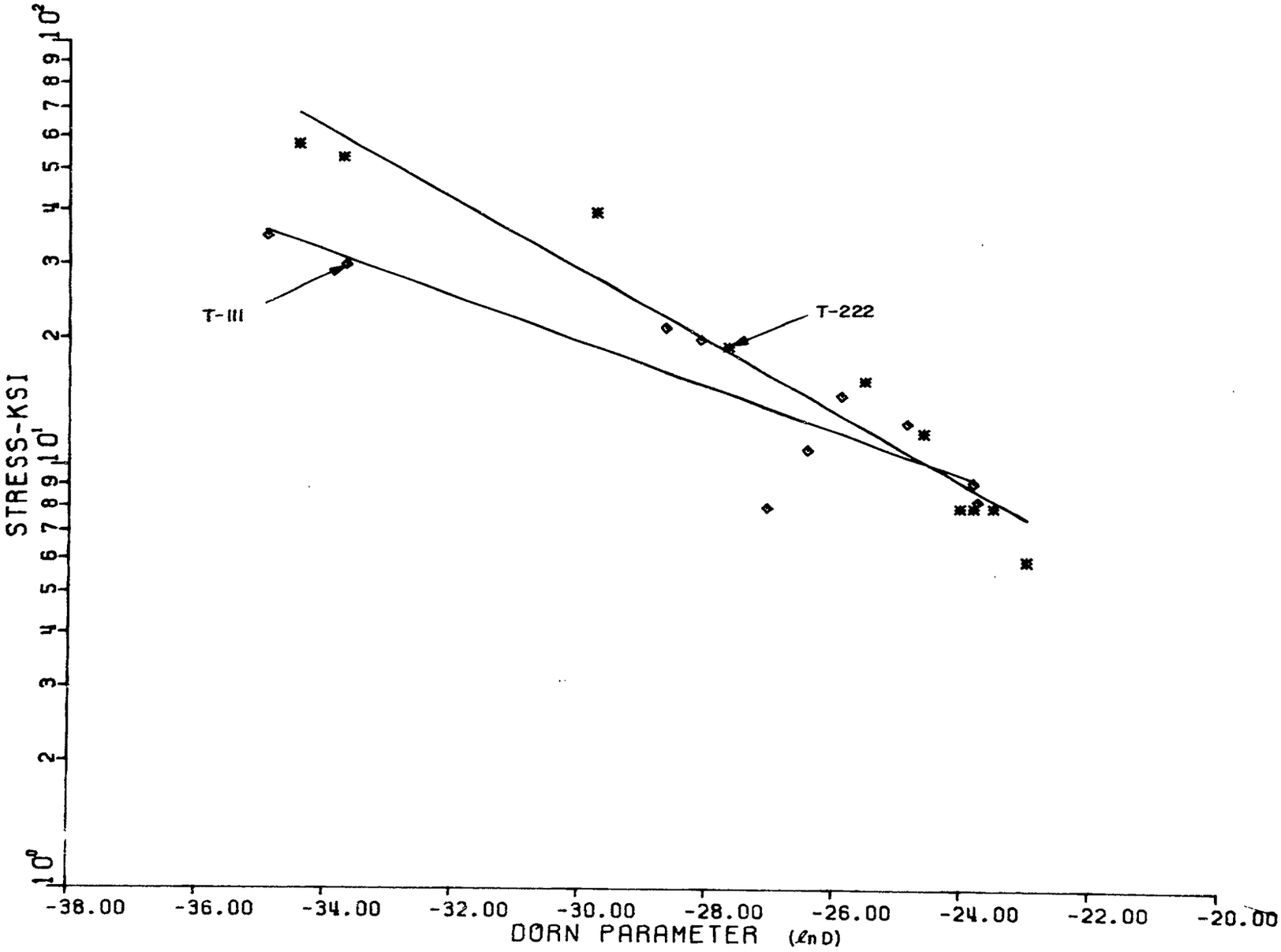

Figure 60. Dorn Parameter Plot (H = 70, 000) for T-222 and T-111 at 0.5% Creep.

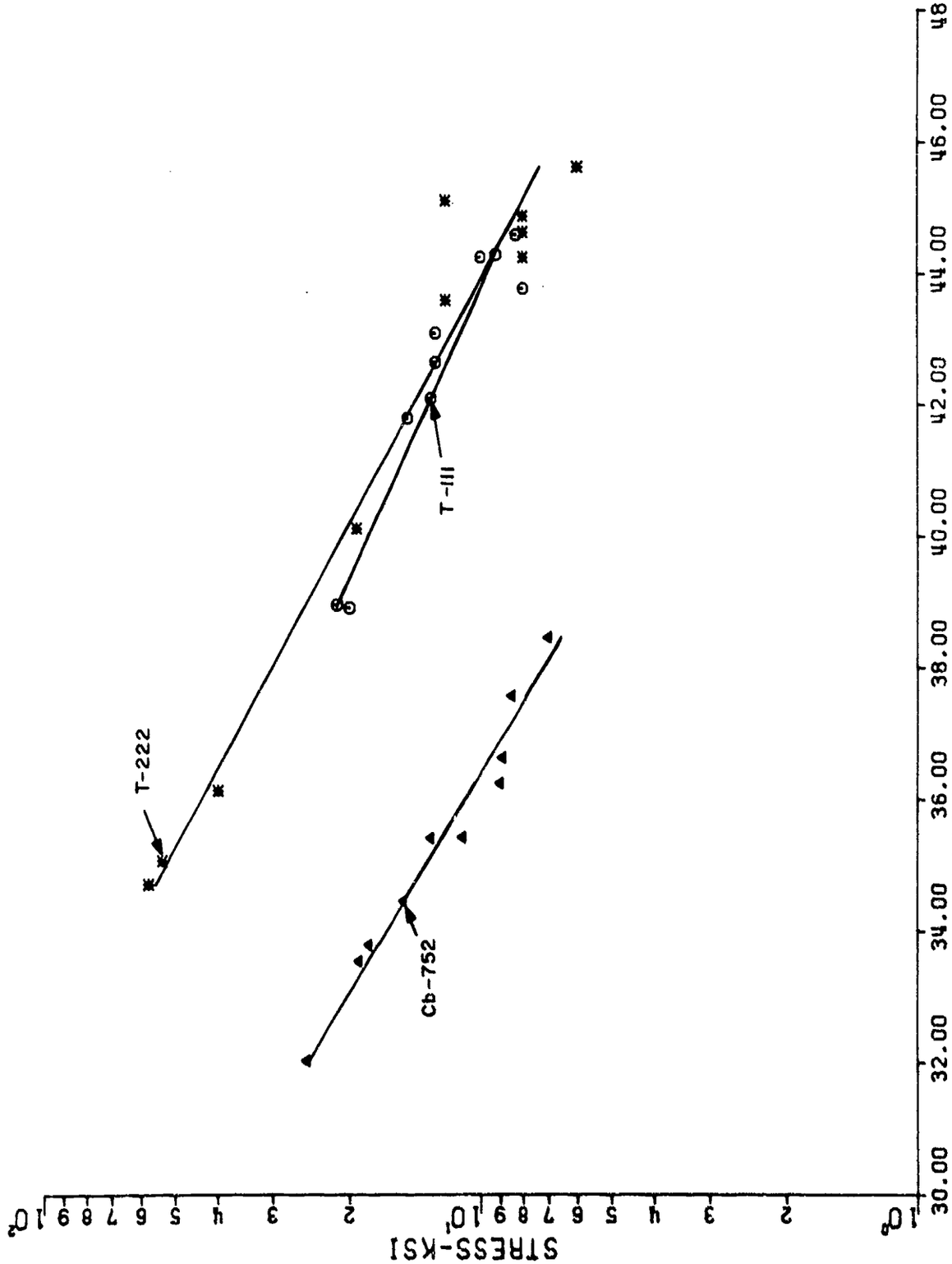

Figure 61. Larson-Miller Parameter Plot (C = 13.5) for T-222, T-111, and Cb-752 at 1.0% Creep.

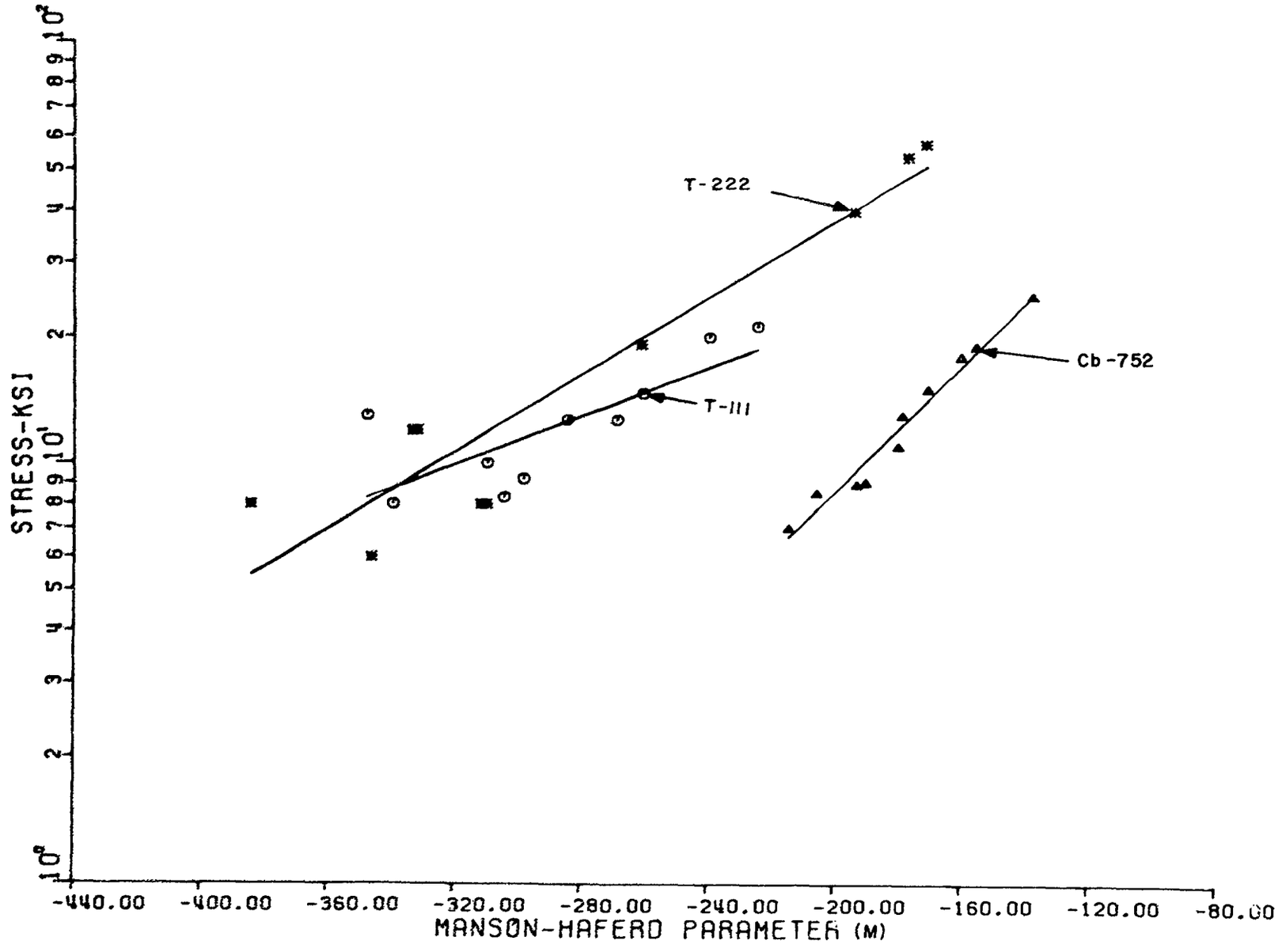

Figure 62. Manson-Haferd Parameter Plot (T_a = 1000, t_a = 7.0) for T-222, T-111, and Cb-752 at 1.0% Creep.

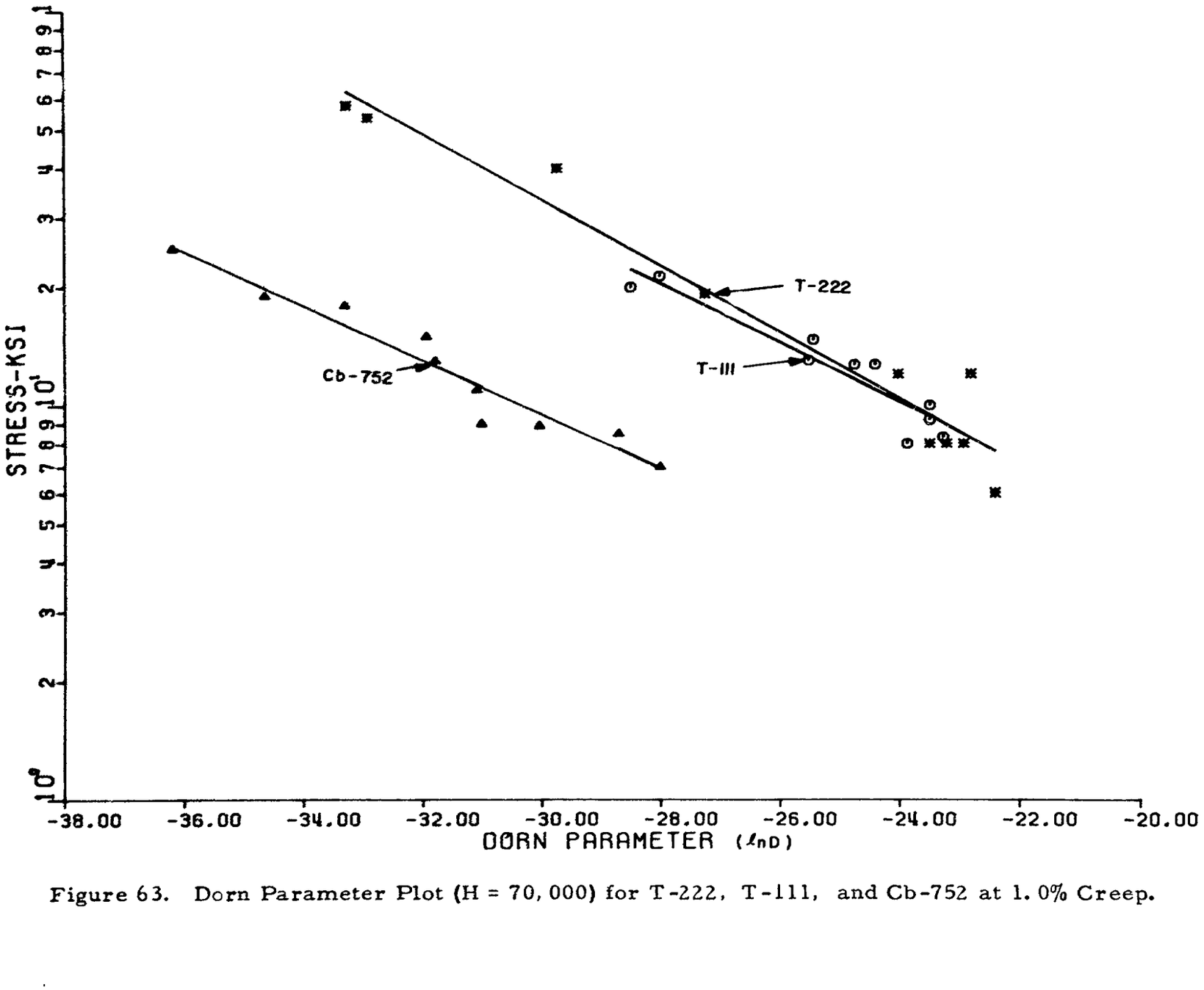

Figure 63. Dorn Parameter Plot (H = 70, 000) for T-222, T-111, and Cb-752 at 1.0% Creep.

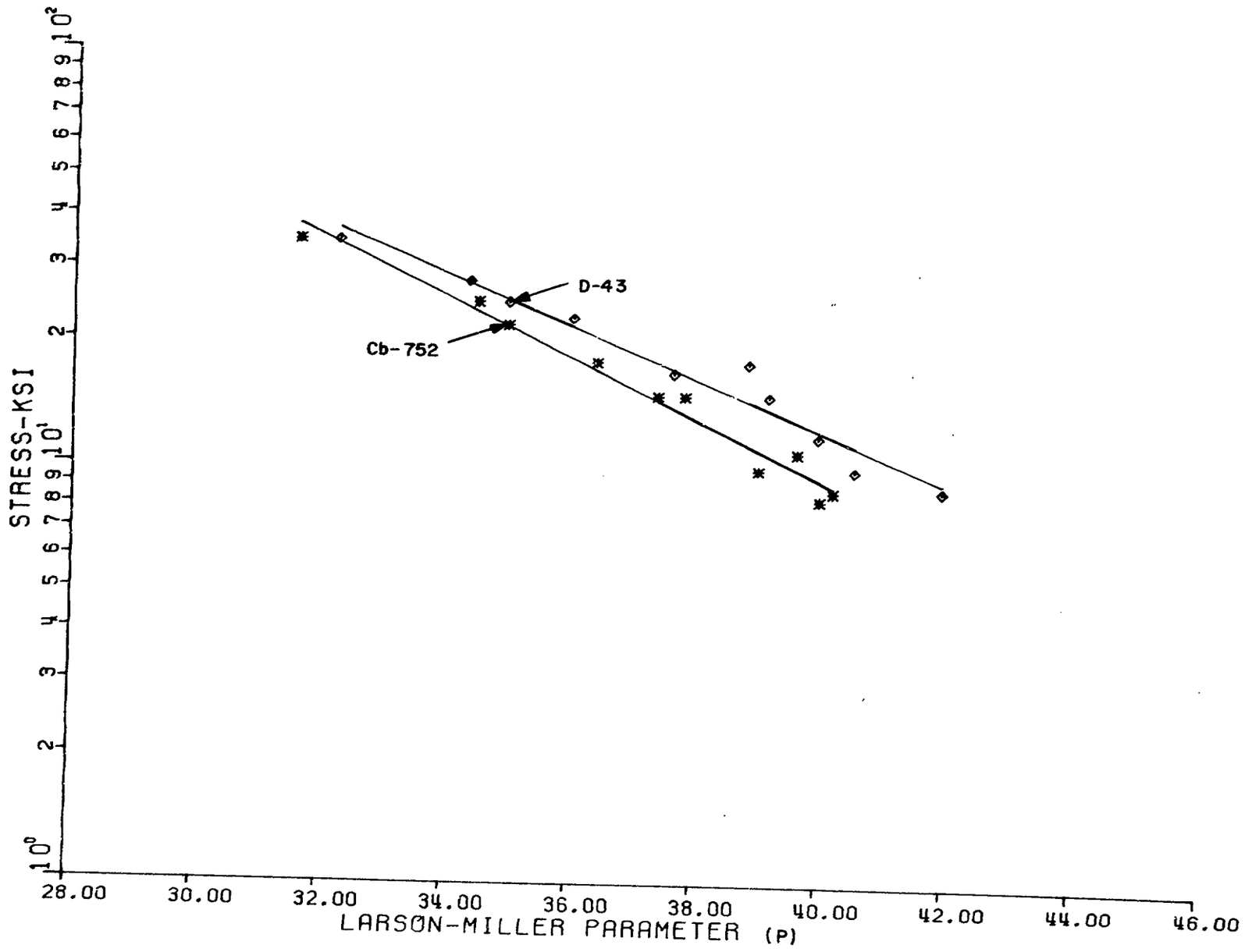

Figure 64. Larson-Miller Parameter Plot (C = 13.5) for D-43 and Cb-752 at 5.0% Creep.

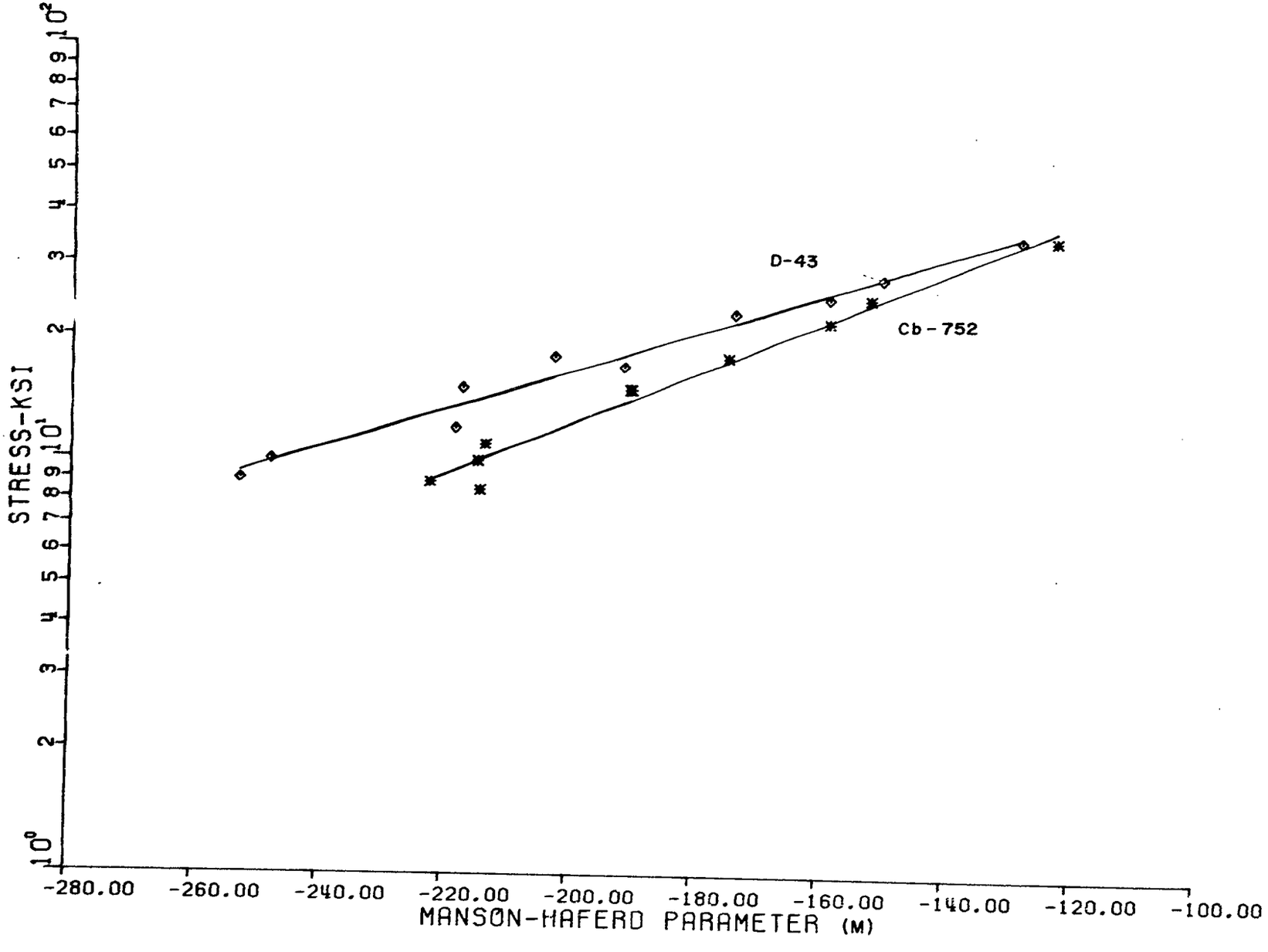

Figure 65. Manson-Haferd Parameter Plot (T_a = 1000, t_a = 7.0) for D-43 and Cb-752 at 5.0% Creep.

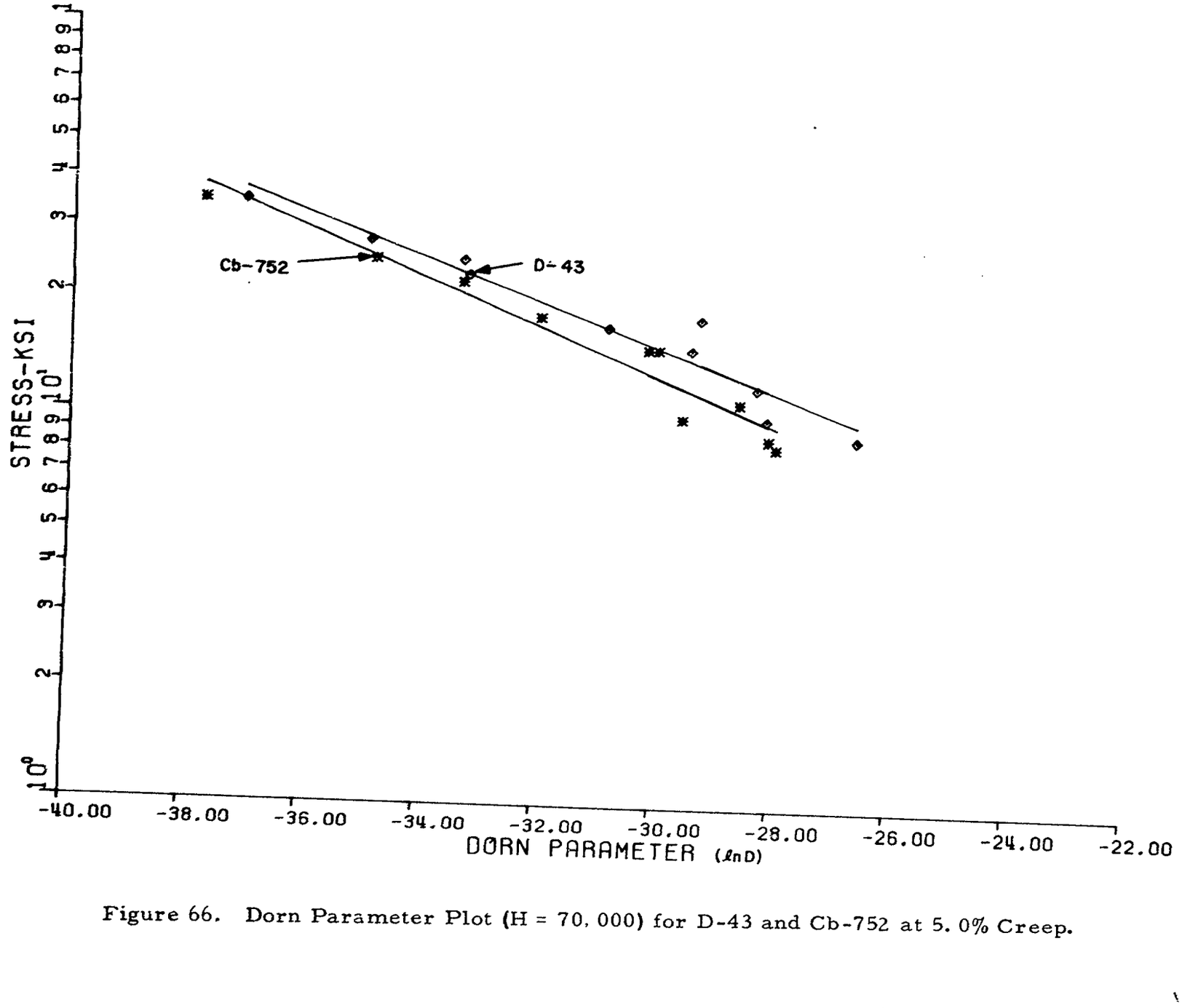

Figure 66. Dorn Parameter Plot (H = 70, 000) for D-43 and Cb-752 at 5. 0% Creep.

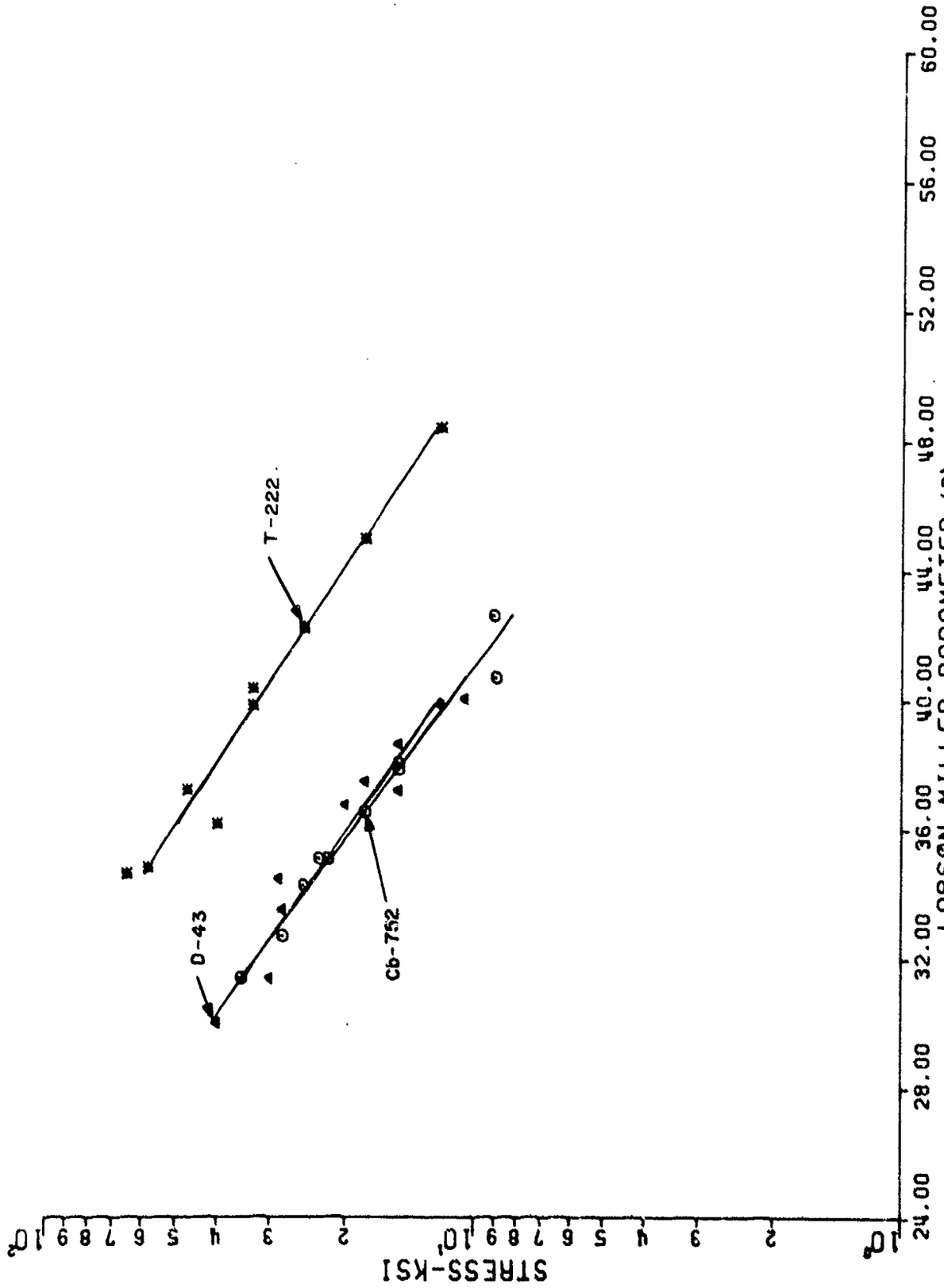

Figure 67. Larson-Miller Parameter Plot (C = 13.5) for T-222, D-43, and Cb-752 at Rupture.

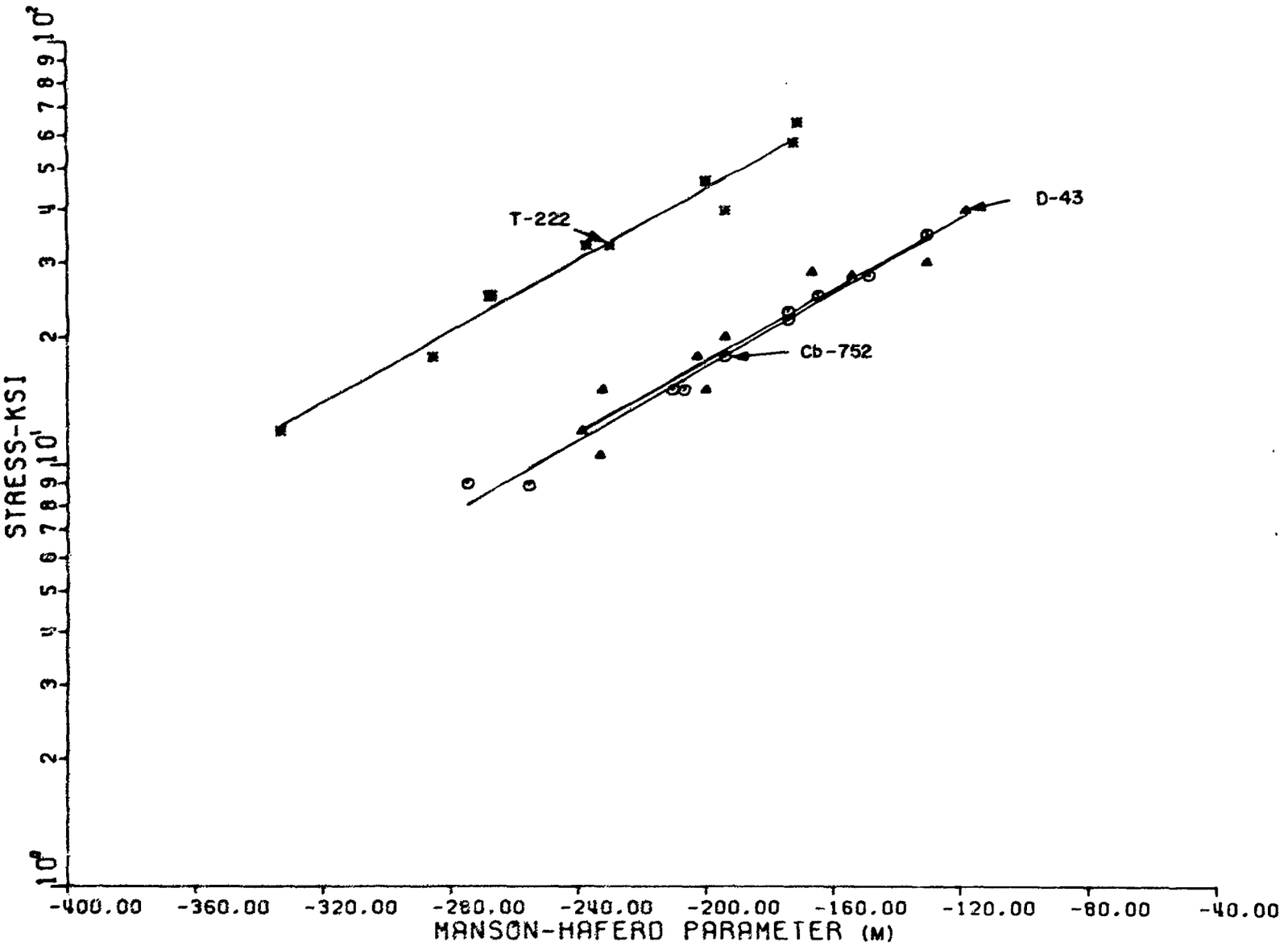

Figure 68. Manson-Haferd Parameter Plot (T_a = 1000, t_a = 7.0) for T-222, D-43, and Cb-752 at Rupture.

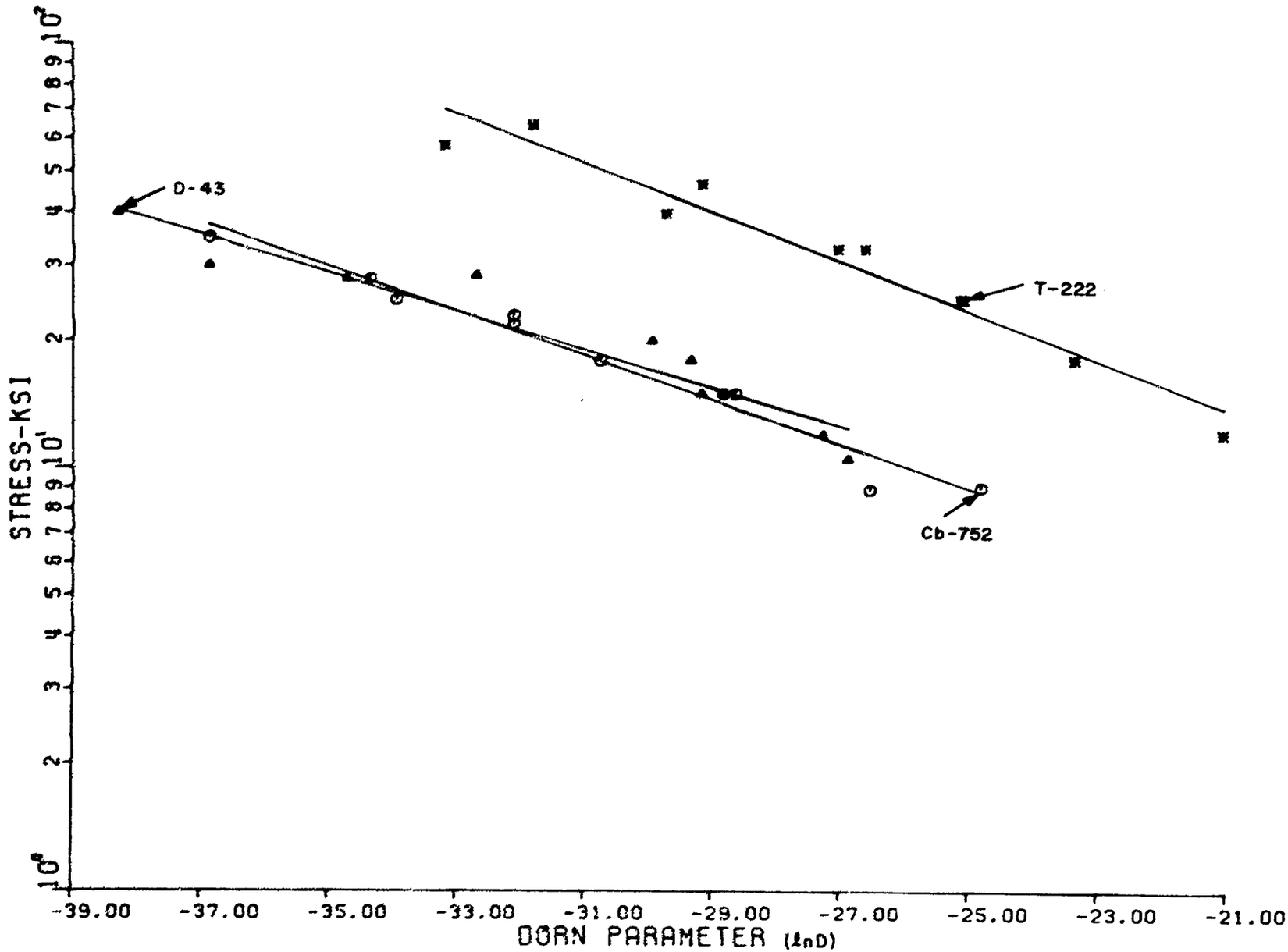

Figure 69. Dorn Parameter Plot (H = 70,000) for T-222, D-43, and Cb-752 at Rupture.

1.3.8 Laminated Metal Composites

The configuration and thickness of load bearing components manufactured from high strength alloys are limited by fracture toughness considerations. It has been proposed that substituting a laminated composite of thin sheets for a bulk section of a given material could be advantageous in certain applications (Reference 49 and 50). The thin sheets in such an adhesively bonded laminate would act in unison to provide the required strength. Since the sheets are separated by a low modulus adhesive, the possibility of crack propagation through the entire section thickness is greatly reduced. The sudden premature failure associated with plane strain fracture is not likely in the thinner sheets.

Because of the inability of the adhesive to transfer the shear load from one thin layer of the composite to another, these layers act essentially independently of each other in modes of loading other than pure tension. In bending, particularly in a plane normal to the surface of the individual sheets, and in compression, this effect could result in a decrease in strength from that of an equivalent bulk section. This program was conducted to determine the mechanical properties of two such laminated composites.

1.3.8.1 Laminated Aluminum

A laminated metal composite was fabricated by adhesive bonding of thin sheets of 2024-T3 aluminum with Dexter EA9500 adhesive. Seventy-two of the aluminum sheets (0.040-inch-thick each) were bonded together resulting in a final composite thickness of approximately 3 inches. The composite was 7-1/2 inches long by 7 inches wide.

Mechanical properties determined included ultimate tensile strength, yield strength, modulus, compressive strength and fracture toughness. All properties were determined in the flatwise direction.

The results of the tensile and compressive tests are shown in Tables XXX and XXXI, respectively. The properties of the laminated composite were calculated based on the overall cross-sectional area of specimens, including the adhesive. Since this adhesive comprised approximately 5% of the overall area, the tensile strength data for the composite appear to be slightly lower than the handbook values (Reference 51).

Two types of compressive specimens were utilized; one being a long column to be tested in a supporting fixture, the other

TABLE XXX

TENSILE PROPERTIES OF LAMINATED ALUMINUM COMPOSITE

Yield Strength at 0.2% Offset (PSI x 10^{-3})	Yield Elongation at 0.2% Offset (%)	Ultimate Strength (PSI x 10^{-3})	Ultimate Elongation (%)	Modulus (PSI x 10^{-6})
38.62	0.64	60.98	25	8.79
39.60	0.56	63.20	26	10.74
40.61	0.58	62.50	24	9.95
39.20	0.56	62.00	27	10.96
50.00	0.69	62.35	28	10.15
37.91	0.65	58.26	25	8.36
Avg. 40.99	0.61	61.55	25.8	9.83

TABLE XXXI

COMPRESSIVE PROPERTIES OF LAMINATED ALUMINUM COMPOSITES

Specimen Size	Yield Strength at 0.2% Offset (PSI x 10^{-3})	Compressive Strength (PSI x 10^{-3})	Compressive Modulus (PSI x 10^{-6})
1/4" x 1/2" x 3-1/8"	39.20	68.40	10.74
	39.20	76.00	9.58
1" x 1" x 1"	44.40	78.60	-----
	41.30	76.80	-----
	43.00	73.50	-----

short, and requiring no lateral support. The short (one-inch cube) specimen was used for yield and compressive strengths only. The long specimen, 1/4-inch by 1/2-inch by 3-1/8-inches was used for yield and compressive strength and modulus. The modulus values were obtained from stress-strain curves obtained by using strain gages bonded to opposite sides of the specimen.

Two large compact tension specimens (Figure 70) were machined from the laminated aluminum composite in an attempt to determine the fracture toughness. The tests were performed in accordance with ASTM Method E-399. The K_Q values obtained were 30.92 and 35.43 KSI IN. In order for a result to be considered valid according to this method, it is required that both the specimen thickness and the crack length exceed 2.5 times $(K_{IC}/\sigma ys)^2$, where σys is the 0.2 percent offset yield strength of the material. The results of these tests were invalid because the thickness and crack length were not sufficiently large. This indicates that the K_{IC} value of the material is too great for the size of the specimen (1.5 inches thick) used in these tests.

The fracture surface of one of the laminated composites compact tension specimens in shown in Figure 71. As can be seen, the sheets of aluminum apparently acted individually, thus, eliminating the possibility of a plane strain condition, as had been predicted. The decrease in thickness and the typical shear fracture of each sheet were easily discernable.

1.3.8.2 Titanium-Boron Composite

A second, more complex, composite was included in this program. This material consisted of alternating layers of Ti-6Al-4V and a boron/epoxy composite. The boron layers were made from 8 plies of 3M "B" staged prepregs in an alternating 0° - 90° layup. A total of four layers of titanium and three layers of boron were bonded together with EA 9500 epoxy adhesive. The resulting composite was approximately 7 inches by 7 inches by 1/4-inch thick.

Tensile, compressive, and compact tension specimens were to be machined from the material and tested. However, this combination of the boron composite and titanium was extremely difficult to machine. As a result, the tensile and compressive specimens were produced but it was not practical to machine the compact tension specimens, as originally planned.

The tensile tests were conducted in accordance with ASTM Method E-8. The results of these tests are given in Table XXXII. The large variation in yield strength can probably be attributed

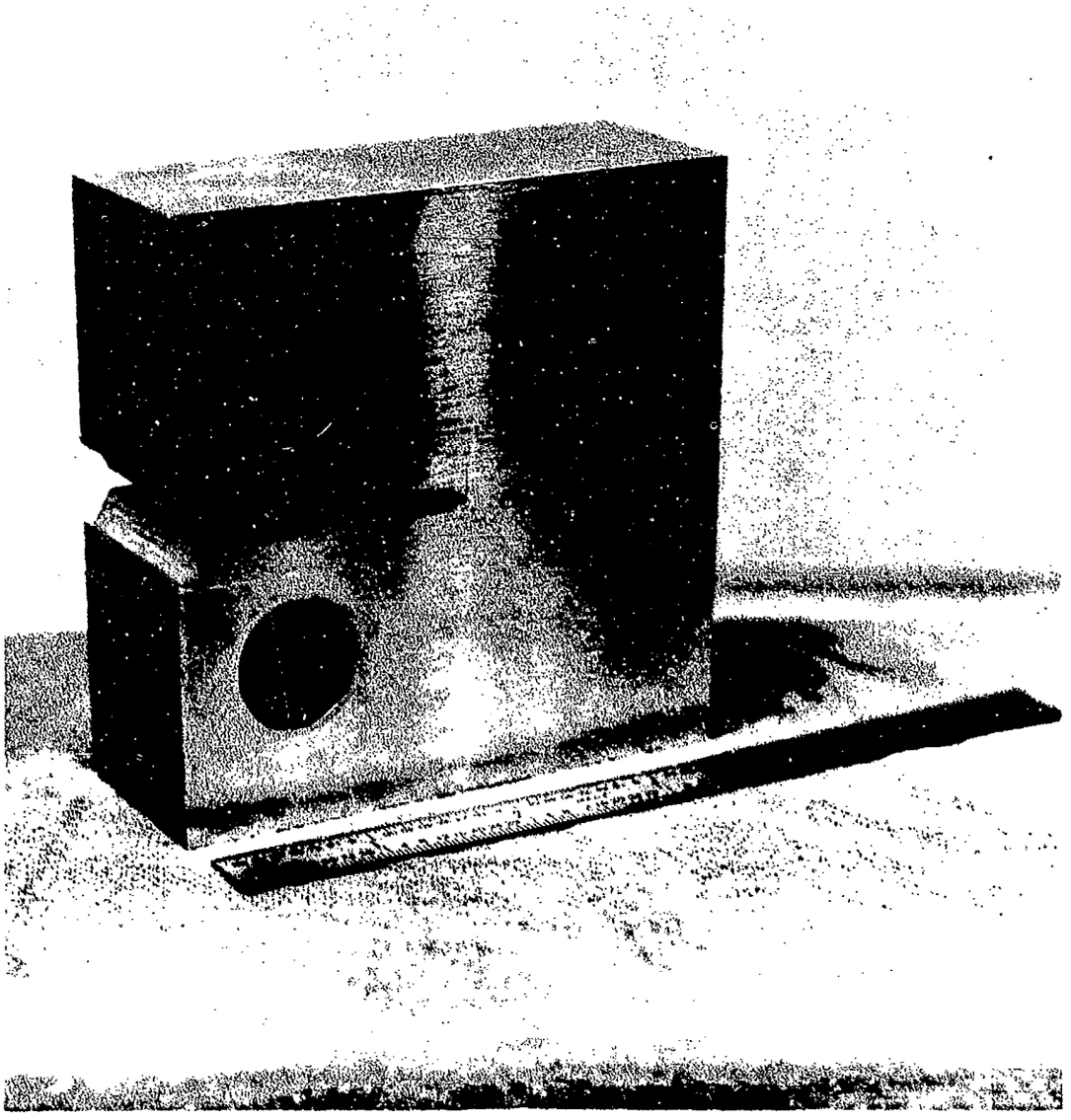

Figure 70. Laminated Aluminum Composite Compact Tension Fracture Toughness Specimen.

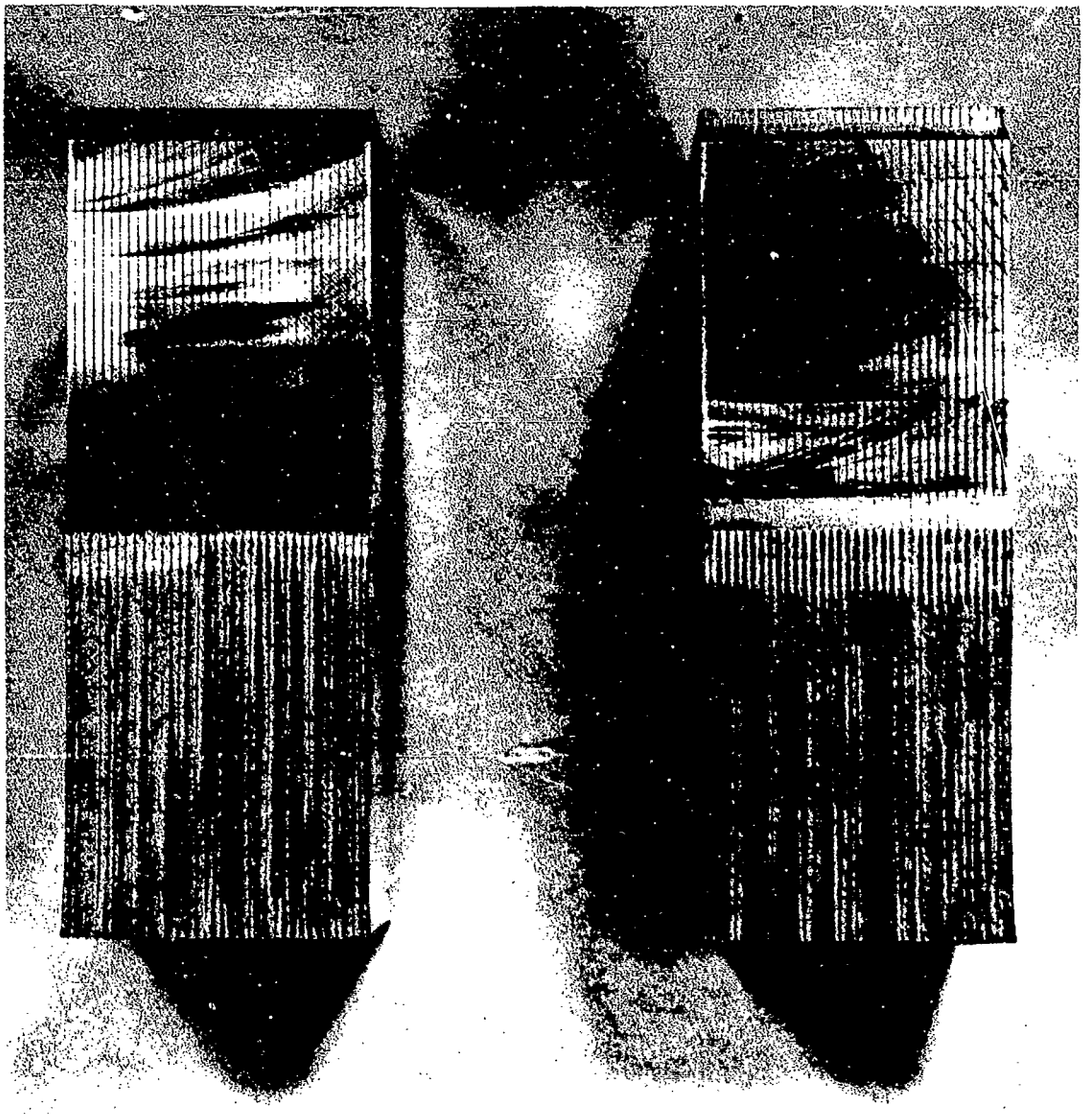

Figure 71. Fractured Surface of Aluminum Composite CT Specimens.

TABLE XXXII

TENSILE PROPERTIES OF TITANIUM/
BORON/EPOXY COMPOSITE

Specimen No.	Yield Strength at 0.2% Offset (PSI x 10^{-3})	Yield Elongation (%)	Ultimate Strength (PSI x 10^{-3})	Ultimate Elongation (%)	Modulus (PSI x 10^{-6})
1	80.00	0.72	92.78	5.3	15.87
2	39.66	0.46	93.18	4.0	14.86
3	38.89	0.46	93.61	5.0	14.13
4	20.80	0.34	93.46	5.6	15.69

to either premature failure of the boron/epoxy composite or failure of the bond between the titanium and the boron/epoxy composite. Visual inspection of the specimens after testing failed to indicate slippage within the bond joint. The stress-strain diagrams for each specimen are shown in Figure 72.

The modulus values obtained from these materials were considerably lower than expected, based on law-of-mixtures calculations. This is probably due to the inability of the adhesive bond to transfer the load from the titanium to the stiffer boron composite.

The compression tests were again conducted on both long and short specimens. Modulus measurements were obtained from specimens approximately 0.285 inch by 0.500 inch by 3.40 inches long. These specimens were instrumented with strain gages for determining the modulus. The compressive strength and yield strength were determined on specimens approximately 0.285 inch by 0.500 inch by 1.00 inch long. Two valid tests were obtained with each of these specimen configurations. The results are given in Table XXXIII.

TABLE XXXIII

COMPRESSIVE PROPERTIES OF TITANIUM/
BORON/EPOXY COMPOSITE

Specimen Type	Yield Strength (KSI)	Compressive Strength (KSI)	Modulus (PSI x 10^{-6})
Short	180.18	183.71	-----
Short	176.02	179.52	-----
Long	------	------	18.08
Long	------	------	17.99

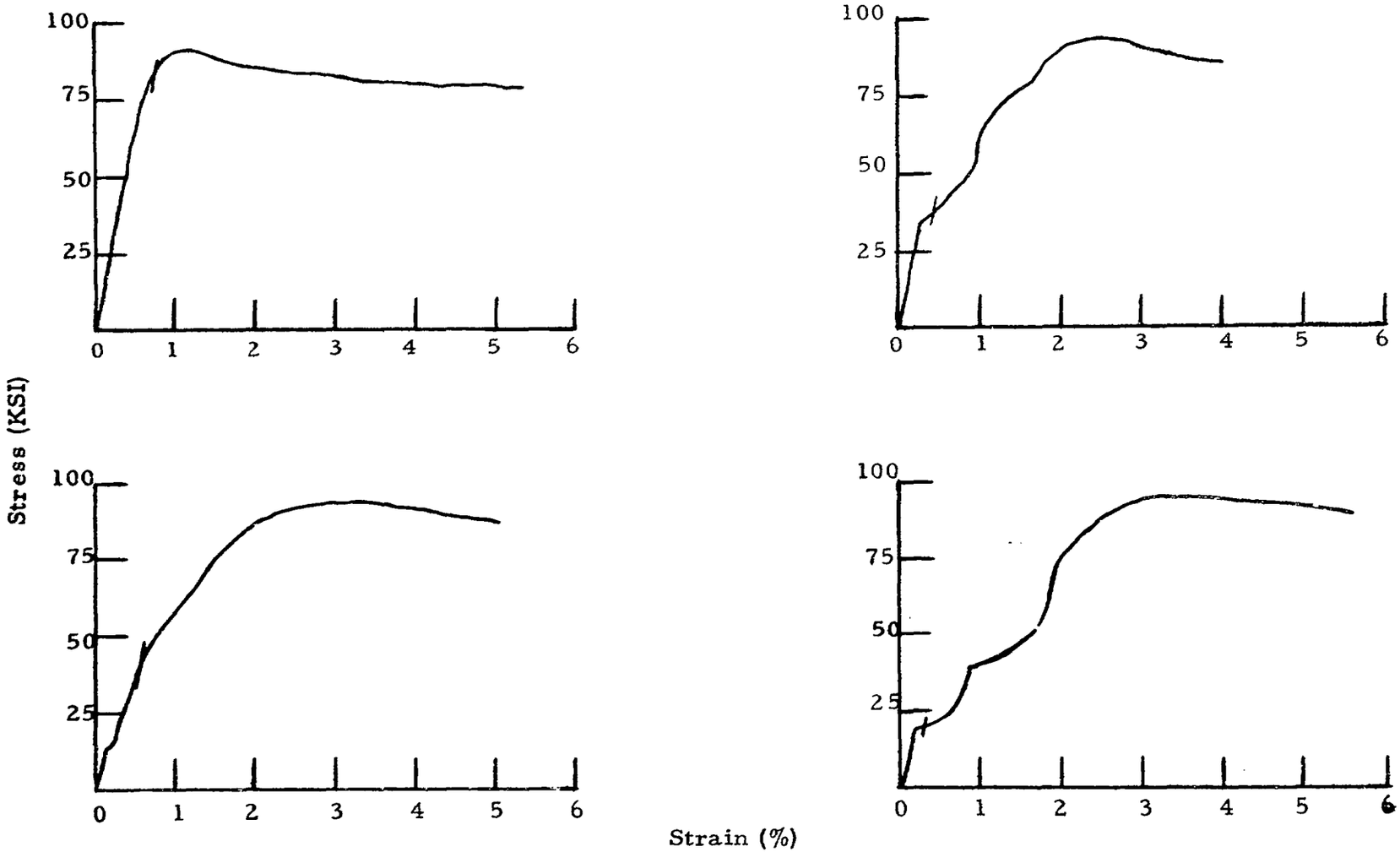

Figure 72. Stress-Strain Curves for Titanium/Boron/Epoxy.

SECTION II

EVALUATION OF NONMETALLIC MATERIALS

2.1 INTRODUCTION

The requirements for nonmetallic materials for applications in present and future aircraft and space vehicles are becoming more stringent. Current environmental requirements for these materials, particularly the elastomers, in many cases exceed the capabilities of well developed and characterized commerically available materials. For these reasons it has been necessary to continually evaluate the characteristics of these as well as any new materials to assure their ability to meet the more severe requirements. The University has been involved in these types of studies.

In addition, programs were undertaken to investigate the causes of failures involving nonmetallic materials in operational Air Force aircraft or systems. In these studies it was usually necessary to determine whether the failure was caused by shortcomings of the material or resulted from improper preparation or application techniques. Several of the more involved nonmetallic materials evaluation programs are summarized in this section.

2.2 STORAGE LIFE TESTING OF FUEL TANK SEALANTS

Current military specifications call for fuel tank sealants to be storable for 9 months from the date of manufacture (Reference 52). Field reports have indicated some sealants used on current operational aircraft are not meeting this 9-month requirement. The sealants in question would not cure within the required time interval. Prompted by these reports, a storage life testing program was initiated to determine the storability of fuel tank sealants that are qualified to MIL-S-8802D. This military specification covers integral fuel tank and fuel cell cavity sealants over a temperature range of -65°F to 250°F.

The test materials for this program were supplied in A-2, B-2 and B-1/2 classifications. The materials were received in Semkit and can forms.

2.2.1 Procedure

To evaluate the curability and storability of these sealants, a testing program employing three tests from MIL-S-8802D was developed. These tests were application life, standard curing rate, and tack-free time. The application life for Class A compounds is determined by a viscosity measurement. For Class B compounds the application life is measured by extruding the sealant through an orifice at a prescribed pressure within a certain time interval. The test data are reported in poises for the Class A compounds and grams per minute for Class B compounds.

The standard curing rate test measures the hardness of the compound following curing times of 72 hours for Class A-2 and B-2 compounds, and 30 hours for Class B-1/2 compounds.

In the tack-free time test, a sheet of polyethylene film is placed on the surface of the sealant, with a pressure of 1/2 ounce per square inch for two minutes. At the end of this two minute period the weight is removed and the film is peeled off the sealant. The polyethylene should come away clean and free of sealing compound.

The thirty-three materials involved in this program were manufactured by five different companies. The companies will be referred to only by code in this report. Two compounds were supplied by Manufacturer SL I. They will be referred to as SL IA and SL IB. SL IA material was tested in A-2, B-2, and B-1/2 classes with can and Semkit (both standard polyethylene and Al foil packaging. Material SL IB was supplied only in classes A-2 and B-2 but in the same three package forms. All three classes were supplied by manufacturers SL II and SL III but only in the can and standard Semkit packages. The SL IV compound was supplied only in class B-2 and B-1/2 can forms. The SL V compound was supplied in Class A-2 and B-2 Semkit and can forms.

The three tests discussed above are scheduled for each of these thirty-three materials following 0, 3, 5, 6, 7, 8, 9, 12, 15, 18, and 24 months of storage. All materials will be stored at room temperature at less than 80°F for the entire 24-month period. This program is continuing and only that portion which has been completed (the first 9 months) is discussed in this report.

2.2.2 Results

The results of these tests are discussed by class and form of the materials evaluated. The application life, standard curing rate, and tack-free time results are discussed separately but are summarized in Table XXXIV.

2.2.2.1 Application Life Tests

The application life test data for the six compounds tested are discussed in the following paragraphs. Figures 73 through 78 are plots of the respective application life parameters as a function of storage time.

The application life tests for the class A-2 materials in Semkit form show that two of the seven materials tested failed the initial test at zero months. After 9 months, only two of the seven materials were passing this test. The SL IA compound failed the application life after 3 months in both Semkit forms. The SL IB compound failed after six months but the aluminum foil Semkit began passing again after eight months. The SL II compounds passed the application in all except one of the months tested. The SL III and the SL V compounds failed all the application life tests.

After 9 months of testing only one of the seven class B-2 compounds in Semkits is passing the application life test (Figure 74). The SL IB compound in the aluminum foil package has passed after each month of storage. Others, such as the SL IA compound with foil package the SL II compound, and the SL III compound have failed after each month of storage. The SL III compound after three months had set up after mixing to the point that no compound could be extruded after the 2 hour application life. However, after seven months a slight improvement was observed.

The B-1/2 class of material performed the best of three classes of Semkits testing in this program. After 9 months of storage only one of the four compounds tested was failing the application life test. These results are shown in Figure 75.

After 9 months storage all the A-2 materials supplied in can form passed the application life test. Two of the compounds

Text continued on page 146

TABLE XXXIV

RESULTS OF STORAGE LIFE TESTS

Material (Class and Form)	Time (Months)	Application Life	Std. Curing Rate Shore "A_2"	Tack-Free Time
SL-IA	2	960 poise	25	P
Class A-2	3	2920 poise	38	P
Form-Al Foil, Semkit	5	4000+ poise	29	P
	6	4000 +poise	32	P
	7	4000+ poise	28	P
	8	4000+poise	35	P
	9	4000+poise	35	P
SL-IA				
Class A-2	2	1280 poise	28	P
Form-Polyethylene,	3	3660 poise	40	P
Semkit	5	4000 + poise	31	P
	6	4000 + poise	34	P
	7	4000 + poise	28	P
	8	4000 + poise	36	P
	9	4000 + poise	35	P
SL-IA	2	520 poise	26	P
Class A-2	3	1660 poise	42	P
Form - Can	5	2000 poise	30	P
	6	1475 poise	33	P
	7	1204 poise	31	P
	8	3480 poise	35	P
	9	1600 poise	37	P
SL-IA	1	11.80 gr/min	41	F
Class B-2	3	14.29 gr/min	43	P
Form-Al Foil, Semkit	5	12.35 gr/min	44	P
	6	10.05 gr/min	46	P
	7	9.47 gr/min	45	P
	8	8.06 gr/min	45	P
	9	10.16 gr/min	49	P

TABLE XXXIV (continued)

RESULTS OF STORAGE LIFE TESTS

Material (Class and Form)	Time (Months)	Application Life	Std. Curing Rate Shore "A_2"	Tack-Free Time
SL-IA	1	19.33 gr/min	38	F
Class B-2	3	11.54 gr/min	40	P
Form-Polyethylene	5	7.98 gr/min	45	P
Semkit	6	7.58 gr/min	47	P
	7	6.48 gr/min	44	P
	8	4.61 gr/min	49	P
	9	8.91 gr/min	44	P
SL-IA	1	39.23 gr/min	49	P
Class B-2	3	14.50 gr/min	44	P
Form - Can	5	5.70 gr/min	48	P
	6	11.53 gr/min	48	P
	7	10.49 gr/min	53	P
	8	5.79 gr/min	51	P
	9	7.79 gr/min	52	P
SL-IA	1	45.56 gr/min	40	P
Class B-1/2	3	36.42 gr/min	42	P
Form-Al Foil,	5	46.32 gr/min	42	P
Semkit	6	44.34 gr/min	42	P
	7	36.84 gr/min	43	P
	8	34.10 gr/min	45	P
	9	34.24 gr/min	45	P
SL-IA	1	47.53 gr/min	38	P
Class B-1/2	3	38.04 gr/min	42	P
Form-Polyethylene,	5	30.33 gr/min	40	P
Semkit	6	27.30 gr/min	42	P
	7	29.40 gr/min	44	P
	8	24.66 gr/min	43	P
	9	23.04 gr/min	41	P

TABLE XXXIV (continued)

RESULTS OF STORAGE LIFE TESTS

Material (Class and Form)	Time (Months)	Application Life	Std. Curing Rate Shore "A_2"	Tack-Free Time
SL-IA	1	28.89 gr/min	41	P
Class B-1/2	3	22.52 gr/min	46	P
Form-Can	5	16.60 gr/min	47	P
	6	16.95 gr/min	48	P
	7	20.07 gr/min	50	P
	8	12.66 gr/min	52	P
	9	12.95 gr/min	53	P
SL-IB	1	1120 poise	40	P
Class-A-2	3	1160 poise	42	P
Form-Al Foil, Semkit	5	2184 poise	41	P
	6	2640 poise	39	P
	7	4000 + poise	44	P
	8	1340 poise	41	P
	9	1060 poise	45	P
SL-IB	1	1480 poise	41	P
Class-A-2	3	1540 poise	45	P
Form-Polyethylene,	5	2360 poise	42	P
Semkit	6	2680 poise	40	P
	7	3200 poise	46	P
	8	3160 poise	44	P
	9	3160 poise	46	P
SL-IB	1	840 poise	42	P
Class-A-2	3	1080 poise	43	P
Form - Can	5	1000 poise	41	P
	6	1340 poise	40	P
	7	980 poise	42	P
	8	800 poise	41	P
	9	800 poise	45	P

TABLE XXXIV (continued)

RESULTS OF STORAGE LIFE TESTS

Material (Class and Form)	Time (Months)	Application Life	Std. Curing Rate Shore "A_2"	Tack-Free Time
SL-IB	2	35.57 gr/min	45	P
Class - B-2	3	32.75 gr/min	47	P
Form-Al Foil, Semkit	5	32.08 gr/min	48	P
	6	34.98 gr/min	39	P
	7	41.83 gr/min	40	P
	8	37.30 gr/min	45	P
	9	31.82 gr/min	45	P
SL-IB	2	32.21 gr/min	43	P
Class - B-2	3	26.09 gr/min	47	P
Form - Polyethylene,	5	25.05 gr/min	45	P
Semkit	6	23.90 gr/min	45	P
	7	26.57 gr/min	45	P
	8	21.43 gr/min	48	P
	9	14.77 gr/min	51	P
SL-IB	2	41.52 gr/min	49	P
Class - B-2	3	39.84 gr/min	50	P
Form - Can	5	48.48 gr/min	50	P
	6	44.36 gr/min	48	P
	7	42.36 gr/min	52	P
	8	48.06 gr/min	48	P
	9	44.48 gr/min	50	P
SL-II	0	1020 poise	22	P
Class - A-2	3	1400 poise	35	P
Form - Polyethylene,	5	1860 poise	26	P
Semkit	6	2340 poise	8	P
	7	1592 poise	30	P
	8	3200 poise	33	P
	9	1500 poise	33	P

TABLE XXXIV (continued)

RESULTS OF STORAGE LIFE TESTS

Material (Class and Form)	Time (Months)	Application Life	Std. Curing Rate Shore "A_2"	Tack-Free Time
SL-II	0	1240 poise	28	P
Class - A-2	3	1940 poise	37	P
Form - Can	5	2020 poise	33	P
	6	2140 poise	33	P
	7	1980 poise	42	P
	8	1400 poise	40	P
	9	1440 poise	40	P
SL-II	0	14.25 gr/min	48	P
Class - B-2	3	14.35 gr/min	46	P
Form - polyethylene,	5	12.14 gr/min	45	P
Semkit	6	16.39 gr/min	47	P
	7	11.05 gr/min	51	P
	8	10.65 gr/min	46	F
	9	13.55 gr/min	45	P
SL-II	0	19.65 gr/min	46	P
Class - B-2	3	19.27 gr/min	46	P
Form - Can	5	24.02 gr/min	48	P
	6	18.74 gr/min	50	P
	7	19.01 gr/min	50	P
	8	19.11 gr/min	52	P
	9	20.43 gr/ min	51	P
SL-II	0	31.19 gr/min	38	P
Class - B-1/2	3	20.81 gr/min	38	P
Form - Polyethylene,	5	20.77 gr/min	38	P
Semkit	6	13.28 gr/min	37	P
	7	17.56 gr/min	40	P
	8	13.68 gr/min	40	P
	9	11.07 gr/min	43	P

TABLE XXXIV (continued)

RESULTS OF STORAGE LIFE TESTS

Material (Class and Form)	Time (Months)	Application Life	Std. Curing Rate Shore "A_2"	Tack-Free Time
SL-II	0	46.28 gr/min	37	P
Class - B-1/2	3	38.44 gr/min	35	P
Form - Can	5	37.30 gr/min	36	P
	6	35.67 gr/min	34	P
	7	31.49 gr/min	36	P
	8	41.61 gr/min	35	P
	9	39.29 gr/min	41	F
SL-III	0	4000 + poise	37	P
Class - A-2	3	4000 + poise	40	P
Form - Polyethylene,	5	4000 + poise	39	P
Semkit	6	4000 + poise	43	P
	7	4000 + poise	43	P
	8	4000 + poise	35	P
	9	4000 + poise	42	F
SL-III	0	4000 + poise	38	P
Class - A-2	3	2560 poise	40	P
Form - Can	5	1960 poise	39	P
	6	1760 poise	44	P
	7	1700 poise	43	P
	8	2400 poise	37	P
	9	2020 poise	43	P
SL-III	0	3.20 gr/min	42	P
Class - B-2	3	0.00 gr/min	45	P
Form - Polyethylene,	5	0.00 gr/min	45	P
Semkit	6	0.00 gr/min	50	P
	7	0.00 gr/min	48	P
	8	2.13 gr/min	43	P
	9	4.39 gr/min	46	P

TABLE XXXIV (continued)

RESULTS OF STORAGE LIFE TESTS

Material (Class and Form)	Time (Months)	Application Life	Std. Curing Rate Shore "A_2"	Tack-Free Time
SL-III	0	12.09 gr/min	43	P
Class - B-2	3	19.78 gr/min	45	P
Form - Can	5	15.43 gr/min	47	P
	6	16.03 gr/min	50	P
	7	13.32 gr/min	50	P
	8	14.02 gr/min	41	P
	9	14.73 gr/min	48	P
SL-III	0	28.31 gr/min	43	P
Class - B-1/2	3	29.06 gr/min	43	P
Form - Polyethylene,	5	22.28 gr/min	45	P
Semkit	6	22.83 gr/min	43	P
	7	17.82 gr/min	47	P
	8	6.47 gr/min	46	P
	9	17.37 gr/min	45	P
SL-III	0	40.11 gr/min	43	P
Class - B-1/2	3	46.40 gr/min	45	P
Form - Can	5	42.78 gr/min	45	P
	6	43.16 gr/min	43	P
	7	34.74 gr/min	45	P
	8	44.09 gr/min	42	P
	9	48.65 gr/min	45	P
SL-IV	0	7.08 gr/min	47	P
Class - B-2	3	12.65 gr/min	47	P
Form - Can	5	15.68 gr/min	50	P
	6	16.30 gr/min	50	P
	7	11.56 gr/min	49	P
	8	10.01 gr/min	48	P
	9	24.50 gr/min	51	P

TABLE XXXIV (concluded)

RESULTS OF STORAGE LIFE TESTS

Material (Class and Form)	Time (Months)	Application Life	Std. Curing Rate Shore "A_2"	Tack-Free Time
SL-IV	0	29.02 gr/min	39	P
Class - B-1/2	3	34.42 gr/min	47	F
Form - Can	5	30.47 gr/min	50	F
	6	35.46 gr/min	47	F
	7	30.44 gr/min	42	F (22 hrs.)
	8	27.68 gr/min	45	P
	9	41.94 gr/min	50	F (18 hrs.)
SL-V	0	3580 poise	35	P
Class - A-2	3	2956 poise	36	P
Form - Polyethylene,	5	4000 + poise	42	F (72 hrs.)
Semkit	6	4000 + poise	36	F (208 hrs.)
	7	4000 + poise	23	F (304 hrs.)
SL-V	0	2952 poise	35	P
Class - A-2	3	1420 poise	35	P
Form - Can	5	840 poise	40	P
	6	780 poise	33	P
	7	680 poise	34	F (138 hrs.)
SL-V	0	17.72 gr/min	42	P
Class - B-2	3	18.14 gr/min	45	P
Form - Polyethylene,	5	13.54 gr/min	46	P
Semkit	6	13.84 gr/min	46	P
	7	14.76 gr/min	45	F (138 hrs.)
SL-V	0	25.36 gr/min	43	P
Class - B-2	3	24.37 gr/min	45	P
Form - Can	5	23.90 gr/min	39	F (46 hrs.)
	6	22.93 gr/min	36	F (67 hrs.)
	7	22.64 gr/min	27	F (138 hrs.)

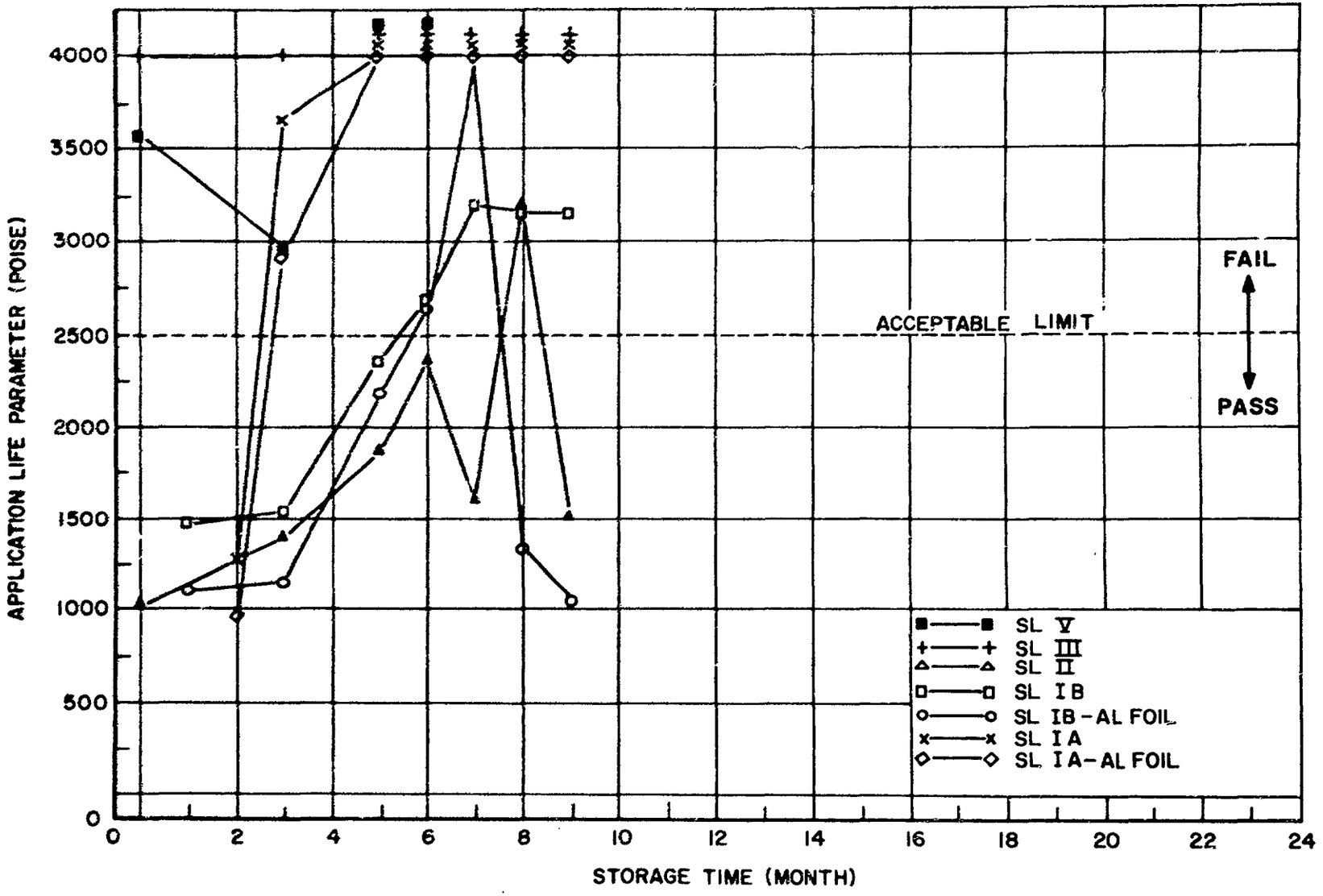

Figure 73. Results of Application Life Tests for Class A-2 Materials in Semkit Form.

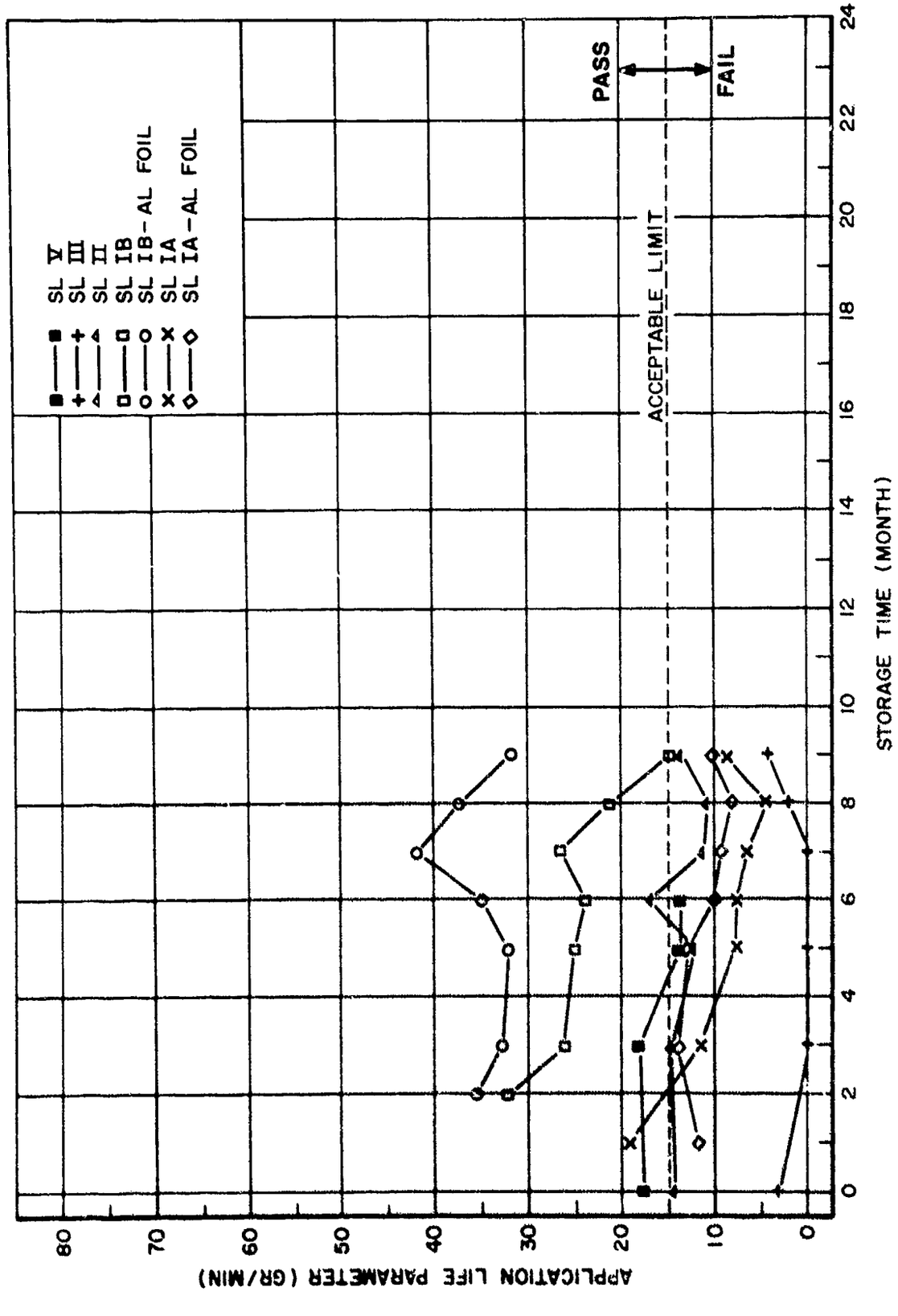

Figure 74. Results of Application Life Tests for Class B-2 Materials in Semkit Form.

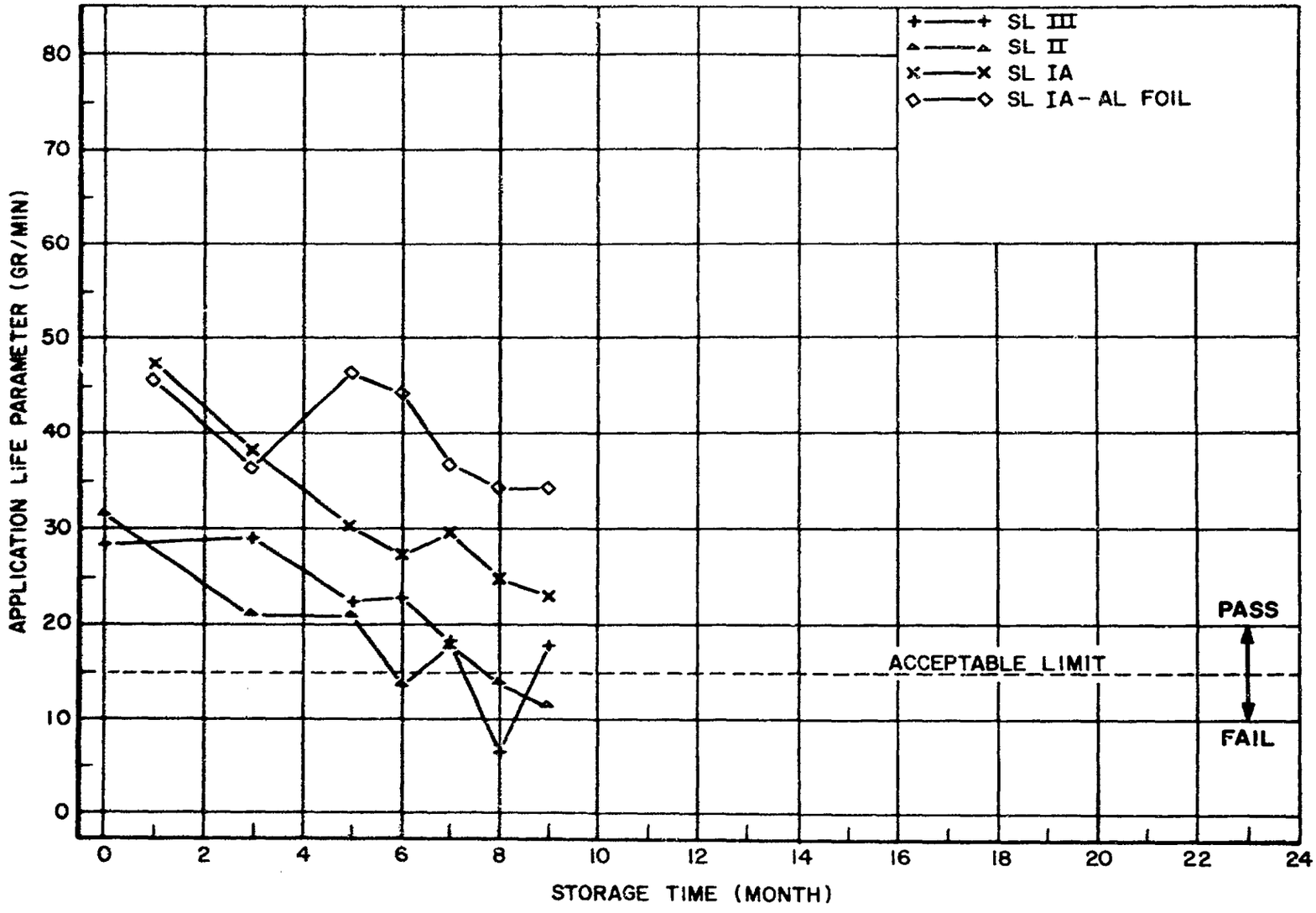

Figure 75. Results of Application Life Tests for Class B-1/2 Materials in Semkit Form.

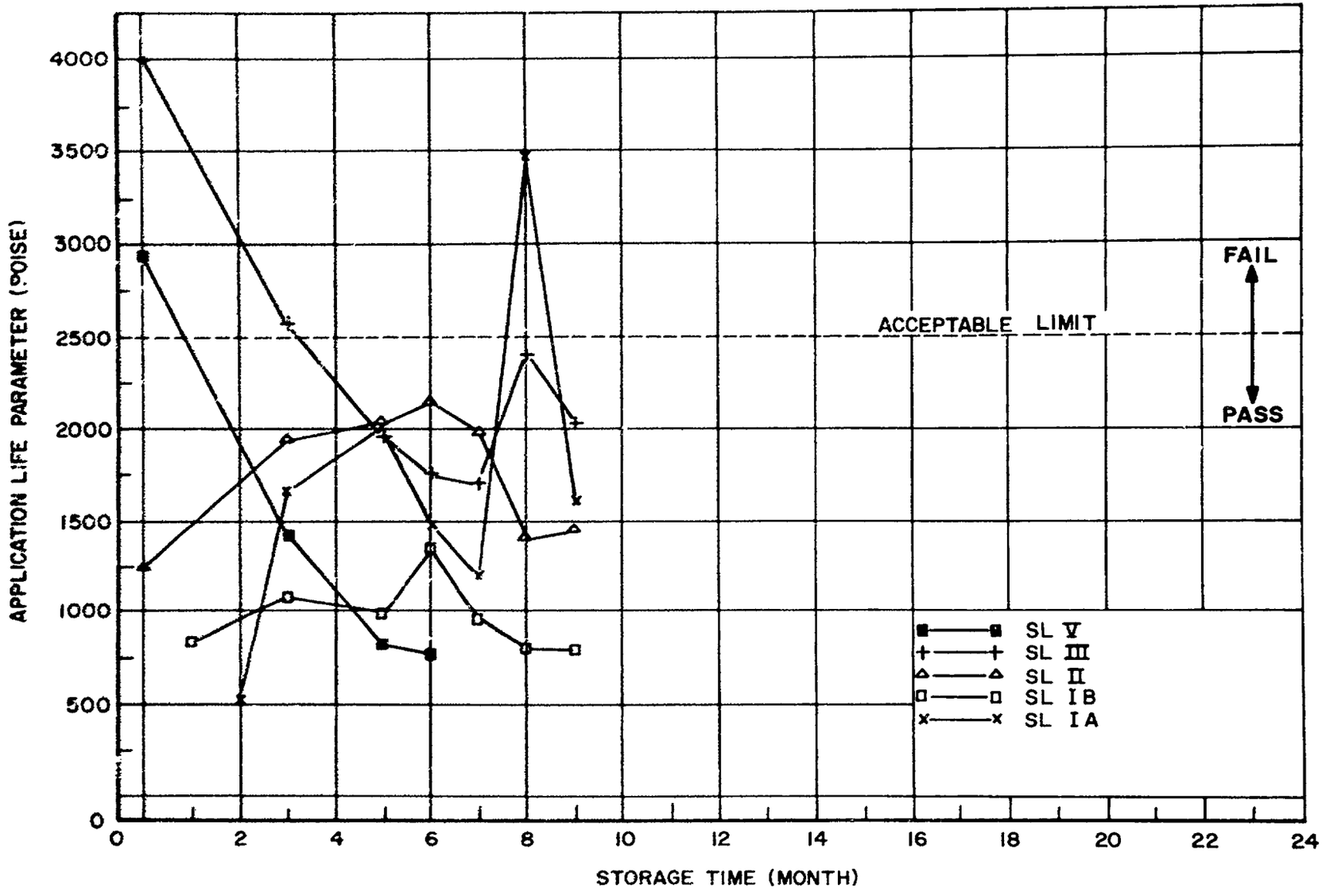

Figure 76. Results of Application Life Tests for Class A-2 Materials in Semkit Form.

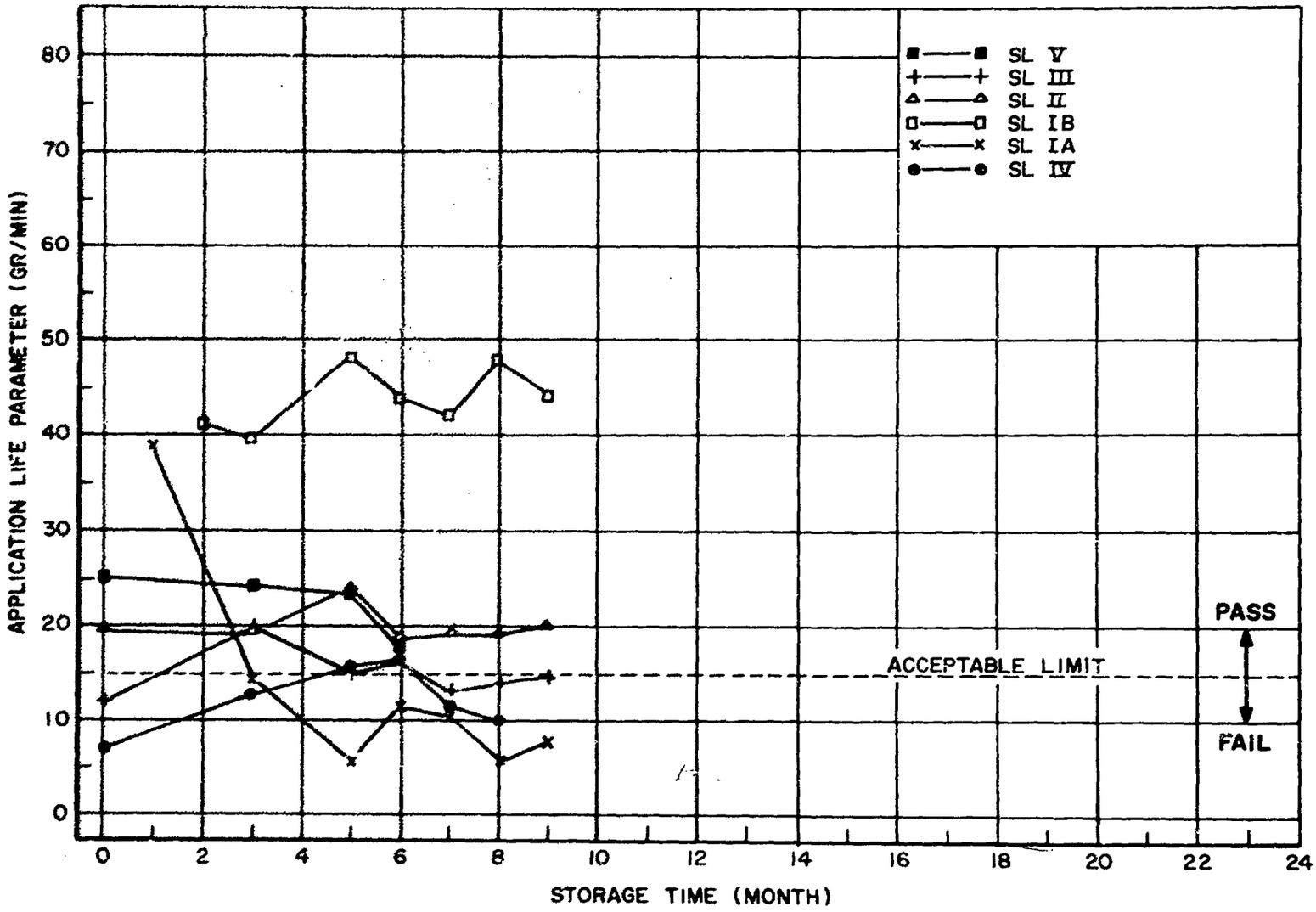

Figure 77. Results of Application Life Tests for Class B-2 Materials in Can Form.

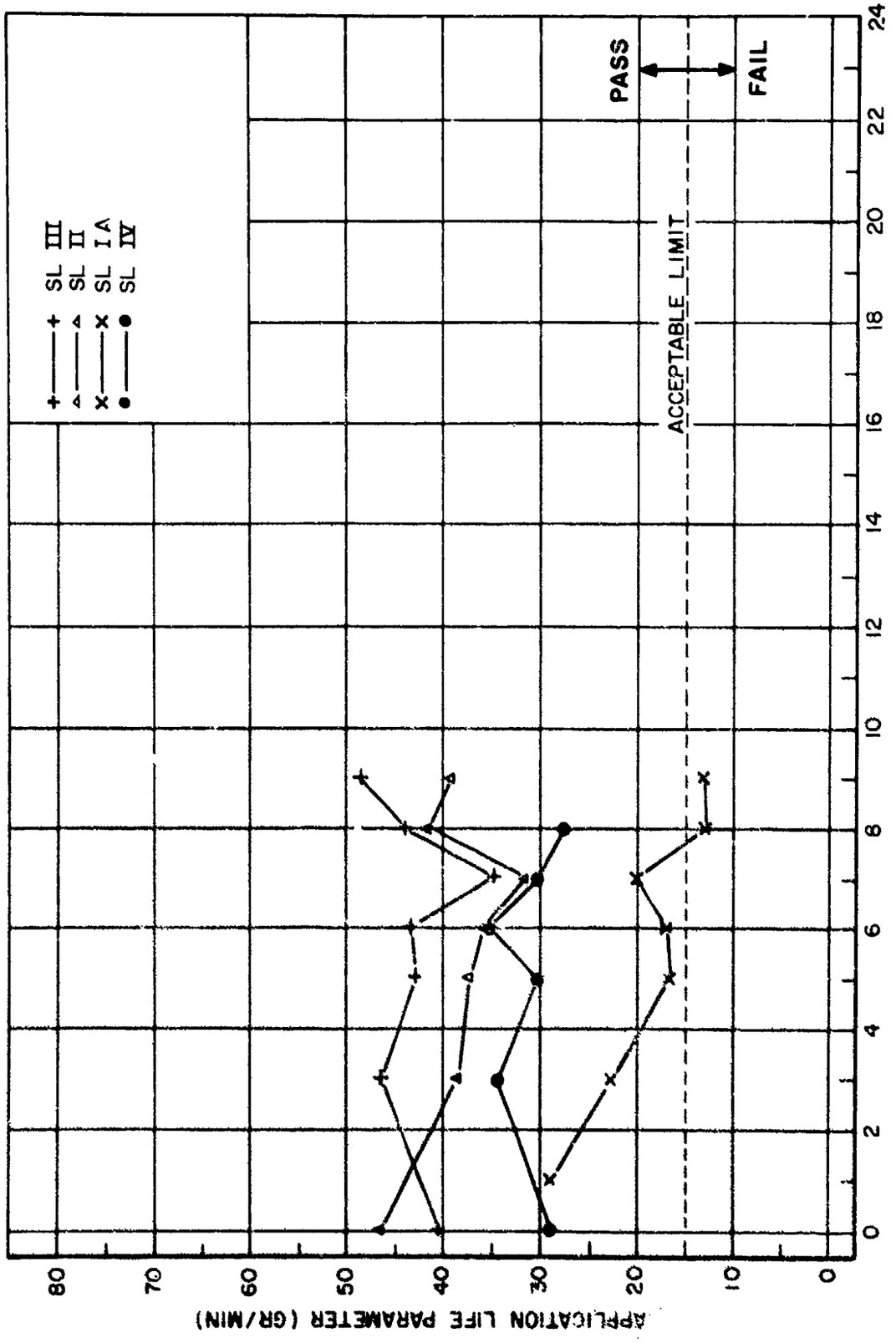

Figure 73. Results of Application Life Tests for Class B-1/2 Materials in Can Form.

tested, SL III and SL V, failed the test initially but recovered in three months (Figure 76).

As shown in Figure 77 the SL IB B-2 compound in cans has the longest application life of the 6 compounds tested. The SL IA compound, SL III, and SL V compounds are all failing this test after 9 months storage. The SL II application life test results were constant throughout the 9 months.

The SL IA B-1/2 compound in cans failed the application life test after 8 and 9 months storage. All of the other compounds in this category passed the test over the 9-month period (Figure 78).

2.2.2.2 Standard Curing Rate Tests

The SL IA class A-2 compound in the aluminum foil and polyethylene Semkit packages failed the standard curing rate test at 2, 5, 6, and 7 months. The same class of the SL II compound failed the standard curing rate tests after 0, 5, 6, 7, 8, and 9 months. This compound passed this test only once during the 9 month test and that was by the minimum acceptable value. The SL III and SL V compounds passed all the standard curing rate tests over the 9-month storage period. All B-2 and B-1/2 Semkit materials tested passed the standard curing rate tests.

SL IA class A-2 compound in cans failed the standard curing rate test after 2, 5, 6, and 7 months. The hardness, however, increased with storage life. The SL II A-2 material in the can form failed this test at 0, 5, and 6 months. It also is indicated an increasing hardness with storage life. The SL V material failed this test after 6 months storage. Its hardness throughout has been close to the minimum acceptable value. All B-2 materials in the can form passed the standard curing rate test.

The SL II B-1/2 compound in can form failed the standard curing rate test after 6 months by one hardness point. It recovered the following month and has been passing since. All other B-1/2 materials are passing after 9 months of storage.

2.2.2.3 Tack-Free Time

The SL III A-2 compound in Semkits was not tack-free in the required 40 hours after 9 months storage. The SL V A-2 Semkit compound did not pass the tack-free time test after 5, 6, and

7 months of storage. After 7 months an additional 240 hours was required before this compound became tack-free.

SL IA B-2 compound in Semkits failed the tack-free time once during these storage tests, at 1 month. It has passed since that time. After 8 months the SL II compound failed to become tack-free in 40 hours, but passed again at 9 months. The SL V compound failed the test for the first time after 7 months of storage. All of the class B-1/2 materials in Semkits have been passing the tack-free time test.

The only A-2 can material failing the tack-free time test was the SL V compound after 7 months of storage and the only B-2 can material failing was the SL V compound after 5, 6, and 7 months. After 7 months exposure this compound did not become tack-free until 138 hours after mixing.

The SL II class B-1/2 compound in cans failed the tack-free time test after 9 months exposure. The similar SL IV compound also failed the tack-free time test after 3, 5, 6, 7, and 9 months exposure. This material was tack-free within 48 hours after mixing.

2.2.3 Discussion

The results of this program show that most of the materials evaluated have difficulty passing the three tests described after 9 months of storage. Several of the compounds evaluated would not pass these tests in the as-received condition. Predicting the storage life for a class of materials is not possible because of the unusual behavior of these materials particularly in the application life testing after storage. Several of these materials cycled from passing to failure and back to passing within a 3 month time interval. Most of the materials that failed the application life test initially were also failing after 9 months. Exceptions to this were the SL III A-2 compound in the can form and the SL V A-2 compound in the can form. This SL V A-2 compound, although passing the application life test after 9 months is failing the tack-free time tests.

As a result of these tests over the first 9 months of storage, the AFML has issued a proposed amendment to Mil-S-8802D. One of the major changes included in this amendment is source inspection of materials qualified to Mil-S-8802D. In addition, these materials are changing during storage, with some materials becoming faster curing and having difficulty meeting application time requirements, and some becoming slower curing and having difficulty meeting the tack-free time. These materials, although not passing these tests, are nevertheless considered usable. Changes in the requirements for the application life, standard curing rate, and tack-free time were issued for materials stored for 9 months and longer. These changes to the specification include a decrease

in the application life by 50% and increases in the standard curing time and tack-free time by 50%. The new values are shown in Tables XXXV and XXXVI. These materials will be reclassified according to these values following 9 months storage.

It is felt that with these changes, the compounds that fail the as-received tests will be eliminated by source inspection and that the relaxing of the requirement for 9 months storage will enable these materials to remain usable over a long storage period.

2.3 HYDROLYTIC STABILITY TESTING OF ELASTOMERS

The high humidity and temperature of a tropical environment to which operational aircraft are being subjected for long periods of time has caused several elastomeric type materials used in these aircraft to revert. The reversion process is a function of relative humidity and is accelerated by high temperatures. Several test programs concerning the hydrolytic stability of elastomeric sealants and electrical potting compounds were conducted to provide engineering data on reversion life.

2.3.1 PC-1 Potting Compound

A two-part testing program involving PC-1 potting compound material was conducted to evaluate its hydrolytic stability. The first part of the program involved the hydrolytic stability of various colorations of the PC-1 compound. The second part of the program was concerned with the effect of mixing ratio on the stability of the compound.

2.3.1.1 Part One Testing

In this portion of the program six colorations of PC-1 were tested for reversion resistance. Six cylinders of premixed PC-1 compound were supplied in the following six colorations: clear, black, yellow, green, red, and orange. All of these cylinders were fully cured and ready for exposure. Test samples were prepared by cutting one-inch thick discs 1.6 inches in diameter from the cylinders.

The test conditions to which the samples were exposed were 160°F and 95% relative humidity, and 200°F and 95% relative humidity for periods of 120 days. Failure was determined by hardness measurements conducted periodically during the 120 day exposure. A 20% loss in hardness was considered a failure. The hardness was determined weekly for the first four weeks and monthly, thereafter, with a Rex A hardness indentor.

The results of these exposures indicate that the color additives to the PC-1 compound have no effect on the hydrolytic

TABLE XXXV

APPLICATION TIME OR WORK LIFE FOR MATERIALS STORED FOR 9 MONTHS

Class Material	Application Time (hours)	Work Life (hours)
A-1/2	1/4	----
A-2	1	----
B-1/2	1/4	----
B-2	1	----
B-4	2	----
C-20	4	8
C-80	4	40

TABLE XXXVI

TACK-FREE TIME AND CURING RATE FOR MATERIALS STORED FOR 9 MONTHS

Class Material	Tack-Free Time (hours)	Curing Rate (hours)
A-1/2	16	64
A-2	64	112
B-1/2	16	45
B-2	64	112
B-4	72	136
C-20	144	---
C-80	180	---

stability of the materials (Table XXXVII). The initial hardness of the samples was 85 points. The samples exposed to the 160°F and 95% relative humidity showed no decrease in hardness until the third week of exposure. The sharpest decrease occurred during the second month of exposure. After four months the hardness had decreased more than the 20% considered as failure but the samples were far from reverted.

The samples exposed to the 200°F and 95% relative humidity environment failed after the third week of exposure. If reversion were defined as the point where the hardness dropped to 20 points, these samples would be considered as having reverted between the second and third month of exposure. After four months, the hardness was only 5 points and the samples were tacky.

During the last month of the 160°F test and the second month of the 200°F test, Rex A hardness readings were supplemented with the Shore A readings. The Shore A instrument is a much easier instrument to read and is more accurate in that it has scale divisions of 1 point versus 5 points with the Rex A. The third and fourth month hardness readings on the 200°F test specimens were all recorded using the Shore A instrument.

All of the samples, except the black ones, underwent a color change during the humidity temperature exposure. The color change was more severe at 200°F than at 160°F but in all cases was complete within two months of exposure. Identification of the test samples by color became very difficult. The color changes which occurred are also listed in Table XXXVII.

2.3.1.2 Part Two Testing

The second testing program involved a study to evaluate the stability of the PC-1 material in high humidity environments as a function of mix ratio. This material is presently being used in the F-4 and F-111 aircraft and has been found to be improperly mixed. The purpose of this program is not to establish why the material was improperly mixed but rather to determine the behavior of the improperly mixed material in a humid environment.

PC-1 is a two part compound that should be deaerated prior to curing to remove entrapped gas bubbles. Sufficient quantities of this compound to prepare approximately 2-inch diameter by 1/4-inch thick specimens were mixed in the following weight ratios: 100/32, 100/27, 100/22, 100/17, and 100/12. The proper mix ratio is 100/22. The compounds were evacuated for 20 minutes and then poured into molds. All samples were cured for 5 hours at 180°F. At 2 hours into the cure, the samples with a mix ratio of 100/12 cracked and began

TABLE XXXVII

HYDROLYTIC STABILITY TEST RESULTS OF SIX COLOR COLORATIONS
PC-1 POTTING COMPOUND

Temp.	Initial Color	Final Color	0 wk.	1 wk.	2 wk.	3 wk.	4 wk.	2 mo.	3 mo.	4 mo.
160°F	black	black	85	85	85	80	80	70	65	65(54)
	yellow	brown	85	85	85	80	80	70	65	65(54)
	green	dark green	85	85	85	80	80	70	65	65(54)
	red	dark red	85	85	85	80	80	70	65	65(54)
	orange	dark orange	85	85	85	80	80	70	65	65(54)
	clear	black	85	85	85	80	80	70	65	65(54)
200°F	black	black	85	75	70	70	65	50(35)	(10)	(5)
	yellow	dark brown	85	75	70	65	65	50(34)	(15)	(5)
	green	black	85	75	70	70	65	50(35)	(15)	(5)
	red	red-brown	85	75	70	65	65	50(35)	(10)	(5)
	orange	red-brown	85	75	70	65	65	50(35)	(15)	(5)
	clear	black	85	75	70	65	65	50(36)	(15)	(5)

NOTE: Values shown in parentheses( ) were obtained with a Shore Type A_2 Instrument; all other values with a Rex Type A.

to swell in the region of the crack. At the end of the cure cycle the specimens were examined and only the samples with the 100/12 mix ratio were tacky, all of the other samples appeared fully cured. The hardness check at a later date indicated that all specimens (including the 100/12 samples) were cured.

All of the samples prepared for this testing program have small bubbles entrapped in the sample despite the vacuum deaeration of the compounds. These bubbles are approximately 10-20 mils in diameter and are dispersed evenly through the specimen. The cause for the bubbles could not be determined.

A new evacuation procedure was developed which yields a completely bubble-free sample. In this procedure, the degassing pressure recommended by the manufacturer is reduced by a factor of 10. To prepare these samples, the premixed compound was poured into a disposable 6-ounce "Semco" plastic cartridge. This cartridge is approximately 1-1/2 inches in diameter and 6 inches deep and was filled approximately 1/2 full with mixed compound. The filled cartridges were placed in a vacuum dessicator and the pressure inside the dessicator slowly reduced to 0.5 torr. Most of the gas bubbles are removed at a pressure of 2 torr but there is still evidence of bubbling until the pressure is reduced to the 0.5 torr level. The cartridge was then removed from the vacuum and placed in an air gun. The cartridge tip was placed about 1/8-inch from the bottom of the mold to be filled. The compound was then expelled from the cartridge while keeping the cartridge tip about 1/8-inch from the rising level of the compound in the mold. This technique is used to prevent "folding in" of air bubbles when filling the mold. The particular mold used in this program was a disposable aluminum foil cup approximately 2 inches in diameter and 1/2 inch high.

Using this technique, ten additional samples were prepared and were tested according to the same procedures as the original samples. In addition, two samples were prepared at a mix ratio of 100/7. These samples cured but the initial hardness was low. All hardness measurements were made on these samples after they were allowed to cool to room temperature (approximately 2 hours after removal from the oven). The stability of these samples was determined by hardness measurements as in Part One. After 90 days exposure, the hardness values were again recorded with both the Rex A and Shore A_2 hardness indentors.

The results of these tests shows that the PC-1 potting compound can be mixed over a wide range of accelerator to base ratios and still cure. Hardness measurements on freshly cured samples, therefore, cannot be used to indicate any change in mixing ratio. The only

change in the as-cured hardness occurred with the 100/7 mix ratio sample. The complete test results (hardness values) are shown in Table XXXVIII.

Using the criteria of 20% loss in hardness as failure, the 160°F bubble-free samples failed between 60 and 90 days and the 200°F samples failed between 13 and 20 days. None of the samples were reverted at this point, but 200°F samples reverted between 90 and 120 days. The 100/7 mix ratio samples decayed at approximately the same rate as the other mix ratios.

These results also show that the reversion time is not seriously altered by mixing ratio until the accelerator to base ratio is reduced to approximately 1/3 of that recommended. Samples mixed at accelerator to base ratio higher than that recommended by the manufacturer had the same behavior as the properly mixed material.

The presence of entrapped gas bubbles in the test samples had little effect on the reversion resistance of the PC-1 compound that was mixed at the proper base accelerator ratio. At the extremes of the mix ratios investigated, slightly longer reversion times were observed with the samples that were bubble free.

2.3.2 Compounds PC-2, PC-3, and PC-4

Three potting compounds were evaluated for humidity resistance and insulation resistance following humidity exposure. PC-2 is a one part flexible epoxy, PC-3 and PC-4 are two-component humidity-resistant polyurethanes. Test samples of the three materials were subjected to 160°F and 200°F at 95% relative humidity environments for 120 days. The electrical insulation resistance and reversion resistance were determined periodically during the four-month exposure.

2.3.2.1 Test Procedure

Two samples of each material were prepared using mixing and curing techniques recommended by the manufacturer. The samples were fabricated in two forms; one for insulation resistance, the other for humidity evaluation. The insulation resistance samples were fabricated by pouring the mixed material into 1-inch long and 1-3/8-inch diameter rigid sections of aluminum conduct, which served as a mold. Following cure, two brass screws were placed into the material 3/4-inch apart to serve as electrodes. The hardness samples were prepared by extruding the premixed, degassed compound from a 6-ounce cartridge into an aluminum foil disposable cup. The cup was approximately 2 inches in diameter by 1/2 inch deep.

TABLE XXXVIII

HARDNESS OF PC-1 POTTING COMPOUND FOR DIFFERENT MIX RATIOS

Samples with Entrapped Gas Bubbles

Test Temperature	Mix Ratio	Time (Days) 0	1	2	3	6	7	8	9	10	13	20	27	58	90	120
160°F	100/32	75	70	70	70	65	65	65	65	65	65	65	65	65	55 (48)	55 (45)
	100/27	80	80	80	75	75	75	75	75	75	75	75	70	65	65 (57)	60 (49)
	100/22	85	85	85	85	85	85	80	80	80	80	75	75	70	70 (60)	65 (51)
	100/17	85	85	85	85	85	85	85	85	85	80	80	70	65	65 (50)	55 (44)
	100/12	75	80	80	80	80	80	80	80	80	75	65	55*	55*	50*(41)	40 (31)
200°F	100/32	75	70	70	65	65	65	65	65	65	60	55*	50*	40*	25*(18)	5*(5)
	100/27	80	80	80	75	75	75	75	75	75	65	65*	55*	45*	35*(25)	15*(10)
	100/22	85	85	85	80	80	80	80	80	80	65	65*	65*	50*	40*(26)	15*(10)
	100/17	85	85	85	85	80	80	80	80	80	70	65*	60*	45*	35*(22)	15*(10)
	100/12	75	80	80	80	75	75	75	75	75	65	50*	45*	30*	25*(11)	5*(5)

Samples without Entrapped Gas Bubbles

Test Temperature	Mix Ratio	Time (Days) 0	1	2	3	6	7	8	9	10	13	20	27	90	120
160°F	100/32	85	85	80	80	80	75	75	75	75	75	75	70	65 (61)	60 (56)
	100/27	85	85	85	80	80	75	75	75	80	75	75	75	70 (61)	60 (56)
	100/22	85	85	85	85	85	80	80	80	80	75	75	75	70 (65)	60 (50)
	100/17	85	85	85	85	85	80	80	80	75	75	75	70	65 (56)	60 (50)
	100/12	85	80	80	80	75	75	70	70	70	70	65	65	55 (47)	50 (36)
	100/7	70	70Δ	70	70	65	60	60	55	50	50	50	45	35 (22)	25 (18)

TABLE XXXVIII (concluded)

HARDNESS OF PC-1 POTTING COMPOUND FOR DIFFERENT MIX RATIOS

Samples without Entrapped Gas Bubbles

Test Temperature	Mix Ratio	Time (Days) 0	1	2	3	6	7	8	9	10	13	20	27	90	120
200°F	100/32	85	80	75	75	75	70	70	70	70	70	65	60	45*(41)	25*(17)
	100/27	85	85	80	80	75	70	70	70	70	70	65	65	45*(41)	25*(17)
	100/22	85	85	85	80	75	75	75	75	70	70	65	65	45*(39)	25*(14)
	100/17	85	85	80	80	70	65	65	65	70	65	60	60	40*(32)	20*(12)
	100/12	85	75	75	75	65	60	60	60	55	55	50	50	35*(21)	10*(5)
	100/7	70	70Δ	65	60	50	50	50	50	35	35	30*	30*	15*(10)	-- (2)

Δ Material puffed slightly

* Indicates sample was tacky

NOTE: Values shown in parentheses ( ) were obtained with a Shore Type A_2 Instrument; all other values with a Rex Type A.

One hardness sample and one insulation resistance sample of each material were exposed to the 160°F and 95% relative humidity and 200°F and 95% relative humidity environments for 120 days. The insulation resistance and hardness measurements were made weekly for the first month and monthly, thereafter.

For the reversion portion of the tests, a decrease in the Shore A hardness to below 20% of the original value was considered as failure. The insulation resistance samples were considered failing when the resistance dropped below 10^2 megohms.

2.3.2.2 Results

The test results in Table XXXIX show that PC-2 failed the hydrolytic stability tests at 200°F and 95% relative humidity after the first month of exposure. PC-3 and PC-4 easily passed throughout the 160°F and 200°F exposure. After 50 days at 200°F the PC-2 samples completely reverted and measurements of insulation resistance and hardness were not possible to obtain. Figure 79 shows the degraded condition of the PC-2 insulation resistance sample.

At 160°F the insulation resistance of the P/C-2 material continually decreased over the 120 day exposure period. The P/C-3 and P/C-4 materials maintained nearly the same insulation resistance throughout the test period. The hardness of all three materials remained constant.

At 200°F the P/C-3 and P/C-4 materials showed only slight changes in resistance during the first two months but decreased sharply during the last two months. The hardness value of the P/C-4 decreased 20% over the 120 day period while the P/C-3 decreased only 11%. As previously mentioned, the P/C-2 material reverted after 50 days of exposure.

2.3.3 Evaluation of PC-5

PC-5 is a two-part polyurethane potting material formulated as a molding compound for electrical cables and as a potting compound for electrical connectors. The manufacturer claims that it is useful over a -70°F to 300°F temperature range. The purpose of these programs was to determine the hydrolytic stability of this polyurethane compound at the less severe conditions of 160°F and 95% relative humidity for 120 days.

2.3.3.1 Procedures

Four hardness samples were prepared from raw materials by hand mixing and degassing at 0.5 torr for 10 minutes. Two of

TABLE XXXIX

HARDNESS AND INSULATION RESISTANCE TEST RESULTS

Insulation Resistance (megohms)

Sample	Test Condition	0 wk.	1 wk.	2 wk.	3 wk.	1 mo.	2 mo.	3 mo.	4 mo.
PC-2	160°F-95% R. H.	6.1×10^5	6.1×10^4	1.7×10^4	7.5×10^3	4.3×10^3	2.6×10^3	2.2×10^3	9.5×10^2
PC-3	160°F-95% R. H.	1.6×10^6	1.5×10^6	1.6×10^6	1.3×10^6	1.5×10^6	1.3×10^6	1.2×10^6	1.4×10^6
PC-4	160°F-95% R. H.	1.6×10^6	1.6×10^6	1.7×10^6	1.4×10^6	1.5×10^6	1.3×10^6	1.2×10^6	1.4×10^6
PC-2	200°F-95% R. H.	7.0×10^5	4.0×10^3	2.0×10^3	1.1×10^3	3.1×10^2	--------REVERTED--------		
PC-3	200°F-95% R. H.	1.6×10^6	1.6×10^6	1.6×10^6	1.3×10^6	1.4×10^6	1.2×10^6	3.0×10^5	2.0×10^4
PC-4	200°F-95% R. H.	1.7×10^7	1.6×10^6	1.6×10^6	1.3×10^6	1.5×10^6	1.3×10^6	7.0×10^4	5.0×10^3

Hardness (points)

Sample	Test Condition	0 wk.	1 wk.	2 wk.	3 wk.	1 mo.	2 mo.	3 mo.	4 mo.
PC-2	160°F-95% R. H.	61	55	56	57	59	64	66	63
PC-3	160°F-95% R. H.	61	60	63	62	62	64	63	63
PC-4	160°F-95% R. H.	88	83	85	87	86	87	86	85
PC-2	200°F-95% R. H.	61	59	60	58	43	--------REVERTED--------		
PC-3	200°F-95% R. H.	61	59	60	59	57	58	56	54
PC-4	200°F-95% R. H.	88	83	84	81	81	80	76	70

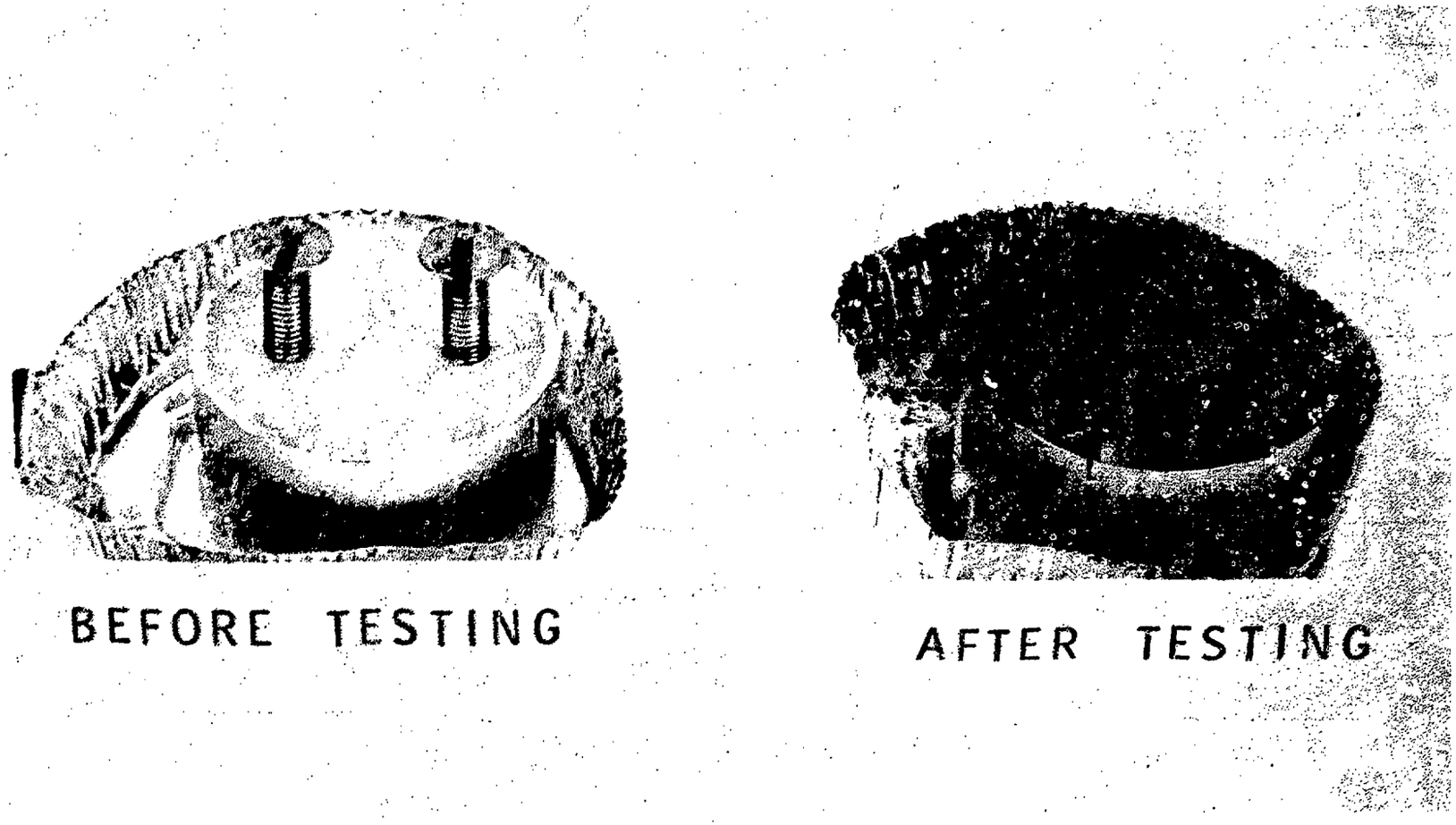

Figure 79. PC-2 Insulation Resistance Sample Before and After Exposure.

the four samples prepared received the standard 14-day cure at room temperature and 50% relative humidity. The remaining two samples received an accelerated cure of 7 hours at 180°F. Both of these cures were suggested in the product literature supplied by the manufacturer. Following the curing cycle, the samples were placed in a humidity chamber at 160°F and 95% relative humidity.

The hardness of the material was recorded at 0, 7, 14, 21, 28, 42, 56, 84, and 120 days. All samples were removed from the humidity chamber and allowed to cool to room temperature. Approximately two hours cooling time was allotted before hardness measurements were made.

2.3.3.2 Results

The early test results indicated that the samples were not fully cured at the beginning of the testing schedule even though the suggested curing procedures were followed. These results show that even after 4 weeks in the humidity chamber, none of the samples had fully cured. In addition the samples had lower hardness values than those suggested by the manufacturer for this sealant following cure. Manufacturer's data indicate that the materials subjected to a 7-hour cure at 180°F should have a Shore A hardness value of 80 points. The samples evaluated in this initial test were approximately 1/2 that value.

Based on these early results, a second batch of samples were prepared from fresh material. Tests on the initial samples were not discontinued but allowed to complete the full 120 day exposure period.

The test results on both the initial and second batch of samples are shown in Table XL. Although the second batch of samples indicate higher hardness values than the initial batch, they are not yet up to advertised values. The second batch of room temperature samples were not fully cured until after 7 days of exposure to the humidity environment.

The hydrolytic stability of these samples was good based on the accepted 20% loss in hardness criteria. The second series of samples lost less than 10% hardness following the 120-day exposure to the 160°F and 95% relative humidity environment.

2.3.4 FTS-B Sealant

An experimental polysulfide based fuel tank sealant was evaluated for qualification to several tests described in Mil-S-8802D. These tests are specific gravity, flow, standard curing rate, peel strength,

tensile strength, elongation, weight loss, and flexibility. FTS-B is a two-component sealant with an application life of two hours.

2. 3. 4. 1 Procedure

All of the test samples were prepared by mixing the two components on a Semco dasher type mixer according to manufacturer's specifications. The test procedures followed will not be discussed in detail here since this is available elsewhere (Reference 53).

2. 3. 4. 2 Results

The test results (Table XI.I) showed that FTS-B failed most of the six tests. The only tests passed were the specific gravity and the flexibility tests. The flow rate was too high for passage, the standard curing rate test failed with a hardness of 9 instead of the 35 points required. The peel strengths were lower than required with all of the panels failing adhesively. The tensile strengths and elongations were very erratic and the material had an overall weight loss of 8. 52% which is above the maximum permitted.

2. 3. 5 FTS-C Sealant

FTS-C is an experimental low density fuel tank sealant. It is a polysulfide based compound that was tested for mechanical and physical properties. The specific tests conducted were peel strength, tensile strength, elongation, and hardness.

2. 3. 5. 1 Procedures

Because the supply of the FTS-C material was limited, the number of tests and the test procedure were slightly modified from those described in Mil-S-8802D.

The FTS-C sealant was mixed in a Semco dasher type mixer. The sealant was allowed to cure for 14 days at room temperature. Tensile and elongation samples were cut from a 1/8-inch thick molded sheet of material fabricated from the mixed sealant. The tensile and elongation samples were dogbone shape and cut with an ASTM "C" die. Hardness measurements were made by folding the 1/8-inch thick dogboned specimen back onto itself to achieve the proper 1/4-inch thickness for hardness measurements. Hardness measurements were made on the tabs only. All specimens were allowed to cool for two hours at room temperature before testing.

Text continued on page 164

TABLE XL

HYDROLYTIC STABILITY OF PC-5 POTTING COMPOUND

Time (days)	Initial Test Series Hardness (points)		Second Test Series (Hardness (points)	
	R. T. Cure	90°F Cure	R. T. Cure	180°F Cure
0	43	41	52	71
7	54	46	69	72
14	55	46	69	71
21	56	53	65	72
28	57	55	66	71
42	59	53	64	71
56	56	53	65	69
84	55	48	62	67
120	52	45	60	66

TABLE XLI

TEST RESULT OF SEALANT FTS-B

Test	Results	Remarks
1. Specific Gravity	Passed	Specific Gravity 1.15
2. Flow	Failed	Flow after 50 min. - 0.94-in. Flow after 90 min. - 0.95-in.
3. Standard Curing Rate	Failed	Hardness after 72 hrs.
4. Peel Strength		
a. Original	Failed	Max. peak load - 15.5 lbs. Cohesive failure
b. 7 days at 140°F in JRF*	Failed	Max. peak load - 4.5 lbs. Adhesive failure from cloth
c. 7 days at 140°F in JRF/ saltwater	Failed	Max. peak load - 4.25 lbs. Adhesive failure from cloth
d. 70 days at 140°F in JRF	Failed	Max. peak load - 4.1 lbs. Adhesive failure from cloth
e. 70 days at 140°F in JRF/ saltwater	Failed	Max. peak load - 5.0 lbs. Adhesive failure from cloth

*JRF: Jet Reference Fluid

TABLE XLI (concluded)

TEST RESULT OF SEALANT FTS-B

Test	Results	Remarks
7. Tensile and Elongation		
a. Standard Cure	Failed Passed	Ultimate Tensile Strength - 172 psi Elongation - 213%
b. 7 days at 200°F	Not identified in Mil -S-8802 D	Ultimate Tensile Strength - 94 psi Elongation - 125%
c. 7 days at 200°F	Passed Failed	Ultimate Tensile Strength - 300 psi Elongation - 92%
d. 14 days at 140°F in JRF	Passed Failed	Ultimate Tensile Strength - 107 psi Elongation - 101%
6. Weight Loss and Flexibility		
a. Weight Loss	Failed	Weight loss - 8.52%
b. Flexibility	Passed	No cracking or chalking

2.3.5.2 Results

The material has a very low specific gravity of 0.58. It does not have good peel strength, tensile strength or hardness (Table XLII). The as-cured tensile strength, elongation, and hardness were 54 psi, 130% and 23 points, respectively. After 30 days at 160°F, the tensile strength increased to 105 psi, the elongation decreased to 67% and the hardness increased to 34 points. This indicates that the material was not fully cured or that it is susceptible to age hardening. Secondly, the cross section of the samples changed during the 30 day heat soak. The as-cured material contains many voids. After exposure, the structure appears to collapse, filling the voids (Figure 80).

The samples exposed to the 200°F heat conditioning for 30 days were not able to be tested because the sample cross section had drastically changed and the samples adhered to the aluminum panel on which they were supported during the exposure. The samples that were exposed to the 160°F and 95% relative humidity for 120 days reverted after 45 days of exposure. At the end of the 120 days, the condition of the samples was too poor to permit testing as they also adhered to the aluminum panel.

2.3.6 Evaluation of MC-A and MC-B Materials

A testing program was conducted to determine the tensile strength, elongation, and hardness of compounds MC-A and MC-B following aging at 160°F and 95% relative humidity. MC-A is a polyester polyurethane that is used as a molding compound and has a prior history of reversion. The MC-B is a polyether polyurethane and is recommended as a reversion-resistant compound. The properties of both of these materials were determined following aging for 0, 28, 56, 84, and 120 days at 160°F and 95% relative humidity.

2.3.6.1 Procedure

The sample configuration was an ASTM "C" size dogbone shaped tensile specimen. The test specimens were placed on aluminum foil and put in desiccators containing a saturated solution of potassium sulfate to maintain the 95% relative humidity. The desiccator was then placed in an oven at 160°F for the 120 day test period. Each compound was kept in a separate desiccator. Hardness readings were made on the tab of the dogbone specimens.

2.3.6.2 Results

The 160°F and 95% relative humidity environment caused all of the MC-A test samples to revert before they could be tested. Only the as-received test data were obtained because of the early reversion.

TABLE XLII

TEST RESULTS OF FTS-C FUEL TANK SEALANT

1. Specific Gravity: 0.58

2. Peel Strength:

Test Condition	Panel	Fabric	Max. Peak Load (lbs.)	Type of Failure
20 days at 140°F 3% saltwater	Mil-A-8625	Duck	3.2	Adhesive to cloth
As Cured	Mil-A-8625	Duck	4.5	Adhesive to cloth
20 days at 140°F 3% saltwater	Mil-C-5541	Duck	4.1	Adhesive to cloth
As Cured	Mil-C-5541	Duck	5.5	Adhesive to cloth

3. Tensile Strength, Elongation, and Hardness:

Test Condition	Ultimate Tensile Strength (psi)	Elongation (%)	Hardness (points)
As Cured	54.0	130	23
30 days at 160°F	105	67	34
30 days at 200°F	-----	---	--
120 days at 160°F and 95% R.H.	----	---	--

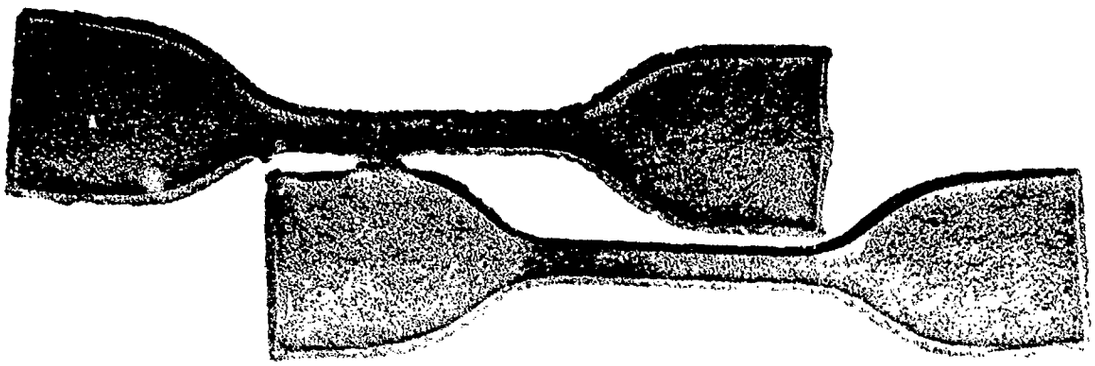

Figure 80. FTS-C Test Specimens Indicating Reversion and Collapsing Voids.

The reversion of the MC-A material was first observed after only 5 days of exposure. The samples were deformed, and in some locations, became liquid. The samples turned color, from clear to manila, during cooling from 160°F to room temperature. The samples were allowed to sit at room temperature for several days after reversion. After two days, the samples returned to the clear color. A slight increase in hardness was observed after this two day exposure to room temperature. After 28 days of exposure, all of the MC-A samples had reverted. All of the samples were stuck to the aluminum foil and could not be removed. The as-received mechanical property data are shown in Table XLIII.

The MC-B completed the 120 day exposure in the test environment. The results of the mechanical property tests on MC-B are also shown in Table XLIII. After 28 days of exposure the ultimate tensile strength dropped 37% with an increase in elongation of 8%. From 28 days through 84 days of exposure, the mechanical property remained relatively constant. From 84 to 120 days of exposure, a slight increase in tensile strength was observed. The MC-B did not show any tendency to revert nor did it adhere to the aluminum foil. The hardness of each of the samples tested was monitored for several days after exposure. Only slight increases (a maximum of 5 points) were found and this increase occurred within the first 3 days of the post-test room temperature exposure.

2.3.7 Cover Material CM-A

Compound CM-A is a polyurethane cover material used for expandable structures. The hydrolytic stability of CM-A was determined by testing the material for hardness, tensile strength and elongation after 0, 28, 56, 84, and 120 days in a test environment of 160°F and 95% relative humidity. The tests were conducted in a humidity-controlled environmental test chamber.

2.3.7.1 Procedure

Material for this program was supplied in sheet form and was only 0.015-inch thick. To obtain a suitable hardness sample, seventeen 2-inch x 2-inch x 0.015-inch sheets were cut from the material and stacked to attain a total thickness of approximately 1/4-inch. The hardness was determined with a Shore A indentor. The tensile specimens were cut from the sheet material with an ASTM size "D" die.

2.3.7.2 Results

The test results showed that the material did not revert during the 120-day humidity exposure. However, the test samples were not completely resistant to the environment. After the initial

TABLE XLIII

MECHANICAL PROPERTY
TEST RESULTS ON MC-A AND MC-B

Specimen	Test Environment	Ultimate Strength (psi)	Elongation (%)	Hardness (points)
MC-A	As Received	3017	787	65
MC-B	As Received	4118	660	81
MC-B	160°F/95% R.H./28 days	2588	717	75
MC-B	160°F/95% R.H./56 days	2583	685	76
MC-B	160°F/95% R.H./84 days	2407	790	72
MC-B	160°F/95% R.H./120 days	2743	783	71

28 days of exposure, blisters were observed on one side only of the test samples. These were particularly evident in the 2 x 2-inch hardness samples where the sheets were stacked upon each other. When the blisters were broken they were found to contain a clear liquid, probably water. The average size of the blisters was about one square millimeter. Although no accurate amount of the blisters was maintained, the blisters appeared to increase in number during the last month of exposure.

The test results in Table XLIV showed that the largest decrease in tensile strength occurred during the first and last months of exposure. The elongation increased sharply after the first month of exposure and then decreased slowly throughout the remaining 90 days. The hardness dropped 80 points during the first month and remained relatively constant for the remainder of the exposure.

2.4 COMPATIBILITY OF ELASTOMERS

Despite extensive materials test programs, difficulties often occur when the materials are in use in an operational system. In many cases the failures are either caused or accelerated by attack from some fluid which contacts the material. Compatibility problems are common causes for failure of elastomeric materials.

The compatibility testing programs discussed here are a result of material problems which occurred in operational systems in the field. They are generally designed to identify or substantiate the existence of a compatibility problem and to recommend a solution to the problem, if possible.

2.4.1 Elastomers in Lubricants

Field tests reported that numerous failures in seals had been located in helicopter jet engines. These reports indicated that the problem was probably the result of the seal being incompatible with the engine lubricant even though these seals and lubricants were approved for use in this particular engine.

2.4.1.1 Procedure

The initial effort in this program was to evaluate the compatibility of the particular helicopter seal in a variety of approved engine lubricants which are qualified to Mil-G-7808.

Thirteen chevron-type seals and eleven lubricants were used in this test program. This seal material was described as a flourosilicone compound and will be referred to as L/C-1. The seals were aged in the lubricating oils for 70 hours at 302°F and then tested for load and elongation in tension, and volume change. Because of the complex shape of the chevron seal, an ultimate tensile strength calculation was omitted and the test results were reported as a tensile load. Test samples were fabricated by cutting the circular shaped seal into three equal length pieces (Figure 81). The 70-hour agings were conducted by suspending the 3 sections of the seal in a mason jar in which the oil level was such that it completely covered the specimens.

2.4.1.2 Results

The results of the initial series of tests (Table XLV) showed that a severe chemical reaction occurred between the chevron seal and the lubricant coded as LO-3. The seal itself had lost all its strength and was soft and tacky. Light rubbing would remove large quantities of the material. The condition of the seal was so poor that tensile and elongation tests could not be conducted.

Text continued on page 174

TABLE XLIV

HYDROLYTIC STABILITY TEST RESULTS
ON CM-A COVER MATERIAL

Time (days)	Tensile Strength (PSI)	Elongation (%)	Hardness (points)
0	3504	537	80
28	2462	718	66
56	2325	697	65
84	2308	672	63
120	1863	662	65

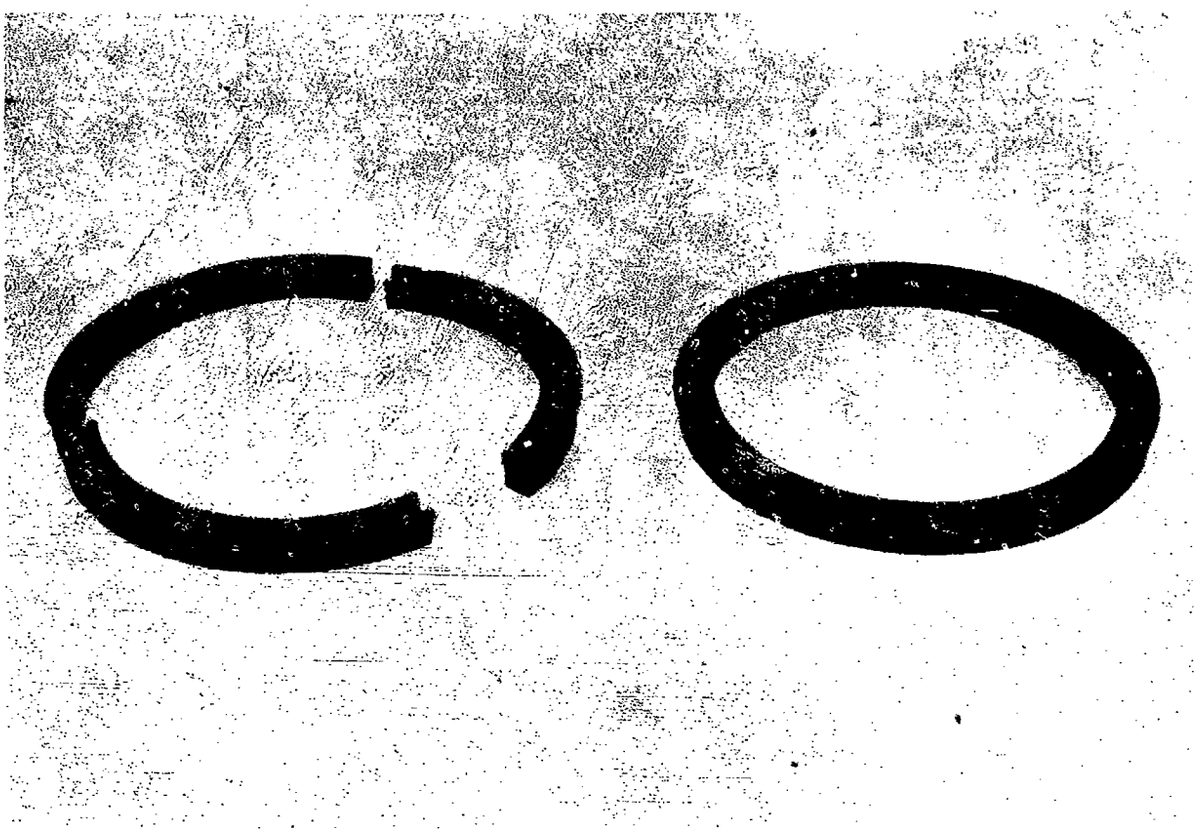

Figure 81. L/C-1 Chevron Helicopter Seal and Cut Test Sections.

TABLE XLV

RESULTS OF L/C-1 CHEVRON TYPE SEAL TESTS

	Load in Tension (lbs)	Elongation (%)	Volume Swell (%)
As Received	23.6	127	----
After exposure to:			
LO-1	14.8	115	28.5
LO-2	15.7	130	25.9
LO-3	----	---	11.4*
LO-4	19.7	113	10.1
LO-5	18.7	110	10.0
LO-6	19.0	118	19.0
LO-7	17.5	101	11.3
LO-8	15.7	97	23.9
LO-9	16.9	99	9.9
LO-10	16.3	94	10.0
LO-11	15.9	124	19.5

* Because of the poor condition of the seal. this is only an approximate value.

Seals evaluated in the other ten lubricating oils suffered losses in tensile strength from 16.5% to 41.5%. Losses in elongation did not exceed 26% of the as-received values. None of these seals showed any visible evidence of chemical attack as was found with the seal aged in the LO-3 lubricant.

As a result of analytical studies conducted at AFML the L/C-1 seal was identified as a silicone rather than a flourosilicone compound. In addition, further materials were scheduled for aging tests in the lubricating oils. These materials are identified as L/C-2, L/C-3 and L/C-4. The L/C-3 and L/C-4 materials were provided in sheet form and were evaluated in the LO-3 lubricant only. The L/C-2 material was an actual chevron seal and test samples were prepared in the same manner as the L/C-1 material. The same tests were conducted on these materials as the L/C-1 samples. However, the L/C-3 and L/C-4 test samples were cut from sheet material using a dogbone tensile cutter. The tests results, therefore, show that the ultimate tensile strength could be calculated and reported rather than simply the load in tension. The results of these tests are shown in Table XLVI.

The results of these tests show that the L/C-2 material is compatible with the lubricants tested. The maximum loss in strength is less than 30% of the as-received value and occurred with the LO-1 oil. Over half of the seals showed increases in elongation after aging, with the others showing slight decreases. The volume swell of these samples ranged from 4.8% to 11.0%.

The L/C-3 and the L/C-4 materials aged in LO-3, however, both demonstrated evidence of incompatibility. The L/C-3 samples became so brittle that they could not be tensile tested in the usual manner. The L/C-4 material, although not showing any visible reactions, lost considerable tensile strength and elongation. The volume swell for this material was 9.5%.

In the third phase of lubricant/compatibility testing program a silicone chevron type seal (L/C-1) was evaluated under identical conditions. These seals, however, were aged in different lubricants than those discussed above. These are candidate lubricants to Mil-L-7808 and are coded as LO-12, LO-13, LO-14, LO-15, LO-16, and LO-17. The test samples were prepared as before by cutting the seal into three equal-length portions. The results are included in Table XLVI.

Three of the five lubricants reacted with the seals. These are LO-13, LO-14, and LO-15. The seals became soft and the surface of the seal could be removed by light rubbing motion along the surface. The load in tension of the samples aged in these oils was approximately 1/2 of the original value. Samples aged in the LO-15 and LO-17 had much higher elongations than others.

TABLE XLVI

RESULTS OF LUBRICANT/SEAL COMPATIBILITY TESTS

Material	Lubricant	Load in Tension (lbs)	Elongation (%)	Volume Increase (%)	Ultimate Tensile Strength (psi)
L/C-2	L/O-1	33.3	163	9.8	----
	L/O-2	45.5	103	8.5	----
	L/O-3	37.3	87	11.0	----
	L/O-4	38.3	81	8.2	----
	L/O-5	31.2	131	6.8	----
	L/O-6	42.6	200	8.0	----
	L/O-7	42.9	92	4.8	----
	L/O-8	39.1	205	9.4	----
	L/O-9	51.3	138	7.9	----
	L/O-10	38.5	89	7.1	----
	L/O-11	41.9	92	8.2	----
	As Received	44.2	97	---	----
L/C-3	As Received	----	540	---	1227
	L/O-3	----	*	5.9	*
L/C-4	As Received	----	230	---	1105
	L/O-3	----	191	9.5	419

*Because of the poor condition of the test sample following exposure, this sample could not be tested.

TABLE XLVI (concluded)

RESULTS OF LUBRICANT/SEAL COMPATIBILITY TESTS

Material	Lubricant	Load in Tension (lbs)	Elongation (%)	Volume Change (%)	Ultimate Tensile Strength (psi)
L/C-1	L/O-12	18.8	57	23.0	----
	L/O-13	12.0	65	18.8	----
	L/O-14	10.8	52	24.6	----
	L/O-15	13.0	125	26.4	----
	L/O-16	15.7	41	20.9	----
	L/O-17	16.1	136	24.8	----
	As Received	23.3	58	----	----

2.4.1.3 Summary

These tests show conclusively that the L/C-1 seal material should not be used in systems where it could come in contact with the LO-3 lubricant. Also, the use of this material in systems containing the LO-13, LO-14, and LO-15 lubricants is questionable and further compatibility tests should be conducted with those combinations. The use of L/C-3 and L/C-4 materials with the LO-3 lubricants also is not recommended.

2.4.2 Elastomers in Fuels

As a result of recent seal failures which occurred in the field, a program was initiated to examine two elastomeric compounds for compatibility with jet fuels. One of the compounds is qualified to Mil-P-5315 and the other qualified to AMS 7271.

2.4.2.1 Procedure

Size 214 O-ring packings of the two compounds designated F/C-1 and F/C-2 were used for these evaluations. Three packings were exposed to each of six test conditions. These tests were conducted at room temperature and under the following conditions.

1. Type I (TT-S-735) test fuel for 70 hours.
2. Type III (TT-S-935) test fuel for 70 hours.
3. JP-4 for 70 hours.
4. JP-7 for 70 hours.
5. Type III test fuel for 70 hours followed by Type I test fuel for 70 hours.
6. JP-4 for 70 hours, followed by JP-7 for 70 hours.

The packings were suspended in the test fuel in covered mason jars. Following exposure, the packings were tested for volume change.

2.4.2.2 Results

The results of these tests revealed that the F/C-2 compound underwent a large change in volume (181.7%) when the samples were exposed to Type III test fuel.

The rings were also found to float in water following exposure. Because of this unusually high volume change, a second batch of the F/C-2 packings were purchased and the same test repeated. The complete test results are shown in Table XLVII.

TABLE XLVII

FUEL COMPATIBILITY TEST RESULTS

Test Environment	Volume Increase (%) F/C-1 Batch 1	F/C-2 Batch 1	F/C-2 Batch 2
1. Type I for 70 hours	1.2	14.9	15.1
2. Type III for 70 hours	32.3	181.7	64.5
3. JP-4 for 70 hours	10.9	41.0	40.5
4. JP-7 for 70 hours	2.2	22.0	21.9
5. Type III for 70 hours Type I for 70 hours	-2.7*	10.8	10.0
6. JP-4 for 70 hours JP-7 for 70 hours	-1.7*	22.4	21.6

*Volume Decrease

The second batch of packings tested indicates essentially the same results as the batch one tests, except for that of the Type III test fuel. The volume swell was only 64.5% versus the 188.7% reported during the earlier exposure.

Both the F/C-1 and F/C-2 compounds underwent the highest volume change when exposed to the Type III test fuel. Also, significant reductions in volume swell were found when the compounds were exposed to the combinations of Type III/Type I and JP-4/JP-7 test fuels. The F/C-1 compounds actually showed a contraction when exposed to the conbined fuels.

2.4.3 Elastomers in a Decontaminant

Recent failures of Buna-n pump seals used in pumping a decontaminating solution prompted a study to determine the compatibility of the seal with the decontaminant. Six materials were evaluated in the testing program, including the troublesome Buna-n seal that was used in the decontaminant pump. The other materials evaluated were an ethylene propylene rubber, a neoprene, and three other Buna-n compounds. The decontaminant used was a mixture of 55% mono-ethanol-amine and 45% mono-isopropyl-amine.

2.4.3.1 Procedure

The six materials to be evaluated were exposed to the decontaminant at 75°F for 72 hours. The test samples were suspended in the decontaminant in mason jars. Following exposure the materials were evaluated for ultimate tensile strength and elongation, volume change, and hardness. All samples, except the neoprene were in the form of O-rings. The neoprene was supplied in sheet form.

2.4.3.2 Test Results

The as-received test results and the post-exposure results are listed in Table XLVIII. E/D-1 is the Buna-n pump seal material, E/D-2 is the ethylene propylene rubber, E/D-3 is the Neoprene, and E/D-4, 5, 6, are other Buna-n compounds.

A close examination of the results in Table XLVIII shows the probable cause for the troublesome decontaminant pump seal. The material used in the pump (E/D-1) had the highest volume change of all the materials tested; but more significantly, the volume change was negative. Thus, the seal after being exposed to the decontaminant solution for a 72 hour period actually shrank 6.1 percent. A comparison of the other materials to E/D-1 shows that it has the lowest tensile strength and nearly the lowest elongation.

TABLE XLVIII

RESULTS OF ELASTOMER/DECONTAMINANT COMPATIBILITY TESTS

	Ultimate Tensile Strength (PSI)	Elongation (%)	Hardness Shore A (points)	Volume Change (%)
As Received				
E/D-1	1250	217	72	----
E/D-2	1348	150	67	----
E/D-3	2050	251	76	----
E/D-4	3437	352	73	----
E/D-5	2093	287	73	----
E/D-6	2000	376	66	----
After 72 Hour Aging in Decontaminant				
E/D-1	1395	169	72	-6.1
E/D-2	1478	162	67	
E/D-3	2163	278	75	0.14
E/D-4	2706	282	74	0.74
E/D-5	2127	291	71	1.13
E/D-6	2130	386	69	0.55

The best seal material, of those evaluated, appears to be E/D-5. This material swells slightly in the decontaminant and has good tensile, elongation, and hardness values after exposure. Other materials, such as E/D-4, had higher tensile properties and approximately the same elongation but lacked sufficient swell. For these reasons the E/D-5 material was recommended as the replacement seal for the decontaminant pump.

2.5 DYNAMIC O-RING EVALUATIONS

All candidate elastomeric O-ring compounds are required to meet current military standards. The University of Dayton, through the use of government-developed equipment and test procedures, is conducting dynamic O-ring tests for candidate compounds.

The test equipment used in this program was developed and fabricated by the Air Force. All testing was conducted according to Mil-P-25732B (Reference 54). The hydraulic fluids used in these tests meet the requirements of Mil-H-5606 (Reference 55).

2.5.1 Modifications to Test Equipment

The test equipment used in the performance of these tests was in need of repair when it was received from the Air Force Materials Laboratory. The schematic of basic design is shown in Figure 82. The test cell is driven by an external driving cylinder located outside the environmental chamber. The test cell pressure is supplied by an air/oil boost unit and is controlled by solenoid valving. The air/oil unit is isolated from the test cell by a transfer cylinder which also serves as a means of determining the total leakage during the endurance tests.

Initial modifications to the tester included the replacement of the badly worn hydraulic power unit for the driving cylinder. Early testing also resulted in the failure of the air/oil boost unit. After several temporary repairs were made, the air/oil pump head was replaced. Repeated failures of this pump head prompted the purchase of a new air/oil boost unit.

Other modifications to the unit included the complete rewiring of the test apparatus and replacement of the heaters in the environmental chamber. The chamber controls were also repaired and improved.

Early test results showed that the 325 size packings exposed to the endurance cycle test were being severely damaged during the test. These packings were already qualified to Mil-P-25732B but were failing far short of the required 12,000 cycles. These test results prompted a close inspection of the test cell with respect to the specification.

All six test cell cylinder barrels provided with the apparatus were checked for surface finish and tolerances. The piston head was closely inspected and the piston rods were checked for surface finish and tolerances. During this inspection, the piston head and rod assembly was found not to be concentric. The cylinder barrels were too smooth and had to be lapped to produce the proper surface finish. The dimensions of the brass spacer rings used in the endurance portion of the test cycle

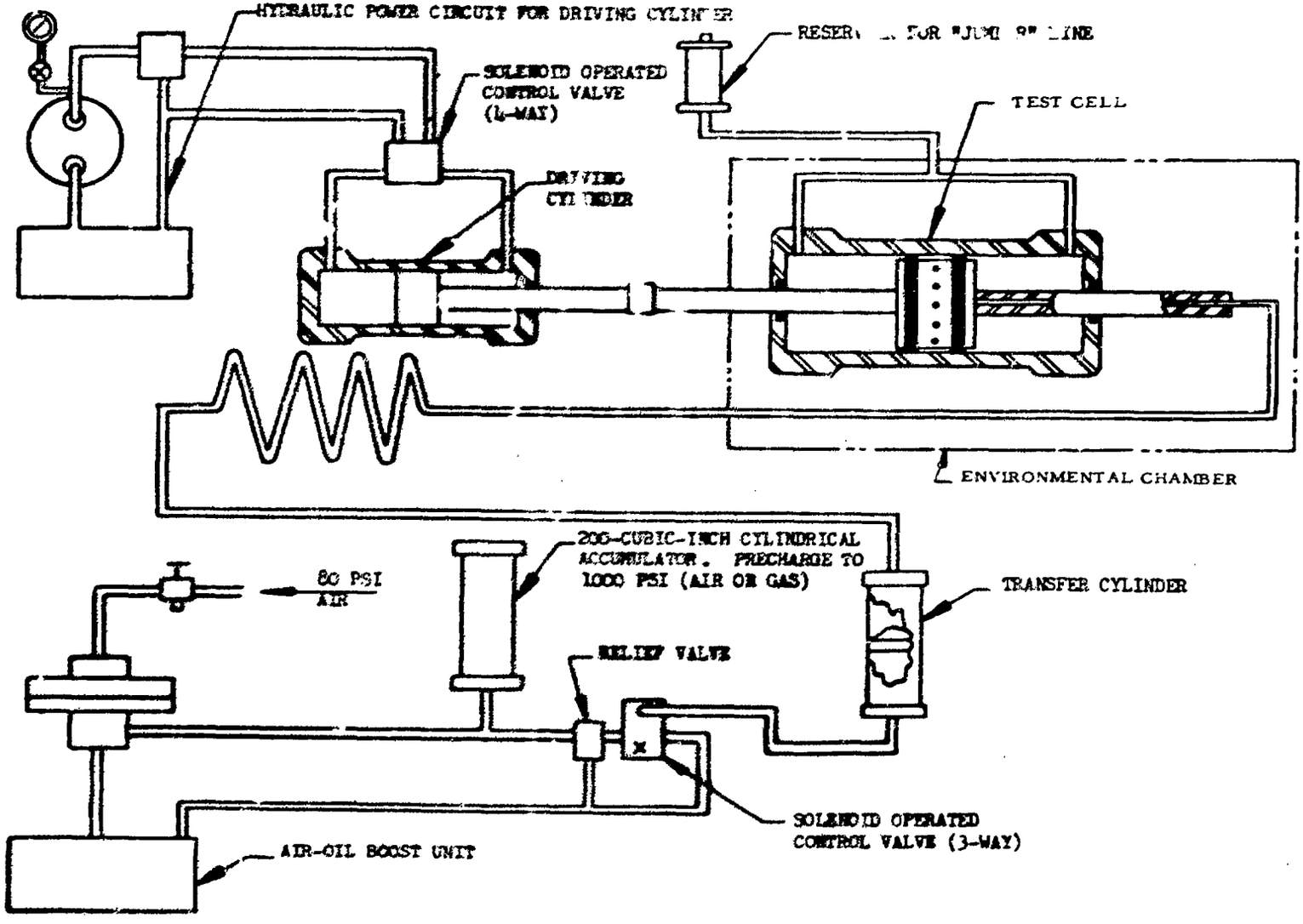

Figure 82. Endurance-Cycling Test Circuit Schematic (Reference 54).

were not within the specified tolerance. New spacer rings were fabricated and rigorously checked before each test run to insure proper diametral clearance between brass ring and cylinder barrel.

Following the completion of these equipment modifications, the average number of cycles the packings would withstand increased from 9,000 to over 100,000 cycles.

2.5.2 Tests Conducted

Because the condition of the equipment was questionable, the initial test program was designed to produce baseline cycling data. The procedure was to operate the tester through the Performance Test A and Endurance Test A of Mil-P-25732B. The endurance portion of the test was carried to catastrophic failure of the O-ring packings rather than the minimum 12,000 cycles required.

Although this test is described in detail in Reference 54, a a brief description is included here. Following a 72-hour aging period at 275°F, the O-ring packings are assembled on a test cylinder for a static pressure test. The test cylinder temperature is then lowered to -65°F and the O-rings are subjected to a low pressure cycling test, a high pressure cycling test, and a high pressure static test. The test cell is then returned to room temperature for a leakage check and O-ring inspection. The same packings are then placed back on the test cylinder for endurance testing. The endurance test is conducted at 275°F and 1500 psi for a minimum of 12,000 continuous cycles.

2.5.3 Results of Baseline Testing

The baseline test results for O-ring packings that were tested to failure are shown in Table XLIX. The results of the endurance tests on the initial packings were quite scattered and averaged below the minimum requirements of the specification. These low results were caused by equipment malfunctions and by the test cell being out of tolerance as described above.

The first of these tests showed a complete O-ring failure occurring at 14,047 cycles. At 9000 cycles the cycle counter was found to be malfunctioning, giving two counts for each cycle. The counter was repaired but the point at which the counter began malfunctioning was not known.

The second test had a left end O-ring failure at 3377 cycles. This premature failure cannot be explained except that it could have been caused by a faulty O-ring. The right end O-ring showed very little damage when examined after the test. The left end O-ring, however, was badly worn.

TABLE XLIX

RESULTS OF BASELINE O-RING CYCLING TESTS

Specimen	Number of Cycles to Failure	Remarks
1	12, 401	Test interrupted twice, net number of cycles at 275°F: 10, 400
2	5, 218	Cold temperature soak at -80°F or below
3	8, 945	Test interrupted, net number of cycles at 275°F: 7945
4	14, 047	Cycle counter malfunction
5	3, 376	Premature O-ring failure
6	10, 001	Test interrupted, net number of cycles at 275°F: 9000

The third test indicated a complete failure after 10,001 cycles. The test was stopped at 2700 cycles to repair a fractured high pressure hydraulic line. Approximately 1000 cycles were required to achieve an equilibrium test temperature after the shut down.

The fourth test indicated a failure of the right end O-ring at 12,401 cycles. During the 275°F cycling portion, the test was stopped on two occasions; once at 6200 cycles, and again at 9800 cycles. These stoppages were caused by fatigue failures in the high pressure tubing inside of the 275°F test box and by failure of the air/oil boost unit discussed earlier. During these stoppages the temperature dropped below 275°F while the repairs were being completed. Approximately 1000 cycles had elapsed after each stoppage before the temperature again stabilized at 275°F. The net number of cycles at 275°F was, therefore, 10,400 cycles. The failed O-ring appeared to have been forced between the brass spacer ring and the shaft. With the O-ring in this position, each stroke pinched and eventually cut a small portion of the O-ring. This cutting action caused the failure of the O-ring. Many small portions of the O-ring were found in the test cylinder when it was disassembled. The left end O-ring also showed similar cuts but to a less extent.

The fifth test showed a right end O-ring failure after 5218 cycles. The premature failure of this O-ring may have been due to the 18-hour cold temperature soak which was performed at a temperature much lower than -65°F. Lack of adequate control over the temperature resulted in the 18-hour soak being conducted at -80°F and below. This extremely cold temperature could conceivable have caused the premature failure. The type of failure was similar to that observed during the first test.

In the sixth test the O-ring on the left end failed at 8,945 cycles. At 4787 cycles of the 275°F cycling test, the test was stopped because of yet another fatigue crack in the high pressure line leading to the test cell. A new high pressure line configuration was developed and the test continued. Approximately 1000 cycles were required to bring the test cell back to 275°F, leaving a net of 7945 cycles at 275°F. The left end O-ring failure was similar to the ones described above.

The Buna-n compound has previously been qualified to this test but these preliminary baseline data indicated an average of only 9000 cycles for 6 test runs. Close inspection of the test equipment revealed that several components did not meet the design specifications. These discrepancies were described in detail above.

After the required modifications and corrections were completed, six additional tests using Buna-n O-rings were conducted. Packing failure was considered to be when the total leakage exceeded 75 ml. The results of these six tests are described as follows.

Test No. 1: O-ring failure occurred on the left end after 61,510 cycles. The leakage was measured several times during the test and was found to be 11 ml after 34,850 cycles, 37 ml after 49,300 cycles, 52 ml after 60,988 cycles, and 128 ml after 61,510 cycles.

Test No. 2: No O-ring failure occurred during this test but the test was terminated because of a hydraulic pump failure at 24,300 cycles. The leakage at that time was 23 ml.

Test No. 3: O-ring failure occurred at 43,086 cycles. The leakage measured was 0 ml after 7,164 cycles, 8 ml after 21,414, 9 ml after 36,009 cycles, and 63 ml after 43,086 cycles. Pump failure caused an early halt to this test.

Test No. 4: The O-ring test was performed continuously over a 24-hour period. O-ring failure occurred between 94,900 cycles and 151,350 cycles. A failure of the automatic shut-down mechanism caused the cycling to continue after the O-ring failure occurred.

Test No. 5: The fifth test was conducted over a five-day period and ran for 54,000 cycles before the O-rings failed. Only the Endurance Test B of Mil-P-25732B was conducted during this evaluation.

Test No. 6: The sixth test was conducted over eleven days. For the first ten days the test was operated for 8 hours per day and shut down at the end of each working day. Up to that time the O-rings were tested through 144,400 cycles and had leaked to a total of 30 ml of test fluid. On the last day this test was allowed to operate overnight. The O-ring failed sometime during this overnight operation and a failure of the automatic shut-off mechanism resulted in the O-rings being cycled beyond the point of failure. The test ran an additional 45,593 cycles during the overnight portion of the test, resulting in a total of 190,093 cycles.

Examination of the O-rings following this test showed that the left end O-ring was in reasonable condition with approximately 1/16-inch of the cross section circumference nibbled. The right end O-ring was split with a large portion of the ring completely missing. The failure appears to be caused by the splitting of the O-ring, not by nibbling action associated with normal wear. The nibbling was just slightly more than that observed on the left end O-ring.

In each of the six tests conducted after the modifications the number of cycles far exceeded those previously obtained. However, during these tests the brass spacer rings were found to be scraping the cylinder wall, causing wear. The wear of these rings causes two effects on O-ring sealing. First, the clearance gap between the ring and the

cylinder wall was increased and caused the O-ring to be pinched and cut during the cycling. Second, brass particles from the spacer ring are embedded in the O-ring causing unnatural wear.

2.5.4 Conclusions and Recommendations

The results of these last six tests indicated that the equipment modifications made to the test apparatus were successful and that the packings being evaluated were not being failed prematurely by the test equipment. With this baseline data completed, other compounds may be evaluated in similar testing programs. If future packing tests with other compounds indicate cycling life far in excess of the minimum 12,000 cycles, as did the Buna-n compound tested, the cycling requirements could be extended to provide a more meaningful evaluation of the packing compounds.

SECTION III

ADDITIONAL AREAS OF ACTIVITY

3.1 INTRODUCTION

Throughout this contract a variety of smaller efforts were undertaken. These tasks included the evaluation of adhesives and adhesive joints, the mechanical properties of several foam sandwich materials, and the effects of disinfectants on clear plastics. Fabrication techniques for ZrO_2 fiber reinforced ceramics and boron patches for helicopter rotor blades were also investigated as were several NDT programs utilizing ultrasonic detection, fluorescent dye penetrants, and photochromic compounds.

Since most of these efforts were relatively small or not of general interest, details are not included in this report. There were three projects, however, which are of sufficient interest to be included. These are summarized in the following paragraphs.

3.2 HOT PRESSING 3-D CARBON COMPOSITES

Both the mechanical and ablative properties of graphitic materials vary as a function of density. Because of the fabrication processes involved, the densities of many of the newly developed carbon/carbon composites tend to be considerably lower than those of good grades of commercial graphite. This is particularly true with the three-dimensionally reinforced carbon matrix composites. A program was therefore undertaken to investigate the feasibility of increasing the density of one such 3-D carbon composite in an attempt to improve certain basic properties.

3.2.1 Procedure

From the data available in the literature (References 56, 57, 58, and 59) it is apparent that most graphite materials would deform easily under conditions of sufficiently high temperature and stress and given sufficient time. It was therefore felt that subjecting the existing material to a hot-pressing operation could result in a significant increase in density, providing the require hot-pressing conditions could be attained.

The 3-D composite used for this study consisted of woven fabric and high modulus fiber reinforcement in a carbon matrix. In this

particular material, conventional WCA flat woven fabric acts as the reinforcement in two dimensions while Thornel 50 fibers, oriented normal to the plane of the fabric, reinforce the composite in the third direction. The bulk density of the material is generally in the 1.62 to 1.65 g/cc range.

The hot-pressing operations were carried out in a resistance heated unit which was developed by UDRI. This apparatus employs a graphite die which doubles in service as the resistance heating element (Figure 83). Although this facility is capable of achieving temperatures up to 3000°C at pressures up to 5000 psi, it was utilized primarily because of the specimen shapes and sizes (rectangular bars up to 3 inches in length) which could be accommodated. It is operated in air but the use of the graphite die results in a reducing environment in the sample cavity. Provisions are included for continuous monitoring of ram travel, thus providing an indication of the densification which the sample is undergoing.

Four pieces of the 3-D carbon/carbon composite were supplied, each 0.75-inch by 0.75-inch by 1.6-inches, with the Thornel fibers oriented in the long direction. The initial piece (designated simply as No. 5) was cut to produce two specimens, each approximately 0.3-inch thick. These were then machined to fit precisely into the cavity of existing molds (1/2-inch wide with semicircular ends). The pressing direction in all of these tests was perpendicular to the Thornel fibers.

3.2.2 Results

The first specimen (No. 5-1) was hot-pressed at a temperature of 2500°C and 2960 psi for approximately 20 minutes. This resulted in a slight reduction in specimen thickness with no measurable change in its length and width. Table L contains the hot-pressing conditions and results of all of these tests. As can be seen from these data the initial pressing operation resulted in a very slight (less than 1/2%) increase in density. The same specimen was then hot-pressed a second time under more severe conditions. The temperature was increased to 2600°C, the pressure to 4450 psi, and the time to 45 minutes. The combined effect of these two pressing operations was an overall increase in density of 4.7%.

For the second test, which was conducted using a similar specimen (No. 5-2), the temperature and time were again increased. The temperature varied during this test but for the majority of the time it was at or near 2800°C. The pressure was maintained at 4450 psi for 95 minutes. The dimensions of the sample underwent considerable change, the thickness decreasing from 0.297 inch to 0.242 inch while the width and length increased by 0.053 inch, and 0.030 inch, respectively.

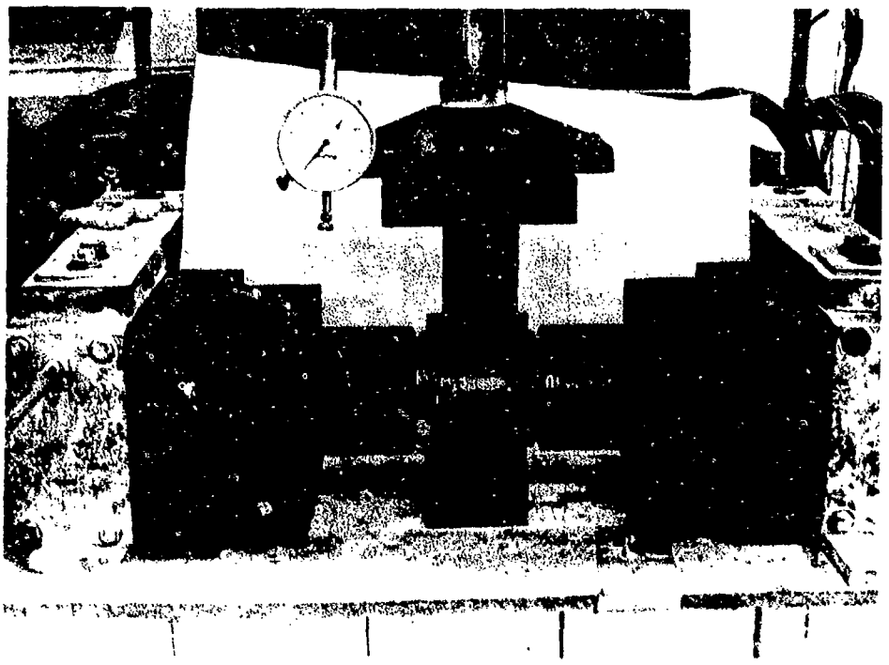

Figure 83. Resistance-Heated Hot Press Graphite Die.

TABLE L

RESULTS OF HOT-PRESSING 3-D
CARBON/CARBON COMPOSITES

Specimen Number	HOT PRESSING CONDITIONS			DENSITY		
	Max. Temp. (°C)	Pressure (PSI)	Time (MIN)	Initial (g/cc)	Final (g/cc)	Increase (%)
5-1 (1st pressing)	2500	2960	20	1.689*	1.696*	0.4
5-1 (2nd pressing)	2600	4450	45	1.696*	1.755*	4.7
5-2	2800	4450	95	1.636	1.788	9.3
4-1	2750	4420	42	1.644	1.711	4.1
4-2	2750	4420	42	1.644	1.716	4.4
22-1	2800	4420	89	1.653	-----	---
22-2	2800	4420	89	1.653	-----	---
D-4	2575	4420	60	1.636	1.751	7.0
D-5	2550	4420	45	1.636	1.718	5.0

*Measured by liquid displacement method. All the densities calculated from dimensional and weight measurements.

These changes in physical dimensions indicates that considerable plastic flow occurred in the matrix. A comparison between a hot-pressed and an as-received sample is shown in Figure 84. The density of this sample increased 9.3% from 1.636 g/cc to 1.788 g/cc. It should be noted that these are bulk densities which were calculated from dimensional and weight measurements.

Because of the apparent success in these initial attempts at increasing the density, it was decided to machine new molds which could accommodate full 3/4-inch wide specimens without the semicircular ends.

Difficulties were encountered during the hot-pressing operation which limited the degree of densification which was obtainable with several of the remaining samples. Intermittent failures in the large electrical power supply resulting in sudden decrease in temperature were the most commonly occurring difficulty. The contraction which occurs during such temperature drops results in loss of electrical contact in the region of the mold end plates. This, in turn, results in the formation of severe hot spots in these areas when the power is again applied. This overheating in the area around the ends of the mold limited both the time and temperature which could be attained.

All of the specimens were forwarded to Southern Research Institute where their mechanical properties were to be evaluated. The results of these tests have not yet been made available. The densification of these materials by hot-pressing was considered successful, however. It is felt that if proper care is taken in preparation for the hot-pressing, density increase of 10% can be realized for composites such as the one involved in this study.

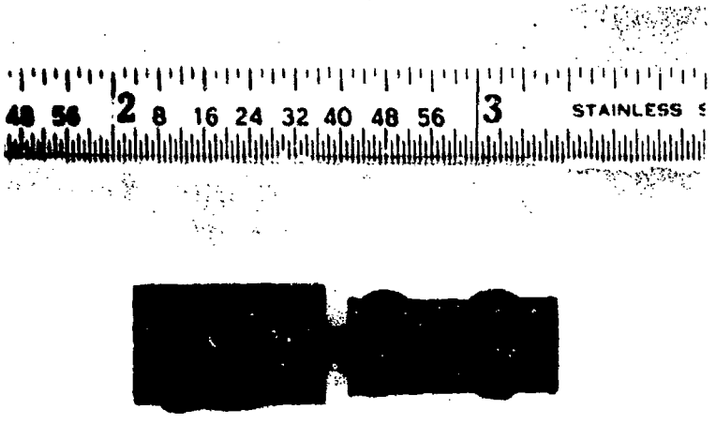

Figure 84. Change in Dimensions Resulting from Hot-Pressing of 3-D Carbon/Carbon Composite.

3.3 DEVELOPMENT OF FOAM-IN-PLACE HELMET LINERS

This program was initiated several years ago and has been discussed previously (Reference 6). Since that time a number of improvements have been made, both in the foam formulation and in the mold used to form the foam-in-place liners.

3.3.1 Improvements in Molds

A program was undertaken to evaluate an improved helmet liner mold. The mold, as shown in place on a person's head in Figure 85, is made up of several separate parts. An aluminum ring is suspended on the head by means of adjustable straps. The height of the aluminum ring on the head is adjustable by turning a windlass to which one of the straps is attached. After the correct height has been determined, four adjustment screws, located around the edge of the aluminum ring, are turned to align the ring on the head. A 1/4-inch thick rubber skull cap is then donned by the individual. The upper surface of the cap is coated with a release agent to facilitate removal of the foam. A rubber ring, which acts as a dam to prevent loss of foam, is then placed over the head and pushed down flush with the aluminum ring. This rubber ring fits tightly against the rubber skull cap to prevent leakage of the foam. On top of this is placed the Teflon coated stainless steel upper mold half. It is locked in place on the rubber ring over the aluminum ring. The rubber ring provides a seal between the steel upper half and the aluminum ring.

The foam is then mixed and poured through the large hole in the top. The mold is then rotated somewhat to distribute the chemicals evenly around the mold before it begins to foam. The head is kept level during the process until the foam begins to set up. Excess foam is expelled through the small blowholes and through the large oval shaped hole on top.

As soon as the foam is firm to the touch, the mold is removed. After the excess materials has been trimmed off, the rubber skull spacer cap removed from the underside. The upper mold half is then separated from the aluminum ring and the rubber ring is removed. Disassembly of this unit is very easy compared to the previous designs.

The foamed liner is allowed to remain in the upper mold half for several minutes until it has cured. The stainless steel shell is then flexed by pushing in on its sides to release the cured foam from the Teflon coated shell. The foam can then be pushed out of the stainless steel shell by means of a jig and special tools included with the kits. The steel shell is supported in a jig which is incorporated in the wooden box in which the mold is packaged. The special lever-type tool is a plunger which has its fulcrum on the stainless steel shell. The lever is attached

Figure 85. Newly Developed Mold For Foam-In-Place Helmet Liners.

to the shell while the shell is in the jig and pressure is applied to the handle of the lever until the liner drops out of the mold half.

The molds are each packaged in a sturdy wooden box, which also contains the accessories needed for the foaming operation, such as the level-type plunger, serrated foam cutting knife, extra rubber ring and skull cap, smock, and instruction booklet. The evaluation of the new molds consisted of making ten foam-in-place liners in each size mold of the improved design. This evaluation indicated that these molds were a great improvement over the molds evaluated previously.

3.3.2 Foam Formulation Improvements

The original foam formulation developed for this program (Reference 60), although satisfactory, suffered some drawbacks. One was concerned with the rapidity with which the foam reaction proceeded once the chemicals were mixed. It was difficult to pour the chemicals into the mold rapidly enough to prevent losing some of the foam in the pouring process. Also, many of the liners foamed had a number of void defects caused by entrapped gases.

In work done at the AFML some years ago, it was observed that the addition of small amounts of stearic acid reduced reaction rate and improved the foam cell structure. It was decided to try to improve the foam with stearic acid additives. It was determined that adding a small amount of stearic acid to the polyol portion of the portion of the foam fomulation alleviated these problems. This addition of stearic acid slowed the reaction down substantially, giving a longer cream time and making it much more convenient for pouring. The quality of the foam was also improved considerably since the presence of voids in the completed liners was reduced. Uniformity of cell size was improved as well.

3.4 PHOTOCHROMIC FILTERS FOR CAMERAS

A very high priority project involved a requirement for an automatically variable density filter to replace fixed value neutral density filters currently in use on gunship cameras. It had been suggested that a photochromic filter could be developed which would lighten and darken according to the ambient light level to automatically provide sufficient filtration for camera protection. The feasibility of such a filter employing photochromic materials was investigated for a two-week period. At the end of this period it was determined that such a filter would indeed be possible, providing time was available for development.

3.4.1 Preliminary Studies

Off-the-shelf as well as highly experimental photochromic compounds developed by the AFML were employed in a variety of solvents and resins. It was determined that side-band filters would have to be used to attenuate wavelengths of the light not attenuated by the photochromic compound, since the compounds could not possible cover the entire visiole, near ultra-violet and near infrared spectra which are involved in this application. Only about 100-nanometer segments of the spectrum can be well attenuated by the photochromics. By choosing a photochromic attenuating in the region of the camera's greatest sensitivity, and by carefully matching a sideband filter to this photochromic, it was possible to obtain the required high densities.

Several systems were assembled which would provide a density change from about neutral density three to neutral density four, which was acceptable. These were, of course, simple exploratory prototype systems and not at all refined nor totally acceptable. However, they did demonstrate conclusively the feasibility of using a photochromic compound for this purpose. Based on these findings, a decision was made to perfect such a system.

3.4.2 Development of Suitable Compounds

It was necessary to provide a photochromic filter which would automatically attenuate the incident sunlight to maintain a light level suitable for the application intended. This same filter must, however, fade as the light level decreases, to let in sufficient light to activate the system. Since the system is sensitive to light of all visible wavelengths as well as near infrared and ultraviolet, it was necessary that the filter attenuate over a wide wavelength range.

Various dyes were tried, the objective being to select a dye which, when dissolved in a particular solvent, will give the strongest coloration and yet will reverse in a reasonable period of time and will

have relatively long fatigue life. It was eventually decided to use an AFML development, a nitro-substituted dye made with the enzyme urease. This compound provided the longest fatigue life consistent with good coloration and reverse times. However, as with all photochromic systems the dye will attenuate the light in a comparatively narrow range of about 100 nanometers. It was, therefore, necessary to provide sideband filters on either side of the "window shade" to give complete protection over the spectrum required.

For the dye selected, it was necessary to determine its peak of maximum absorption in order to determine which side-band filter would be required. It was also found that a certain type of blue filter had to be placed in front of the photochromic filter to protect it from the bleaching effect of the longer wavelength light present in sunlight.

As a result of experimentation, it was determined the best method of preparing these filters was by pouring a solution of vinyl butyral, Butvar B-76, in toluene containing the dye, onto a circular plate of glass the size of the filter required (approximately 4-1/2-inches in diameter). The mixture was then permitted to dry for a specific time interval to obtain the desired concentration of solvent. It was found that the density and reverse time of the filter could be controlled by varying the drying time of the resin-solvent compound once it was poured on the glass plate.

After the required drying time had elapsed, a cover glass plate was placed on top, the assembly placed in a press and the excess compound pressed out. This pressing also assures intimate contact between the glass and the resin, giving good optical properties to the filter. It was decided to prepare several filters using different drying times, in order to provide the testing personnel with filters giving different densities and reverse times.

3.4.3 Evaluation of Filters

A number of filters were prepared and installed on the system in aircraft. A series of tests were conducted, under various light conditions to check the response of the filter, both in coloration and in fade rates. Several filters were evaluated, each with a different solvent concentration.

REFERENCES

1. Gunderson, A. W., "Preliminary Mechanical Property Evaluation of D6ac Steel in Support of the F-111 Aircraft Recovery Program," MAA 70-6, AFML, WPAFB, Ohio, July 1970.

2. ASTM Standard E399-70T, "Test for Plane Strain Fracture Toughness of Metallic Materials," May 1969.

3. Anctil, A. A., and Kula, E. G.., "Fatigue Propagation in Armor Steels," AMMRC TR-69-25, November 1969.

4. Crooker, T. W., and Lange, E. A., "Corrosion-Fatigue Crack Propagation Studies of Some New High Strength Structural Steels," ASME Paper No. 69 MET-5.

5. Crooker, T. W., and Clark, W. G., "Factors Determining the Performance of High Strength Structural Metals," Report of NRL progress, NRL Problem No: M0p-25, Project No: RR007-01-46-5432, March 1970.

6. Clark, W. G., "Subcritical Crack Growth and its Effect Upon the Fatigue Characteristics of Structural Alloys," Engineering and Fracture Mechanics, 1968, Vol. I, pp. 385-397.

7. "Steel Alloy Selection of F-111 Justification Data for D6ac Steel," FZM-12-408, General Dynamics Corporation, Ft. Worth, Texas, February 1964.

8. Cummings, Harold N., "Some Quantitative Aspects of Fatigue of Materials," WADD-TR-60-42, Curtis-Wright Corporation, Propeller Div., Caldwell, N. J.

9. Gott, J. E., and Lynch, J. M., "A Production Process for Large Solid Motor Cases Internal Roll-Extruded," AFML-TR-68-116, May 1968.

10. Harmsworth, C. L., and Cervay, R. R., "Fracture Toughness Evaluation of D6ac Steel in Support of the F-111 Aircraft Recovery Program," Tech. Memo AFML/LAE-71-2.

11. Petrak, G. J., "Fracture Toughness and Stress Corrosion Properties of 7175-T736," UDRI-TR-69-01, January 1969.

12. Kaufman, et al., "Fracture Toughness, Fatigue, and Corrosion Characteristics of X7080-T7E41 and 7178-T651 Plate and 7075-T6510, 7075-T3510, X7080-T7E42, and 7178-T6510 Extruded Shapes," AFML-TR-69-255, November 1969.

13. Brownhill, et al, "Mechanical Propagation Rates of Stress-Relieved Aluminum Alloy Hand Forgings," AFML-TR-70-10, February 1970.

14. Jones, R.E., "Comparison of Fracture Toughness Values Obtained Using Semi-Infinite Aluminum Plates with Values Using Laboratory Size Specimens," AFML-TR-69-58, April 1969.

15. Kaufma et al., "Fracture Toughness of Aluminum Alloys," Metals Engineering Quarterly, August 1969.

16. Dubensky, R.G., "Fatigue Crack Propagation in 2024-T3 and 7075-T6 Aluminum Alloys at High Stresses," NASA CR-1732, March 1971.

17. Wei, R.P., "Fatigue-Crack Propagation in a High-Strength Aluminum Alloy," International Journal of Fracture Mechanics, Vol. 4, No. 2, 1968.

18. Johnson, H.H., and Wilner, A.M., "Moisture and Stable Crack Growth in High Strength Steel," Applied Materials Research, Vol. 4, p. 34, 1965.

19. Kaufman, et al., "Fracture Toughness, Fatigue, and Corrosion Characteristics of X7080-T7E41 and 7178-T651 and 7075-T6510, 7075-T7351, X7080-T7E42 and 7178-T6510 Extruded Shapes," AFML-TR-69-255.

20. Brownhill, et al., "Mechanical Properties, Including Fracture Toughness and Fatigue, Corrosion Characteristics and Fatigue-Crack Propagation Rates of Stress-Relieved Aluminum Alloy Hand Forgings," AFML-TR-70-10, February 1970.

21. Dubensky, Robert G., "Fatigue Crack Propagation in 2024-T3 and 7075-T6 Aluminum Alloys at High Stresses," NASA CR-1732, Langley Research Center, Hampton, Virginia, 1971.

22. Harmsworth, C. L., McClaren, S. W., Cook, O. H., "Titanium Castings," Machine Design, Vol. 40, No. 15, pp. 166-171.

23. Bass, Collin D., 1/Lt., USAF, "Evaluation of Ti-6Al-4V Castings," AFML-TR-69-116, Wright-Patterson Air Force Base, Ohio, 1969.

24. McClaren, S. W., Cook, O. H., and Pascador, G., "Processing Evaluation and Standardization of Titanium Alloy Castings," AFML-TR-68-264, Wright-Patterson Air Force Base, Ohio, 1969.

25. "Marine Corrosion Studies," Third Interim Report of Progress: NRL Memorandum Report 1634, July 1965.

26. Hudson, C. M., "Fatigue-Crack Propagation in Several Titanium and Stainless Steel Alloys and One Superalloy," NASA TN D-2331, October 1964.

27. Report of NRL Progress, March 1970.

28. Crack Growth Data from Aerospace Corporation.

29. Letter and Attachments from R. A. Davis to J. L. Bickhard concerning the transmittal of material and data to C. L. Harmsworth, March 20, 1970.

30. "Report of NRL Progress," June 1970.

31. McDonnell-Douglas Phase 3 Data.

32. Amateau, M. F. and Kendall, E. G., "F-15 Ti-6Al-6V-2Sn Crack Propagation Program," The Aerospace Corporation, November 10, 1970.

33. Conway, J. B., "Stress-Rupture Parameters for the Refractory Alloys," presented at ASM-AIME Materials Engineering Exposition and Congress, October 14-17, 1968.

34. Mendelson, A., Roberts, E. Jr., and Manson, S. S., Optimization of Time-Temperature Parameters for Creep and Stress-Rupture with Application to Data from German Cooperative Long-Time Creep Program, NASA TN D-2975, August 1965.

35. Goldhoff, R. M., "Comparison of Parameter Methods for Extrapolating High-Temperature Data," Journal of Basic Engineering, December 1959.

36. Titran, R. H., Creep of Tantalum T-222 Alloy in Ultrahigh Vacuum for Times to 10,000 Hours, NASA TN D-4605, May 1968.

37. Sawyer, J. C., and Steigerwald, E. A., "Generation of Long Time Creep Data of Refractory Alloys at Elevated Temperatures," 13th Quarterly Report for period July 26, 1966 to September 26, 1966, TRW Contract NAS-3-2545, October 14, 1966.

38. Buckman, R. W., Jr., and Goodspeed, R. C., "Development of Precipitation Strengthened Tantalum Base Alloy," ASTAR-811C, Summary Topical Report, Contract No. NAS 3-2542.

39. Sheffler, K. D., Generation of Long Time Creep Data on Refractory Alloys Elevated Temperatures, Final Report Advance Information copy, TRW-ER-7442.

40. Sheffler, K. D., and Sawyer, J. C., "Generation of Long Time Creep Data on Refractory Alloys at Elevated Temperatures," 18th Quarterly Report, NAS-CR-72524, January 15, 1969.

41. Bartlett, E. S., and Van Echo, J. A., "Creep of Columbium Alloys," DMIC Memo 170, June 24, 1963.

42. Stephenson, R. L., Creep-Rupture Properties of Cb-752 Alloys and Their Response to Heat Treatment, Tech. Report No. ORNL-TM-1577, August 1969.

43. McCoy, H. E., Creep-Rupture Properties of Tantalum-Base Alloy T-222, Rep. ORNL-TM-1576, Oak Ridge National Lab., September 1966.

44. Titran, R. H., and Hall, R. W., Ultra-High Vacuum Creep Behavior of Cb and Ta Alloys at 2000°F and 2200°F for Times Greater than 1000 Hours, NASA TN D-3222, January 1966.

45. DMIC Report 212, "Pilot Production and Evaluation of Tantalum Alloy Sheet," Westinghouse Electric Corp., Contract N-600(10)-59762.

46. Filippi, A. M., Production and Quality Evaluation of T-222 Tantalum Alloy Sheet. Final Report (January 1968), Navy Contract No w 66-0538-d, Westinghouse Astronuclear Lab., Report PR-(KK)-003.

47. Beck, E.H., and Schwartzberg, F.R., Determination of Mechanical and Thermophysical Properties of Refractory Metals, Martin Co., Tech. Report AFML-TR-65-247, July 1965.

48. Bewley, J.G., and Schussler, M., Final Report on Process Improvement of Columbium (Cb-752) Alloy, Tech. Report AFML-TR-65-63, March 1965.

49. Brown, W.F., Jr., and Srawley, J.R., "Plane Strain Crack Toughness Testing of High Strain Metallic Materials," ASTM Special Technical Publication No. 410.

50. Gerdeman, D.A., et al., "The Evaluation of Aerospace Materials," AFML-TR-68-53, March 1968.

51. "Aerospace Structural Metals Handbook," Volume II, Non-Ferrous Light Metal Alloys, Fourth Revision, Syracuse University Press, March 1967.

52. Private Communication with Mr. Philip A. House, Materials Engineer, Materials Support Division, Air Force Materials Laboratory.

53. Military Specification Mil-S-8802D, Sealing Compound, Temperature-Resistant, Integral Fuel Tanks and Fuel Cell Cavities, High-Adhesion, September 1, 1967.

54. Military Specification Mil-P-25732B, Packing, Preformed, Petroleum Hydraulic Fluid Resistant, 275°F, January 11, 1967.

55. Military Specification Mil-H-56-6B, Hydraulic Fluid, Petroleum Base; Aircraft, Missile, and Ordance, June 26, 1963.

56. "The Industrial Graphite Engineering Handbook," Union Carbide Corporation, New York, 1962.

57. "The Reactor Handbook," Vol. 3, Materials, Section I, General Properties, September 1953, AECD-3647.

58. Wagner, P., Driesner, A.R., and Kmetko, E.A., "Some Mechanical Properties of Graphite in the Temperature Range 20° to 3000°C," Prepared for Second U.N. International Conference on Peaceful Uses of Atomic Energy, 1958.

59. Digesu, F.J., and Pears, C.D., "The Determination of Design Criteria for Grade CFZ Graphite," AFML-TR-65-142, May 1965.

60. Gerdeman, D.A., Berner, W.E., and Petrak, G.J., "Evaluation and Application of Materials for Unusual Aerospace Systems," AFML-TR-70-288, December 1970.

Unclassified

Security Classification

DOCUMENT CONTROL DATA - R & D

(Security classification of title, body of abstract and indexing annotation must be entered when the overall report is classified)

1. ORIGINATING ACTIVITY *(Corporate author)*

University of Dayton Research Institute
Dayton, Ohio 45469

2a. REPORT SECURITY CLASSIFICATION

Unclassified

2b. GROUP

3. REPORT TITLE

Evaluation of Materials Applicable To Aerospace Systems

4. DESCRIPTIVE NOTES *(Type of report and inclusive dates)*

Summary Report (1 September 1970 through 29 February 1972)

5. AUTHOR(S) *(First name, middle initial, last name)*

Dennis A. Gerdeman
William E. Berner
Gerald J. Petrak

6. REPORT DATE	7a. TOTAL NO. OF PAGES	7b. NO. OF REFS
June 1972	205	60

8a. CONTRACT OR GRANT NO.	9a. ORIGINATOR'S REPORT NUMBER(S)
F33615-71-C-1054	UDRI-TR-72-39
b. PROJECT NO. 7381	
c.	9b. OTHER REPORT NO(S) *(Any other numbers that may be assigned this report)*
d.	AFML-TR-72-95

10. DISTRIBUTION STATEMENT

Distribution limited to US Government agencies only; report covers test and evaluation of commercial products or military hardware; 9 June 1972. Other requests for this document must be referred to the Air Force Materials Lab. Attn:

11. SUPPLEMENTARY NOTES	12. SPONSORING MILITARY ACTIVITY
	AFML/LAE Air Force Materials Laboratory Wright-Patterson Air Force Base, Ohio

13. ABSTRACT

This report describes the materials evaluations and related efforts completed under contract to the Air Force Materials Laboratory. The crack growth properties of D6ac steel were determined and actual components constructed of D6ac and 4340 were fatigue tested. The tensile, crack growth, and fracture toughness properties of roll-extruded HP 9-4-25 were determined as a function of degree of roll-reduction. Fracture and fatigue crack growth studies were conducted on 7175-T736 aluminum forgings. Design data were generated on the newly developed 7049 aluminum alloy extrusion in the T73 and T76 conditions. The effect of annealing on the tensile and fatigue properties of centrifugally cast Ti-6Al-4V were investigated as were the tensile, fracture, fatigue crack growth and stress corrosion properties of beta annealed Ti-6Al-4V plate. Tensile, fracture, fatigue, and static crack growth, and notched and unnotched fatigue test data were generated for Ti-6Al-6V-2Sn. A parametric analysis of creep and stress rupture data as it pertains to the refractory metal alloys is presented. Two laminated composites were also evaluated. One was a simple adhesively bonded 2024 aluminum composite and the other was composed of alternating layers o Ti-6Al-4V and boron/epoxy. The results of the preliminary evaluation of these composites are presented. Thirty-three elastomeric materials manufactured by five different companies are being evaluated in a 24-month storage test program. The hydrolytic stability of several potting compounds was also determined. Compatibility studies involved a silicone compound helicopter engine seal in eleven approved engine lubricants, two O-ring packings in Type I, Type III, JP-4, and JP-7 fuels, as well as Buna-n, ethylene propylene, and neoprene pump seals in a 55% mono-ethanol-amine/45% amon-isopropyl-amine decontaminant. The hot pressing conditions which were used to increase the density of 3-D carbon/carbon composites are described. Additional development of a foam-in-place liner for helmets and the development of suitable photochromic compounds for camera filters are also discussed.

DD FORM 1 NOV 68 1473

Unclassified

Security Classification

14 KEY WORDS	LINK A		LINK B		LINK C	
	ROLE	WT	ROLE	WT	ROLE	WT
fracture mechanics						
aluminum alloys						
creep rupture						
tantalum alloys						
titanium alloys						
stress corrosion						
crack initiation						
crack arrest						
fuel tank sealants						
elastomers						
potted electrical connectors						
helmet design						
foam-in-place liners						